SCUOLA DI DOTTORATO
UNIVERSITÀ DEGLI STUDI DI MILANO-BICOCCA

Department of

Medicine and Surgery

PhD program in Neuroscience Cycle XXXII

Curriculum in Clinical Neuroscience

TMS-EEG: a promising tool to study the cathodal tDCS effects on cortical excitability

Surname Varoli Name Erica

Registration number 727850

Tutore / Tutor: Leonor Josefina Romero Lauro

Cotutore / Co-tutor:
(if there is one)

Supervisor:
(if there is one)

Coordinator: Guido Angelo Cavaletti

ANNO ACCADEMICO / ACADEMIC YEAR 2018/2019

Contents

Abstract

Transcranial direct current stimulation (tDCS) is a non-invasive neuromodulatory technique able to induce plasticity-related alterations in neuronal excitability. There is a growing interest in the use of tDCS in both experimental and clinical settings; in particular, the chance to induce long-term effects fostered the used of the technique to treat cognitive impairments associated with different neuropsychological and psychiatric disorders.

Although tDCS is increasingly used, presently little is still known about its neurophysiological underpinnings, particularly concerning the activity on the brain regions that underlie high cognitive brain functions. In these cases, optimal tDCS stimulation parameters also have yet to be clearly defined. This issue is particularly true for the cathodal polarity of tDCS stimulation, that is reported as less effective, or it is not explored at all. For instance, recent evidence-based guidelines for clinical use of tDCS do not include cathodal stimulation for the treatment of any disease. A deeper understanding of the mechanisms underpinning this technique would be crucial to achieving a better refinement of stimulation protocols for clinical and research purposes.

For this reason, a systematic and comprehensive study of its cortical effects acquires a critical relevance. In the last years, there has been indeed a keen interest in understanding the working mechanisms of this technique. To address this issue, in this project we explored the cortical plasticity modulation induced by cathodal stimulation on healthy subjects while resting or during task execution, using an integrated system of Transcranial Magnetic Stimulation and Electroencephalography (TMS-EEG). TMS-EEG is indeed a promising tool to explore the effects of different non-invasive brain stimulation techniques because it allows measuring directly cortical excitability modulation all over the cortex and effective connectivity.

In this dissertation are reported a total of three studies. In the first study, starting from the results obtained from the same research group with anodal tDCS, the effects of cathodal stimulation over the right Posterior Parietal Cortex (PPC) were explored during resting state. The contralateral homologue brain area, namely the left posterior parietal cortex (PPC), was targeted with TMS before, during, and after cathodal stimulation.

In the second study, we explored the behavioural effects induced by the application of cathodal tDCS over right PPC during the execution of two tasks, one of visuospatial working memory and a second tapping visual attention reorienting, which are known to involve this brain area. Within the research project of this dissertation, the aim of this second study was to find tasks sensitive to the effect of cathodal tDCS over the right PCC, to be used in the third study. In particular, a disruption of the performance was found for a modified version of the Posner Cueing Task.

In the third study, we employed again TMS-EEG to track the neurophysiological effects of cathodal tDCS on right PPC at an active state, i.e. while the participants were performing the task tested on the second study.

In the first and third studies, the EEG was concurrently recorded from 60 channels, and each participant underwent an additional control session in which sham tDCS was delivered. Indexes of global and local cerebral excitability were obtained, (Global Mean Field Power, GMFP and Local Mean-Field Power, LMFP) on mean TMS-evoked potentials (TEPs). A source modelling analysis was also performed, computing global and local current density at the cortical level for each subject, to better define the localization of the induced tDCS effects, avoiding the potential confound of volume conduction.

The results at resting state for cathodal tDCS, both at sensors and cortical sources levels, converge in showing no differences during and after tDCS compared to pre-stimulation sessions, both at a global and local level. The previous results with anodal tDCS, instead, reported a widespread rise of cortical excitability along with a bilateral frontoparietal network, following structural connections.

On the other hand, at an active state, cathodal, as well as anodal, tDCS stimulation induced modulation of cortical excitability only in the task-relevant brain regions.

Several significant findings emerged from this empirical work. First of all, these data highlight a non-linear impact of anodal and cathodal stimulation on cortical excitability at rest that is not depicted by the simplistic view of anodal-excitatory and cathodal-inhibitory effects. Another relevant point is the crucial role played by the different cortical states (resting vs active). These results seem to point out that the level of cortical state can contribute to modulate the tDCS effects, in line with “activity-selectivity” hypothesis. The level of cortical state needs to be taken into account, especially to observe neuromodulatory effects also with cathodal tDCS. All these findings hold relevant implications for tDCS setup in both cognitive neuroscience experiments and rehabilitation protocols.

Glossary of abbreviations

AD	Anno Domini
ADHD	Attention Deficit Hyperactivity Disorder
AEP	Auditory Evoked Potential
AG	Angular Gyrus
ANOVA	ANalysis Of Variance
ANT	Attentional Network Test
BA	Brodmann's Area
BDNF	Brain-Derived Neurotrophic Factor
BF	Bayesian Factor
BOLD	Blood Oxygen Level-Dependent
CBZ	Carbamazepine
CDA	Contralateral Delay Activity
cm	centimetre
CRT	Choice Reaction Task
CSE	CorticoSpinal Excitability
dB	deciBel
DC	Direct Current
dCS	dynamic Contrast Sensitivity
DLPFC	DorsoLateral PreFrontal Cortex
DMO	Dextromethorphan
ECT	ElectroConvulsive Therapy
EEG	Electroencephalography
EF	Electric Field
EOG	ElectroOculoGram
ERP	Event-Related Potential
FA	False Alarm

FDR	False Discovery Rate
fMRI	functional Magnetic Resonance Imaging
FWER	Family Wise Error Rate
GABA	gamma-Aminobutyric Acid
GLMER	Generalised Linear Mixed-Effects R
GMFP	Global Mean Field Power
H&E	haematoxylin–eosin
HD-EEG	High Definition-EEG
HD-tDCS	High Definition-transcranial Direct Current Stimulation
Hz	Hertz
I	Input
I/O	Input/Output
ICF	IntraCortical Facilitation
IFG	Inferior Frontal Gyrus
IPL	Inferior Parietal Lobe
IPS	IntraParietal Sulcus
ISI	Inter-stimulus Interval
kΩ	kiloohm
LA	Left Anodal
LC	Left Cathodal
L-dopa	Levodopa
LMER	Linear Mixed-Effects R
LMFP	Local Mean Field Power
LRT	Likelihood Ratio Test
LTD	Long-Term Depression
LTP	Long-Term Potentiation
M	Mean

m	metre
M1	Primary Motor cortex
MA	Massachusetts
mA	milliAmpere
MCP	Multiple Comparison Problem
MDD	Major Depression Disorder
MEP	Motor Evoked Potential
min	minute
mm	millimetre
MNI	Montreal Neurological Institute
MR	Magnetic Resonance
ms	millisecond
NBS	Navigation Brain Stimulation
NIBS	Non-Invasive Brain Stimulation
NL	Nederland
NMDA	N-methyl-d-aspartate
O	Output
PA	Pennsylvania
PAS	Paired Associative Stimulation
PC	Personal Computer
PD	Parkinson’s Disease
PET	Positron Emission Tomography
PFC	PreFrontal Cortex
PPC	Posterior Parietal Cortex
PT	Phosphene Threshold
RA	Right Anodal
RC	Right Cathodal

rCBF	regional Cerebral Blood Flow
REM	Rapid Eye Movement
RGB	Red Green Blue
ROI	Region Of Interest
RT	Reaction Time
rTMS	Repetitive Transcranial Magnetic Stimulation
RVP	Rapid Visual Processing
s	second
S1	Primary Sensory cortex
SCD	Significant Current Density
sCS	static Contrast Sensitivity
SD	Standard Deviation
SE	Standard Error
SEP	Somatosensory Evoked Potential
SICI	Short-IntraCortical Inhibition
SMA	Supplementary Motor Area
SPL	Superior Parietal Lobe
T	Tesla
tACS	transcranial Alternating Current Stimulation
TBS	Theta-Burst Stimulation
tDCS	transcranial Direct Current Stimulation
TEP	Transcranial magnetic stimulation Evoked Potential
tES	transcranial Electric Stimulation
TMS	Transcranial Magnet Stimulation
TMS-EEG	TMS with co-registration of EEG
tRNS	transcranial Random Noise Stimulation
USA	United States of America

V	Volt
V1	Primary Visual cortex
VC	Virtual Cortex
VEP	Visual Evoked Potential
VWM	Visuospatial Working Memory
VWMT	Visual Working Memory Task
WM	Working Memory
μA	microampere

Chapter One: "The neuromodulatory techniques"

1.1 Chapter overview

In this Chapter, we will discuss the historical development of the brain stimulation techniques, starting from the first medical uses of electricity, in Roman Epoque, to the contemporary non-invasive electrical brain stimulation techniques. After an overview of the main different types of transcranial electrical stimulation techniques, we will mainly focus on the transcranial direct current stimulation (tDCS). In particular, we will discuss all the stimulation parameters that need to be taken into account in the design of an experimental study.

At the end of this Chapter, the reader will have an overall idea of how to design an experimental or clinical study using the tDCS, and which are the limits and the advantages in using this particular technique.

1.2 An historical overview

Transcranial Direct Current Stimulation (tDCS) is a Non-Invasive neuromodulatory Brain Stimulation (NIBS) technique, based on a weak electric current flow able to modulate the underlying brain activity, passing through the scalp. It is one of the most used technique belonging to the wider category of transcranial Electric Stimulations (tES). In the last two decades, the impressive potential of these simple and easy-to-apply techniques has become clearer as the use has increased (Dubljević, Saigle, & Racine, 2014). TES can be used as a treatment for neuropsychiatric disorders and to improve and enhance cognitive functions in both patients and healthy subjects (Fertonani & Miniussi, 2017). In particular, many of these techniques can be used in place or in combination with pharmacological, cognitive and behavioural treatments, with the purpose of increasing the beneficial effects (Giordano et al., 2017).

Despite the employment of these techniques had an impressive growth in the last twenty years, the use of electricity for both investigational and therapeutic purposes, can be traced back for centuries (Beaudreau & Finger, 2006), with an history characterized by a meandering path, replete with both missteps and triumphs (Wexler, 2017).

Even if the earliest documented medical electricity usage came from the first century in the Roman age, around 1 – 50 AD (Coffman, Clark, & Parasuraman, 2014; Zago, Priori, Ferrucci, & Lorusso, 2016), it was during the Enlightenment that a real interest in the use of electricity for medical purposes has grown up. During the 18th century, for example, a various technological innovation made easier to govern electrical therapies. In particular, it was thanks to the Leiden jar first and then to the voltaic pile, the first electrical battery invented by Alessandro Volta in 1799 (Piccolino, 2000),

that became possible to apply a continues electric current to a body. This technique is nowadays known as galvanism.

At the beginning galvanism was commonly used to treat a various form of post-stroke paralysis and movement disorders, as well as some cases of hysterical seizures (Finger, 2006). Its application was generally confined to the body affected parts, rather than being applied directly to the patient’s head. The first transcranial applications of a current flow were mainly, as it happened for many important discoveries, consequences of incidents. A well-documented early case of transcranial stimulation occurred in 1755, when the French physician Charles Le Roy was able to induce phosphenes (perceived transient flashes of light) in a blind patient by stimulating via a conducting wire wrapped around his head. Le Roy’s goal was to treat the blindness, and even though the patient’s sight was not restored - in this sense the experiment was a complete failure - this was the first single-case study able to demonstrate the possibility to induce eyes and/or optic nerves response by mean of electrical stimulation (Lewis & Rosenfeld, 2016; Wagner, Valero-Cabre, & Pascual-Leone, 2007). In the same year Benjamin Franklin described his second serious incident and he explained how electricity could be applied directly to the head without dangerous and significant long-lasting effects (Beaudreau & Finger, 2006). Again, in the same trend, we have to acknowledge the contribution of Jan Ingenhousz in the 1783, who described a sort of alteration in his cognitive functions together with a positive change in the mood after a frightful incident that left him unconscious and confused (Beaudreau & Finger, 2006; Elliott, 2014). Although anecdotal, these stories nevertheless represent some of the first documented evidences of a putative cognitive modulation related to a head electrical stimulation. Between the end of the 18th and the beginning of the 19th century the use of electrical stimulation to treat psychiatric disorders obtained first experimental successes in pioneering clinical studies by the English surgeon John Birch and the Italian physician Giovanni Aldini. Their works were mostly focused on depression (melancholia) and schizophrenia (Beaudreau & Finger, 2006; Elliott, 2014; Parent, 2004). In particular, Aldini’s work inspired many different electrotherapies that are still in use today, and it could be considered as the turning point towards the contemporary neuroscience concept of *animal electricity*, that marked the beginning of the era of DC stimulation for the treatment of neurological and psychiatric disorders (Parent, 2004; Sarmiento, San-Juan, & Prasath, 2016).

From the beginning of the 20th century the use of electrostimulation began to decline due to a combination of factors: the controversial reported results, some positive and other completely negative, a lack of understanding of its mechanisms of action, and the consequent increase in the concerns about safety and participant tolerability (Sarmiento et al., 2016; Steinberg, 2013). At the same time, the setting up of new and different methods for the treatment of psychiatric disorders, such

as the birth of psychoanalysis at the end of 19th century and the development of the Electroconvulsive Therapy (ECT) in 1938 (Taylor, 2007), followed by the discovery and the introduction of the first-generation antipsychotic drugs in the early 1950s (Dubljević et al., 2014; Shen, 1999), contribute to the gradual abandonment of electric stimulation.

Finally, it was only around twenty years ago that the use of direct current stimulations started again to increase significantly. In particular, thanks to the work of Priori and colleagues (1998) first, and then to the contribution of Nitsche and Paulus (i.e. 2000, 2001) who dedicated their entire careers to study of direct current stimulation, the peculiar characteristics of modern tDCS became well established. It is a non-invasive and well tolerated stimulation, with only mild adverse effects. These findings renewed the interest in the clinical usage of tDCS (Brunoni, Ferrucci, Fregni, Boggio, & Priori, 2012).

TDCS is today a very promising tool both for neuroscientists, to enhance cognitive functions in healthy people (Dubljević et al., 2014), and for clinical neurologists and psychiatrists, to facilitate the treatment of different neuropsychiatric disorders generally resistant to the traditional approaches (Schlaug & Renga, 2008). Although tDCS has definitely demonstrated its benefits, a deeper understanding of its neurophysiological mechanisms of action would be nowadays crucial to achieve a better refinement of stimulation protocols for clinical and research purposes.

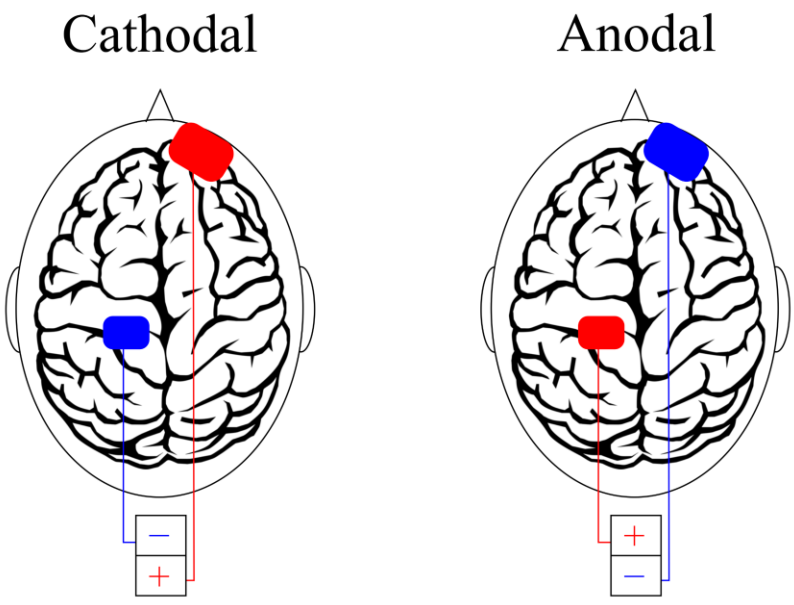

Figure 1.1: *Montage of tDCS. On the left side is possible to observe a cathodal tDCS montage in which the blue electrode is the target one, while the red one, the anode, is the reference. Beyond the head, a schematic representation of a battery with the negative pole linked to the cathode and the positive one on the anode. On the right side, the opposite schematic representation was depicted, namely anodal tDCS montage.*

1.3 Contemporary tES

TES is a generic term that refers to a class of NIBS techniques based on the use of low intensity currents (typically 1 – 2 mA) on the brain scalp, with a stimulation method that is similar for all the different tES (Paulus, Nitsche, & Antal, 2016). The current is delivered from a battery-driven stimulator, using two or more rubber electrodes. The electrodes are wrapped in a viscose sponge that can be soaked in an isotonic saline solution or fixed directly on the scalp with a conductive paste. Generally, one electrode is defined as the target electrode and it is positioned above the cortical region of interest, while the other one is usually referred to as the reference, or return electrode (see Figure 1.1; Bikson, Datta, Rahman, & Scaturro, 2010).

TES devices are referred to as sub-threshold neuromodulatory technologies. It means that the strength of the injected current falls below the required threshold to directly elicit an action potential in the stimulated neuronal populations. Instead, these techniques modulate the neurons spontaneous firing activity in a bi-directional way, via subthreshold alterations of the resting membrane potentials (Giordano et al., 2017; Miocinovic, Somayajula, Chitnis, & Vitek, 2013; Paulus et al., 2016). This is one of the main aspects that distinguish tES from Transcranial Magnetic Stimulation (TMS). The latter is one of the main supra-threshold NIBS techniques, which is capable of directly induce firing in underlying neuronal populations (Paulus et al., 2016). The electrical currents induced in the brain

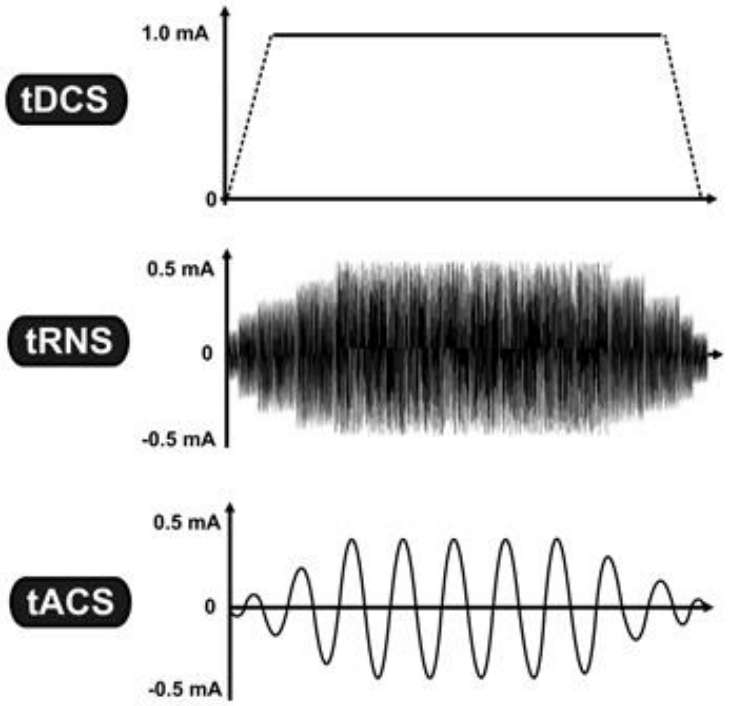

Figure 1.2*: Different types of tES with their characteristic waveforms. From the top: tDCS delivers a constant current which can be either positive (anodal) or negative (cathodal); tRNS delivers instead stimulation at multiple and different frequencies**;** tACS uses a sinusoidal current at a specific frequency which continuously alternates between positive and negative (Saiote et al., 2013).*

by TMS are two to three orders of magnitude bigger than those produced using tES (Salvador, Wenger, & Miranda, 2015). Whereas the spatial and temporal resolution of TMS is considerably better, when applied for an extended period of time, tES techniques have shown to be able to elicit changes in cortical excitability that can endure beyond the initial stimulation period, with effects that can last from several minutes up to over an hour (Kuo et al., 2013; Nitsche, & Paulus, 2000, 2001). Moreover, tES tools are generally more cost-effective, easier to operate, and easily adaptable for double-blind and sham-controlled studies. For example, the concurrent application of a stimulation with behavioural tasks is more difficult with TMS compared to tES. In fact, the supra-threshold activations may inevitably disrupt task-relevant activities, while the sub-threshold polarization induced by tES allows the online stimulation to enhance or reduce task-dependent neuronal activation, without interfering with the concurrent activity (Paulus et al., 2016).

In conclusion, tES and TMS can be considered as complementary and both of them are valuable adjunctive tools in neuroscience research, having both the potential to overcome an inherent limitation of neuroimaging techniques: the difficulty to infer causal involvement of brain areas or functional networks in specific motor, perceptual, or cognitive processes.

Focusing on tES, it is possible to differentiate sub-categories based on the type of electricity used for the stimulation (see Figure 1.2): direct currents (transcranial Direct Current Stimulation, tDCS), alternating currents (transcranial Alternating Current Stimulation, tACS), or random noise currents (transcranial Random Noise Stimulation, tRNS) (Yavari, Jamil, Samani, Vidor, & Nitsche, 2018).

TDCS is the most widely used among the tES techniques, mainly due to its simplicity in design. The conventional tDCS paradigm uses a single current amplitude maintained constant during the entire stimulation session, except for one ramp-up and one ramp-down period, typically with an 8–30 s linear ramp. This fade-in and fade-out periods are introduced in order to minimize the probability of unexpected and unintended skin and visual sensations induced by retinal stimulation after switching on or off the stimulation suddenly. The current flow is not restricted to the area underneath the electrodes, but rather spreads around in the areas near to the target one (Miranda, Mekonnen, Salvador, & Ruffini, 2013; Opitz, Paulus, Will, Antunes, & Thielscher, 2015; Ruffini, Fox, Ripolles, Miranda, & Pascual-Leone, 2014). The High-Definition tDCS (HD-tDCS) is a variant of the conventional design tDCS with a significant improvement in the stimulation physical focality, that is commonly known as one of the limits in traditional tDCS based study design (Kuo et al., 2013; Villamar et al., 2013a). The HD-tDCS can be delivered through a concentric-ring electrodes configuration with the active electrode centred on the target area, surrounded by four return electrodes (see Figure 1.3). According to different modelling studies, this electrodes configuration results in a

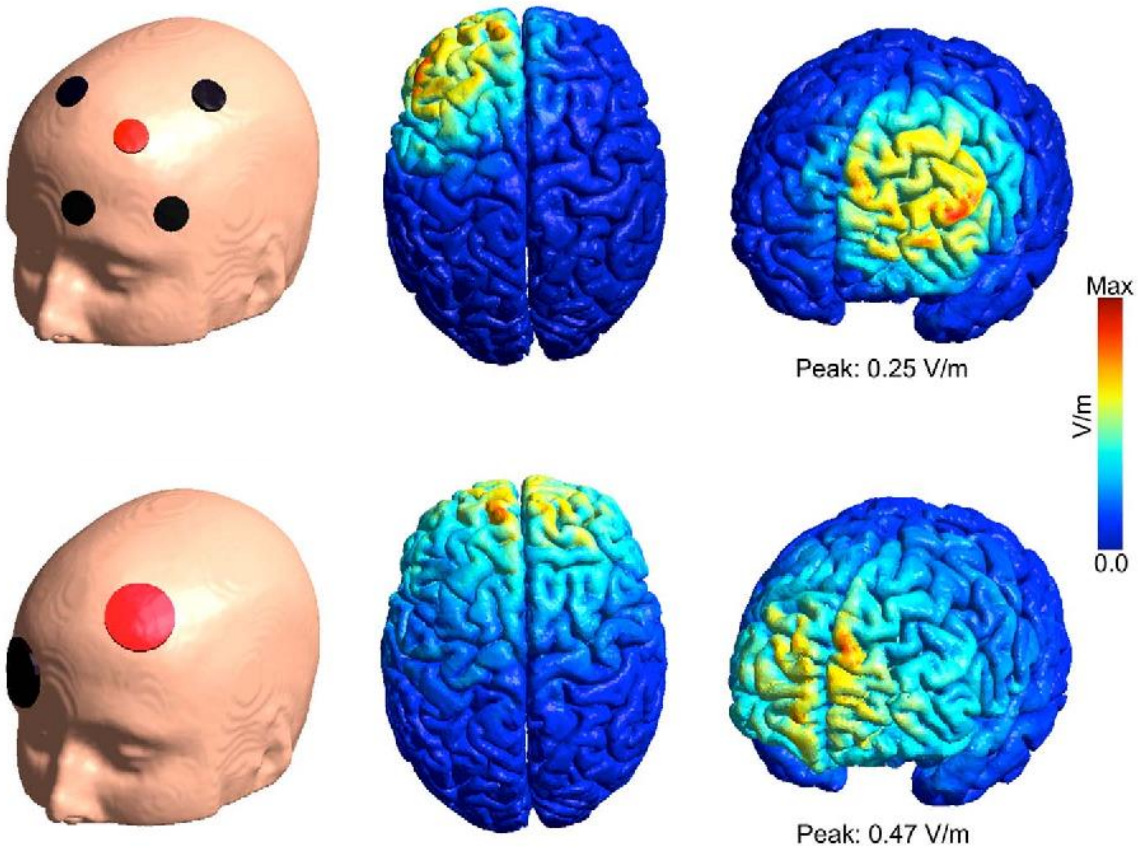

Figure 1.3: *Example of a HD-tDCS montage in the top half, together with a simulation of electrical current flow in the cortical brain region illustrating electric field magnitudes. In the bottom part, the same is illustrated for a traditional tDCS montage. It can be clearly seen that HD-tDCS produces a more focal electrical field mainly confined to the left stimulated region (Hill et al., 2017).*

maximal electric field (EF) strength under the target electrode with the brain current flow constrained by the 4 x 1 ring radius, that is defined as the distance between the active and each of the return electrodes, and thus it has a more spatially restricted electric field (Datta et al., 2009; Datta, Elwassif, Battaglia, & Bikson, 2008).

Although the best configuration of the parameters of the stimulation may vary from experiment to experiment, the current density (i.e., current intensity/electrode size), duration, polarity, and location of the electrodes have been shown to have important implications in the neuromodulatory outcome of the stimulation (Zaghi, Acar, Hultgren, Boggio, & Fregni, 2010).

Given the remarkable effects of tDCS, the use of low intensity nonconstant currents may also be an attractive option. In tACS, the externally applied alternating current has been demonstrated to induce endogenous neural oscillations by increasing the oscillations power or the phase-locking index between the driving and endogenous oscillations (Antal et al., 2008; Antal & Herrmann, 2016).

The application of tACS provides sinusoidal currents across the scalp with a given frequency. During the oscillations, both the electrodes works alternately as anode or as cathode, and the current

intensity increases and decreases following the sinusoidal wave. For tACS the most effective parameters to influence the efficacy of the stimulation are frequency, intensity, and phase, while the polarity-dependent effects become completely inconsistent (Antal et al., 2008; Antal & Herrmann, 2016; Zaehle, Rach, & Herrmann, 2010).

This specific technique was developed in order to investigate the possible causal relationship between brain oscillations and cognitive functions, and, consequently, as a possible therapeutic tool to restore disturbed oscillations that characterise different diseases, such as Parkinson’s and schizophrenia (Paulus et al., 2016).

TRNS is a particular type of tACS. During tRNS a low intensity alternating current is applied with intensity and frequency of the current as random parameter, left free to vary in a given range (Antal & Herrmann, 2016; Paulus et al., 2016). In a similar vein to tACS, different forms of noise can be applied, depending on the frequency ranges. In most of the studies using tRNS, a frequency spectrum between 0.1 Hz and 640 Hz (full spectrum) or 101–640 Hz (high-frequency stimulation) were used (Fertonani, Pirulli, & Miniussi, 2011; Terney, Chaieb, Moliadze, Antal, & Paulus, 2008). The probability function of the noisy current stimulation follows a Gaussian or a bell-shaped curve with mean zero and a variance chose in a way that the 99% of all generated current levels are within ±1 mA. In the frequency domain all coefficients of the random sequence have a similar amplitude (“white noise”).

In conclusion, all these sub-categories of tES, even if based on different low-intensity current applications, are effective in modulating the neural brain activity, and they are increasingly used both for research and clinical purposes. However, there is still some work to do in order to fully understand their mechanisms of action, particularly true for the tDCS, even if it is the widespread one.

For these reasons, this dissertation will present and discuss the results of our works aiming for a more deeply understand of the mechanisms of action of tDCS. The following paragraphs will describe the basic methodological and functional knowledge of tDCS.

1.4 tDCS stimulation parameters

From a practical point of view, the setting and the usage of tDCS are relatively straightforward. The traditional and more common application requires only two electrodes, an anode and a cathode, attached to the scalp, through which a low intensity current flow passes. tDCS is indeed often advocated for its relative simplicity compared to other NIBS techniques (e.g., Brunoni, Nitsche, & Loo, 2016; Yavari et al., 2018). However, despite its relative “ease-to-use reputation”, tDCS can be very fruitful if applied within rigorous protocols (Woods et al., 2016) and by considering correctly all the stimulation parameters (Fertonani & Miniussi, 2017). For this reason, researchers need a deep knowledge of both behavioural and cognitive processes as well as of the more recent advances in

stimulation theories, in order to better predict what will be the outcomes of the stimulation protocols (Monte-Silva, Kuo, Hessenthaler, Fresnoza, Liebetanz, Paulus, & Nitsche, 2013). A list of the key stimulation parameters which experimenters should consider includes, but it is not limited to: current polarity, density and intensity, duration of the stimulation, size and position of electrodes on the head. In the following paragraphs these technical aspects will be explored more in detail.

1.4.1 Polarity

In literature, the anode is usually defined as the electrode through which the positive current enters the head. The cathode, or the negative pole, instead closes the electric circuit by letting the current exiting. (Jackson et al., 2016; Merrill, Bikson, & Jefferys, 2005).

In human tDCS studies, anodal tDCS refers to a stimulation montage in which the anodal electrode is placed above the target brain region. On the other hand, cathodal tDCS refers to any montage in which the cortical target underlies the cathode. As mentioned above, the electrode over the non-target region is not physiologically inert and, for this reason, its position and size can have a considerable impact on the effects of the stimulation on the brain, even if it is placed over an extra-cephalic site such as the chin or deltoid (Bikson et al., 2010; Im, Park, Shim, Chang, & Kim, 2012; Moliadze, Antal, & Paulus, 2010; Nasseri, Nitsche, & Ekhtiari, 2015).

Relatively to single neuron registrations, the effects of tDCS are generally considered polarity-dependent, with anodal stimulation increasing the neurons’ spontaneous firing rate and evoked potentials, and cathodal tDCS leading to the opposite effect. This effect was demonstrated in first pioneering *in vitro* animal studies. In those works, indeed, it has been observed that the application of a direct current can depolarize, in case of anodal stimulation, or hyperpolarize, in case of cathodal one, the neuron membrane potential and enhancing or diminishing the neuron firing rate, respectively (Bindman, Lippold, & Redfearn, 1962, 1964; Creutzfeldt, Fromm, & Kapp, 1962; Purpura & McMurtry, 1965). This kind of opposite effect was observed also in human studies when tDCS was applied on M1 (Kirimoto et al., 2011; Nitsche & Paulus, 2000, 2001; Nitsche et al., 2003; Priori, Berardelli, Rona, Accornero, & Manfredi, 1998), or in correspondence with somatosensory (Kirimoto et al., 2011), and visual cortices (Accornero, Voti, La Riccia, & Gregori, 2007; Antal, Kincses, Nitsche, Bartfai, & Paulus, 2004). However, this is a relatively simplistic dichotomy largely based on the effects of radial currents applied to pyramidal neurons oriented perpendicularly to the surface of the cortex, and it is not always completely fulfilled. For instance, the interaction between polarity and stimulation intensity seems to induce non-linear tDCS effects also in motor areas (Batsikadze, Moliadze, Paulus, Kuo, & Nitsche, 2013). The application of both 2 mA anodal and cathodal tDCS on the left M1 for 20 minutes was able to induce an increase in cortical excitability. In contrast, usually 1 mA cathodal tDCS produces a reduction in it. These results suggest that an enhancement of

tDCS intensity does not necessarily increase the efficacy of stimulation but might also shift the direction of excitability alterations (Batsikadze et al., 2013).

Non-linear and non-additive phenomena may also occur when tDCS is associated with a task, in line with the “neural noise” model (Miniussi, Harris, & Ruzzoli, 2013). In a more recent study, Bortoletto and colleagues (2015) observed that the activity of the motor system, at the moment of the stimulation, plays a crucial role in determining the effects of anodal tDCS on the ability of motor learning. In particular, the authors observed that 1,5 mA of anodal tDCS for 20 minutes reduced motor learning if applied during the execution of a task that induces learning and increasing cortical excitability. The same stimulation parameters, instead, caused facilitation in learning processes when applied during the task that neither induces learning nor changes cortical excitability (Bortoletto et al., 2015).

Therefore, clear-cut polarity-dependent effects of tDCS may not be achieved using all the different stimulation conditions and across all brain regions. This may be particularly true in humans, whose complex and diverse cortical architecture is likely to differentiate the shape of current flow across various brain regions (Jacobson, Koslowsky, & Lavidor, 2012).

The state-of-art about the tDCS mechanisms of action will be discussed more deeply in a following Chapter.

1.4.2 Electrode Position

Electrode positions and montage are crucial aspects that should be taken into consideration according to which functions of the human brain are the focus of interest.

Usually the target electrode is placed over the brain region that needs to be modulated. What is even more important is the position of the return electrode. Since the electric current flow goes

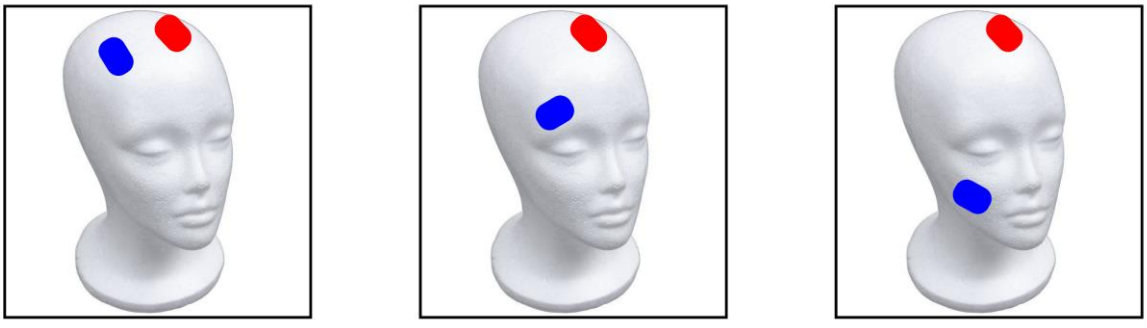

Figure 1.4*: Example of a schematically representation of different types of tDCS montage. On the left the intra-cephalic montage, in which both electrodes are positioned on the head in correspondence of the two targeted contralateral brain regions. In the middle an intra-cephalic montage again, but in this case, the return electrode, the blue one, is positioned in the supraorbital region that are usually considered inert. The last on the right is an extra-cephalic montage in which the return electrode is located on a body region outside the head, usually the cheek.*

through the cortical regions between the two electrodes, the position of the return one determines which will be the areas interested by the stimulation. Today, advances in the precision of computational models helps researchers with the simulation of the tDCS current flows in the brain, allowing a better definition of the electrodes montage (Bikson, Rahman, & Datta, 2012; Bikson et al., 2016; Miranda, Lomarev, & Hallett, 2006).

Currently, two main electrodes montages are used: the intra-cephalic, in which both electrodes are positioned on the head, and the extra-cephalic montage in which the return electrode is located on a body region outside the head, usually the cheek or the shoulder (see Figure 1.4).

In their original tDCS publication, Nitsche and Paulus (2000) conduced a pilot experiment testing different electrodes positions to find the optimal arrangement to achieve current driven cerebral excitability changes and to evaluate any possible rapid modification in the excitability during the current flow. They observed that the optimal electrodes configuration to stimulate M1 require to put the return electrode over the supraorbital area in the contralateral hemisphere. After this pioneering study, it became the classical intra-cephalic montage, that consists in placing the return electrode on a contralateral brain area not involved in the target network, or on the contralateral orbit (Nitsche & Paulus, 2000).

A similar result was also found in a more recent study by Moliadze et al. (2010). The authors observed that positioning the return electrode on an extra-cephalic location – e.g. the upper arm – could lead to a reduction of the after-effects when compared to the intra-cephalic montage over the contralateral forehead. However, even if the extra-cephalic montage seems to be more efficient in reducing the effects induced by the return electrode, computational model reports an unintentional shifting of the current flow more posteriorly (Bikson et al., 2010), and, in some cases, a stimulation of deeper sub-cortical structures as well as of the midbrain and brainstem (Noetscher, Yanamadala, Makarov, & Pascual-Leone, 2014).

For all these reasons, it is usually preferred the intra-cephalic montage over the extra-cephalic one. Furthermore, to reduce the activity of the return electrode, it is a relatively common practice to increase its size, in order to decrease the current density and therefore its functional efficiency (Nitsche et al., 2007).

A last, but not less important, parameter that requires to be consider is the current shunting. Shunting through the skin and skull reduces considerably the amount of current that reaches the brain from the surface of the electrodes (Datta, et al., 2009). Increasing the anode-to-cathode inter-electrode distance can help to reduce the degree of shunting, resulting in a higher effective current flow (Dmochowski, Bikson, & Parra, 2012; Faria, Fregni, Sebastião, Dias, & Leal, 2012). Another expedient can be to reduce the dimension of the target electrode in order to increase the focality of

the electric field produced in the brain (Dmochowski et al., 2012; Nitsche et al., 2007; Wagner, Fregni, et al., 2007).

1.4.3 Current Intensity and Electrode Size

As discussed in the previous paragraph, the different stimulation parameters cannot be considered singularly since they interact one with each other, and this is particularly truth for the intensity of the injected current and the size of the electrodes. The *current density*, indeed, is defined as the ratio between the *stimulation intensity* (mA) and the *electrode size* (cm^2), and it is a crucial factor to take into account in order to determine the desired tDCS physiological effects.

Starting from the results of Nitsche and Paulus (2000) original study, it is still nowadays a common practice to use 5 x 7 cm rectangular pads, with a surface area of 35 cm^2. This correspond to a current density of 0.029 mA/cm^2 and 0.057 mA/cm^2 for stimulation intensities respectively of 1 mA and 2 mA. Despite these are the common parameters, it is not unlikely to find studies in literature with different current settings. As an example, a target electrode with reduced size in order to increase focality, or, on the opposite side, a reference electrode with bigger dimensions to increase its inactivity (e.g. Nitsche et al., 2007). Moreover, also the spread in current intensity values used in human experiments is quite notable, and it is scattered around from 0.1 mA to 4.0 mA, depending on the studies (Bikson et al., 2016). Nevertheless, when researchers have to define these parameters for the design of a new experiment, they should remember two aspects: first the safety limitation, and second the non-linear relation between current density and tDCS effects. Indeed, even if high stimulation intensities, up to 4 mA, seems to be well within the safety limits based both on predictions from animal and computational modelling analyses (Bikson et al., 2016), they are very infrequently used. In fact, it was demonstrated that high current intensities are normally associated with more intense and sometime even painful scalp sensations. This could also make more difficult to design a blind experiment since during the sham trials this scalp sensations are less pronounced in comparison to the active conditions (Wallace, Cooper, Paulmann, Fitzgerald, & Russo, 2016).

The second point is that, although a larger current density results in stronger and more prolonged after-effects (Nitsche & Paulus, 2001), this relationship is not always linear. In a recent study, Bastani and Jaberzadeh (2013) compared the effects of anodal tDCS stimulation with an intensity of 0.3, 0.7, 1.4 and 2 mA. They observed that the smallest current density (0.3 mA) produced significantly larger corticospinal changes than the next two higher. Another study also investigated both anodal and cathodal tDCS stimulation for four different stimulation intensities: 0.5, 1.0, 1.5 and 2.0 mA (Jamil et al., 2017). Results showed that for anodal tDCS, all the intensities resulted in equivalent facilitatory effects relative to sham, whereas for cathodal tDCS, only the stimulation with an intensity of 1.0 mA seemed to induce an excitability reduction (Jamil et al., 2017). These studies

are only two examples in support of the non-linear intensity-dependent neuroplasticity related after-effects of tDCS.

1.4.4 Stimulation Duration

The duration of the stimulation also affects the lasting and the magnitude of the after-effects, and the tDCS literature is full of studies with a wide range of different stimulation durations. In fact, depending on which type of effects one is interested in, the duration of the stimulation can vary noticeably. For instance, a 4 s stimulation is well suited to obtain only acute effects on excitability, which are membrane polarization-driven, but do not include synaptic plasticity (Nitsche, Nitsche, et al., 2003; Nitsche & Paulus, 2000). In contrast, to observe after-effects, tDCS stimulation has to be delivered for at least 3 minutes. Even longer stimulations lead to more pronounced changes (Nitsche & Paulus, 2000, 2001), although, also in that case, the relationship is not strictly linear. In a similar vain to stimulation intensity, initial studies by Nitsche and Paulus (2000, 2001) demonstrated an incremental linear effect on cortical excitability induced by different stimulation durations. In particular, they observed that up to 13 minutes of stimulation lead to longer-lasting plastic changes. Nevertheless, in a more recent study, Monte-Silva and co-workers (2013) observed opposite effects when the tDCS stimulation window was extended even more. Their results showed that 26 minutes of 1 mA anodal tDCS stimulation induced a reduction in cortical excitability, while they registered instead an increase after a single session of 13 minutes. Moreover, the authors observed that two 13 minutes long blocks of tDCS, with a short interval of 3 or 20 minutes in between, induced an enhancement of cortical excitability not immediately after the end of the stimulation, but some hours later, and this effect lasted for over 24 hours (Monte-Silva et al., 2013).

This study demonstrated that the long-lasting tDCS effects depend on a non-linear connection between stimulation duration, plasticity duration, and impact direction. Moreover, this becomes even more crucial if tDCS is used to study cognitive functions or in rehabilitation protocols. In cognitive paradigms, it is common to perform stimulation session up to 20 minutes (e.g. Brunoni & Vanderhasselt, 2014; Giustolisi, Vergallito, Cecchetto, Varoli, & Romero Lauro, 2018). This difference in duration becomes even more evident in clinical studies that investigate the use of tDCS as a therapeutic intervention (Bolognini et al., 2011; Brunoni et al., 2012; Kekic, Boysen, Campbell, & Schmidt, 2016). Nevertheless, it is worth to consider that a prolongation of stimulation duration might not result in a higher efficacy for each case (Monte-Silva et al., 2013).

1.4.5 Timing of stimulation - Online Versus Offline Effects of Stimulation

Timing of stimulation is also an important issue, especially in cognitive neuroscience experiments. Related to this point, the state of the cortex during the stimulation is also a determining

factor for the effects of tDCS (Lafon, Rahman, Bikson, & Parra, 2016; Silvanto, Muggleton, & Walsh, 2008). Many different works aimed to investigate the optimal timing for combining tDCS with different cognitive tasks in order to maximize the behavioural after-effects (as discussed in the Chapter Five, e.g. Martin, Liu, Alonzo, Green, & Loo, 2014; Pirulli, Fertonani, & Miniussi, 2013; Stagg & Nitsche, 2011). As an example, after-effects are significantly modulated by cognitive and motor activities, compared to the resting conditions (Antal, Terney, Poreisz, & Paulus, 2007). These evidences show that the effects of tDCS may depend on the background level of activity in the system, for this reason the cortical state of the neural population at the time of stimulation need to be taken into account to the effectiveness of tDCS stimulation (Bortoletto, Pellicciari, Rodella, & Miniussi, 2015; Matsunaga, Nitsche, Tsuji, & Rothwell, 2004). For instance, if the resting state is characterised by a low level of spontaneous discharge, the plasticity effects of tDCS may result smaller than expected. At the same time, if the system is already activated at high level it could be possible that tDCS excitatory effects results less evident.

1.5 Summary

In this paragraph, we described all the main stimulation parameters that need to be taken into account during the design process of any study or experiment. On the other hand, these specific technical knowledges have to go hand in hand with an equally good theoretical preparation on the mechanisms underlying tDCS. In the next Chapter, we will describe in detail what is the state-of-art of the knowledge about the working mechanism of the tDCS.

Chapter Two: “State-of-art about the tDCS mechanisms of action”

2.1 Chapter overview

A deep understanding of the neurophysiological underpinnings of tDCS effects is crucial to achieve a better refinement of stimulation protocols for clinical and research purposes. Current knowledge attribute the acute effects of tDCS to a shift in the membrane potential (Liebetanz, Nitsche, Tergau, & Paulus, 2002; Nitsche & Paulus, 2000), but the exact mechanisms underlying this effect as well as the after-effects of tDCS are still object of further investigations. Even so, the number of studies that address this issue remain still relatively little and, consequently, several complex neurobiological mechanisms are still not well understood. In this Chapter, we will try to bring together the results from many diversified studies to describe the current knowledge of the physiological effects of tDCS. We will start from *in vitro* and animal models, to move then on pharmacological, neurophysiological and computational studies in humans, ending with researches that used other techniques to record stimulation-effects on cortical excitability and connectivity induced by tDCS (for a more systematic review see Medeiros et al., 2012; Stagg & Nitsche, 2011).

2.2 Studies on animal models

Many hints on the neuronal mechanisms of online and offline tDCS effects come from the translational approach of animal models.

The first pioneering *in vitro* studies using direct current stimulation provided evidence for a polarity-dependent modulatory action, according to which anodal DC increases neurons' spontaneous firing rate and evoked potentials, while cathodal tDCS leads to the opposite effect (Bindman et al., 1962, 1964; Creutzfeldt et al., 1962; Purpura & McMurtry, 1965). However, already in the Purpura and McMurtry study, it has been showed that neurons throughout the cortex were not modulated in a homogeneous manner. In particular, the authors observed that the neurons in deep cortical layers often responded in a opposite way; the result was that anodal DC reduced neurons activity, while the cathodal one increased it (Purpura & McMurtry, 1965). Moreover, they observed that the different subpopulations of neurons seem to respond to DC with different thresholds. In particular, non-pyramidal neurons were stimulated at lower total charges compared to pyramidal tract neurons, which were instead modulated only at higher charge densities (Purpura & McMurtry, 1965). These findings suggest that the relation between the orientation of the neurons and the electrical field is crucial to observe a stimulation response. This relation becomes even more relevant for human studies, in which tDCS could stimulate both pyramidal tract neurons and interneurons.

More recent *in vitro* animal models confirmed the complexity of tDCS effects, showing that the modulation of neuronal excitability results from the interaction of several factors. Among all of them, the interaction between the different neuronal compartments seems to play a crucial role (Bikson et al., 2004). In their work, Bikson et al. (2004) studied the effects of DC on neuronal excitability in rat hippocampal slices. They observed that the peak amplitude and the time of membrane polarization vary along the axis of neurons, with the maximal polarization at the tips of basal and apical dendrites. Additionally, in the mid-apical dendrites the polarization was biphasic: the authors observed a time-dependent shift in the polarity reversal site. This means that a negative electrode very close to the apical dendrite of a pyramidal cell hyperpolarizes the soma and depolarizes apical dendrites; whereas a positive electrode depolarizes the soma and hyperpolarize apical dendrites. Lastly, electric fields perpendicular to the apical–dendritic axis do not induce any somatic polarization, but they determine an effect at the level of afferents. The results of this study seem to demonstrate that DC fields could modulate neuronal excitability in a time-dependent manner with a not clear threshold. This modulation seems to be the result of interactions between different neuronal compartments, the non-linear properties of the cell membrane, and effects on afferents. Radman and colleagues (2009) found that the cortical neuron morphology related to electric fields and the cortical cell type are crucial factors in determining sensitivity to sub- and supra-threshold brain stimulation. In particular, pyramidal neuronal soma of layer V seems to be the most sensitive to polarization from optimally oriented subthreshold fields. Instead, regards to suprathreshold electric fields, neurons of the layer IV and V had a lower sensitivity. Moreover, DC stimulation is able to induce plasticity effects in neuronal networks thanks to the glia role (Gellner, Reis, & Fritsch, 2016). Glia represents approximately the 50% of all the cells present in the brain. Even if they are not able to generate action potentials, they are electrically active, and they participate in synaptic plasticity because their cellular properties potentials allow for sensitivity to voltage changes.

When the duration of the stimulation exceeds 5 min, tDCS can induce long-lasting after-effects, presumably deriving from changes in synaptic strength. These after-effects are dependent upon continuous protein synthesis during stimulation (Gartside, 1968), likely mediated by mechanisms such as Long-Term Potentiation and Depression (LTP and LTD; Fritsch et al., 2010; Hattori, Moriwaki, & Hori, 1990; Islam, Aftabuddin, Moriwaki, Hattori, & Hori, 1995; Moriwaki, 1991; Ranieri et al., 2012; Rohan, Carhuatanta, Mcinturf, Miklasevich, & Jankord, 2015).

Changes in Ca homeostasis are likely to play a role in the mechanisms of cortical excitation following anodal polarization, and in particular in long-lasting changes in synaptic plasticity (Islam et al., 1995). Repeated anodal polarizations increase Ca^{2+} intracellular amount, affecting calcium and sodium membrane channels and inducing morphological changes in neurons. Fritsch et al. (2010)

have recently investigated the synaptic effects of DC stimulation in an *in vitro* animal study, using slices of mouse primary motor cortex (M1). The authors showed that, without a simultaneous synaptic activation, anodal DC stimulation elicits only a short-lasting synaptic enhancement. This effect becomes instead a long-lasting LTP when a 0.1 Hz stimulation was combined with DC. LTP effects seem also to be polarity-specific: in fact, only anodal polarization induces them, dependently on N-methyl-d-aspartate (NMDA) receptor activation and it requires also an activity-dependent brain-derived neurotrophic factor (BDNF) secretion. Starting from these results, Ranieri and co-workers (2012) applied DC stimulation to rat's brain slices and they observed an LTP polarity-specific modulation: anodal DC increased LTP, while the cathodal one decreased it. Also, this study evidences that LTP is not induced by DC stimulation alone, but only in the compresence of simultaneous synaptic activation (Fritsch et al., 2010; Ranieri et al., 2012).

The present data on animal model demonstrate that DC stimulation is able to modulate LTP. They also provide the rationale for its use in neurological diseases in order to intervene at a level of brain plasticity, promoting the adaptive and suppressing the maladaptive processes.

The results from animal models can also provide information on the current threshold limits and, in addition, they can be used to validate and improve the computational models used in the determination of predictive safety thresholds in humans (Bikson et al., 2016). However, the main limitation of the studies with animal models remains the considerable complexity of translating the findings to human beings, considering the notable differences in the parameters and settings.

As an example, three different research groups tested in animal studies what is the lowest current density able to generate any histological damage. Liebetanz and colleagues (2009) applied a current with intensity of 500 μA through a 2.1 mm diameter circular electrode-contact for 10 minutes, assessed by haematoxylin–eosin (H&E) stain. Fritsch and colleagues (2017), applied a 600 μA current through a 4 mm diameter circular electrode-contact for 20 minutes, assessed by FluoroJade C stain. Finally, Jackson et al., (2017) used a 500 μA current through a 5 × 5 mm square electrode-contact for 60 minutes, assessed by H&E stain (Bikson et al., 2016). Despite these high values of intensity of current used in animals' studies, as already mentioned in the previous chapter, in humans protocols the safety boundaries for current intensities are set within 0.1 – 4.0 mA (Bikson et al., 2016; Nitsche et al., 2008). In fact, it is known that higher intensities usually generate more painful sensations on the skin in the region under and around the electrodes, reducing also the blindness in the sham control condition (Wallace et al., 2016).

2.3 Human studies

In humans, the mechanisms underlying tDCS effects have been mainly investigated by means of pharmacological interventions (for a review: Medeiros et al., 2012), usually targeting sensory-

motor areas since these are cerebral regions where the amplitude of evoked activity is easier to measure. More recently, a growing number of studies have been focused on computational models of the current flow (e.g., Lafon et al., 2016; Miranda et al., 2013), and on recording stimulation-effects on cortical excitability and connectivity by means of other techniques such as functional Magnetic Resonance Imaging (fMRI), Positron Emission Tomography (PET), TMS and Electroencephalography (EEG).

This paragraph aims to illustrate more in detail the wide range of human studies that contributed to increase the knowledge about the mechanisms underlying tDCS effects.

2.3.1 Pharmacological interventions to understand tDCS neurobiological mechanisms

Several pharmacological approaches have been used to understand the mechanisms of tDCS. The dextromethorphan (DMO), a NMDA-receptor antagonist, is able to suppress the effects of both anodal and cathodal tDCS stimulation (Liebetanz et al., 2002). This result suggests the involvement of NMDA in plastic excitability changes induced by both type of polarity stimulation. In the same study, Liebetanz and colleagues (2002) also administered the carbamazepine (CBZ), a Na^+-channel-blocking that selectively eliminated the effect of anodal tDCS. These results suggest that anodal tDCS after-effects require a depolarization of membrane potentials, and also that a combination of glutamatergic and membrane mechanisms is necessary to induce the neuroplasticity tDCS effects (Liebetanz et al., 2002). To understand the changes in motor cortical excitability elicited by tDCS, Nitsche et al., (2003a) used the flunarizine, a Ca^{2+} channel blocker, and they obtained results similar to the ones observed in the previous study with CBZ.

Moreover, the administration of Lorazepam, a GABAergic agonist, seems to induce a selective modulation of the after-effects elicited by anodal tDCS only (Nitsche et al., 2004a). Anodal tDCS indeed elicits a reduction of short-intracortical inhibition (SICI) and an increase in I-wave mediated intracortical facilitation (ICF): both of them are indicators of GABAergic inter-neuronal activity (Nitsche et al., 2005).

These first studies suggest that the plastic changes induced by tDCS affect different neuronal membrane channels, such as Na^+ and Ca^{2+} ions, and they are influenced by GABAergic neurotransmission and by the potentiation of synaptic glutamatergic receptors (Nitsche et al., 2003a).

tDCS plastic changes also involved the regulation of a multiple variety of neurotransmitters, including dopamine, acetylcholine, and serotonin (Kuo, Grosch, Fregni, Paulus, & Nitsche, 2007a; Monte-Silva et al., 2009; Nitsche et al., 2009). In two very similar studies Kuo and co-workers (Kuo et al., 2007a; Kuo, Paulus, & Nitsche, 2007b) investigated the role of dopamine and acetylcholine. In the first study, they administered the dopamine precursor levodopa (L-dopa) together with tDCS and paired associative stimulation (PAS), a motor cortex stimulation protocols able to induce

neuroplasticity changes. The authors observed that the administration of L-dopa inhibits the enhancement in the excitability induced by anodal tDCS, while it prolongs the cathodal reduction effects. These results demonstrate that the dopamine plays a significant role in the neuroplasticity mechanisms in human brains. The authors obtained similar results also with the administration of rivastigmine, a cholinesterase inhibitor. Rivastigmine essentially blocked the enhancement in the global excitability elicited by anodal tDCS and revealed a tendency to firstly reduce and then stabilize cathodal tDCS-induced inhibitory after-effects (Kuo et al., 2007b). These results were confirmed by Monte-Silva et al. (2009) in a study in which different doses of ropinirole were given to the subjects. The ropinirole is a D_2/D_3 dopamine agonist which generated D_2-like receptor activation in an inverted “U”-shaped dose response curve.

At last, the serotonin-dependent modulation of plasticity was investigated using the citalopram, a serotonin reuptake blocker (Nitsche et al., 2009). Citalopram enhanced and prolonged the facilitation effects induced by anodal tDCS, whereas it reversed the inhibitory effect of cathodal tDCS. These data confirmed that serotonin has a prominent impact on neuroplasticity in humans, which is in favour for facilitatory plasticity (Nitsche et al., 2009).

In summary, the results described in these pharmacological studies in humans seem to demonstrate that tDCS modulates cortical excitability during stimulation by non-synaptic cells changes, but the after-effects should be driven by synaptic modification (Stagg & Nitsche, 2011). In particular, after-effects of anodal tDCS are dependent on modulation of both GABAergic and glutamatergic synapses, while the cathodal ones are dependent on the glutamatergic synapses. For both tDCS polarities, the modulatory effects seem to be controlled by dopamine, acetylcholine, and serotonin neurotransmitters (Stagg & Nitsche, 2011). Since different neurophysiological studies in healthy individuals have established the presence of an interaction between tDCS and pharmacological agents, it is essential, especially for clinical studies, to take into account which kind of pharmacological treatment is in use by the patient. In this way, it is possible to monitor the emergence of potential synergic effects as well as the increase of serious risks for the patient (Bikson et al., 2016; McLaren, Nissim, & Woods, 2018).

Despite these promising results, a more thorough understanding of the cellular changes underlying the effects of tDCS is essential in order to actually make tDCS a promising and powerful clinical tool.

2.3.2 Computational models of current flow

As mentioned in the previous paragraph, in vitro and in vivo studies cannot easily and completely reproduce the behaviour of tDCS electric filed in the brain. For this reason, much of our knowledge comes from modelling representations. The first computational models were very

simplistic since they represented the electrodes like a point and the head like a perfect sphere (e.g. Ferdjallah, Bostick, & Barr, 1996).

Following studies tried to improve these aspects using, for example, ring- or disc-shaped electrode configurations model (Datta et al., 2008), or rectangular-shaped pad model (Miranda et al., 2006). Other studies, instead, used Magnetic Resonance (MR) images to generate more realistic and complex head models, able taking into account the geometries and the tissue properties (e.g. Sadleir, Vannorsdall, Schretlen, & Gordon, 2010; Suh, Lee, & Kim, 2012).

In Miranda et al., 2013 work, the authors calculated the tDCS electric field generated in the brain using a realistic finite element model from MR images. In particular, they simulated an accurate representation of all the interfaces between tissues with different electrical conductivities, and they looked at the effect of the differences in the cortical shape on the electric field in the cortex.

The main finding of this work was that the complex cortical geometry combined with the high conductivity of the cerebrospinal fluid - which covers the cortex and fills its sulci - generates a very distinctive electric field distribution in the cortex. Using an electrodes montage suitable for the motor cortex stimulation – namely, the anode positioned over the hand area and the cathode placed above the contralateral eyebrow – the authors registered a higher value for the normal component of the electric field to the bottom of sulci and near the electrode, together with a weaker tangential component that covered large areas of the gyri, flowing in the direction of the other electrode (Miranda et al., 2013).

In an interesting recent study, Lafon and colleagues (2016) combined *in vitro* animal experiments together with computational modelling in order to investigate whether DC stimulation is able to affect the neuronal input/output (I/O) function. This function represents the relation between the synaptic efficacy (Input, I) and the likelihood of eliciting an action potential (Output, O). In other words, whether the biphasic membrane polarization induced by DC stimulation could be related to the independent modulation of input and output processes (Bikson et al., 2004; Lafon et al., 2016). Results showed, for the first time, that DC stimulation can modulate the output obtained for a given and fixed synaptic input. In particular, anodal stimulation seems to generate an opposite polarization of soma and dendrite that increases the likelihood to elicit an action potential and, simultaneously, increases also the synaptic current entering in the cells. On the opposite side, cathodal DC stimulation seems to induce a decrease in the output likelihood caused by soma hyperpolarization, even if this effect is partially cancelled by the depolarization of the dendrites that increases the probability of spikes in this area. Therefore, cathodal DC stimulation, if compared to the anodal one, creates an opposite shift in the threshold of I/O function, but with an overall weaker impact because of these two counterbalancing opposite effects on the two neuron's compartments (Lafon et al., 2016).

Starting from the results of these computational modelling studies the next important step is to verify the validity of these predictions through neurophysiological experiments. If successful, such experiments could validate the models presented and, at the same time, provide a better understanding of the mechanisms underlying the effects of tDCS. For example, a precise knowledge of the relative weight of each component of the electric field in the outcome of the stimulation is crucial to calculate the focality of any montage. This information become relevant also to decide the electrodes position and current intensity for optimal stimulation of a predetermined target (Dmochowski, Datta, Bikson, Su, & Parra, 2011; Miranda et al., 2013).

2.3.3 Recording stimulation-effects on cortical excitability and connectivity by means of other techniques

Robust evidences of tDCS polarity-dependent effects have been shown by stimulating in correspondence of sensory-motor areas, probably because in these regions is easier to measure changes in cortical excitability. In a memorable study of Priori et al. performed in 1998, the authors applied tDCS on M1 and measured the changes in the amplitude of motor evoked potentials (MEPs) by TMS. In the study, TMS pulses were delivered after the onset of tDCS that could be anodal (+), cathodal (-) or sham (0). In each trial the three conditions were alternated with the sequence 0, +, -, 0. The results showed a significant reduction of MEPs amplitude after anodal tDCS, while cathodal stimulation did not induce any changes in the activity of M1. In their work, Nitsche and Paulus (2000, 2001) demonstrated the possibility of a non-invasive modulation of motor cortex excitability in a polarity-dependent way, by the application of weak direct current through the scalp. In particular, anodal tDCS increased selectively the cortical excitability, while the cathodal stimulation inhibited it. These effects could be controlled in terms of magnitude and duration by varying the current intensity and the duration of the stimulation. Moreover, the authors hypothesised that the changes in cortical excitability were probably induced by a modification in the membrane polarization. In particular, short-term potentiation and processes similar to post excitatory central inhibition were the likely candidates for the excitability changes after the end of stimulation. These pioneering studies started to show the importance of this technique as a tool to induce neuroplasticity modulation in a non-invasive, painless and reversible way (Nitsche & Paulus, 2001).

Similar polarity-dependent results were obtained by targeting the primary visual cortex (V1) and by measuring phosphene thresholds (PTs) evoked by short trains of TMS (Antal, Kincses, Nitsche, & Paulus, 2003), or static and dynamic contrast sensitivities (sCS and dCS, respectively; Antal, Nitsche, & Paulus, 2001). An increase in PTs and a loss of sCS and dCS were found during and immediately after cathodal stimulation. A similar but opposite effect was observed during and after anodal tDCS, with a reduction in the PTs and no evidence of any effects on sCS and dCS. These

results reveal that elementary visual functions, such as contrast detection and phosphene perception, can be transiently altered by tDCS by modulating neural excitability, has already shown in the motor cortex. However, since CS and PT are strongly subjective parameters, following studies focused on recording visual evoked potentials (VEPs) that are a direct electrophysiological measure such as MEPs, by combining tDCS with EEG (Accornero et al., 2007; Antal et al., 2004). In agreement with the previous studies on M1, these studies demonstrated that tDCS was able to modify the amplitude of cortical VEPs in a polarity-dependent way. Cathodal stimulation reduced the amplitude of N70, while anodal tDCS increased it, even if with lower efficiency. Furthermore, a weak tendency of increased P100 amplitude was observed only after cathodal tDCS (Antal et al., 2004) This last result was confirmed by Accornero et al. (2007). In the study a reduction of VEP-P100 amplitude during and after anodal polarization is reported, together with a significant increase during and after cathodal stimulation. It has also been observed that both polarities left latency statistically unchanged. Also for V1 the effects of tDCS seems to be modulated by the intensity and the duration of the stimulation session.

In a more recent and very interesting study, Kirimoto and colleagues (2011) recorded MEPs and somatosensory evoked potentials (SEPs) before, immediately after, and 15 minutes after the application of tDCS on supplementary motor area (SMA). They interestingly observed that anodal tDCS on SMA induced an increase in the amplitude of N20 and P25 SEPs components that led to a reduction of MEPs in M1. Instead, cathodal stimulation induced opposite effects. The results of this study seem to reflect an inhibitory connection between M1 and SMA. They also reveal that tDCS, beyond modulating the excitability of the stimulated area, can also alter cortical connectivity from the targeted area, and thus affecting broader brain networks.

When combining tDCS on M1 and fMRI, anodal stimulation induced a large increase in regional cerebral blood flow (rCBF). This effect was observed during stimulation and the rCBF returned to baseline level as soon as the current was turned off, but it increased again in the post-stimulation period. Cathodal polarity, in contrast, induced a smaller increase during the stimulation, a significant decrease right after, and a continuous decreasing in post-stimulation period (Zheng, Alsop, & Schlaug, 2011). The differences in rCBF after-effects observed for the two tDCS polarities support the evidences of behavioural and cognitive after-effects. They also show again that tDCS not only modulates activity in the brain region directly underlying the stimulating electrode but also in a network of brain regions that are functionally related to the stimulated area (Zheng et al., 2011).

By targeting brain regions different from the primary sensory-motor cortices, Stagg et al. (2013) showed that anodal tDCS on left dorsolateral prefrontal cortex (DLPFC) increased perfusion in a wide set of brain areas, including the left primary sensory cortex (S1), the midcingulate cortex,

the paracingulate cortex and the left parietal cortex. An increase in the connectivity between the stimulated area and the contralateral homologous one (i.e., right DLPFC) and the left sensorimotor cortex was also found, together with a decrease in the connectivity with the bilateral thalamus. Cathodal tDCS, instead, decreased perfusion in the bilateral thalami and right middle and inferior temporal gyri and led to a decrease in the connectivity between the left DLPFC and an extensive region in the left temporal, parietal, and occipital lobes. In contrast, an increased functional connectivity was observed after cathodal but not anodal tDCS over M1 within the motor and non-motor network, such as the default mode brain network (Amadi, Ilie, Miranda, & Stagg, 2014).

Clemens and colleagues (2014) combined tDCS and fMRI measurements to investigate possible changes in resting-state networks and to more deeply understand how tDCS could modulate intrinsic brain activity. In their work, the authors stimulated the parietal cortex applying anodal tDCS on the right angular gyrus (AG). They measured the changes in blood oxygen level-dependent (BOLD) signal within any of the canonical resting-state networks. They found that after tDCS stimulation, the BOLD signal at rest decreased in the bilateral primary and secondary visual areas, and in the right putamen. An increased BOLD signal at rest, instead, was found in widely distributed brain regions covering thalamic, frontal, parietal, and occipital clusters of activity. From these exploratory results, it was possible to conclude that a single session of anodal tDCS over the right AG could be enough to induce large-scale changes in resting-state activity. These changes were localized in sensory and cognitive areas, covering regions both close to and distant from the stimulation site (Clemens et al., 2014). Data in support of the tDCS neuromodulatory effects in non-motor areas are also reported in other studies in which tDCS was used to modulate the functional activity of the bilateral parietal brain regions. Those areas are known for underling allocentric and egocentric navigation processes (Hampstead, Brown, & Hartley, 2014). During task performance, results supported the neuromodulatory effects of tDCS by revealing polarity-dependent changes in both the magnitude of BOLD signal and in the effective connectivity's patterns. Same results were found with resting-state functional connectivity suggesting that the stimulation primes not only the areas underling the target electrode, but also a more extended network that can be recruited during task execution (Krishnamurthy, Gopinath, Brown, & Hampstead, 2015)

It turns out to be particularly evident that tDCS can be used for probing functional brain connectivity, but also as a newel and promising therapeutic intervention in psychiatric and neurological disorders (Wörsching et al., 2016). It highlights the need for understanding the interplay between neural systems and stimulation protocols, requiring essential methodological work. In a fascinating and recent study, the authors combined tDCS and fMRI aimed to examine the test-re-test characteristics of the tDCS modulation effects at resting state (Wörsching et al., 2017). Twenty

healthy participants received 20 minutes of both 2 mA active and sham tDCS on DLPFC. In order to target the area bilaterally, a bipolar montage was used: the anode was placed in correspondence of F3, while the cathode on F4 (according to the international 10–20 system). Results revealed low reliability of resting-state functional-connectivity after active tDCS. The intra-individual variations observed in this study resembled the variability of tDCS effects in motor regions. It may be one of the reasons why, in some researches, robust tDCS effects at a group level were missing (Wörsching et al., 2017).

In another interesting study fMRI data and GABA levels, assessed by Magnetic Resonance Spectroscopy, were measured before and after 20 min of 1 mA anodal and sham tDCS (Bachtiar, Near, Johansen-Berg, & Stagg, 2015). Even if the results were in line with previous studies, showing a reduction in GABA concentration and an increase of functional connectivity induced by anodal tDCS, these changes are not correlated. Particularly the researchers showed that the magnitude of the changes in both GABA level and functional connectivity does not correlate across subjects, suggesting that they could be guided by different mechanisms (Bachtiar et al., 2015).

Taken together, all these findings suggest that, to effectively modulate relevant neural circuits, additional and systematic researches on tDCS mechanisms of action are still needed. In this sense, the use of neuroimaging and neurophysiological measures are a crucial starting point to better define target regions and to adjust the method to physiological requirements (Esmaeilpour et al., 2019; Wörsching et al., 2016)

2.4 Using TEPs to explore brain response to tDCS

Recently, the effects on cortical excitability and connectivity of tDCS were directly evaluated by the use of an integrated system that combine TMS and co-registration of EEG (TMS-EEG). Through the activation of a cortical area via TMS stimulation, it is possible to measure in real time the brain response over the cortex by means of HD-EEG recordings. Transcranial magnetic stimulation evoked potentials (TEPs), recorded with this technique, reflect the cortical excitability and connectivity of the targeted area, and represent a direct measure of the neural state.

Pellicciari and colleagues (2013) performed a very well-designed experiment in which they recorded both MEPs and TEPs, one time before and two times after anodal and cathodal tDCS on the left M1. The first after stimulation recording session was performed immediately after the 13 minutes long tDCS stimulation with an intensity of 1 mA, while the second one was performed 30 minutes later. All TEPs and MEPs recording sessions were followed by a behavioural block in which participants performed a very simple detection task used to evaluate the potential tDCS effects on the performance.

To investigate whether tDCS induces any short-term and/or long-term polarity-dependent change in the cortical responses, the authors computed the Local Mean Field Power (LMFP) of the TEPs in clusters of electrodes that covered the left and right motor regions. Results demonstrated that tDCS on motor cortex induces polarity specific changes in cortical reactivity. In particular, anodal tDCS determined an increase in TEPs amplitude in both hemispheres, while cathodal tDCS led to a decrease of LMFP values in the left cluster and an increase in the right hemisphere. These were long-lasting effects; indeed, the TEPs recorded 30 minutes after the end of tDCS stimulation revealed that these amplitude changes persisted over time.

MEPs measurements showed polarity specific effects as well, quite overlapping the TEPs results. In particular, for anodal stimulation, the amplitude of the MEPs immediately after tDCS stimulation increased, and this modulation persisted over time. However, for cathodal tDCS, the reduction in MEPs amplitude was recorded only in the first TMS-EEG session, the one immediately after the end of tDCS stimulation. The results of this study therefore demonstrate that TEPs response provides a viable direct measurement to investigate the polarity-specific changes induced by means of tDCS, that can be used in addition to the better-known MEPs, recorded peripherally (Pellicciari, Brignani, & Miniussi, 2013).

In the following year, Romero Lauro and colleagues (2014) investigated the effects of anodal tDCS applied on the right PPC, by the use of TMS-EEG. They recorded TEPs from the contralateral homologue area, namely the left PPC, before, during and 15 minutes after 10 minutes of tDCS stimulation while participants were at rest. The authors targeted the posterior regions in order to maximise the advantage in using TMS-EEG, which allows for exploring cortical reactivity of areas otherwise not functionally measurable, since they cannot produce a direct TMS output such as MEPs for M1. From a theoretical point of view, indeed, the tDCS has been already successfully applied on PPC for modulating both sensory and cognitive functions (e.g. Berryhill, Wencil, Branch Coslett, & Olson, 2010; Bolognini, Olgiati, Rossetti, & Maravita, 2010a; Bolognini, Spandri, Olgiati, Fregni, Ferraro, & Maravita 2013; Convento, Vallar, Galantini, & Bolognini, 2013). In the Romero Lauro et al. (2014, 2015) studies, different expedients were used in order to deal with the electrical artefacts produced by tDCS, especially when tDCS and TMS-EEG were performed concurrently. In particular, they avoided the contact between tDCS and EEG electrodes by removing the EEG electrode under the tDCS patch and by positioning both the EEG ground and the reference far away from the tDCS electrodes.

The results showed that, at a global level, anodal tDCS induces an increase in cortical excitability both during and after the stimulation, in an early time windows (from 0 to 100 milliseconds after TMS pulse). The local analysis was performed on four clusters of electrodes: two

parietals, corresponding to the TMS and the tDCS hotspots; and two frontals. The enhancement of the local excitability was observed after tDCS stimulation, in an earlier time window (between 0 to 50 milliseconds), and in a more widespread brain area, including left and right parietal and frontal regions, thus indicating a diffuse modulation of the cortical network activity. These results were also confirmed by the source modelling analysis that revealed a significant and widespread increment of cortical excitability, in both during and after tDCS recording sessions, that was not due to volume conduction. Therefore, in this study, data both at the sensor and source levels converge in suggesting a diffuse rise of cortical excitability due to anodal tDCS, mediated by fronto-parietal connections (Romero Lauro et al., 2014, 2015).

Finally, few studies recently started to investigate the tDCS mechanisms of action during task performance in healthy and clinical population, targeting brain regions different from the primary sensory-motor cortex. In Cipollari et al. (2015) work, TMS-EEG recordings were combined with anodal tDCS and language treatment in post-stroke aphasic patients. Despite quite a number of studies have used the tDCS to treat aphasia, to which level the stimulation of a cerebral region may affect the activity of anatomically connected regions remains still unclear. For this reason, the authors applied both anodal and sham tDCS over the right inferior frontal gyrus (IFG), while the patients underwent three weeks of language treatment. TEPs were recorded both before and at the conclusion of the sessions, from clusters of electrodes close to the tDCS hotspot, in order to measure any possible change induced by it. Behavioural results demonstrated a greater improvement in accuracy and speech articulation in the participants that performed language training coupled with anodal tDCS stimulation. This observation was accompanied by neurophysiological data that showed, after anodal tDCS, a more pronounced increase of cortical excitability in ROI electrodes located over the stimulated region.

Other studies investigated the causal relationship between the enhancements in cognitive performance and the supposed plastic changes in the related cortical sites induced by anodal tDCS, in healthy population (Pisoni et al., 2017). Also in that case, the TMS-EEG recording sessions were performed before and immediately after anodal tDCS stimulation on left IFG, while participants were involved in a verbal fluency task. In order to keep under control the effects that may be induced by the tDCS protocol and TMS target location, the authors assessed three different conditions: (1) anodal tDCS with TMS over left premotor cortex; (2) same stimulation locations but with sham tDCS; (3) anodal tDCS with TMS over left posterior parietal cortex. Data suggested a positive correlation between the degree of cognitive improvement and the increase of cortical activity. In particular, the cortical excitability modulation, measured both at sensors and sources level, occurred only in the left areas related to the language production cerebral network (left Brodmann’s areas 6, 44, and 45).

Pisoni and colleagues (2017) demonstrated that, in healthy humans, the cognitive enhancement caused by anodal tDCS is affected by ongoing brain activities, increasing cortical excitability of task-related functional brain networks only.

Hill, Rogasch, Fitzgerald, and Hoy (2019) applied HD-tDCS over the left dorsolateral prefrontal cortex (DLPFC) of a sample of twenty healthy participants. Also in this study, the authors assessed three different experimental conditions pseudorandomised: (1) anodal HD-tDCS stimulation was delivered at rest; (2) anodal HD-tDCS was coupled with the execution of a cognitive task that engaging WM; (3) sham HD-tDCS was administered during task performance. TEPs were recorded applying the TMS coil directly over the anode, in correspondence with the F3 EEG electrode. The neurophysiological changes were also probed using ERPs, recorded both during n-back WM tasks and at rest. All the recording sessions were performed before and after HD-tDCS stimulation. The data highlight a complex pattern of findings. From a physiological point of view, HD-tDCS induced a modulation of TEPs amplitude regardless the task engagement. Changes in ERPs amplitude recorded during the n-back task were observed instead only when the stimulation was delivered during a task performance. However, no differences were observed, regardless of stimulation condition, on neither the EEG data at rest, nor WM performance. In contrast with the results of the previous studies, these findings paint a more complex picture of neural and behavioural responses to prefrontal stimulation in healthy subjects and provide only limited support for state-dependent effects of HD-tDCS over the DLPFC overall (Hill et al., 2019).

Experimental paradigms incorporating TMS-EEG would allow for further exploration of these brain-behaviour relationships through the evaluation of changes in TEPs amplitude (Ferrarelli et al., 2008; Rosanova, Casali, Bellina, Resta, Mariotti, & Massimini, 2009). Furthermore, the possibility to record TEPs over the entire scalp allows for the investigation of connectivity changes across multiple structurally and functionally connected brain regions, providing important information about the effects of tDCS on distributed cortical networks (Miniussi, Brignani, & Pellicciari, 2012; Romero Lauro et al., 2014). Finally, the present knowledges about the current flow induced in the brain by tDCS are largely based on evidences deriving from computational models. However, the brain reactivity profiles produced by TMS-EEG experiments could provide important additional physiological evidences of the neuromodulation effects induced by different tDCS configurations.

Furthermore, future TMS-EEG studies which investigate the effects of tDCS on a combination of excitatory and inhibitory processes and their correlation with cognitive performance could help to throw light on neurobiological response of specific cortical regions to mild electrical stimulation.

The studies described so far seem to demonstrate that tDCS, when applied on primary sensory-motor cortices, induces polarity-dependent opposite effects: anodal excitatory and cathodal

inhibitory. This evidence becomes more controversial when higher cognitive functions and the underlying brain areas are targeted (Jacobson et al., 2012). However, as mentioned above, few recent studies started to question this rigid dichotomy by showing different results also for motor and visual cortices. For example, Batsikadze et al. (2013) showed how different tDCS intensities on M1 can generate non-linear effects regardless the polarity of the stimulation. Furthermore, in the visual domain, anodal tDCS seems to increase cortical excitability and to improve visual discrimination learning, while with cathodal stimulation no significant effects on excitability nor on learning are reported (Sczesny-Kaiser et al., 2016). Typically, anodal tDCS has been observed to enhance the targeted cognitive function, whereas cathodal stimulation is reported as less effective or it is not explored at all. For instance, recent evidence-based guidelines for clinical use of tDCS (Lefaucheur et al., 2017) do not include cathodal stimulation for the treatment of any disease.

However, some clinical studies reported significant results also with cathodal tDCS in rehabilitative protocols of both neuropsychological and psychiatric diseases. In the domain of language, in particular in relation to the aphasia, the use of cathodal tDCS improves auditory verbal comprehension in subacute stroke patients when applied on the right Wernicke’s area and combined with the conventional speech and language therapy (You, Kim, Chun, Jun, & Park, 2011). Same positive results and benefits for aphasic patients was found by applying cathodal tDCS over the healthy right Broca's homologue area (Kang, Kim, Sohn, Cohen, & Paik, 2011). The results showed that cathodal tDCS induced a significant improve in picture naming after 1 hour from the end of the last treatment session, the fifth (Kang et al., 2011). These results are consistent with the role of Wernicke's and Broca’s area in language, and with the therapeutic effect that cathodal tDCS has on aphasia patients. This suggests that tDCS may be an adjuvant treatment approach for aphasia rehabilitation therapy in patients in an early stage of stroke (You et al., 2011).

Also, in the general domain of pain, cathodal tDCS seems to be sometime effective in the treatment of fibromyalgia (Villamar et al., 2013b) and migraine (Antal, Kriener, Lang, Boros, & Paulus, 2011). Villamar and colleagues (2013b) used a 4 × 1-ring configuration of HD-tDCS with the centre electrode on the left M1. The authors observed that both anodal and cathodal HD-tDCS stimulation conditions led to significant reduction in overall perceived pain as compared to sham. This effect occurred immediately after cathodal HD-tDCS, and it was also evident for both anodal and cathodal HD-tDCS 30 minutes after the stimulation (Villamar et al., 2013b). Concerning the migraine, even if cathodal tDCS on V1 did not reduce the frequency of the attacks, it was able to significantly reduce the intensity of pain if compared to the sham stimulation (Antal et al., 2011).

For what concern the psychiatric diseases, the use of cathodal tDCS has been investigated in particular for the treatment of Major Depression Disorder (MDD). Brunoni and colleagues (2014a)

performed a randomized, double-blind and controlled study on MDD patients. They used an intra-cephalic montage with the anode on the left DLPFC (F3) and the cathode over the right DLFPC (F4). The main advantage in using this specific montage derives from the simultaneous increase of the left DLFPC activity and the decrease the right one, which are respectively hypo- and hyperactive in depression (Brunoni et al., 2014a). Results showed that cognitive control therapy combined with tDCS treatment might be more beneficial for older depressed patients, particularly for those who have cognitive resources to adequately learn and improve task performance over time (Brunoni et al., 2014a). Last but not least, a preliminary and open pilot study showed that the use of bifocal tDCS can be an interventional treatment also for refractory symptoms in schizophrenia (Brunelin et al., 2012).

All these studies converge in demonstrate that the behavioural outcomes of cathodal tDCS, both in research and in clinical settings, are less predictable in comparison to those induced by anodal tDCS. Following this, a systematic and comprehensive study of cathodal tDCS mechanisms of action and its cortical effects acquires a critical relevance.

2.5 Summary

In this Chapter an overview, as comprehensive as possible, of the state-of-art about theoretical knowledge concerning tDCS mechanisms of action has been presented. This project aims to provide new and further evidences to improve the knowledge on the neurophysiological basis of tDCS by applying the TMS-EEG approach to explore the effects induced by cathodal tDCS. In the following chapters, after an introduction to TMS-EEG to provide a rationale for its use as a method for exploring the physiological effects of tES techniques, we will present the experimental corpus of this dissertation. In these Chapters, the two primary studies carried out in order to understand the cathodal tDCS mechanisms of action, both at rest and during task execution, will be described.

Chapter Three: "TMS-EEG integrated system: methodology and applications"

3.1 Chapter overview

The aim of this chapter is to present the TMS-EEG integrated system from both a theoretical and a practical point of view, and to provide a rationale for its use as a method to explore the physiological effects of tDCS. In the last years the TMS-EEG has been increasingly used as a non-invasive technique for different purposes: to probe the brain's excitability, time-resolved connectivity, and instantaneous state. This spread in the usage of TMS-EEG is largely due to its excellent temporal resolution and to its ability in probing changes in cortical plasticity outside the motor cortex. However, only in the last decade few studies have started to employ TMS-EEG to study the tES's mechanisms of action and their effects on the brain. This chapter will firstly introduce the technical characteristics and methodological peculiarities of the TMS-EEG system. Subsequently, it will present the advantages of using this technique for studying tDCS mechanisms of action, and it will describe the results obtained from the first studies.

3.2 Introduction to TMS-EEG integrated system

The operating principle of TMS is electromagnetic induction, as discovered by Michael Faraday in 1838. A pulse of current, with enough strength and short enough duration, passes through a coil placed over a person's head and generates a rapidly changing magnetic field that penetrates scalp and skull reaching the brain with negligible attenuation. These pulses, in turn, induce a secondary ionic current in the brain that can elicit post-synaptic potentials in the neural tissue under the stimulating coil, leading to alterations in the cortical activity (Pascual-Leone, Walsh, & Rothwell, 2000; Walsh & Cowey, 2000; Walsh & Pascual-Leone, 2003). In the studies described in the previous chapters, TMS was used to target the primary motor (Barker, Jalinous, & Freeston, 1985) or visual (Meyer, Diehl, Steinmetz, Britton, & Benecke, 1991) cortex. In these regions, the induced polarization generates respectively a transient activation of extremity muscles, directly measurable with surface electromyographical electrodes (Pascual-Leone et al., 1998), or the phosphenes, that are brief flashes of light (Antal et al., 2003; Kammer & Baumann, 2010). The greater limit of TMS is that outside the visuomotor cortices the effects of stimulation are not directly measurable (Fitzgerald, 2010; Ilmoniemi & Kičić, 2010) and can be inferred only indirectly by observing the effects on the performance of a wide range of behavioural tasks. Today, the combination of TMS and EEG allows going beyond this limit. Indeed, using the integrated TMS-EEG system is possible to directly measure cortical reactivity, through the recording of the electrical activity all over the scalp. Furthermore, this

technique can provide relevant information regarding the spread of current throughout the brain (Bortoletto, Veniero, Thut, & Miniussi, 2015; Ilmoniemi et al., 1997; Siebner et al., 2009).

The first successful use of the combination of TMS and EEG was reported by Cracco et al. (1989), who recorded TMS-evoked cortical responses in the hemisphere contralateral to the stimulation. As one could expect, the large electromagnetic discharges of TMS were able to saturate the EEG amplifier, preventing the extraction of any useable brain responses from the EEG recordings (Ilmoniemi & Kičić, 2010; Veniero, Bortoletto, & Miniussi, 2009).

A first attempt to reduce the magnetic artefacts was done by suitably adjusting the geometrical arrangement between the coil and the EEG electrodes, and also by putting a metal strip between the electrodes, as a scalp-grounded (Amassian, Cracco, Maccabee, & Cracco, 1992). However, only the use of electronics to decouple the electrode signals from the amplifier stages during the pulse makes possible to map the electric scalp distribution due to the stimulation of the motor and visual cortices (Ilmoniemi et al., 1997).

In addition to standard evoked responses, TMS may also trigger oscillatory activity (Paus, Sipila, & Strafella, 2001; Fuggetta, Fiaschi, & Manganotti, 2005; Rosanova et al., 2009) or perturb ongoing rhythms (Rosanova et al., 2009). Also in these cases, the measured signals can provide relevant information about the functional state of the brain. For these reasons, TMS-EEG system has also been used to examine neurophysiological processes across cortical regions (Paus et al., 2001) and to study different clinical conditions such as schizophrenia (Ferrarelli et al., 2008), major depression (Casarotto et al., 2013), and consciousness disorders (Ragazzoni et al., 2013; Rosanova et

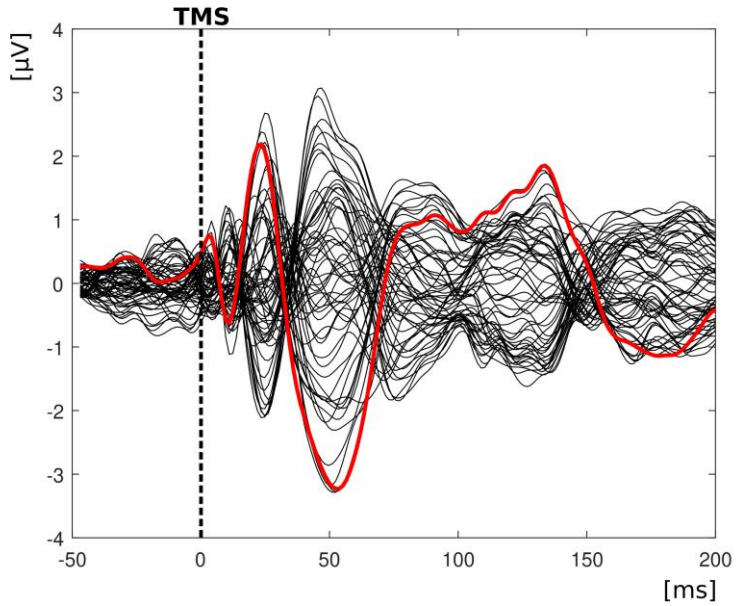

Figure 3.1*: Example of a TEP recorded during one of the experiments that are part of this work. The black part of the butterfly plots represents the mean signal from all the sixty channels. The red line represents the mean signal of the electrodes under the TMS.*

al., 2012). The recording and analysis of TMS-evoked responses mostly follow the same logic and principles as for any other evoked response data, but with some unique features that will be described in the following paragraphs.

3.3 TMS-evoked potentials (TEPs)

The TEP is a complex waveform which consists of several peaks and valleys with various latencies and follows the TMS pulse, as it can be clearly seen from the example in Figure 3.1. Each of these components represent the combination of excitatory and inhibitory post-synaptic potentials from large populations of neurons (Rogasch & Fitzgerald, 2013). In contrast to the high variability of MEPs, TEPs’ responses are generally highly reproducible. This is valid only under the condition that the TMS delivery and targeting are well controlled and stable from pulse to pulse and between experiments (Ilmoniemi & Kičić, 2010). The sensitivity and the repeatability of this measure is a crucial point to evaluate the potential of TMS-EEG not only as a research tool but also as a diagnostic and monitoring instrument (Casarotto et al., 2010). In their work performed explicitly to evaluate the sensitivity and repeatability of TMS-EEG potentials, Casarotto et al. (2010) modified, in a controlled way, the stimulation parameters while performing repeated longitudinal measurements. They completed pairwise comparisons to assess the sensibility of TMS-EEG’s response to changes in the stimulation parameters and the replicability. To evaluate TEPs sensibility, different measurements were recorded varying target site, stimulation intensity and angle, on the same participant. Furthermore, to verify the replicability, different stimulation sessions were performed over one week, maintaining constant all stimulation parameters. Results show that the EEG responses to TMS perturbations are essentially sensitive to changes and repeatable over time.

This finding permits to consider TEPs a promising measure to detect longitudinal changes in the state of cortical circuit.

TEPs also appear to be sensitive to changes in the brain state. For example, changes in TEP’s waveform morphology have been noted during non-Rapid Eye Movement (REM) sleep compared both to awake subjects and during REM sleep (Massimini et al., 2005, 2010); as well as in patients in vegetative state compared to ones in minimal conscious state (Casarotto et al., 2016; Ragazzoni et al., 2013; Rosanova et al., 2012). Furthermore, changes in TEPs amplitude have also been reported following NIBS protocols such as repetitive TMS (rTMS - Casula et al., 2014), theta-burst stimulation (TBS - Vernet et al., 2013), or even during and after tDCS stimulation (Hill et al., 2019; Pisoni et al., 2017; Romero Lauro et al., 2014, 2015),

All these studies seem to confirm that TEPs can provide a quantifiable marker of the neurophysiological brain state also in non-motor regions, in a similar way to how MEPs provide

information regarding corticospinal excitability (CSE). TEPs also can provide important information about the functional dynamics of distributed cortical networks (Miniussi & Thut, 2010).

3.4 Peculiarity and challenges in combining TMS and EEG

3.4.1 Amplifiers

The first obstacle that bumps in when combining TMS with EEG is the sizeable electromagnetic artefact induced by TMS that can saturate the recording amplifiers for a not negligible time. As pointed out above, there are different methods generally used to reduce or eliminate this artefact. One of the possibilities is to use an amplifier that includes an attenuator and a semiconductor switch (Iramina, Maeno, Nonaka, & Ueno, 2003). This system provides an attenuation of the signal for the entire duration of the TMS pulse: the EEG amplifiers are switched off 10 milliseconds before the TMS pulse and then switched on again after 1 millisecond. In this way, the TMS artefact is not completely eliminated but it is attenuated, and it remains for about 10 milliseconds post-stimulus (Iramina et al., 2003). Ives and co-workers (2006) and Thut et al. (2005) have developed an EEG recording system that includes an amplifier with a limited slew-rate so that the TMS pulses did not saturate the electronics. Similar to what happens for the previous method, also in this case the system does not completely eliminate the electromagnetic artefact. However, since the EEG signal can be recorded without interruption, the artefact can be removed by computing a subtraction in order to isolate the electrophysiological signals from possible residual TMS-induced contaminations. As a main limitation, this system requires baselines or control measurements in order to perform the subtraction. This additional procedure usually increases the level of noise (Ilmoniemi & Kičić, 2010).

The most effective, and less noisy alternative to deal with the electromagnetic artefact is to use a sample-and-hold TMS-compatible system, which is able to prevent the passage of large artefacts through the amplifier circuits. It was developed in 1999 by Virtanen and co-workers, and then commercialized by Nexstim, Helsinki, Finland. It works using an external trigger that blocks the passage of signal inside the amplifier immediately before the TMS pulse. This amplifier permits to record artefact-free continuous EEG in the presence of TMS pulses and scalp distributions of evoked potentials, starting at 2.5 millisecond after each TMS pulse (Virtanen, Ruohonen, Naatanen, & Ilmoniemi, 1999). A continuous recording mode without the use of sample-and-hold circuits is also possible. In fact, using a BrainAmp amplifier (BrainProducts GmbH, Munich, Germany; Veniero et al., 2009), it is possible to adjust the sensitivity and the operational range of the instrument in order to match the applied TMS strength. The results have shown that, regardless of the different experimental conditions, the electromagnetic artefact lasts approximately 5 milliseconds after TMS onset (Veniero et al., 2009).

3.4.2 Electrodes Type

In the TMS-EEG system, the EEG electrodes need to satisfy different physical requirements in order to operate in the extreme electromagnetic environment induced by TMS. In particular, the electrodes need to be, at the same time, small enough not to overheat and not to be affected by the induced current, and covered with a suitable surface material for the best interface with the skin. For these reasons, the best electrodes for TEPs recording seem to be conductive plastic electrodes with a silver pin, such as an Ag/AgCl surface, for ensuring high-quality recordings (e.g. Ives, Rotenberg, Poma, Thut, & Pascual-Leone, 2006; Thut, Ives, Kampmann, Pastor, & Pascual-Leone, 2005; Veniero et al., 2009).

Before recording TMS-EEG, it is usually recommended to reduce the electrode impedance under 5 kΩ. This precaution guarantees to have small artefacts induced by possible electrodes movements or polarization (Ilmoniemi & Kičić, 2010). To achieve a low electrode impedance, it is needed to clean the skin under it. During the preparation of the EEG cap, it can be useful to scrub the skin surface before applying electrode paste in order to further reduce the resistance. As the electrodes' resistance may change during the experiment, it is recommended to keep controlled the electrode impedance, at least during long recording sessions.

3.4.3 Other artefacts in TMS-EEG experimental design

In the TMS-EEG system, the induced electromagnetic interference in EEG registration is only the main artefact generated by the combination of these two techniques. However, other issues should be considered if we are interested in performing a successful TMS-EEG recording session.

3.4.4 Electrode movement and polarization

When an electrode is moved or mechanically pressed, it generates a short potential change that lasts until the equilibrium is re-established. This movement artefact is a substantial interference in the EEG recording. In most of the cases, such artefacts are caused by the contact between the TMS coil and the electrodes, and this could generate a vibration in the electrodes due to the TMS pulse or to any pressure by the experimenter. Especially when the coil is held manually by the experimenter, it is not possible to completely remove physical movement. For this reason, the noise signal is removed during data pre-processing, after the recording.

The electrode polarisation is caused by electric currents between the electrolyte and the electrode. Usually, the polarised state of the real electrodes is somewhere along a continuum between the two extremes: perfectly polarised and perfectly non-polarised (Ilmoniemi & Kičić, 2010). In TMS-EEG studies, however, it is challenging to analyse the EEG response for several tens of milliseconds immediately after the TMS pulse. In fact, a polarised electrode needs hundreds of

milliseconds to return to the equilibrium potential after a TMS pulse (Litvak et al., 2007). Thanks to the technological development, a particular recording system has been developed which, combined with a special software for the removal of polarisation artefacts, allows to remove most of them and to analyse the cortical response starting already 10 milliseconds after the TMS pulse (Litvak et al., 2007).

3.4.5 Eye movements

Eye movements also cause a transient potential at the vertex, which can induce a considerable interference to the EEG signal. Usually, a TMS-EEG recording session is longer than a traditional EEG registration; therefore, the participant will surely need to move her or his eyes. In this situation, it could help to train the subjects to synchronise the eye movements with the preparatory interval between two TMS pulses. However, the TMS per se can trigger eye movements or blinks due to the stimulation of the eye-controlling brain areas or eye muscles. A way to reduce these kinds of eye contractions is to adjust the coil position, sometimes it can be sufficient a shift of few millimetres in the target point or a small change in the coil inclination. Instead, the eye movements due to a startle response to TMS sound or to tactile sensation are generally more difficult to control. In any case, a solution to these problems is to monitor blinks and eye movements with specific electrodes, usually placed on the face of the subjects, near the eyes. In this way, it is possible to record the electrooculogram (EOG) and remove the EEG trials with big eye movement’s artefacts during the pre-processing analysis.

3.4.6 Muscle activity

As for the eye contractions, TMS can induce the activation of different muscles, usually those of the neck, jaw and face, depending on the position of the coil. If these muscles are close to the EEG electrodes, this can induce strong artefacts in the recording EEG signal. The muscle artefacts can be reduced by moving or re-orienting the coil, by reducing TMS intensity or by a combination of these two.

3.4.7 Sound induced by coil “click”

Every TMS pulse is accompanied by a click with an intensity up to 100–120 dB (Counter & Borg, 1992; Starck, Rimpiläinen, Pyykkö, & Esko, 1996) due to the abrupt electromagnetic forces in the coil (Tiitinen et al., 1999). This auditory effect generates an auditory evoked potential (AEP) recording by EEG. It is important to note that the sound can be spread both by air and by bone conduction, reaching the cochlea directly (Nikouline, Ruohonen, & Ilmoniemi, 1999). For this reason, simple hearing protections can help to reduce, but not to eliminate the AEPs. To do that it is necessary

to use a noise masking at the same frequency spectrum as the TMS sound, that is able to conceal the click perception (Massimini et al., 2005).

3.4.8 Somatic scalp sensations

TMS can also elicit SEP (Somatosensory Evoked Potential) arising from muscle contraction and sensory-neurons direct stimulation. The action potential propagation in peripheral sensorimotor axons results in twitches of cranial muscles, which cause, on one hand muscle potentials and electrode movement artefacts in the TEP recordings (Mutanen, Mäki, & Ilmoniemi, 2013), and, on the other hand, a twitch-induced sensory input to the brain (Conde et al., 2019).

In the brain, this evoked response is characterised by a larger amplitude in the contralateral hemisphere compared to the stimulation side. In contrast, the TEPs prominent response amplitudes usually are in the regions around the stimulated point. Even more, the SEPs most significant peak is at a latency of 80 milliseconds, while the largest TEPs amplitude is observed in the 100 to 200 millisecond interval.

To examine the contribution of multisensory co-stimulation on TEPs, in the Conde et al. (2019) experimental design, a realistic sham condition was included. The results show a substantial similarity between the EEG responses evoked by real TMS stimulation and the ones evoked by realistic sham session, both for early and late TEP components. These findings stress the need to control the remaining non-transcranial evoked potentials using a realistic multisensory sham stimulation, that have to be designed to mirror as closely as possible the features of the real TMS multisensory stimulation. It is clear that disentangling the contribution of somatosensory sensations from the TMS response in the EEG trace is very difficult. Nevertheless, researchers have concluded that this is not a significant problem for a TMS-EEG study if these effects are correctly suppressed or controlled by experimental design (Ilmoniemi & Kičić, 2010).

3.5 Methodological arrangements to perform a successful TMS-EEG study

As it emerges from what has been described so far, combining TMS with EEG requires technical and methodological ability. In order to keep under control the large number of sources of potential artefacts, proper technical solutions are needed, already during the data-taking. In this paragraph, I will describe some suggestions about how to prepare the experimental setting before starting the recording session and how to monitor crucial elements during the registration.

The first step is the preparation of the experimental setting, with particular focus on the EEG cap montage. As described before, in order to obtain a high-quality EEG recording session is strictly essential to reduce the impedance under the electrodes. To do that, the skull has to be scrubbed using a specific paste, and the hairs under the electrodes need to be moved to leave the pin directly in contact

with the skin. After that, it is essential to put attention on the application of a relatively small amount of gel in order to avoid the formation of potential contact between neighbour electrodes.

Another critical point is to precisely locate the target area and to maintain a good control on the position of the coil for the whole duration of the recording session. This procedure is more straightforward when the area of interest is in the visuo-motor cortex. As mentioned in the previous chapter, the stimulation of those areas evokes a motor or visual potential that is directly measurable, that allows for adjusting the coil position in order to maximise or minimise the motor or visual threshold. For other areas that are not functionally directly measurable, the precise targeting requires a navigation technique that starts from the coil coordinates theoretically defined, and then translates on the subject’s own MRI. More specifically, starting from the coil location and orientation, the neuronavigation system is able to compute the induced electric field distribution in the brain, taking into account the subjective characteristics of the brain structures. It is essential, indeed, that in the navigation brain stimulation (NBS) system the individual MRI of every subject is used. Using such a system, the cortical target, as well as coil position and orientation, can be monitored in real-time throughout the sessions. These recorded parameters can be recalled to help in reproducing the location and orientation (direction and angle) of the coil in subsequent stimulation sessions. In TMS-evoked EEG, an accurate reproducibility of the stimulation parameters is essential for any comparative or longitudinal study.

3.6 TEPs data analysis

After the data-taking, but before starting with the data analysis, the EEG data need to be pre-processed. This procedure consists of an epoch-by-epoch inspection in which trials with artefacts due to eye blinks or movements and spontaneous muscle activities are removed, usually by the use of a semi-automatic procedure (e.g. Casali, Casarotto, Rosanova, Mariotti, & Massimini, 2010). Data pre-processing allows to increase the signal-to-noise ratio.

3.6.1 Global and Local Mean Field Power

One of the main advantages in performing TMS-EEG study is the possibility to collect information about the brain connectivity. Indeed, TEPs can be recorded not only from the area directly targeted, but also from the electrodes positioned over more distant brain regions (Massimini et al., 2005; Romero Lauro et al., 2014, 2015; Rosanova et al., 2009).

To obtain information about the activity of the entire brain, usually an index of global excitability, known as Global Mean Field Power (GMFP), is computed averaging the TEPs signal deriving from all the EEG channels. The GMFP represents the standard deviation across electrodes at a given time point, and it is calculated using the following formula:

$$\mathrm{GMFP(t)} = \sqrt{\left[\frac{\sum_i^k (V_i(t) - V_{mean}(t))^2}{K}\right]}.$$

In the above formula, *t* is time, *k* defines the number of channels, V_i corresponds to the voltage in the i-th channel averaged across subjects and V_{mean} is the voltage value averaged over all channels (Lehmann & Skrandies, 1980).

To further identify the specific contributions of the different cortical regions, it is also possible to measure an index of local excitability, the local mean field power. For that, clusters of electrodes are selected as ROI to address specific local excitability changes. The optimal number of EEG channels that define a ROI needs to be small enough to keep focal information, but at the same time, it should include enough channels to capture the most pronounced EEG activity (Ilmoniemi & Kičić, 2010). Usually, the clusters are composed of 1 to 4 electrodes to provide a local and focused information about the cortical processing. However, if the interest is to have information about a more global hemispheric activation, the number of electrodes in a single cluster could be bigger, for example from 10 to 15 (e.g. Nikulin, Kičić, Kähkönen, & Ilmoniemi, 2003). For instance, in the Romero Lauro et al. (2014) work, the analysis of the TEPs amplitude in four different ROI, defined by four electrodes each, permitted to better understand which brain region were mostly contributing to the increase of cortical excitability observed at a global level during and after the tDCS stimulation.

3.6.2 Sources modelling analysis

Another possible TMS-EEG data analysis method consists in a source modelling reconstruction and then in computing the current density at the source level. In this way the TEPs analysis can be performed avoiding the potential confound of volume conduction.

A TEP measurement $v(x_e,t,k)$, registered by the e-th sensor at the x_e position and time t, for the k-th trial, can be parametrised as function of the distribution of the signal at the level of the cortical surface using:

$$v(x_e,t,k) = G(x_e,x_j) * j(x_j,t,k) + \varepsilon(x_e,t,k),$$

where $j(x_j,t,k)$ is the source vector that generated the signal, $\varepsilon(x_e,t,k)$ is an instantaneous noise at the time t and position x_e, and $G(x_e,x_j)$ is the operator defining the propagation of the electrical signal in the head tissue. The operator G depends only on the positions of the source and of the sensor, respectively x_j and x_e, and on the physical and geometrical properties of the head. These properties are usually modelled using the 3-spheres BERG method (Berg & Scherg, 1994) that includes three concentric spheres with different homogeneous conductivity: cortex, skull and scalp. For a better definition of these compartments, in the work of this dissertation, the model is fitted on an individual MRI for every subject. If the MRI is not available, it is also possible to use a template model, even if

this will inevitably decrease the precision of the compartments’ definition. The spatial solutions of the equation above are then constrained within a rigid and defined 3D grid with a fix number of points, that has to be much bigger than the number of sensors (i.e. 3004, 2000, 2000 vertexes for the 3 different layers).

The condition $N_{sources} >> N_{sensors}$ gives many solutions to the inverse equation; this means that many different sources configurations can bring to the same cortical response at the sensors lever. To further constrain the solution, a Bayesian analysis is performed in order to find the sources configuration that better describe the measured signal. A more detailed explanation of this analysis technique can be found in Casali et al., 2010.

3.6.3 Cluster analysis

The cluster-based analysis is a powerful analysis tool whether we do not have a priori knowledge of where and when the effect of interest is expected. This technique is particularly useful in the analysis of EEG data were the number of samples, (sensor, time)-pairs, is extremely large and it brings to the Multiple Comparison Problem (MCP). This means that it is not possible to control the so-called Family Wise Error Rate (FWER) using standard parametric statistical techniques. The FWER is the probability of falsely find a difference between different experimental conditions, under the hypothesis of no-effect. Usually, in the case of EEG experiment, the number of samples can easily be of several thousands, making practically no possible to control the FWER with standard techniques.

Starting from the example of a multi-subject experiment, with multiple sensors and multiple time samples, in which we want to compare two different experimental conditions, the procedure for a non-parametric cluster-based analysis requires some work.

Firstly, we can average over all the trials of each subject and used the averaged (sensor, time)-pairs for the rest of the analysis. This is useful since it reduces the number of random extractions needed in the next steps, but if the number of subjects is too small ($N < 8$), it will not be possible to get p-values smaller than a given threshold. Then, we have to define the clusters of sensors and time regions. For the sensors, normally the clusters include all the sensors within a given area. For the time clusters, an idea could be to perform a standard parametric t-test to find time windows with a possible significant effect, or at least to cluster together all the subsequent time sample with a t-test of the same sign (positive or negative). After this, for each cluster, the non-parametric test is performed following these steps: (1) the trials of the two conditions are collected in a single set; (2) randomly partition this set in two subset with the same dimension of the initial ones; (3) perform the test statistic of this random partitions and plot the result in a histogram; (4) repeat steps 2 and 3 many times; (5)

calculate the proportion of random partitions that has a larger t-test that the observed one. This last number is the so-called permutation p-value. If this is smaller than the critical alpha-level decided a priori, the two data in the two experimental conditions are significantly different.

It can be demonstrated that the choice of the critical alpha-level does not affect the FWER, so it does not affect the rate of false positive. However, on the other hand, a large threshold can reduce the sensitivity of the test, cutting out weak but long-lasting effects. A more exhaustive and detailed description of this technique can be found in Maris & Oostenveld, 2007.

3.6.4 Time-Frequency analysis

In TMS-EEG studies, an alternative way to investigate brain states and their dynamics, in terms of oscillatory cortical activity, is to perform time-frequency analyses (Pellicciari, Veniero, & Miniussi, 2017). This procedure provides a way to extract a matrix of the EEG signal that represents the oscillatory power as a function of time and frequency. To obtain this matrix, it is possible to average the time-frequency signal deriving from each single trial, resulting in a total oscillatory response that capture phase-locked and non-phase-locked response to stimulus onset: in this case, the TMS pulse. Another possibility is to average the activity across trials, time- and phase-locked to the event onset (Herrmann, Rach, Vosskuhl, & Strüber, 2014). Due to its ability to capture possible changes in EEG power over time, the time-frequency analyses provide a powerful tool for exploring transient, non-stationary, neural oscillations (Cohen, 2017; Jahankhani, Kodogiannis, & Revett, 2006).

Several methods are available to decompose event-related EEG oscillations in the time-frequency domain. Among them, the most used, in particular in TMS-EEG studies, are the ones based on the Wavelet Transformation (Ferrarelli et al., 2008; Harris, Schwerdtfeger, & Strauss, 2011; Rosanova et al., 2009). This procedure is based on a series of oscillatory functions defined starting from a prototypical wavelet, usually the Morlet wavelet, that has a good trade-off between time and frequency resolution. However, the main limitation with this particular approach comes from the changing in wavelet length. In fact, a longer wavelet will improve the frequency resolution but, on the same time, it will reduce the temporal resolution. Consequently, a single oscillatory event well-defined in frequency, cannot be exactly localised in time (Gross, 2014; Pigorini et al., 2011).

To disentangle this issue, a different procedure based on Hilbert–Huang Transform (Huang et al., 1998) was implemented, to decompose TMS-evoked EEG oscillations with a simultaneous high resolution both in the time and in the frequency domain. In contrast to Wavelet Transformation analysis, the Hilbert–Huang Transformation is based on adaptive oscillatory functions derived from the data (Gross, 2014). Every adaptive function can change amplitude and frequency over time. The

subsequently transformation leads to an estimate of an instantaneous frequency and amplitude for each function, that are then combined into a time-frequency spectrum.

The full potential of TMS-EEG for studying the oscillatory cortical activity, depends strongly on the understanding of possible neural effects of single TMS pulse on baseline cortical activity and the best method to adequately measure the cortical oscillatory responses triggered by TMS. The greater relevance of this analytical approach in TMS-EEG is related to the possibility of defining causal relationships in the connection across brain areas and their involvement in time. The spatiotemporal pattern of the brain responses to TMS can contribute to defining causal relationships in the connections across brain areas and can reveal their activation at the time of stimulation (Bortoletto et al., 2015).

3.7 Summary

In this Chapter, the integrated technique TMS-EEG was described. We discussed in detail its peculiarities, the main advantages as well as the complexities and challenges that arise from the integration of these two techniques. As already discussed in the overview, the aim of this Chapter is to provide the basic knowledge to fully understand the next experimental part of the thesis, that is the main core of this work.

Chapter Four: "Tracking the effects of cathodal tDCS at resting state by means of TMS-EEG"

4.1 Chapter overview

In this Chapter, it will be presented the first study of the project, aimed to explore the effects of cathodal tDCS over the right PPC using TMS-EEG. This study mirrored a previous one (Romero Lauro et al., 2014, 2015) in which the effects of anodal tDCS were investigated at rest, as mentioned before (Chapter Two, Section 2.4).

The results showed the existence of non-linearity between the effects induced by the two different stimulation polarities that do not match the well-known anodic-excitatory and cathodic-inhibitory coupling, which emerged when sensorimotor areas are targeted (Kirimoto et al., 2011; Nitsche & Paulus, 2000, 2001). This study represents one of the first attempt to focus on the mechanisms underlying cathodal tDCS effects on humans, which are usually less investigated. Thus, it represents a starting point to deepen tDCS knowledge, better clarifying the role that could be played by this polarity of stimulation, both for clinical and research purposes.

4.2 Manuscript

The present study has been published as an Open Access article in: **Varoli, E.**, Pisoni, A., Mattavelli, G. C., Vergallito, A., Gallucci, A., Del Mauro, L., ..., & Lauro, L. J. R. (2018). Tracking the effect of cathodal transcranial direct current stimulation on cortical excitability and connectivity by means of TMS-EEG. Frontiers in neuroscience, 12. doi: 10.3389/fnins.2018.00319*

4.3 Aim of the study

In the present study, we aimed at further complementing previous knowledge on the neurophysiological basis of tDCS by applying TMS-EEG to explore the effects induced by cathodal tDCS. Addressing the cortical effects of cathodal tDCS acquires peculiar relevance considering that the behavioural outcomes of this stimulation are more uncertain in comparison to those induced by anodal tDCS (e.g. Jacobson et al., 2012 for a review). Indeed, whereas polarity-dependent opposite effects – anodal excitatory and cathodal inhibitory -, are usually reported when stimulating the primary sensory, motor or visual, cortices, the evidence becomes more controversial when higher cognitive functions and the underlying brain areas are targeted (Jacobson et al., 2012). Typically, anodal tDCS has been found to enhance the targeted cognitive function, whereas cathodal stimulation

* Reprinted with the permission of Frontiers in Neuroscience, the full text is available in the Appendix 1

is reported as less effective or is not explored at all. For instance, recent evidence-based guidelines for clinical use of tDCS (Lefaucheur et al., 2017) do not include cathodal stimulation for any disease.

To mirror previous data (Romero Lauro et al., 2014, 2015), in the present study we applied cathodal tDCS over the right PPC, and we tracked its effects on cortical excitability and connectivity performing TMS-EEG co-registrations before, during and 10 minutes after the end of the stimulation. As in the previous study, the PPC was chosen as TMS hotspot for two main reasons. The first one is that we were interested in maximizing the advantage in using TMS-EEG technique. TMS-EEG, indeed, allows exploring cortical reactivity and connectivity of areas, otherwise not functionally measurable, since they cannot produce a direct TMS output such as MEPs for M1 and phosphenes for the primary visual cortex (V1). The second reason is that, from a theoretical perspective, the PPC plays a crucial role in different sensorimotor and cognitive functions (e.g. Andersen & Cui, 2009; Fogassi & Luppino, 2005; Ikkai & Curtis, 2011; Shomstein, 2012). Moreover, as mentioned above (see Chapter Two, Section 2.4), the tDCS has been successfully applied to this area for modulating sensory (e.g. Bolognini et al., 2010a, 2010b; 2013; Convento et al., 2013) and cognitive processes (Berryhill et al., 2010; Sparing et al., 2009; Stone & Tesche, 2009) in healthy participants.

Based on what observed when the primary motor or sensory area are targeted, as well as for what reported in in vivo/vitro studies, we hypothesized a reduction of cortical excitability and connectivity during and following the stimulation.

4.4 Material and Methods

4.4.1 Participants

Fifteen healthy, right-handed volunteers (five males, mean age 25.4 years, SD 3.5, range 21-32) took part in the study. Each participant completed an Adult Safety Screening Questionnaire (Keel, Smith, & Wassermann, 2001) and gave informed written consent prior to study procedures. Participants did not report any contraindication to non-invasive brain stimulation (Rossi et al., 2009), namely no history of medical disorders, no substance abuse, no use of central nervous system-effective medication, no psychiatric and neurological disorders, including brain surgery, tumour, or intracranial metal implantation. The study was performed in the TMS-EEG laboratory of the University of Milano-Bicocca, was approved by the local Ethics Committee and it was carried out in accordance with the ethical standards of the revised Helsinki Declaration.

4.4.2 Procedure

For each participant, the experimental session consisted in three blocks of TMS-EEG recordings performed before (pre-tDCS), during (during-tDCS) and 10 min after cathodal tDCS (post-tDCS) applied over the right PPC. Each recording session lasted about 7 min during which

participants were in a resting condition, fixating a white cross in a black screen (17’’). A second group of fifteen participants took part in a control Sham session. Six of them were taken from a previous study (Romero Lauro et al., 2014), while the remaining nine were recruited from the present sample. Sham sessions were identical to the cathodal ones, but tDCS was turned off 30s after the start. The order of the two sessions (cathodal and sham tDCS) was counterbalanced across subjects.

4.4.3 TMS stimulation parameters

TMS was delivered with an Eximia™ TMS stimulator (Nexstim™, Helsinki, Finland) using a focal figure-of-eight bi-pulse 70 mm-coil. As in Romero Lauro et al. (2014), the stimulation target was the left PPC, between P1 and CP1 EEG electrodes. High-resolution (1 x 1 x 1 mm) structural magnetic resonance images (MRI) were acquired for each participant using a 3 T Intera Philips body scanner (Philips Medical Systems, Best, NL). TMS target was identified on individual MRIs using a Navigated Brain Stimulation (NBS) system (Nexstim™, Helsinki, Finland), which employs infrared-based frameless stereotaxy to map the position of the coil and of participant's head, within the reference space of the individual's MRI space. Mean Montreal Neurological Institute (MNI) coordinates for the target site were X = -31 (SD = 5.2) Y = -70 (SD = 6.6) Z = 54 (SD = 3.7). The NBS system allowed for a continuous monitoring the position and orientation of the coil, thus assuring precision and reproducibility of the stimulation across sessions. Moreover, the NBS system estimated on-line the distribution and intensity (V/m) of the intracranial electric field induced by TMS. It uses a locally best-fitting spherical model, accounting for the head and brain shape of each participant, and taking into consideration the distance from scalp, coil position and orientation. Mean stimulation intensity, expressed as a percentage of the maximal output of the stimulator, was 58%, (range = 50 - 63%), corresponding to an electric field of 100 ± 14 V/m. The coil was placed tangentially to the scalp and adjusted for each participant in order to direct the electric field perpendicularly to the shape of the cortical gyrus, following the same procedure of previous studies (Casarotto et al., 2010; Mattavelli, Rosanova, Casali, Papagno, & Romero Lauro, 2013; Romero Lauro et al., 2014). Since TMS over parietal sites can activate temporal and frontal muscles, hence eliciting artefacts in the EEG recordings, the site of the stimulation was individually adjusted, in order to avoid or reduce as much as possible muscle twitches. TMS pulses were delivered at an inter-stimulus interval (ISI) randomly jittered between 2000 ms and 2300 ms (.4 - .5 Hz). 180 TMS pulses were delivered for each session.

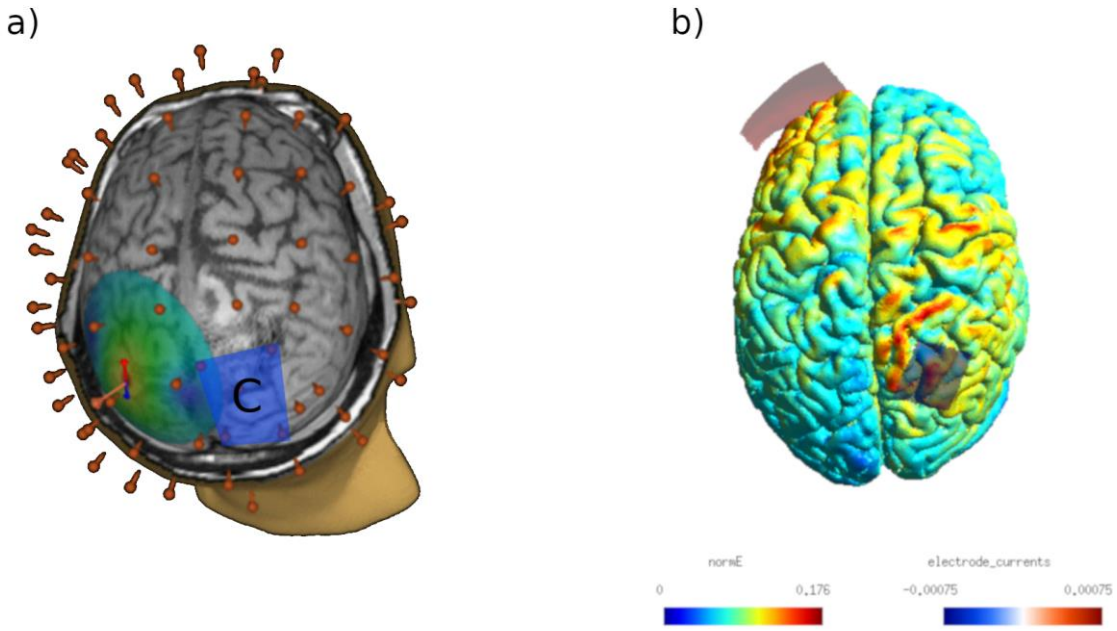

Figure 4.1: *In the left side, panel a), a 3D reconstruction of the individual MRI is depicted, showing the electrical field induced by TMS on the left parietal cortex. The blue rectangle represents the cathode patch position over the right parietal cortex; the 60 red points correspond to the position of the EEG cap electrodes. On the right side, panel b), the estimated current flow related to the specific tDCS montage and parameters used in the study.*

4.4.4 tDCS stimulation parameters

tDCS was delivered by a battery driven constant current stimulator (Eldith™, Neuroconn, Ilmenau, Germany) using a pair of rubber electrodes and a conductive paste (Ten20 conductive EEG paste, Kappamedical™, USA) to attach them to participants’ head and reduce impedance. An intra-cephalic montage was used. The cathode (size = 9 cm²; current density = .08 mA/cm²) was placed over the right PPC under the EEG cap, in a site corresponding to P2 electrode, which was previously removed from the cap as the CP2, as in Romero Lauro et al., 2014. The anode (size = 25 cm², current density = .03 mA/cm²) was positioned over the left supraorbital area. A constant current of .75 mA was applied for 15 min, with 8 s of fade-in/fade out period. Different sized electrodes were used to increase the stimulation focality (Nitsche et al., 2008); in the Figure 4.1 is possible to see the correspondent model of the current flow generated by this specific electrodes montage (SimNIBS v 3.0.7). For sham tDCS, the same electrodes arrangement and stimulation parameters were used, but the stimulator was turned off after 30 s (Gandiga, Hummel, & Cohen, 2006). The feasibility of concomitant EEG recording and tDCS application has been recently probed (Faria et al., 2012; Schestatsky, Morales-Quezada, & Fregni, 2013; Wirth, et al., 2011). In order to avoid tDCS induced artefacts in the EEG trace, the tDCS electrodes and the conductive gel never came in contact with the surrounding EEG recording leads and they were far away from the ground electrodes (see Figure 4.2).

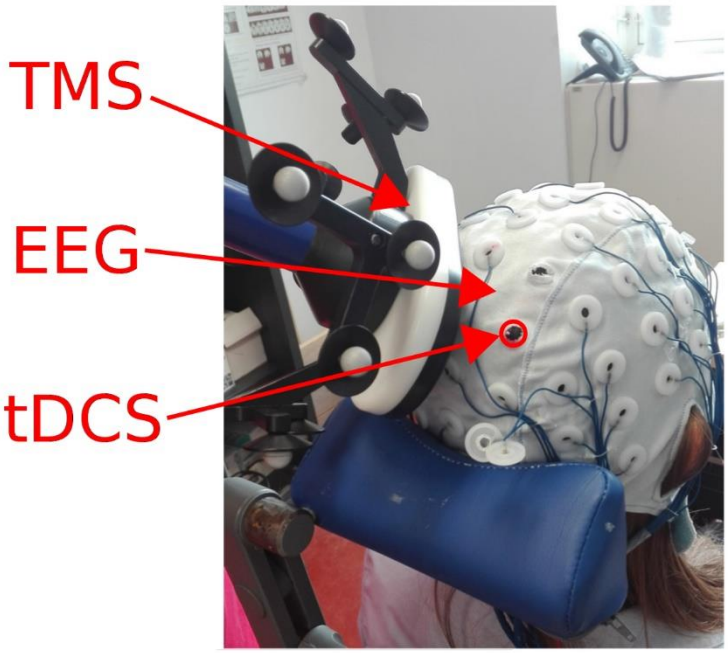

Figure 4.2: *Combined tDCS and TMS-EEG system used for the experiments discussed in the present dissertation. In particular, here it is possible to see that in correspondence of the tDCS patch, the EEG electrodes (P2 and CP2) were removed in order to reduce the potential noise coming from electrical stimulation.*

Transient EEG artefacts were observed only during the fade-in and fade-out phases of tDCS stimulation, while TMS-EEG trials were never affected by those transient artefacts.

4.4.5 EEG Recording data during TMS

TEPs were continuously recorded using a TMS compatible 60-channels amplifier (Nexstim Ltd., Helsinki, Finland), which gates the TMS artefact and prevents saturation by means of a proprietary sample-and-hold circuit (Virtanen et al., 1999). EEG signals were referenced to two electrodes placed over the forehead and used as ground. Eye movements were recorded with two additional electrodes placed near the eyes, in order to monitor ocular artefacts both in the vertical and horizontal axes. As in previous studies (Casarotto et al., 2010; Massimini et al., 2005), in order to prevent auditory potentials due to TMS pulses, a masking noise, which reproduced scrambled TMS “click” time varying frequency components, was continuously played into earplugs worn by participants during the experimental sessions. Electrodes impedance was kept below 5 kΩ, and EEG signals were recorded with a sampling rate of 1450 Hz.

4.4.6 EEG data analysis

EEG data were pre-processed using MATLAB R2016b® (MathWorks, Natick, MA, USA). First, recordings were downsampled to 725 Hz. Continuous signal was then split in single trials, from 800 ms before to 800 ms after the TMS pulse. Trials with artefacts due to eye blinks/movements, or spontaneous muscle activity were removed following a semi-automatic procedure (Casali et al.,

2010), and the visual inspection of the signal by trained experimenters (A.P., E.V.). The average number of trials considered in the analysis was 123 (SD ± 3) for the pre-tDCS, 123 (SD ± 5) for the during tDCS session, and 122 (SD ± 3) for the post-tDCS condition. TEPs were computed by averaging selected artefact-free single trials and by filtering them between 2 and 40 Hz. Bad or missing channels, as P2 and CP2 for each session, were interpolated using the spherical interpolation function of EEGLAB (Delorme & Makeig, 2004). TEPs were then referenced and baseline corrected between -300 and -50 ms before the TMS pulse. For each condition, as an index of global excitability, Global Mean Field Power (GMFP, Casarotto et al., 2010; Pisoni et al., 2017; Romero Lauro et al., 2014, 2015) was computed on averaged TEPs of 60 channels for three temporal windows defined in an interval between 0 to 150 ms from TMS pulse onset. The three time windows were: 0-50 ms, 50-100 ms and 100-150 ms. To further identify the specific contributions of different cortical regions to the modulation of global cortical excitability, indexes of local excitability (Local Mean Field Power, LMFP) were measured following the same procedure used for GMFP. Four clusters of electrodes, with 4 electrodes each, were selected based on anatomical locations. Two parietal clusters: the left one corresponding to TMS hotspot (CP1, CP3, P1, and P3), and the right one corresponding to the area covered by the tDCS cathode (CP2, CP4, P2, and P4). Two frontal clusters corresponded to the areas structurally and functionally connected to the parietal ones: the left frontal cluster (F1, F5, FC1, and FC3) and the right frontal cluster (F2, F6, FC2, and FC6). In order to obtain a synthetic index of global and local cortical excitability, GMFP and LMFP values were cumulated within the three time windows (0-50 ms, 50-100 ms and 100-150 ms after the TMS pulse) and for each experimental condition (pre-, during- and post-tDCS).

4.4.7 Source modelling

Source modelling was performed in order to assess the impact of tDCS on cortical excitability avoiding the potential confound of volume conduction, allowing a better definition of the spatial distribution of the tDCS effects (as in Romero Lauro, et al., 2015). The analysis was run on 14 out of the 15 participants enrolled in the experiment, since in one of them the MRI data were not suitable for source reconstruction (see for details on the procedure see Casali et al., 2013). Firstly, individual standardized meshes were reconstructed for each participant starting from their structural MRIs (SPM8, Ashburner et al., 2011), obtaining meshes of cortex, skull and scalp compartments (containing 3004, 2000 and 2000 vertices, respectively), normalized to the MNI atlas (Casali et al., 2010). Then, for each participant, EEG sensors position was aligned to the canonical anatomical markers (pre-auricular points and nasion), and the forward model was computed. The inverse solution was computed on the average of all artefact-free TMS-EEG trials, using the weighted minimum norm estimate with smoothness prior, following the same procedures as in Casali et al. (2010). This method

is advantageous because it provides stable solution also in the presence of noise (Silva, Maltez, Trindade, Arriaga, & Ducla-Soares, 2004), and it does not require any a priori assumption about the nature of the source distribution (Hämäläinen & Ilmoniemi, 1994). After source reconstruction, a statistical threshold was computed in order to assess when and where the post-TMS cortical response differed from pre-TMS activity (i.e., to identify TMS-evoked response). To do so, a nonparametric permutation-based procedure was applied (Pantazis, Nichols, Baillet, & Leahy, 2003). A binary spatial-temporal distribution of statistically significant sources was obtained and thus only information from significant cortical sources was used for further analyses. As a measure of global cortical activation, we cumulated the absolute Significant Current Density (global SCD, measured in mA/mm^2, Casali et al., 2010) over all 3004 cortical vertexes and over the three time windows (0-50 ms, 50-100 ms and 100-150 ms) for each recording session (pre-tDCS, during-tDCS and post-tDCS). Finally, in order to mirror the LMFP EEG data analysis of the study, for each time window and each experimental condition, a local SCD was computed in the vertexes within four different Brodmann's areas (BAs), identified by means of an automatic tool of anatomical classification (WFUPickAtlas tool; http://www.ansir.wfubmc.edu). These BAs approximately corresponded to the original four clusters of LMFP (left/right BA 6 and 7).

4.5 Analyses

To estimate whether tDCS affected global or local cortical excitability, GMFP and LMFP values were submitted to a series of linear mixed effects models (Baayen, Davidson, & Bates, 2008) in R statistical computing software environment (R Development Core Team, 2013) with the "lme4" package (version 0.6-82, Bates, Maechler, Bolker, & Walker, 2014). In particular, GMFP was considered as a continuous dependent variable, while *Condition* (factorial, 3 levels: pre-, during- and post-tDCS) and *Time Window* (factorial, 3 levels: 0-50ms; 50-100ms and 100-150ms) were tested as fixed factors. The by-subject intercept was included as random factor. The inclusion of a main effect or interaction in the final model was assessed by means of Likelihood Ratio Test (LRT, see Baayen et al., 2008), including a parameter if it significantly increased the model's goodness of fit. The same procedure was adopted for LMFP values, which were analysed separately for each electrodes cluster. A further test with a Bayesian ANOVA on the same values was performed to test for the null hypothesis (Etz, Gronau, Dablander, Edelsbrunner, & Baribault, in press; Rouder, Speckman, Sun, Morey, & Iverson, 2009) by means of the Bayesian Analysis of Variance (ANOVA) using "JASP" software environment (version 0.8.2.0, JASP team, 2017).

The same analysis was performed for source modelling data on global and local SCD values.

The whole procedure was adopted also to analyse sham session data.

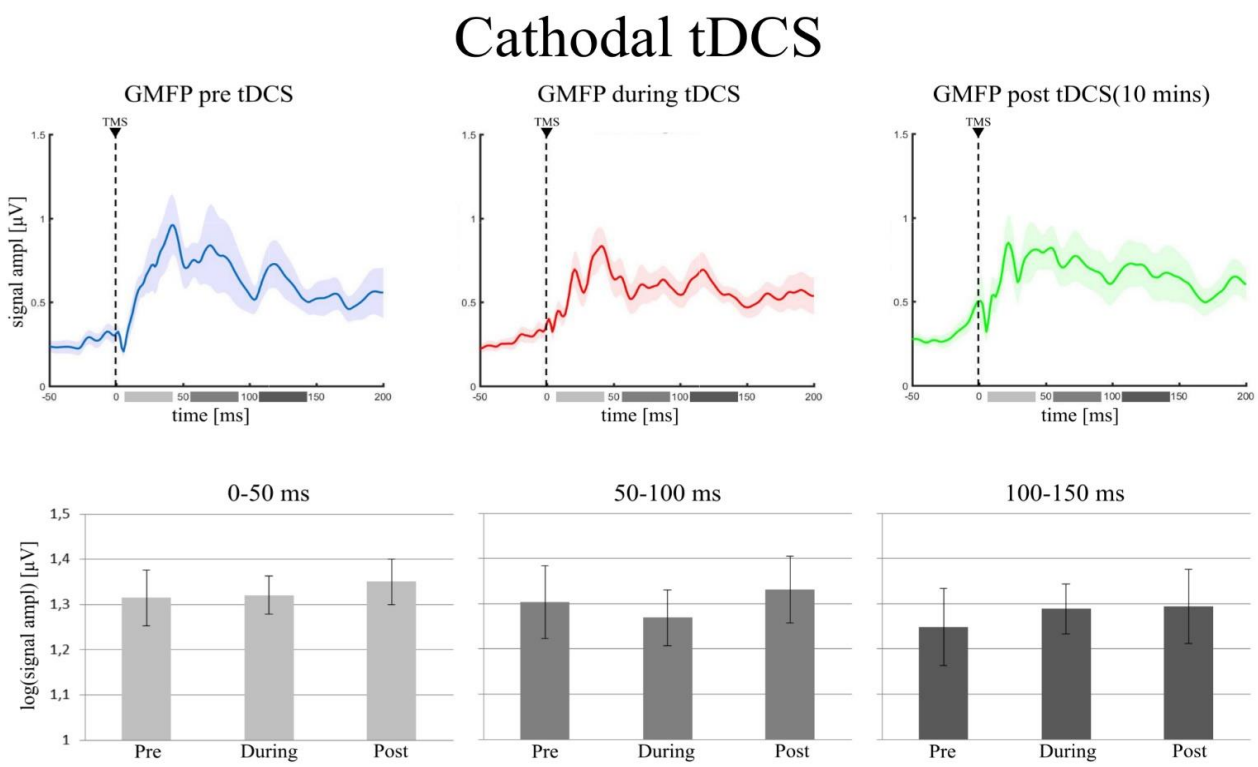

Figure 4.3: *In the upper row it is shown the Grand Average of GMFP in the three experimental conditions (pre tDCS = blue trace; during tDCS = red trace; post tDCS = green trace). Shadowed areas represent ± SE. In the lower row, the bar histograms represent the mean values of the log-GMFP in the three time-windows of our interest (0–50 ms = light gray, 50–100 ms = gray, 100–150 ms = dark gray) for each recording session. The error bars represent ± SE (Varoli et al., 2018).*

4.6 Results

4.6.1 Cathodal stimulation - Sensor analysis

GMFP

The final model on GMFP values did not include the main effect of *Condition* in the 0-50 ms ($\chi^2(2) = 1.15$; p=.56), in the 50-100 ms ($\chi^2(2) = 0.26$; p=.87) and in the 100-150 ms ($\chi^2(2) = 1.62$; p=.44) time windows. GMFP thus did not change when recorded before, during or after cathodal tDCS (see Figure 4.3). Bayesian analysis, indeed, provided a moderate support in favour of the null hypothesis for the first (BF_{01}= 5.1), the second (BF_{01}= 4.6) and the third (BF_{01}= 5.3) time window.

LMFP

Analyses run on LMFP values did not support any effect of cathodal tDCS in any of the considered clusters of electrodes (see Figure 4.4).

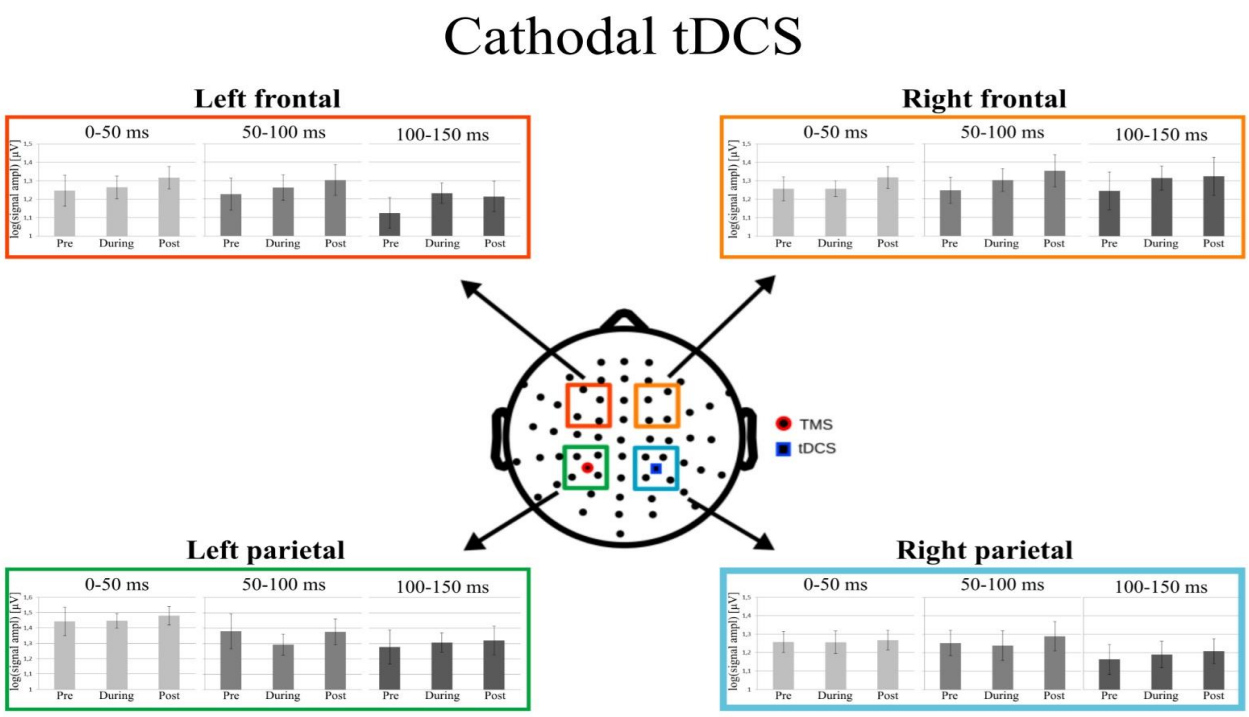

Figure 4.4: *Mean log-LMFP for the four clusters of interest. Coloured squares on the head model represent the electrodes clusters in the parietal and frontal regions. The blue square in the right parietal region represents the location of the tDCS cathode, whereas the red dot in the left parietal cluster represents the TMS position. For each cluster, the bar graphs represent mean log-LMFP in the baseline, during and post tDCS conditions, for the three temporal windows: 0–50 ms (light gray), 50–100 ms (gray), and 100–150 ms (dark gray). Error bars represent ± SE. (Varoli et al., 2018).*

In particular, concerning C1, the cluster under the tDCS cathode, LRT indicated not to include *Condition* in the model run on LMFP values in the first ($\chi^2(2)= 1.53$; $p=.46$) second ($\chi^2(2)= .63$; $p=.73$) and third ($\chi^2(2)= 1.36$; $p=.51$) time window. Critically, Bayesian analyses moderately supported the null hypothesis, indicating no effect of tDCS on LMFP computed in this cluster for the first ($BF_{01}= 5.5$), the second ($BF_{01}= 3.9$) and the third ($BF_{01}= 5.7$) time window.

Analysing C2, the cluster under the TMS coil, LRT indicated not to include *Condition* in models for any time window (0-50ms: $\chi^2(2) = 1.12$; $p=.57$; 50-100ms: $\chi^2(2) = .99$; $p=.61$; 100-150ms: $\chi^2(2) = 1.22$; $p=.54$). Crucially, Bayesian analyses moderately supported the null hypothesis, indicating no effect of tDCS on LMFP computed in this cluster in any time window (0-50ms: $BF_{01}= 6$; 50-100ms: $BF_{01}= 5.3$; 100-150ms: $BF_{01}= 5.5$).

Similarly, in C3 LRT indicated not to include *Condition* in models for any time window (0-50ms: $\chi^2(2) = 1.03$; $p=.6$; 50-100ms: $\chi^2(2) = 2.78$; $p=.25$; 100-150ms: $\chi^2(2) = 1.08$; $p=.58$). Yet, Bayesian analyses moderately supported the null hypothesis, indicating no effect of tDCS on LMFP computed in this cluster in any time window (0-50ms: $BF_{01}= 3.8$; 50-100ms: $BF_{01}= 3$; 100-150ms: $BF_{01}= 4.9$).

The final model on C4 values did not include the main effect of *Condition* in the 0-50ms ($\chi^2(2) = 1.4$; p=.49) in the 50-100ms ($\chi^2(2) = 2.38$; p=.30) or in the 100-150ms ($\chi^2(2) = 3$; p=.22) time windows. Even in this case, Bayesian analysis supported moderately the null hypothesis, indicating no effect of tDCS on LMFP computed in this cluster in any time window (0-50ms: BF_{01}= 4.5; 50-100ms: BF_{01}= 4.4; 100-150ms: BF_{01}= 3.5).

4.6.2 Cathodal Stimulation - Source modelling analyses

Source modelling analyses confirmed results from the sensor analyses. A full report of statistical results of analyses run on Global and Local SCD is reported in the full paper version (Appendix 1). The final model on Global SCD did not include *Condition* in any time window, indicating no effect of cathodal tDCS on cortical activation induced by TMS (see Figure 4.5). Similarly, for both left and right BA7, LRT indicated no inclusion of the factor *Condition* in the final model, suggesting no influence of cathodal tDCS on local cortical activity in the left and right parietal cortices. The same result holds for the left and right BA6, where no effect of tDCS was highlighted on local SCD.

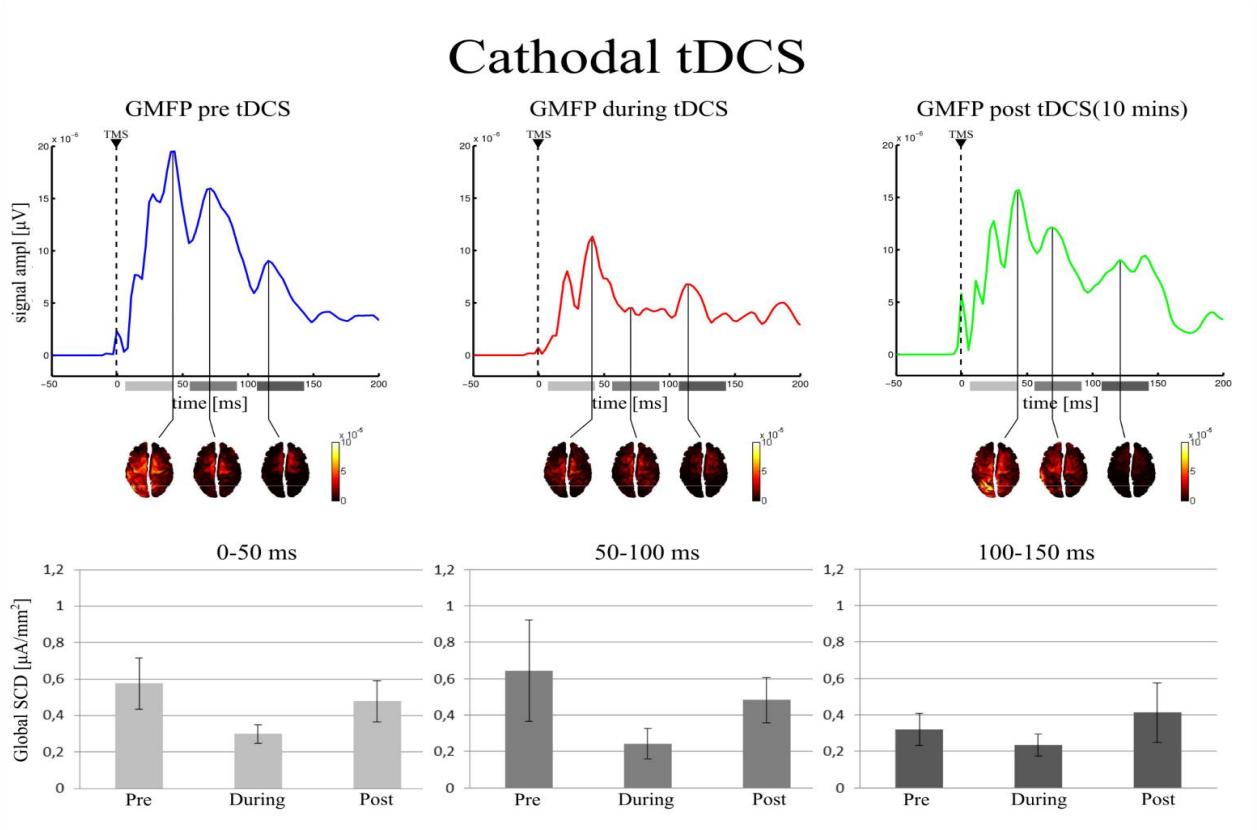

Figure 4.5: *Active vertexes and current spread at the local maxima in the GMFP for the three time-windows. For each recording session, the GMFP is shown on first top row, with the area beneath the curve divided in the three tested time windows (0–50 ms: light gray; 50–100 ms: gray; 100–150 ms: dark gray). The second row shows the estimated cortical sources in time coincidence with the maximum GMFP value, for each time window. In the last row are reported the mean values of the Global SCD for each condition and in each time window. (Varoli et al., 2018).*

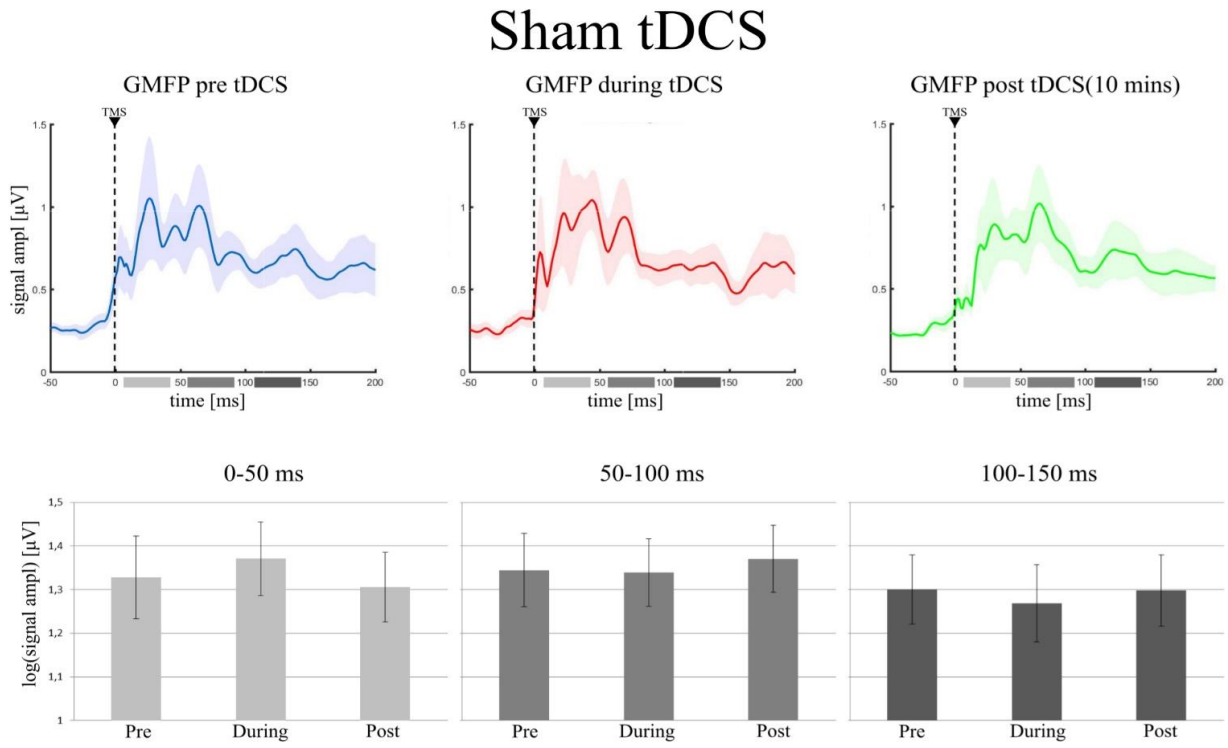

Figure 4.6: *Results for the Sham tDCS condition. In the upper row, it is presented the Grand Average of GMFP in the three experimental conditions, while, in the lower row, the bar histograms represent the mean values of the log-GMFP in the three time-windows of our interest (Varoli et al., 2018).*

4.6.3 Sham stimulation - Sensor analysis

GMFP

As expected, sham stimulation did not modulate global indices of cortical excitability. In particular, the final model run on GMFP did not include the main effect of *Condition* in any time window (0-50 ms: $\chi^2(2) = 1.2$; p=.55; 50-100 ms: $\chi^2(2) = .43$; p=.81; 100-150 ms: $\chi^2(2) = .18$; p=.91 see Figure 4.6). Bayesian analyses moderately supported the null hypothesis for the inclusion of the factor *Condition* in the final model (0-50ms: BF_{01}= 3.9; 50-100ms: BF_{01}= 5.1; 100-150ms: BF_{01}= 5.4).

LMFP

Analyses run on LMFP confirm the lack of any effect of cathodal tDCS in any of the considered clusters of electrodes in modulating local cortical excitability (see Figure 4.7).

In C1, LRT values were non-significant for the first ($\chi^2(2) = 2.4$; p=.3), the second ($\chi^2(2) = .98$; p=.61) and the third ($\chi^2(2) = 2.29$; p=.32) time window. Bayesian analyses moderately supported the null hypothesis, indicating no effect of tDCS on LMFP computed in this cluster (0-50ms: BF_{01}= 2.3; 50-100ms: BF_{01}= 4.73; 100-150ms: BF_{01}= 3.3).

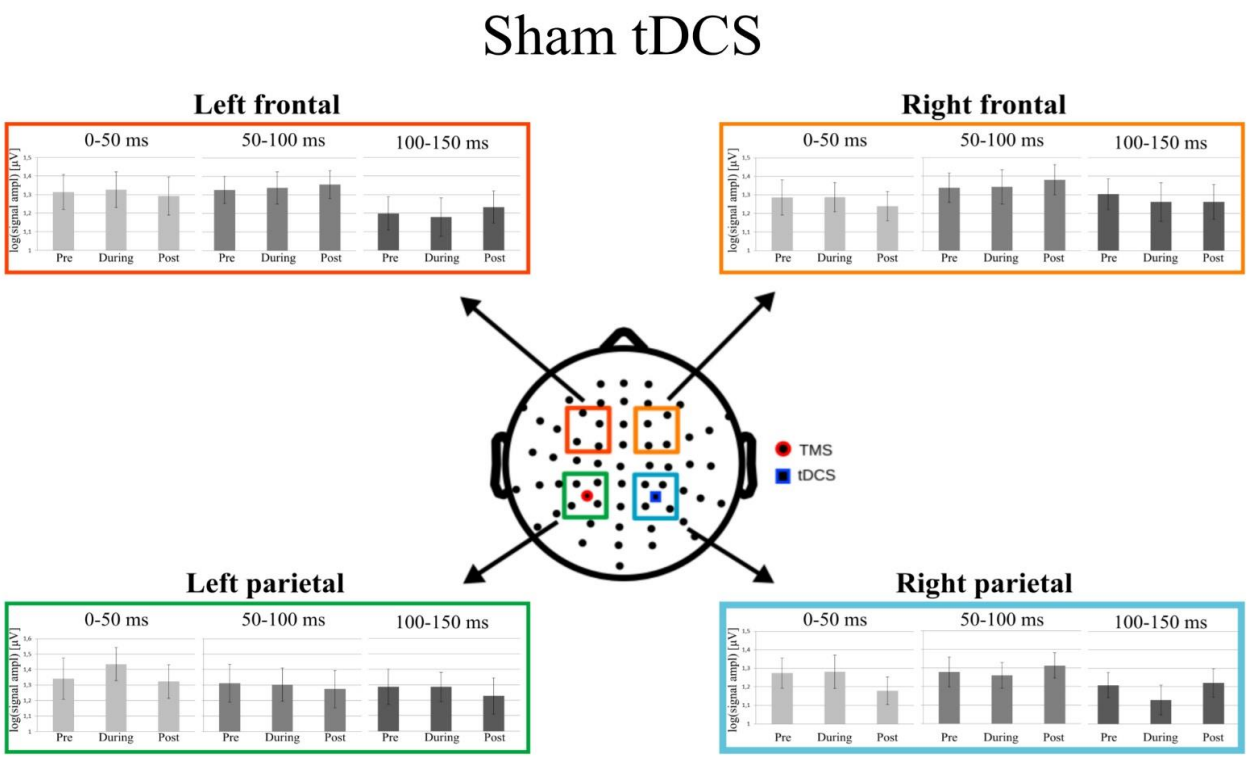

Figure 4.7: *Mean log-LMFP for the four clusters of interest in Sham tDCS stimulation condition (Varoli et al., 2018).*

The same holds for C2. LRT values were not significant for the factor *Condition* in any time window (0-50ms: $\chi^2(2) = 1.28$; p=.53; 50-100ms: $\chi^2(2) = .86$; p=.65; 100-150ms: $\chi^2(2) = .2$; p=.9). Similarly, Bayesian analyses moderately supported the data under the null hypothesis for the first (BF_{01}= 3.4), the second (BF_{01}= 5.4) and the third (BF_{01}= 5) time window.

Similarly, in C3 LRT indicated not to include the factor *Condition* for any time window (0-50ms: $\chi2(2) = 1.94$; p=.38; 50-100ms: $\chi2(2) = .74$; p=.69; 100-150ms: $\chi2(2) = .09$; p=.95) in the final model. Yet, Bayesian analyses moderately supported the data under the null hypothesis for the first (BF_{01}= 4.7), the second (BF_{01}= 5) and the third (BF_{01}= 5.4) time window.

Finally, also for C4 LRT values were non-significant for the first ($\chi^2(2) = .08$; p=.95), the second ($\chi^2(2) = .3$; p=.86) and the third ($\chi^2(2) = .22$; p=.89) time window. Even in this case, Bayesian analyses moderately supported the null hypothesis, indicating no effect of tDCS on LMFP computed in this cluster (0-50ms: BF_{01}= 5.4; 50-100ms: BF_{01}= 5.4; 100-150ms: BF_{01}= 5.1).

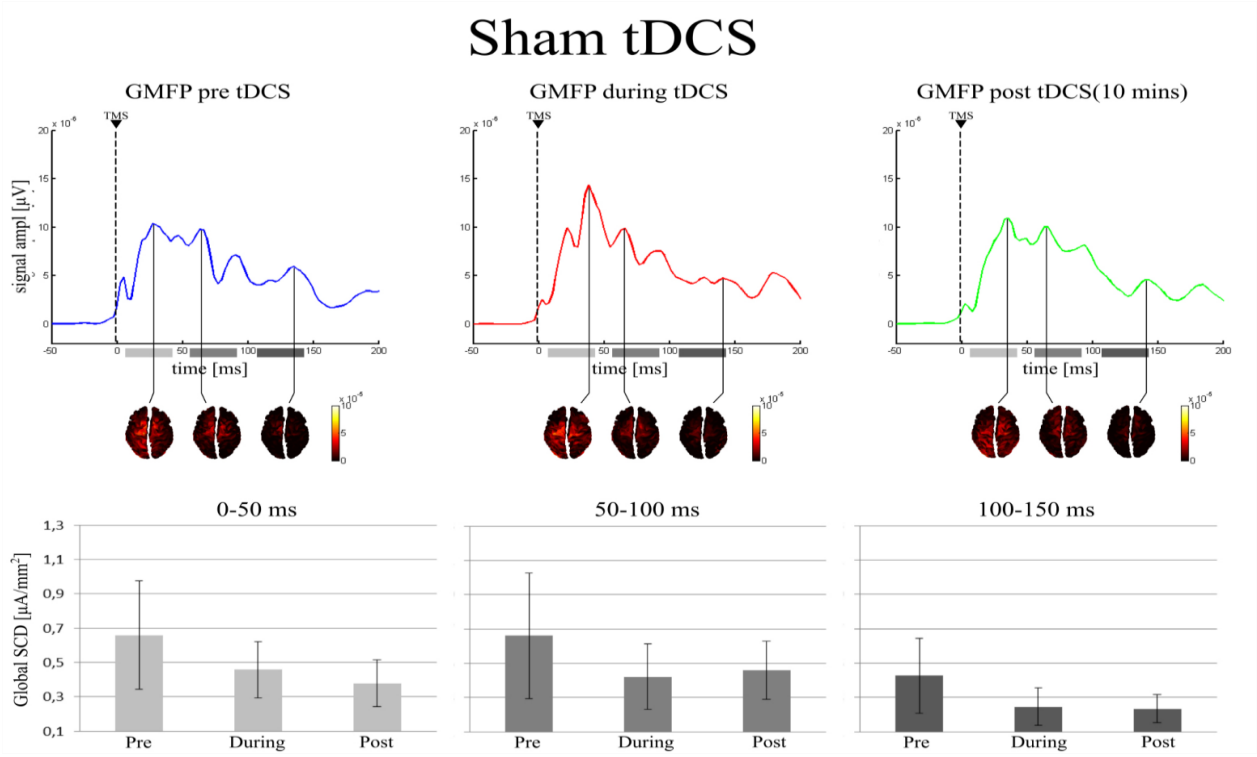

Figure 4.8: *For the Sham tDCS group, active vertexes and current spread at the local maxima in the GMFP for the three time-windows (Varoli et al., 2018).*

4.6.4 Sham Stimulation - Source modelling analyses

Source modelling analyses on sham recordings mirrored the results from the sensor analyses. A full report of statistical results of analyses run on Global and Local SCD is reported in the full paper version (Appendix 1). Global SCD final model did not include *Condition* in any time window, indicating no effect of sham stimulation on cortical excitability (see Figure 4.8). The same holds for both left and right BA7 and BA6, where LRT indicated no inclusion of the factor *Condition* in the final model.

4.7 Discussion

In this study, we ought to investigate the effects on cortical excitability induced by 10 minutes of cathodal stimulation over the right PPC. To this purpose we measured TEPs by means of TMS-EEG recordings before, during and 10 minutes after the end of the stimulation. TMS was applied over the left PPC. As a control condition, 15 participants underwent an additional session in which sham tDCS was delivered. Indices of local and global activity were computed at both the sensors and cortical sources level.

At the sensors level, no significant modulation of cortical excitability was observed during and after cathodal stimulation in comparison to pre-tDCS session, neither at a global (GMFP) nor at a local level (LMFP for 4 clusters of electrodes). Furthermore, no significant results were found for

any of the considered TEPs’ temporal windows, namely an early (0-50ms), a middle (50-100ms) and a late (100-150ms) one, chosen to assess different TEP’s components. Source modelling confirmed the results observed at the sensor level, since SCD did not change during or after stimulation with respect to pre-tDCS condition, both when computed at a global level or in BAs matching the clusters of the LMFP analysis. A similar pattern of results without any significant changes on cortical excitability among the three tDCS conditions was found when sham stimulation was delivered. This result confirms the reliability of the TMS-EEG approach and no effect of test-retest of TEP-derived indices of brain activation (Casarotto et al., 2010; Kerwin, Keller, Wu, Narayan, & Etkin, 2017; Lioumis, Kičić, Savolainen, Mäkelä, & Kähkönen, 2009).

The absence of significant changes among pre-, during- and after-tDCS conditions by itself does not provide evidence that the three conditions are the same. To check further this chance, a Bayesian analysis was performed to directly test the null hypothesis of no change among the three conditions. Despite subtle differences, all the results of the Bayesian analysis converge in suggesting a moderate indication toward the null hypothesis.

Although results suggest a null effect of cathodal tDCS on cortical excitability, further corroborating evidence from different approaches is needed to support such a negative conclusion. Importantly, evidence of the modulatory effects of cathodal tDCS has been provided so far by different approaches. First, a reduction of neurons’ firing rate was observed after cathodal tDCS in animal studies (Bindman et al., 1964; Creutzfeldt et al., 1962; Purpura & McMurtry, 1965). Furthermore, when applied over M1, cathodal tDCS resulted in a decrease of corticospinal excitability assessed by MEPs (Lang, Nitsche, Paulus, Rothwell, & Lemon, 2004; Nitsche & Paulus, 2000); led to a widespread decrease of regional blood flow as measured by PET (Lang et al., 2005; but see also Baudewig, Nitsche, Paulus, & Frahm, 2001); and increased the inter-hemispheric coherence of the resting fMRI signal between the left and right homologues regions of the motor system (i.e. M1 and SMA) as well as the functional connectivity in the motor and default mode networks (Amadi et al., 2014).

The conclusion that instead can be firmly drawn from the present set of results is that cathodal effects on cortical excitability differ from the ones induced by anodal tDCS. The present study indeed mirrored a previous one from our group (Romero Lauro et al., 2014, 2015), where the same procedure and data analysis resulted in a significant rise of cortical excitability during and after anodal tDCS. The significant findings in these previous studies confirm the feasibility of TMS-EEG approach to tap tDCS effects on cortical excitability. Moreover, TEPs have been shown to be a reliable measure of cortical excitability when the same parameters are maintained (Casarotto et al., 2010). For these reasons the lack of significant effects in the present study cannot be attributed thus to the experimental

paradigm, rather indicates a crucial imbalance between anodal and cathodal impact on cortical excitability.

In a qualitative review and meta-analysis, Jacobson and co-authors (2012) revealed how the coupling of anodal-excitatory and cathodal-inhibitory effect is robust in the motor and perceptual domains, but controversial when cognitive functions are addressed. In most of the cases, indeed, when memory, language ore higher cognitive functions are tested, an excitatory/enhancing effect of anodal tDCS is observed, whereas cathodal tDCS effects are less effective or ineffective. The frequent lack of significant behavioural effects induced by cathodal tDCS is possibly the reasons why many studies, performed both in healthy and clinical population, focused only on testing the anodal vs sham modality of stimulation (Jacobson et al., 2012). It has to be noted that studies investigating tDCS-induced cognitive modulations do not target M1. It follows that cathodal effects targeting this region could be due to a greater sensitivity of M1 to cathodal tDCS, having a different cortical organization compared to the rest of the homotypic isocortex.

Nevertheless, there are examples of tDCS effects limited to anodal polarity also in the heterotypic isocortex, such as in the motor (Baudewig et al., 2001; Priori, 2003), visual (Antal et al., 2004; Sczesny-Kaiser et al., 2016) and somatosensory systems (Matsunaga et al., 2004). Critically, with a methodology similar to that applied in the present study, a previous TMS-EEG research (Pellicciari et al., 2013) found the coupling of anodal-excitatory and cathodal- inhibitory modulation on TEPs by stimulating M1. However, also in this case, the effect of the two polarities was different, since increased excitability after anodal stimulation was found over both hemispheres whereas the cathodal stimulation induced opposite effects over the two hemispheres, namely reduced excitability over the stimulated hemisphere and facilitation in the contralateral one.

The mechanisms underlying this non-linearity in the effectiveness of tDCS polarity-dependent effects are still unclear. Jacobson et al. (2012) suggested that the lack of cathodal-inhibitory effects when tapping cognitive functions could be due to several factors, including the recruitment of broader cortical networks, the greater susceptibility to external noise of the behavioural measured adopted, the influence of the initial activation state and the greater occurrence of bilateral interactions supporting contralateral compensation. The hypothesis of a link among anodal tDCS - increased neuronal excitability/enhanced behavioural performance - at odd with cathodal tDCS - decreased neuronal excitability/reduced behavioural performance - run the risk to oversimplify the pattern of possible behavioural and neurophysiological outcomes, especially outside the sensorimotor domain. This simplistic proposal does not take into account indeed the complex combination of excitatory and inhibitory connections within broader cortical networks, the dependence upon the network state activation, the level of performance or task engagement, the well-known inter-individual variability

and other factors affecting the current diffusion in the brain, such as different neural population and orientation (see Fertonani & Miniussi, 2017).

The contribution of inter-individual factors should also be taken into account when discussing the present results. In a recent and well done review (Li, Uehara, & Hanakawa, 2015), the role of these factors – such as neurophysiological state and features, anatomy, genetics, and age – has been deeply discussed in determining the tDCS response variability. In our study, the majority of these aspects has been considered in order to minimize the inter-variability effects. In particular, we homogenize the participants recruitment in relation to age and handedness. Moreover, since our experimental design was a within subject study, we tested each subject at similar times in the day for the two different experimental sessions. Nevertheless, it has been difficult to fully control the anatomical-functional differences. Even if an individual MRI has been used for each subject, this anatomical information guided the definition of TMS stimulation parameters only, while the tDCS ones have been kept fixed in order to have a direct comparison among all the subjects. This choice may have had an effect on the results since it is known that interindividual differences in the brain and cranial anatomy can affects how the tDCS current is received by the brain (Li et al., 2015).

Among these explanations, the most compelling seems to be the initial activation state of the target area. More specifically, whereas addressing motor functions could be done using simple tasks (i.e. reaction times) or passively (i.e. recording MEPs), exploring tDCS effects on cognitive functions entails the use of complex tasks, prompting high activations of the target regions. It is possible then, that the effect of cathodal tDCS are counterbalanced by the activations due to the task, leading to a null effect (Jacobson et al., 2012)

An alternative explanation is that the effects of tDCS may depend in an opposite way on the background level of activity in the system (Matsunaga et al., 2004). For instance, if cathodal stimulation reduces the level of neural discharge, then it may produce effects in systems with high levels of basal activity. However, if the resting state is characterized by low levels of spontaneous discharge, then cathodal tDCS may have little or no effect.

Recently, the results of Lafon et al. (2016) work unveiled how the effects of DC stimulation are dependent upon the location and frequency of active synapses, more than from the polarity of stimulation. Therefore, these data seem to indicate that the active state of the cortex, deriving from a concurrent brain activity such as task performance, could be a crucial aspect to take into account for tDCS application.

In conclusion, the results of the present study show no significant modulation of cortical excitability as measured by TEPs, when the cathodal tDCS is applied over the right parietal cortex. In contrast, previous studies showed a significant rise of cortical excitability stimulating the same

area at resting state (Romero Lauro et al., 2014, 2015); these results show a non-linear impact of anodal and cathodal stimulation on cortical excitability, in line with previous behavioural, neurophysiological and computational modelling studies. Another important point regarding our results is that we recorded TMS-EEG data while our participants were in resting state. We have recently shown how cortical excitability, as measured by means of TEPs, is modulated by the activation state of the target area (Pisoni et al., 2017). In particular, during task execution the induced rise of cortical excitability spread following functional rather than structural connections, encompassing only task relevant brain regions. Whether cathodal effects on cortical excitability would be different by administering a task involving the target region is a crucial question.

The next steps of this project focused on this crucial point in order to investigate if cathodal tDCS may produce different effects in systems with high level of basal activity. For this reason, we performed a new study using the same methodological setting, in order to compare the new data with the previous one, but, in this case, participants were involved in tasks during tDCS stimulation.

Chapter Five: “The effects of cathodal tDCS on high cognitive functions during task performance”

5.1 Chapter overview

This Chapter reports a behavioural study in which we tested whether the performance at a visuospatial working memory and attentional tasks, likely involving the right PPC, is modulated by cathodal tDCS applied to this brain region. As mentioned in the previous Chapter, indeed, we aimed at understanding whether the absence of cathodal tDCS effects over the right PPC at resting state could be due to the inactive state of the cortex. To test this chance, we planned a second TMS-EEG study (Chapter Six) in which participants will be performing a task during the stimulation. For the sake of comparability among these studies, we wanted to keep the right PPC as a target of cathodal tDCS. Therefore, we first needed to find a task sensitive, at least at a behavioural level, to the modulations induced by cathodal tDCS.

5.2 Introduction to the behavioural Study

The right parietal cortex plays a crucial role in several cognitive functions, among which Working Memory and Attention, which play a crucial role for the adaptation in our everyday life, even if we are generally not aware about it.

Impairments of these cognitive functions are frequent concomitant symptoms in several psychiatric and neurologic diseases. For instance, patients suffering from Alzheimer’s disease (AD) (Huntley & Howard, 2010), as well as the ones affected by Parkinson’s disease (PD - Lees & Smith, 1983; Lee, Nagano, Taylor, Lim, & Yao, 2010), exhibit specific deficits in visuospatial WM (VWM) performance. Furthermore, stroke could generate deficits in attention such as unilateral spatial neglect (Làdavas, Del Pesce, & Provinciali, 1989; Vallar, 1998) or spatial extinction, that consists in a reduced ability to detect stimuli in contralesional hemifield, whenever is present a competitor on the other side (Karnath, Himmelbach, & Küker, 2003). In addition to neurological populations, also psychiatric and psychopathological patients are widely affected by specific WM and attentional impairments, such as comprehensive visual WM abnormalities in patients with schizophrenia (Barch, Sheline, Csernansky, & Snyder, 2003) and depression (Rose & Ebmeier, 2006); or the difficulty in sustaining attention in ADHD child (Swaab-Barneveld et al., 2000). In the recent years, the use of NIBS, and in particular tDCS, has been growing as an alternative, or a combining, treatment for these particular pathological conditions, becoming also interesting for cognitive enhancement in healthy person.

Before going into the procedural details of the study, a brief introduction to the cognitive domains tested is provided.

5.3 Visual working memory

Working memory can be generally defined as our ability to temporary grab onto and hold in mind task-relevant information. It is a system with limited capacity that places restrictions to the amount of information that can be held within the storage, although the discussion about these limits remains still controversial (Baddeley, 2010; Cowan, 2010; Eriksson, Vogel, Lansner, Bergström, & Nyberg, 2015). WM has become a central construct in cognitive neuroscience, and one of the most successfully investigated domain within tDCS paradigms. This is not only due to its importance for a wide range of related cognitive abilities, but also its relevant role in several psychiatric and neurological disorders (Johnson et al., 2013; Perlstein, Carter, Noll, & Cohen, 2001; Santarnecchi et al., 2015).

Thanks to the pioneering work of Baddeley and Hitch, a multicomponent and more complex model of WM was first proposed in 1974, and then enriched and developed in further following versions (Baddeley & Logie, 1999; Baddeley, 2010). Since the beginning, this model put emphasis on the importance of the dynamic processing of the information, which occurs in addition to the storage. According to the model WM comprised an attentional control system (the central executive), which works in cooperation with two further slave storage systems – the visuospatial storage, which deals with visual information, and the phonological loop, for verbal material (Baddeley & Hitch, 1974; Baddeley, Logie, Bressi, Sala, & Spinnler, 1986). Subsequently the episodic buffer was also added: a mechanism with integrative function allowing for linking together visual and auditory information, and serving to aid in sending and retrieving information from episodic long-term memory (Baddeley, 2000).

For the aim of this dissertation, we will focus on visuospatial working memory (VWM) that is, as described for the first time in Baddeley and Hitch model (1974), the system responsible for the maintenance and detection of information in the visual modality. VWM is an essential psychological construct since it keeps enough traces of our visual world such that our perception of this world does not fall apart when, as an example, the vision is turned off momentarily during blackout periods due to blinks or eyes movements (Juan, Tseng, & Hsu, 2017). VWM capacity is limited as any other WM storage, and the limitations are reached when individuals try to retain from three to four pieces of information, as it has been observed by several different paradigms (Cowan, 2001; Luck & Vogel, 1997). The nature of this strict limit is related to the object complexity. The task performance, indeed, in most cases is less accurate for complex objects than for the simple ones (Awh, Barton, & Vogel,

2007; Brady, Konkle, & Alvarez, 2011). The theoretical bases for these limitations constitute two distinct yet related abilities. The first one, referred to as the VWM capacity (k), is the amount of information that can be held at any given time. The other one is the ability to gate access of information to WM, sometimes referred to as the control of attention or filtering (Cowan et al., 2005; Cowan, Naveh-Benjamin, Kilb, & Saults, 2006; Cowan & Morey, 2006; Vogel, McCollough, & Machizawa, 2005). Regard the extremely limited capacity of VWM, is general agreement to assume that its capacity is a flexibly divisible resource that can be spread among all the items in the display, but with fewer resources per item and therefore reduced precision as the set size increases. These theories can also be framed in terms of increased neural noise as the set size increases (Anderson, Vogel, & Awh, 2011; Luck & Vogel, 2013). Ideally, individuals can maintain and operate upon many goal-relevant pieces of information in the execution of effective ongoing cognitive processes. Further, people must prevent irrelevant data, either from the external stimulus environment or from internal representations, from gaining access to WM.

The neural correlates of WM are associated with a level of activity both in the dorsolateral prefrontal cortex (Curtis & D'Esposito, 2003; Postle, 2006) and in the posterior parietal cortex (Todd & Marois, 2005; Vogel et al., 2005; Xu & Chun, 2006). These findings were firstly derived from lesion-based studies in both humans and animal's models. They demonstrate the crucial role of the dorsolateral prefrontal cortex in the monitoring and manipulation of items during WM tasks (Barbey, Koenigs, & Grafman, 2013; Duncan & Owen, 2000; Miller & Cohen, 2001). Similarly, in animal models, electrophysiological single unit recordings studies demonstrated the involvement of PPC in working memory processes (Pesaran, Pezaris, Sahani, Mitra, & Andersen, 2002). This arises from the strong structural and functional connections with the DLPFC (Jarbo & Verstynen, 2015; Petrides & Pandya, 1999; Sauseng, Klimesch, Schabus, & Doppelmayr, 2005). In fact, the activation during WM tasks has been shown to co-occur across these two different regions (Friedman & Goldman-Rakic, 1994).

More recently, thanks to technological innovation, several techniques have been used to examine how WM operates. For example, different neuroimaging studies highlighted the topological complexity of the cerebral networks that underlying WM function, with multiple brain regions typically active during task performance. In particular, strong and consistent activations across fronto-parietal networks for both visuospatial and verbal WM tasks have been confirmed (Cohen et al., 1997; Darki & Klingberg, 2014; Klingberg, Forssberg, & Westerberg, 2002; Olesen, Westerberg, & Klingberg, 2004; Owen, McMillan, Laird, & Bullmore, 2005; Schlösser, Wagner, & Sauer, 2006). There are also evidences for a certain degree of hemispheric lateralisation, related to the specificity of WM task requests. With regards to VWM, stronger activations in the right hemisphere were often

demonstrated (D'Esposito et al., 1998; Rottschy et al., 2012; Sarnthein, Petsche, Rappelsberger, Shaw, & Von Stein, 1998; Smith et al., 1995). However, these findings have not been consistently replicated (e.g., Nystrom et al., 2000), and other studies have reported bilateral prefrontal involvement, also during visio-spatial tasks (Cohen et al., 1997; Haxby, Petit, Ungerleider, & Courtney, 2000; Nagel, Herting, Maxwell, Bruno, & Fair, 2013; Sarnthein et al., 1998). Nevertheless, a commonality between all of these findings is the observation of an increase in haemodynamic activity across fronto-parietal networks (Nee & D'Esposito, 2016; Rottschy et al., 2012).

Taken together, all these results contribute to define relevant cortical hubs for the application of NIBS-based approaches, such as tDCS, to explore complex brain-behaviour relationships through the modification of neural circuits involved in WM. However, among the cortical hubs, most of the studies have focused on DLPFC, while only a few of that have investigated the tDCS effects over PPC (e.g. Hill, Fitzgerald, & Hoy, 2016).

In one of that study, Heimrath et al. (2012) delivered anodal, cathodal and sham tDCS stimulation on right PPC during a delayed matching-to-sample working memory task, with a bilateral electrodes montage. In each trial, participants were presented with a memory array consisting of eight dots, with randomized colour and position, which appeared four on the right and four on the left side of the screen, to a fixation cross. Each participant took part in the three stimulation conditions, performed in different days, separated by at least 24 hours to avoid carry-over effects. The results showed a polarity dependent effect on VWM capacity, but in opposite direction respect to the well-known anodal-improvement/cathodal-impairment dichotomy. In particular, they observed a significant reduction of VWM capacity during anodal tDCS for stimuli on the left hemifield, and an increase of that the same capacity with cathodal stimulation compared to the sham condition. For ipsilateral stimuli, both anodal and cathodal tDCS significantly reduced visual WM capacity compared with sham stimulation (Heimrath, Sandmann, Becke, Müller, & Zaehle, 2012). These behavioural data were related to electrophysiological changes that report a significant decrease in oscillatory power in the alpha band for the cathodal tDCS over the parietal cortex. This apparent dissociation between an increase in performance and a decrease in power alpha band could be explained as a result of more general tDCS effects on the underlying fronto-parietal network involved in VWM (Heimrath et al., 2012; Keeser et al., 2011). In a similar study, Tseng et al. (2012) showed significant improvements in VWM capacity following anodal stimulation to the right PPC, compared with sham, but this effect interacted with the participant’s natural VWM capability. In particular, the authors observed that only individuals who had low baseline VWM capacity benefitted more from the stimulation concerning the high-performer. Also in that study behavioural data were confirmed by electrophysiological results showing an increase in N2pc and in contralateral delay activity (CDA),

which implies an improvement in the allocation of attention and memory access, only in the low-WM group compared to sham stimulation condition (Tseng et al., 2012). These results suggest that the effects of tDCS may only arise when participants have some room for improvement, even if Jones and Berryhill (2012) showed an opposite pattern of findings. More specifically, data reported a significant increase in VWM capacity following anodal and cathodal tDCS, compared with sham condition, for high-capacity individuals only. On the other hand, the low-WM group showed a decrease in VWM following both real tDCS stimulation sessions compared to the sham one. These findings provide evidence that parietal involvement in VWM performance depends on both VWM capacity and task demands. The authors speculated around these findings arguing that alternative VWM strategies could be employed by low and high level of VWM individuals (Jones & Berryhill, 2012). To better understand how different applications of tDCS over the right PPC affected different aspects of VWM, Heinen and co-workers (2016) performed a very interesting series of experiments in which they compared bilateral versus unilateral montage, and anodal versus cathodal tDCS polarity in the case of unilateral experimental design. They observed that VWM precision was enhanced when tDCS was applied bilaterally on PPC, independently from polarity. Nevertheless, in the experiment in which they compared the polarity effects on right PPC, when the reference electrode was placed on the opposite arm, the same enhancement in VWM precision was observed only after cathodal tDCS stimulation and exclusively for low-performers (Heinen et al., 2016). In order to study which brain regions are involved in VWM processes and how they interact with tDCS stimulation, in a more recent work Li et al. (2017) aimed to provide causal evidence for the neural dissociation of two mechanisms underlying VWM capacity, namely, the scope and control of attention. In their study, the researchers delivered anodal tDCS to three different areas across three different sessions separated by at least 48 hours: right prefrontal cortex (PFC), right PPC, and visual cortex (VC). In each session, participants completed a change detection task that required them to remember target stimuli and to ignore the distractors one, as well as to ignore the stimuli that appeared on the non-target screen side. The results showed a significant improvement in VWM capacity in the distractor-absent condition after anodal tDCS stimulation on the right PPC, whereas the same stimulation on the right PFC determined the same result but specifically for the distractor-present trials. These results suggest that the activation of right PPC determines the amount of information that can be maintained in VWM, whereas the right PFC is involved in the control of attention (Li et al., 2017). Starting from these results and using a very similar experimental design, Robison and collaborators (2017) performed a study aimed to disentangle the role of right PPC and right PFC in VWM processes (i.e., McNab & Klingberg, 2008; Vogel et al., 2005). The results, both for right PPC and right PFC, shown no significant effects induced by anodal tDCS on alteration of VWM performance.

The heterogeneous results reported in these studies highlight the existence of a non-linear interaction between attentional and VWM processes, as well as between these two cognitive functions and the underlying activity of the involved brain areas. It is likewise essential to take into account that the different results described until now could also be due to various methodological aspects. The differences, indeed, could also be dependent to the different tDCS montages used (intra-cephalic vs extra-cephalic), the different areas targeted, as well as various procedures (online vs offline) and different tasks employed.

Despite the heterogeneity of the results, all studies described so far seem to indicate the involvement of the right PPC in VWM tasks. By the way, to the best of our knowledge, only in the Heimrath et al. (2012) work was observed a significant enhancement in VWM performance after cathodal tDCS stimulation, targeting the right PPC. For this reason, in the present study, we selected the same specific task to better understand if and how the use of cathodal tDCS can modulate performance in such a task. If significant results will be obtained, then the selected VWM task could be considered a good choice for studying the cathodal tDCS mechanisms of action during task performance.

5.4 Visual attention

Attention is a fundamental cognitive process that can be defined as the ability to prioritise processing of goal-relevant information, in order to help humans in driving through a world overloaded of sensory inputs. Attention process refers to a series of cognitive operations in selecting, filtering, and using information for further processing (Lo, van Donkelaar, & Chou, 2019).

Historically, Posner and Petersen (1990) described the attention as a system articulated in three different networks: alerting, orienting and executive; each of them with an own anatomical location, circuitry and function. After twenty years, the two authors demonstrated their theoretical operation thanks to a significant amount of elaboration and evolution happened during that timeframe (Petersen & Posner, 2012).

The alerting network, that is the first part of the attentional system described by Posner and Petersen (1990; Petersen & Posner 2012), consists in triggering and sustaining an arousal status and engaging the reticular activating system, located in the brainstem and thalamus, as well as the parietal and frontal areas related to the norepinephrine system (Aston-Jones & Cohen, 2005; Lo et al., 2019; Moruzzi & Magoun, 1995).

The executive network, which mainly relies on the prefrontal cortex and the anterior cingulate gyrus, is associated with conflict resolution related to the limited capacity of the attention system (Cieslik, Mueller, Eickhoff, Langner, & Eickhoff, 2015; Dosenbach, Fair, Cohen, Schlaggar, &

Petersen, 2008). In particular, the role of the anterior cingulate gyrus is mainly related to a control function, whereas the fronto-parietal system is more related to real-time switching, initiation and adjustment of information processing (Dosenbach et al., 2008).

The spatial orienting consists in the ability to prioritise sensory inputs in order to allocate spatial attention to relevant parts of the visual field. The underlying network relies on cortical areas such as the superior and inferior parietal areas and the frontal eye fields, as well as subcortical regions, such as the pulvinar, thalamus and the superior colliculus (Corbetta & Shulman, 2002; Posner, 1980). Attention orientation can be driven by endogenous, top-down, or by exogenous, bottom-up, stimuli. In the first case, attention is wilfully directed to the left or right hemifield following a central cue, whereas exogenous stimuli generally are peripheral cues that oriented attention automatically. While endogenous orienting is associated with activity in a more dorsal fronto-parietal network, a mostly right-lateralized network of ventral frontal and parietal areas underpins exogenous orienting (Corbetta & Shulman, 2002).

Although these three networks were described as independent from each other, they cooperate closely together to accomplish goal-directed tasks (Petersen & Posner, 2012; Raz & Buhle, 2006).
In this work, we will focus on visuospatial attention orienting because, for this particular cognitive function, the PPC plays a critical role (Corbetta, Patel, & Shulman, 2008; Vandenberghe & Gillebert, 2009). The PPC is located at the portion of parietal cortex posterior to the primary somatosensory cortex. The intraparietal sulcus (IPS) separates the PPC into the superior parietal lobe (SPL) and the inferior parietal lobe (IPL). SPL and IPL represent two mechanisms: SPL, along with the superior frontal cortex, contributes to top-down or goal-directed actions, whereas IPL, along with the inferior frontal cortex, contributes to bottom-up or stimulus-driven effects, and establishes attentional priority maps and calibrating attentional weights (Corbetta & Shulman, 2002; Lo et al., 2019; Molenberghs, Mesulam, Peeters, & Vandenberghe, 2007). Moreover, Kravitz, Saleem, Baker, and Mishkin (2011) suggested that PPC contributes to the selection of relevant visuospatial signals for goal-directed movements and that are hemispheric specialisations to these contributions. More precisely, the cerebral activity appears to be lateralized to the hemisphere contralateral to the visual field to which attention is directed, but with an overall dominance of the right hemisphere. Right PPC, indeed, carries and processes visuospatial information from both the left and right visual fields (Heilman & Van Den Abell, 1980), and it directs spatial attention signals toward either side of space (Szczepanski, Konen, & Kastner, 2010).

These results appear to be confirmed by neuropsychological and clinical studies. In stroke patients, indeed, damage to the PPC often causes deficits in attention in the contralateral visual field, a condition known as unilateral spatial neglect (Kleinman et al., 2007; Làdavas et al., 1989; Suchan,

Rorden, & Karnath, 2012). This condition is typically longer lasting and it causes more severe following damages in the right hemisphere, compared to the left one (Molenberghs, Sale, & Mattingley, 2012; Vallar, 1998). Damages to the right PPC can also cause an additional neurological condition, spatial extinction. In this condition the detection of a stimulus on the contralesional side is reduced or eliminated only in the presence of a competing stimulus on the ipsilesional side (Karnath et al., 2003). Although extinction has been suggested as representing a mild form of neglect (Heilman, Bowers, Coslett, Whelan, & Watson, 1985), the two conditions seem to be associated with different lesion sites. Specifically, extinction has been associated with damage to the right PPC, whereas spatial neglect typically occurs after injury to more ventral cortical areas, in particular the right temporo parietal junction (Karnath et al., 2003; Molenberghs et al., 2012). It has been suggested that this dissociation may reflect the different pathological effects of disruption of the ventral (neglect) and dorsal (extinction) visual pathways (Milner & Goodale, 1995).

In agreement with what has been observed in patients, several brain stimulation experiments have revealed modulation of spatial attention after right, but not left, hemisphere stimulation. In Bolognini et al. (2010b) work, the authors applied anodal tDCS on right PPC during a brief presentation of target stimuli either on the left or on the right visual field, and they found a decrease in reaction time (RT) only for contralateral targets, in the left hemifield. Sparing and co-workers (2009) reported a tDCS polarity-dependent effect. In particular, they observed that anodal tDCS increased accuracy and reduced RT for contralateral stimuli, whereas cathodal stimulation impaired performance in detecting stimuli in the contralateral hemifield, but increased accuracy for stimuli presented bilaterally. However, other studies found opposite results. As an example, Filmer et al. (2015) observed a performance reduction for contralateral stimuli after anodal tDCS stimulation on right PPC, while, for bilateral stimuli, a polarity non-specific performance impairment was observed for both anodal and cathodal tDCS compared with sham stimulation. This discrepancy is unexpected if compared with the Sparing et al. (2009) study, in which they used a similar experimental design. They observed that cathodal stimulation over the right PPC increased performance for ipsilateral targets (Sparing et al., 2009), but decreased it for contralateral targets as well as for bilateral stimuli presentation (Filmer, Dux, & Mattingley, 2015; Sparing et al., 2009). A possible explanation of this discrepancy could be related to the role of right PPC in encoding ipsilateral stimuli, that is enhanced by cathodal stimulation.

To summarise, although some studies have reported unilateral modulations in the expected direction, thus polarity-dependent effects on RT and accuracy for stimuli in the contralateral hemifield, the overall findings were not consistent. When high cognitive functions are involved, the stimulation did not necessarily act in a polarity-dependent and linear way.

One of the most used tasks to tap attentional orienting is the Posner Cueing Task. The Posner Cueing Task is a neuropsychological test, formulated by Michael Posner (Posner, 1980), used to assess the ability to orienting attention. The task performance is measured through RT and accuracy response to target stimuli, to investigate the effects of covert orienting attention respect to different cue conditions. In the traditional paradigm, the participant seats in front of a screen, and he/she has to maintain the gaze on a fixation cross, which is placed at a central point. On the left and the right side of the cross, there are two boxes, in one of that, a target stimulus appears after a brief presentation of a cue. The participant is instructed to respond, indicating the target stimulus position, ignoring the one showing by the cue (Bashinski & Bacharach, 1980). Usually, two main types of cue are used. The endogenous one is commonly an arrow presented in the centre of the screen, namely the same position in which is focused the attention. The arrow can point the left or the right side of the screen. The exogenous cue, instead, is generally presented outside of the centre of the attentional focus, but still within the visual angle. The combination of cue and target position create two different scenarios: valid or invalid trials. In the valid trials, the cue pointed precisely the place in which will appear the target; while in the invalid trials, cue and target appear in the opposite side of the screen. In the original study, Posner used a ratio of 80% valid and 20% invalid trials (Posner, 1980). In this way, the participant learns that more likely the cue is valid, and this reinforces his/her tendency to orient the attention through the cue side. The performance comparison on valid and invalid conditions allows for the analysis of whether cues orienting attention to a particular area benefit or hinder the attentional performance. Since the participant is forced to maintain the gaze fixed in response to the cue, differences in response's RTs between valid and invalid conditions indicates that covert re-orienting of attention has been employed (Posner, Nissen, & Ogden, 2014).

So far, studies employing tDCS stimulation with Posner tasks have yielded to markedly different results. Bolognini et al., (2010a) applied anodal tDCS stimulation on the right PPC improving the performance, but surprisingly for both valid and invalid endogenous cues. In a very interesting study, Li and colleagues (2015) required to eighteen healthy right-handed participants to perform three different tDCS sessions on PPC: sham, and two real sessions with an intra-cephalic montage, namely right anodal and left cathodal (RA/LC), and left anodal and right cathodal (LA/RC). During each session, participants had to perform a number comparison task, which is a modified version of Posner task, a choice reaction task (CRT) and a rapid visual processing task (RVP). Results showed no tDCS effect on Posner task and RVP performance, while the stimulation affected both numerical performance and vigilance level in a polarity-dependent manner: anodal tDCS increased while cathodal decreased the abilities. In this study, the behavioural effects of tDCS seem to be related to high task demands, demonstrating the consequences of the interaction between stimulation

condition and cognitive load (Li et al., 2015). Using a more comprehensive version of Posner's paradigm that can measure spatial re-orienting, alerting and executive attention (see for details about Attention Network Test – ANT Fan, McCandliss, Sommer, Raz, & Posner, 2002), Roy et al. (2015) found that anodal tDCS on the right PPC enhanced spatial re-orienting for target presented in the contralateral left visual field, whereas the stimulation of left dorsolateral and left parietal cortex did not affect performance. These results were corroborated in a more recent study in which participants performed an Attentional Network Task before and after anodal or sham stimulation on the right PPC (Lo et al., 2019).

Taken together, all these results showed a heterogeneous panorama about the involvement of PPC in attentional processes and the possible modulatory effect induced by tDCS. The reason why relatively similar studies produce so disparate results could be related to methodological differences, and in particular to the use of different tDCS montages (intacefalic-extracefalic or bilateral-unilateral). It is crucial, indeed, to take into account that even if the referent electrode is generally considered silent, it actually plays an active role and the current spreads through the two electrodes, affecting different areas structurally and functionally connected to the target one (Romero Lauro et al., 2014, 2015). For this reason, the current flow could actually affect the activity of different areas that play different roles in the attentional network, and this pattern of activations could generate different behavioural outcome. Future studies need to investigate this field combining neuromodulatory and neuroimaging techniques, in order to obtain not only a behavioural output but also a direct observation of implicit indexes.

5.5 Summary

Despite the exploration of attention and visual working memory using tDCS is only at its beginning, the first results are encouraging, and they seem to show that this technique is a useful tool to enhance these high cognitive functions, even though further studies and investigations are required.

The crucial role of these cognitive functions in the daily life, and their active interactions (Baddeley, 2003; Juan et al., 2017), are the main reasons why we are interested in going more in-depth about the possible advantages in tDCS application. Inside this very promising area of research, we decided to perform a study to explore how the activity of different networks could be modulated by applying tDCS on right PPC that appears to be a junction area between the cerebral circuits that underlie these cognitive functions (Juan et al., 2017). Since the literature overview presented so far seems to underline the crucial role of right PPC for both VWM and visuospatial orienting attention, we oriented our choice on those tasks that underlying these cognitive functions, both for the behavioural than for the subsequent TMS-EEG study. In particular, in the following paragraph I will

describe the behavioural study in which our participants performed both a modified version of Posner task and a visuospatial working memory task, during tDCS stimulation.

5.6 Material and Methods

5.6.1 Participants

Thirty-eight healthy, right-handed volunteers (fourteen males, mean age = 22.8 years, SD ± 4.1, range 19-39, mean Oldfield) took part in the study. All participants declared to be right-handed, and this was confirmed by the Edinburgh Handedness Inventory (Oldfield, 1971; mean laterality coefficient = 0.88, SD=0.13).

Each participant completed the Adult Safety Screening Questionnaire (Keel et al., 2001) and gave informed written consent before study procedures. Participants with any contraindication to tDCS procedures were excluded (Rossi, Hallett, Rossini, Pascual-Leone, & Safety of TMS Consensus Group, 2009).

The experiment took place at the laboratory of the Psychology Department at the University of Milano-Bicocca. The local ethical committee approved the study, and the participants' ethical treatment was in accordance with the principles stated in the Declaration of Helsinki.

5.6.2 Procedure

Participants were tested in a single blind, sham-controlled and randomized study. Each subject underwent two different experimental sessions, which differed for the type of stimulation received, namely a real cathodal condition and the sham/placebo one. The two sessions were separated by at least 48 hours, in order to reduce any long-lasting effects (Nitsche et al., 2008). During the stimulation, participants had to perform two consecutive tasks: a modified version of the Posner Cueing Task (Posner, 1980), and a working-memory task (Vogel & Machizawa, 2004), displayed in a 1280 x 800 pixel PC screen settled at 80 centimetres in front of them.

The order of the two experimental sessions and of the tasks within the session were counterbalanced across subjects; both tasks were presented using E-Prime 2.0 software (Schneider, Eschman, & Zuccolotto, 2002 Psychology Software Tools, Pittsburgh, PA).

5.6.3 TDCS stimulation

TDCS was delivered using a BrainSTIM stimulator (EMS, Bologna, Italy) which provided constant current stimulation through a pair of rubber electrodes, covered by two rectangular synthetic sponges soaked by saline solution, in order to increase their conductivity and reduce the skull impedance. To achieve results comparable with the previous studies in which our research group targeting the right PPC (Romero Lauro et al., 2014, 2015; Varoli et al., 2018; described in Chapter

Four), we kept the same stimulation parameters. In particular, we used an intra-cephalic montage with the active electrode, namely the cathode (size=3x3 cm), placed over the right PPC, while the reference electrode, i.e. the anode (size=5x5 cm), positioned over the left supraorbital area. The location of the active electrode was determined according to the 10-20 EEG standard montage, placing the electrode over P2. In the real stimulation session, a constant current was delivered with an intensity of 0.75 for 15 minutes, and 10 seconds of fade-in/fade-out during which current ramped on and off (see Figure 4.1 in the Chapter Four for an estimate of the electric field induced by the stimulation). For the sham condition, the stimulator turned off automatically after 30 s, a procedure which is typically used to induce similar kin sensation as compared to the real stimulation and is known to be effective in blinding participants from their assigned condition (Ambrus et al., 2012; Gandiga et al., 2006; Woods et al., 2016).

5.6.4 Posner Cueing Task (PCT)

During the Posner Cueing Task, participants had to fix a central cross, located in the middle of the display, to the side of which there were two squares, one on the left and one on the right. After 2000 ms a bright cue appeared in correspondence of one of the squares for 80 ms. After an inter-stimulus interval, varying from 200 to 700 ms, a target stimulus appeared inside the right or left square. Participants were instructed to respond, as fast and accurate as they could, indicating the location of the target by pressing two different keys on a keyboard using their two index fingers. Two different combinations of cue and target location was possible: in the congruent or valid condition the target appeared on the same side of the bright cue; otherwise, if target and cue appeared on the opposite side, the condition was considered invalid or incongruent. A third situation was also possible when any target didn’t follow the bright cue, and the trial was considered neutral (false alarm - FA; see the Figure 5.1 for a procedure graphical representation). The task comprised 96 trials: 42 congruent (21 located on the right side and 21 on the left side), 42 incongruent (21 located on the right side and 21 on the left side), and 12 FA trials. Reaction time (RT) and accuracy of response were recorded.

5.6.5 Visual working memory task (VWMT)

The VSTM task was modified from Vogel and Machizawa (2004) and in Heimrath et al. (2012). It was made up of 106 trials, split into two blocks, separated by a 30 s time interval. In each trial, participants maintained their gaze fixed on a cross in the middle of the screen and, after 200 ms, an arrow appeared on the top of the fixation point, pointing either to the left or to the right hemifield, followed by a visual matrix. It comprised eight coloured dots (size= 80 pixels; diameter= 1.75 cm), half of them localized on the right side of the screen, while the other half on the left. Within any visual

matrix all the eight dots appeared with a different colour, and in a different position, varying within a rectangular portion of the hemifield. The possible colours combinations were BLACK (RGB = 0, 0, 0); WHITE (RGB = 255, 255, 255); YELLOW (RGB = 255, 255, 0); CYAN (RGB = 0, 255, 255); RED (RGB = 255, 0, 0); PINK (RGB = 255, 105, 180); ORANGE (RGB = 255, 128, 0); GREEN (RGB = 0, 153, 0); BLUE (RGB = 0, 0, 255); BROWN (RGB = 150, 75, 0). The colours and the positions were randomly assigned in order to avoid the compresence of two or more dots with the same shade and to reduce any sort of facilitation effects. The visual matrix lasted for 250 ms on the screen and was followed by a retention interval of 2000 milliseconds. After that, a coloured dot (target stimulus) appeared in concomitance with the fixation point, and participants had 2000 ms to establish if the target was included (80% of the trials) or not (20% of the trials) in the initial matrix taking into consideration its colour and ignoring its position (Figure 5.1). Participants were asked to press two different keys on the keyboard to perform their choices, using their index fingers.

We recorded the RT and response accuracy. Prior to the first experimental session, participants performed a training session in order to become familiar with the task. The training session was made up of 53 trials and each trial was supplied with a feedback of response.

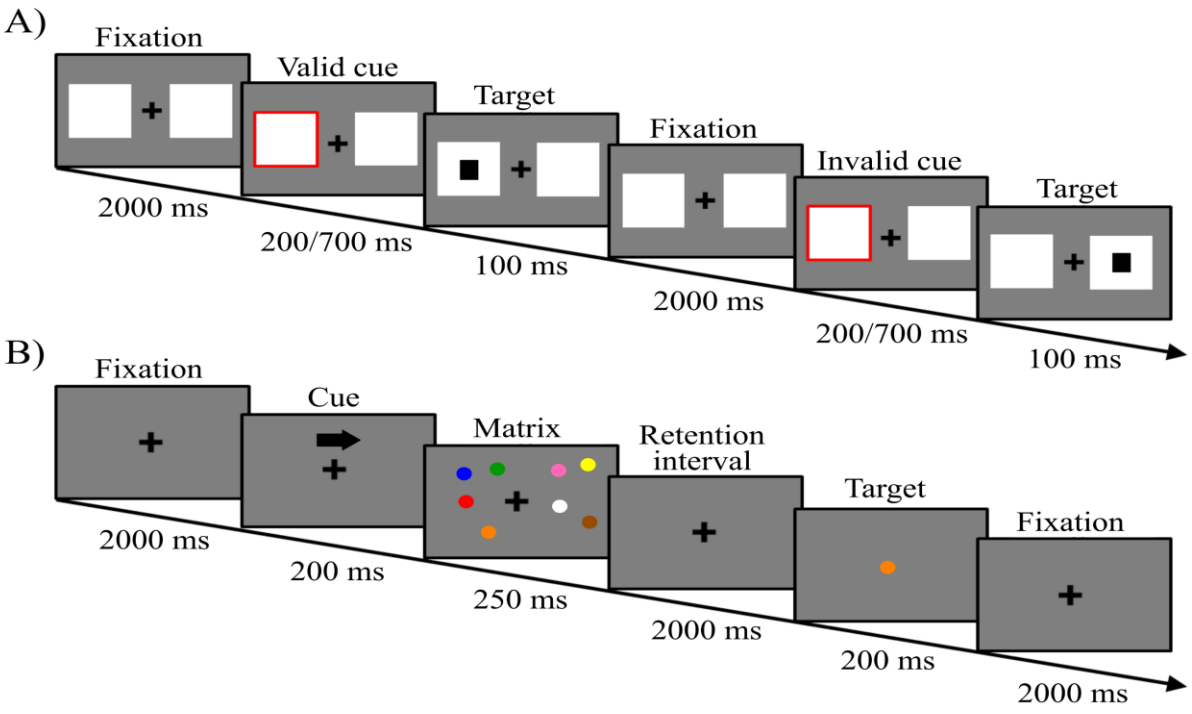

Figure 5.1: *Graphical representation of the tasks' procedure. In the panel A it is reported the procedure of the Posner Cueing Task, with an example of a valid (the first) and an invalid (the second) trials. In the panel B, it is presented the procedure of the Visuospatial Working Memory Task.*

5.7 Statistical Approach and Analysis

PCT and VWMT tasks were analysed separately. Statistical analyses were performed in the statistical programming environment R (R Development Core Team, 2019).

For each task, two steps of analysis were performed: firstly, we run a mixed model regression with the entire sample of participants; secondly, we performed the same statistical procedure splitting the sample according to the task order. Specifically, one subsample (*Sub1*), comprised to nineteen-participant, performing first the Posner Cueing Task and then the Visuospatial Working Memory Task; while the other subsample (*Sub2*) completed the tasks in the opposite order (first VWMT and then PCT).

For the Posner Cueing Task, the accuracy dichotomous variable was analysed using general mixed effects models (Baayen et al., 2008), fitted using the GLMER function of the "lme4" package (Bates, Maechler, Bolker, & Walker, 2015). RTs log-transformed values were analysed according to linear mixed effects regression using the LMER procedure available in the "lme4" R package (version 1.1-5, Bates et al., 2014).

Fixed predictors inclusion in the final models have been tested with a series of likelihood ratio tests by progressively removing those parameters which did not increased the overall model goodness of fit (Gelman & Hill, 2006). For RTs the automatic backward procedure *step* was used, while for the accuracy variable this procedure was performed manually[1]. For a detailed report of the results see the Supplementary Materials in Appendix 2.

A by-subject random intercept was included to account for participant-specific variability (Baayen et al., 2008).

Concerning the VWMT, in order to assess the individual WM performance, we calculated the WM capacity K factor (Cowan, 2001), for each tDCS condition (cathodal vs sham) and accordingly to the attending hemifield (left vs right). K factor was estimated for each subject by performing the following formula: K =S (H–F). In the formula, K represents the number of items that can be held in WM from an array of S objects. It assumes that the target item would have been one of those held in memory respects to K/S of trials such that the performance will be correct on K/S on the change trials (= hit rate H). To correct for guessing, this procedure also takes into account the false alarm rate F (Heimrath et al., 2012). In the end, in order to mirror the statistical analysis performed in the Heimrath et al., 2012 work, K values were analysed using 2 × 2 repeated-measures ANOVA with the within-

[1] The R function *step* can be used only with linear variables and linear mixed models. Instead it does not work properly for dichotomous variables, as it is the variable accuracy in this case.

subject factor *Stimulation Condition* (two levels: cathodal and sham) and *Attended Hemifield* (two levels: left and right).

5.8 Results

5.8.1 Posner Cueing Task.

Two participants were removed from the analysis due to their chance-level performance (accuracy was lower than 50% in both sessions).

Baseline Performance

For the sham condition, statistical analysis was performed apart in order to obtain a behavioural baseline and verify the effectiveness of manipulation comparing our results with those usually observed in literature for the Posner Cueing Task.

Accuracy was analysed on 3456 data points. *Cue validity* (factorial, two levels: valid vs invalid) and *Target side* (factorial, two levels: left vs right) and their possible interaction were entered in the model as fixed factors.

The best fitting model included the simple effect of *Cue validity* since it was significant ($\chi^2_{(1)} = 21.8$, $p<.001$): as expected, accuracy was higher when the target appeared in the valid position (M= 99.7, SE ± 0.12) as compared to the invalid (M= 98.6, SE ± 0.41) one.

For the log transformation of the dependent variable RTs (log-RTs), statistical analysis was performed on 3253 data points, selecting only RTs of correct responses and within two standard deviations. In this case, the best fitting model was the one including the interaction between *Cue validity* and *Target side*. The main effect of *Cue validity* was significant ($\chi^2_{(1)} = 15,9$, $p <.001$), with slower RTs in the invalid condition than the valid one. The interaction effect also resulted significant ($\chi^2_{(1)} = 6.7$, $p =.009$), and post-hoc analysis performed with *fdr* adjustment method showed that when the target was presented on the left side of the screen the RTs were slower in the valid vs invalid condition ($p < .001$).

Main analysis: tDCS effects

The statistical analysis performed within the whole group, for the dependent variable accuracy, was run on 6912 data points. *Cue validity* (factorial, two levels: valid vs invalid), *Target side* (factorial, two levels: left vs right) and *Stimulation condition* (factorial, two levels: cathodal vs sham) and their possible interaction were entered in the model as fixed factors.

The best fitting model was the one including the simple effect of *Cue validity* ($\chi^2_{(1)} = 34.6$, $p<.001$): as expected accuracy was higher in the valid (M= 99.5, SE ± 0.13) vs invalid (M= 98.2, SE ± 0.30) condition.

Concerning log-RTs, analysis was run on 6532 data points. Indeed, correct response and values falling within the range of two standard deviations from the mean. The best fitting model was the one excluding the three-way interaction but including the two-way interactions between *Stimulation condition* and *Target side*, *Stimulation condition* and *Cue validity*, *Cue validity* and *Target side*, plus the three simple effects.

The simple effect of *Cue validity* was significant ($\chi^2_{(1)} = 7.4$, p=.006), with lower RTs in the valid condition despite of the invalid one. The simple effect of *Target side* showed a trend towards significance ($\chi^2_{(1)} = 3.4$, p=.064), with lower RTs when the target appeared on the right side compare to the left. No significant simple effect of *Stimulation condition* resulted.

Concerning the two-way interaction, the one between *Stimulation condition* and *Target side* was significant ($\chi^2_{(1)} = 5.0$, p=.025), and post-hoc analysis performed with *fdr* adjustment method showed that cathodal tDCS increased RTs when the target was presented on the right side of the screen (p = .008). The interaction between *Stimulation condition* and *Cue validity* was significant ($\chi^2_{(1)} = 8.2$, p=.004), post-hoc analysis showed a significant increase of RTs (p < .001) in the invalid condition during sham stimulation. The interaction between *Target side* and *Cue validity* ($\chi^2_{(1)} = 9.6$, p=.002) was also significant with higher RTs when the target appeared on the right side of the screen and the cue was invalid (p < .001).

Effect of task order

As second step, in order to control for the effect task order, we split the sample in the two subgroups described above: *Sub1* that performed first the VWMT and then the PCT, and *Sub2* for whom the task order was the opposite (PCT and VWMT).In both subgroups the statistical analysis was performed separately.

For *Sub1* accuracy, the best fitting model included the main effects of *Cue validity* ($\chi^2_{(1)} =$ 22,3, p<.001) coherently with results on the entire group and literature, the accuracy was higher in the valid (M= 99.7, SE ± 6.7 x 10^{-4}) vs invalid (M= 98.2, SE ± 6.7 x 10^{-3}) condition. Moreover, the model included the interaction between *Cue validity* and *Target side* plus the simple effect of *Stimulation condition* resulted with a trend of significance. In particular, the simple effect of *Stimulation condition* was significant ($\chi^2_{(1)} = 3.4$, p < .001) with lower accuracy during cathodal tDCS stimulation (M= 99.1, SE ± 2.7 x 10^{-3}) in comparison to the sham condition (M= 99.5, SE ± 1.9 x 10^{-3}). The interaction between *Cue validity* and *Target side* was significant ($\chi^2_{(1)} =$ 22,3, p<.001): post-hoc test revealed higher accuracy in the valid condition when the target appear on the right side (p < 001).

Concerning the log-RTs the best fitting model included the interaction between *Stimulation condition* and *Target side*, plus the three simple effects of *Stimulation condition*, *Cue validity* and

Target side. In particular, the main effect of *Stimulation condition* was significant ($\chi^2_{(1)}$ = 8.6, p=.003), with slower RTs in the cathodal tDCS condition vs sham. The main *Cue validity* effect also resulted significant ($\chi^2_{(1)}$ = 9.5, p=.002), with a decrease in RTs when the target appeared in the congruency with the cue. The interaction between *Stimulation condition* and *Target side* was significant ($\chi^2_{(1)}$ = 4.3, p=.038), and the post-hoc analysis revealed an increase in RTs during cathodal tDCS stimulation when the target was on the right side of the screen compared to the left one.

In the *Sub2*, the sample in which participants performed the PCT as the first task, the analysis on the accuracy showed as the best fitting model the one including the simple effect of *Cue validity* ($\chi^2_{(1)}$ = 14.6, p<.001): as in the other groups, accuracy was higher in the valid (M= 99.2, SE ± 0.21) vs invalid (M= 97.8, SE ± 0.43) condition.

Concerning the dependent variable log-RTs, the model that best describe the data included the interactions between *Stimulation condition* and *Target side,* plus *Stimulation condition* and *Cue validity*, and the simple effects of the three variables. The simple effect of *Stimulation condition* was significant ($\chi^2_{(1)}$ = 8.0, p=.005), with slower RTs in the cathodal tDCS condition vs sham. The interaction between *Stimulation condition* and *Cue validity* was significant ($\chi^2_{(1)}$ = 5.4, p=.020), post-hoc analysis showed a significant RTs increasing (p < .001) in the invalid condition during sham stimulation.

5.8.2 Visual Working Memory Task

Statistical analysis was performed on 148 observations on the entire sample. Results shown no significant effects of *Simulation condition* and *Target side* or their interaction.

Subsequently, the same statistical analyses were carried out on the two subgroups defined according to the order of tasks, the *Sub1* and *Sub2* described before. In both groups no significant results were found, neither as main effects nor as interaction.

5.9 Discussion

The study aimed to investigate the possible effects due to the application of cathodal tDCS over the right PPC on the performance at two different cognitive tasks, namely on visuospatial attention and one tapping visual working memory processes. Specifically, in the study, participants took part in two different experimental sessions, corresponding to two tDCS stimulation conditions: cathodal and sham condition. In both experimental sessions, during tDCS stimulation participants performed two separate tasks consecutively: a Posner Cuing Task, in order to assess the eventually tDCS effects on visuospatial attention orientation; and a Visual Working Memory Task, to evaluate the behavioural tDCS effects on the individual visuospatial working memory capacity. The order of

the two tasks was counterbalanced across participants, hence half sample performed first the Posner cuing task and then the VWMT (*Sub1*) and the other half the other way around (*Sub2*).

Baseline Performance

The results in the Posner Cueing Task at sham served as a baseline, since no effect of stimulation was expected. The results showed that the accuracy was higher and the RTs were lower in the congruent trials, namely when the target stimulus appears at the same side previously indicated by the cue. The main effect of *Cue validity*, both on accuracy and RTs, resulted from all the subsequent analysis that we performed, as a demonstration of the task effectiveness.

In the same line, analysis on the whole sample and in the *Sub2*, when the Posner Cueing Task was performed as the first task, showed an interaction between *Cue validity* and *tDCS stimulation*, according to which only in sham condition RTs were slower for invalid cues.

These results are in line with what the performance usually observed at PCT (Posner, 1980), thus they provide a manipulation check on the effectiveness of our task in visual attention orienting.

In sham condition, regarding only RTs, we also found an interaction between Cue Validity and Target Side, according to which when the stimulus appeared on the left side of the screen participants responded faster in congruent condition rather than in the incongruent one. The main effect of *Cue validity*, both on accuracy and RTs, resulted from all the subsequent analysis that we performed, as a demonstration of the task effectiveness.

Effect of Cathodal Stimulation

As stated, the performance at sham served as a baseline to detect eventual effect due to the real condition of stimulation, namely the cathodal one. The analysis performed on the whole sample showed no significant main effects of tDCS stimulation condition, neither on response accuracy nor on RTs. However, in RTs, interaction effects with the stimulation condition were observed. In particular, cathodal tDCS affected the performance, reducing the rapidity in orienting the attention on the right side of the screen, which, in our experiment, is the ipsilateral one. Moreover, cathodal tDCS eliminated the advantage for RTs in the valid cue condition, as observed in the sham condition, since no difference was observed between valid and invalid cues.

This result contributes to the previous knowledge about the role of right PPC in the cognitive process of orienting attention. Despite Li et al. (2015) did not observe any significant results induced by cathodal tDCS during the execution of the Posner Cuing Task, our data seem to demonstrate an opposite trend. Specifically, in our study, cathodal tDCS stimulation, applied on the right PPC, appears to disrupt attentional reorienting after a cue, cancelling the advantage for the valid ones. Moreover, this effect seems to be particularly pronounced when attentional reorienting occurs towards the ipsilateral hemifield, regardless of the type of cue.

Our results are in line with previous ones that investigated the role of different parietal areas in attention orienting processes. For instance, in a TMS study in which slow (1 Hz) rTMS was applied on right frontal eye field area (FEF) before performing a spatial cueing task, the authors observed slower RTs for valid trials only (Sauseng, Freunberger, Feldheim, & Hummel, 2011).

In another experiment, to probe the attentional function of the parietal cortex, a rapid train of event-related rTMS was delivered on the angular gyrus (AG) synchronously with cue onset. The results reflected an impairment of spatial attention by a slowing RTs on valid trials and a recovery of RTs on invalid trials, consistent with attenuated orienting toward the cue (Chambers, Payne, & Mattingley, 2007).

Overall, these results indicated that disruption of the right parietal regions impaired covert orienting attention to visual targets. Thus, it is possible to remark the crucial role of the right parietal cortex for orienting spatial attention (Chambers et al., 2007).

The selective effect of cathodal tDCS on the stimuli appearing in the right field seems to be partially in line with the data previously reported by Filmer et al. (2015). The authors observed contrasting effects of anodal and cathodal tDCS on the perception of single and competing stimuli. In particular, both anodal and cathodal tDCS affected the performance in detecting stimuli that appeared bilaterally. This effect suggests dissociable neural coding properties within the right PPC that our data partially confirmed.

Effect of Task Order

It is presumable that the long-term effect of tDCS and the coupled plastic effect of Long-Term Potentiation/Depression need a certain amount of time to occur (Kronberg, Bridi, Abel, Bikson, & Parra, 2017; Monte-Silva et al., 2013; Ranieri et al., 2012). Therefore, the effect of tDCS on a task might differ according to the timing at which the task occurs since the stimulation onset. In our sample, the task order was counterbalanced across participants. meaning that half of the participant performed first the VWMT and then the Posner (*Sub1*) and the other half first the PCT and then the VWMT (*Sub2*). For this reason, we run a further analysis comparing the effect on PCT according to the timing at which the task was performed, namely immediately after the 30 seconds fade in interval (as a first task, *Sub2*) or after 7 minutes from the stimulation onset (as a second task, in *Sub1*)

A principal effect of cathodal stimulation on both accuracy and RTs resulted in the subgroup that performed the PCT as the second task (*Sub1*). In this group, participants resulted less accurate and with slower RTs during cathodal tDCS as compared to the sham condition. This result was also observed in the second subgroup (*Sub2*), but only for the RTs and in a less consistent way concerning the power of the effect.

Therefore, the disruptive effect of cathodal tDCS over PPC in reorienting the attention becomes even more evident, affecting both RTs and accuracy when the task is performed after a certain amount of time since the stimulation onset.

In literature, to best of our knowledge, no cognitive studies have specifically addressed the minimum duration of stimulation required to stabilize the current flow, and not many studies have discussed which is the best timing for tDCS delivery and task performance, either. On the other hand, many works have investigated the optimal timing for combining tDCS with different cognitive tasks in order to maximize the behavioural effects after the end of the stimulation (e.g. Martin et al., 2014; Pirulli et al., 2013; Stagg & Nitsche, 2011).

For instance, Pirulli et al. (2013) demonstrated how the same tES protocols, with different timing, can bring to opposite effects on the performance. In particular, they showed how the impact of anodal tDCS is grater when applied offline, namely after task execution, rather than online. Even though the online anodal tDCS triggered initial facilitation, this effect was quickly followed by an absence of enhancement in the successive blocks. It could be explained by the fact that anodal tDCS generates an initial depolarization of the neuronal membrane, with an intracellular increase of the ions Na+ and K+. However, prolonged exposure to the anodal tDCS can consequently cause an excessive concentration of these ions, that induces a saturation resulting in a rebalancing of this ion channel conductance. This kind of response can prevent further enhancement of behavioural performance and, even more, it may become an inhibitory effect in case of longer stimulation timing (Monte-Silva et al., 2013; Pirulli et al., 2013). If the stimulation is given alone, before the task, this sort of saturation mechanism could not take place. Therefore, the observed enhancement effects of the offline anodal tDCS can be caused by an optimal intracellular concentration of the ions Na+ and K+. However, these data cannot be generalized to any cognitive functions.

In Martin and co-workers (2014) study, indeed, the authors showed that online anodal tDCS could better enhance skill acquisition in working memory task. Results in the same direction was found in another study that investigated the timing-dependence of interactions between anodal tDCS and motor learning (Stagg & Nitsche, 2011). The authors performed different studies on healthy participants in which they delivered different tDCS stimulation polarity during the execution of an explicit sequence-learning task. They found that the application of tDCS during task led to a polarity-dependent behavioural modulation: compared to sham condition, anodal tDCS enhanced the learning ability, while cathodal stimulation was associated with slower performance. Offline tDCS, instead, led to slower learning for both the polarities, when compared with sham.

Taken together, these results from previous studies shed light on the relevance of stimulation timing, suggesting that tDCS effects are strictly dependent on the level of activation of the neuronal population involved in the task, as well as on the cognitive function targeted (Pirulli et al., 2013).

Although the results are not always coherent, the more pronounced tDCS effects seem to occur when it is delivered online instead of offline. In online protocols, however, whether and how it matters the amount of time since the onset of stimulation, it is still not clear.

Usually, in online experiments, participants are initially stimulated at rest for a variable time, at least 5 - 10 minutes before the onset of the task (e.g. Boggio et al., 2006). Accordingly, our neurophysiological data on anodal tDCS (Romero Lauro et al., 2014) showed significant effects both during and after the end of the stimulation. More specifically, in our experiment, TMS-EEG recording during stimulation started around seven minutes after the onset of the stimulation. While, in the study presented here, the online tasks were performed immediately after the starting of tDCS stimulation. The absence of an interval between the start of stimulation and the onset of the task might explain why the observed cathodal stimulation effects were less marked when the task was performed as first task. As argued before, the reason could be that tDCS effects require a certain amount of time to appear. Accordingly, when Posner task is executed after a certain amount of time, (around 7 minutes) tDCS begins to be effective.

However, regarding the specific domain of tDCS effects on right PPC, in Li et al. (2015) study, the Posner task started 10 min after the onset of stimulation during which participants listen to an audio podcast. Even so, the authors did not observe any tDCS effects on performance.

Therefore, at least for the stimulation of right PPC, it seems that there might be an optimal time window to perform a task under the effect of the stimulation, which presumably falls within the stimulation duration but after a certain amount of time (around 7 minutes). This issue needs to be further explored, taking into account not only the behavioural response but also neurophysiological data.

Concerning the VWMT, our results did not confirm those of other research in the literature (Heimrath et al., 2012; Tseng et al., 2012). We did not observe any significant effect due to tDCS stimulation on WM capacity.

A possible explanation may lie in the task complexity, that required cognitive functions not exclusively and closely related to the visuospatial working memory. Thus, the task might require the activation of a wider network of areas, than those directly stimulated by tDCS.

It is therefore important to be cautious in connecting precise cognitive processes to a single area, generally the one closest to the target electrode: other neighbouring regions could be involved, as well as influenced by current widespread, leading to a modulation of more extensive cortical

networks (Filmer et al., 2015; Romero Lauro et al., 2014, 2015). Berryhill et al. (2014) reported how, in addition to other factors (such as sample homogeneity and motivation of participants), the difficulty of the task could influence the results of performance in cognitive tasks. The latter, indeed, must be balanced to allow the tDCS effects clearer. Thus, according to Berryhill et al. (2014), the experimental design should include adaptive tasks, so that each participant can perform a demanding task, regardless of his working memory capacity. Other differences concerning the experimental design and the methodology may help to clarify the reasons why our results did not replicate those reported in the Heimrath et al. (2012) study. As mentioned above, a crucial element is the number of trials. Notably, in the present study, the task consisted of 96 trials: this number was certainly smaller if compared to the 256 one in the Heimrath et al. (2012) study. This significant reduction of the trials number was necessary to ensure that both the tasks were performed within the stimulation time window, that was of 15 minutes. Moreover, the stimulation interval differs in the two studies: in the Heimrath et al., (2012) work the stimulation session ended after 30 minutes, while in our study the tDCS stimulation last after 15 minutes. Finally, also the intensity of stimulation differs in the two experimental designs, being equal to 0.75 mA in the current experiment, while in the Heimrath experiment was 1 mA.

In our experiment, the choice of these specific stimulation parameters was based on the need to obtain data that could be compared with our previous studies. In particular, we were interested in understanding which task and cognitive function, underlying the right PPC, was effectively modulated by cathodal tDCS.

As mentioned above, the first aim of this project is to investigate the cathodal tDCS mechanisms of action, both at resting state and during task execution. Namely, when the basal level of activity in the target area has already been modified by the concurrent execution of a task (Lafon et al., 2016; Matsunaga et al., 2004). Specifically, from our behavioural study, the most effective and sensitive behavioural paradigm described resulted the one with the VSWM as the first task and the PCT as the second, therefore this will be the one used in the next experiment, in which the modulations of cortical excitability induced by tDCS during the execution of a task will be investigated with the use of the integrated TMS-EEG system. On the basis of our results, we expect to find a behavioural effect only at the PCT.

Chapter Six: "Tracking the effects of cathodal tDCS during task performance by means of TMS-EEG"

6.1 Chapter overview

In this Chapter, the third study of this project will be presented. Specifically, starting from the results discussed in the previous Chapter, a second TMS-EEG study was conducted in which the participants, during cathodal tDCS stimulation, were no longer at rest but engaged in the execution of a task. The purpose of this third and final study is exactly to investigate whether and what kinds of modulatory effects on cortical excitability can be observed following cathodal tDCS stimulation when the target area has already been activated by the execution of a task.

6.2 Introduction to the experiment

The results of the previous study shed light on the feasibility of using cathodal tDCS over PPC to modulate task performance. In particular, we applied tDCS on the right PPC during the execution of attentional and working memory tasks, which are cognitive function involving this area. We observed an increase of RTs in PCT that could be related to a tDCS induced modulation of cortical excitability and reactivity of this brain area. Starting from these results, in this third study, we were interested in understanding how this behavioural change could be translated at cerebral level. In particular, we sought to track changes in cortical activity and signal spread through the areas involved in the attentional and working memory network. Lafon and colleagues (2016) suggested that the effects of tDCS are more dependent to the level of basal activity than to the polarity of the stimulation, and, consequently, cathodal tDCS may produce observable effects in systems with a high level of basal activity. Moreover, in a recent study with TMS-EEG, Pisoni et al. (2018) observed that during task execution the rise of cortical excitability induced by anodal tDCS spread following functional connection involving only brain regions crucial for the task execution.

In the following experiment, we are interested in investigating the effects of cathodal tDCS on cortical excitability when delivered during the execution of a task involving the stimulated region.

6.3 Material and Method

6.3.1 Participants

Sixteen healthy, right-handed volunteers (seven males, mean age 25.2 years, SD 3,6, range 20-33) took part in the study. Each participant completed an Adult Safety Screening Questionnaire (Keel et al., 2001) and gave informed written consent prior to study procedures. The right-handed was confirmed by performing the Edinburgh Handedness Inventory for all participants (Oldfield, 1971; mean laterality coefficient = 0.88, SD= 0.15). Also for this experiment, we verified that

participants did not report contraindications to non-invasive brain stimulation (Rossi et al., 2009). The study was performed in the TMS-EEG laboratory of the University of Milano-Bicocca, was approved by the local Ethics Committee and it was carried out in accordance with the ethical standards of the revised Helsinki Declaration.

6.3.2 Procedure

As in the previous TMS-EEG study described above, for each participant, the experimental session consisted of two blocks of TMS-EEG recordings performed before (pre-tDCS) and 10 minutes after tDCS stimulation (post-tDCS). TEPs was recorded on left PPC; see. Figure 6.1 for a graphical explanation about the procedure. Each recording session lasted about 7 min, during which 180 pulses were collected, and participants remained in a resting condition, fixating a white cross on a black screen (17’’).

Differently from the previous TMS-EEG study at resting state (Chapter Four), here during tDCS participants were asked to perform the two tasks selected and described in the second study: the VWMT, and the PCT, performed in this specific order. We decided to not randomise the tasks’ order because, in the second study, results showed greater evidence of cathodal tDCS effects when the PCT was performed as second task (see discussion Chapter Five, Paragraph 5.6.), whereas no effects emerged for VWMT regardless of the order.

All participants took part to two experimental sessions, performed at least one week apart, corresponding to cathodal and sham tDCS condition. The order of the two sessions (cathodal and sham tDCS) was counterbalanced across subjects.

For collecting data comparable to the previous one, we performed the experiment with the same tDCS and TMS parameters used in the Varoli et al. (2018) experiment (see also Chapter Four). In particular, tDCS was applied (0.75mV intensity) with an intra-cephalic montage, with the cathode (3x3 cm) over the right PPC (P2), and the anode (5x5 cm) in the contralateral supraorbital region. Duration was 15 minutes for the real (cathodal) stimulation and 30 sec for the sham condition.

In TMS-EEG recording, single pulses TMS were delivered to the left PPC while concomitantly recording EEG from a 60 channels cap. Mean stimulation intensity, expressed as a percentage of the maximal output of the stimulator, was 64%, (range = 60 - 73%), corresponding to an electric field of 105 ± 12 V/m. Participants heard a noise-masking trace during the TMS-EEG recording

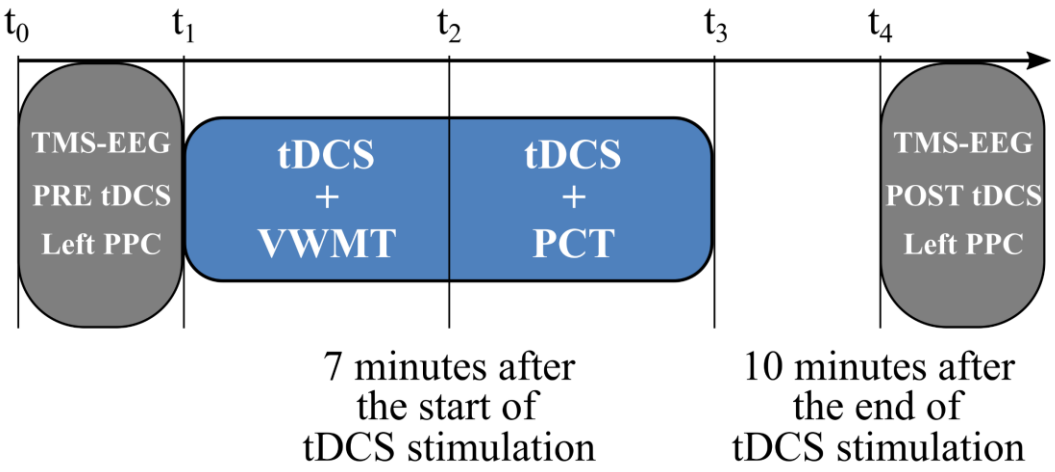

Figure 6.1: *Graphical explanation of TMS-EEG experimental procedure. The arrow on the top represents the experimental timeline. The grey boxes represent the two TMS-EEG recording sessions, one before and one after tDCS stimulation. To be able to compare the data of the two TMS-EEG studies, the TEPs recording sessions post tDCS was performed 10 minutes after the end of tDCS stimulation (t4). The blue box represents the tDCS stimulation session. For all the participants at t1, immediately after the switching on of the tDCS, the VWMT started; at t2, 7 minutes after, started the PCT.*

6.4 Results

6.4.1 Behavioural data

Statistical approach

In order to compare the results, we mirrored the statistical analysis performed in the second study described before (for more detail about statistical approach see the paragraph "Statistical Approach and Analysis"). PCT and VWMT data were analysed separately, and statistical analyses were performed in the statistical programming environment R (R Development Core Team, 2019).

For PCT the dependent variable accuracy was analysed using general mixed effects models (Baayen et al., 2008), fitted using the GLMER function of the lme4 package (Bates et al., 2015). RTs values were analysed according to linear mixed effects regression using the LMER procedure available in the "lme4" R package (version 1.1-5, Bates, Maechler and Bolker, Walker, 2014). Fixed predictors inclusion in the final models have been tested with a series of likelihood ratio tests by applying a backward selection procedure to simplify each statistical model, thus eliminating non-significant fixed effects. For RTs, *step* function from *lmerTest* package (version 2.0, Kuznetsova et al., 2015) was used to automatically perform backward procedure. Details of model selection are reported in the Supplementary materials in the Appendix 3.

For the VWMT as in the behavioural study we calculated the WM capacity K factor (Cowan, 2001), for each tDCS condition (cathodal vs sham) and accordingly to the attending hemifield (left vs right). K factor were then analysed using 2 × 2 repeated-measures ANOVA with the within-subject

factor *Stimulation Condition* (two levels: cathodal and sham) and *Attended Hemifield* (two levels: left and right).

Results of Posner Cueing Task

Statistical analysis was performed on 2880 data points. The best fitting model for the dependent variable accuracy was the one including the two main effects of *Cue validity* and *Target side*. The simple effect of *Cue validity* was significant ($\chi^2_{(1)}$ = 12.1, p<.001): as expected accuracy was higher in the valid (M= 99.2, SE ± 36.4) vs invalid (M= 97.9, SE ± 30.3) condition. The simple effect of *Target side* was at the boundary of significance ($\chi^2_{(1)}$ = 3.7, p=.055), accuracy was higher for the right (M= 98.9, SE ±33.8) as compared to left side (M= 98.2±30.9).

Concerning RTs, analysis was run on 2717 data points. The best fitting model was the one including the interactions between *Stimulation condition* and *Target side* and the one between *Cue validity* and *Target side*, plus the three simple effects.

Crucially, the simple effect of *Stimulation condition* was significant ($\chi^2_{(1)}$ = 7.9, p=.005), with slower RTs during the cathodal as compared to sham stimulation. The interaction between *Stimulation condition* and *Target side* was significant $\chi^2_{(1)}$ = 4.8, p=.028), post-hoc analysis with *fdr* method showed that cathodal tDCS increased RTs when the target was presented on the left side of the screen (p < .001).

The interaction between *Target side* and *Cue validity* was also significant $\chi^2_{(1)}$ = 3.9, p=.048), post-hoc analysis showed a trend for slower RTs when the target appeared on the left side of the screen and the cue was invalid (p=.157).

Results of Visual Working Memory Task

Statistical analysis was performed on 60 observations on the entire sample. The results showed no significant main effects as well as no significant interaction effects between *Simulation condition* and *Target side*.

6.4.2 TMS-EEG data

Statistical analysis approach

In order to directly compare the results of the two TMS-EEG studies with cathodal tDCS over PPC, namely at resting and during task performance, also for this data we performed the same statistical analysis described above, in Chapter four. In particular, we calculated the GMFP and the LMFP values for three time-windows: 0-50 ms, 50-100 ms, 100-150 ms. Then we submitted this data to a series of linear mixed models (Baayen et al., 2008), using the "lme4" package (version 1.1 5 Bates, Maechler and Bolker, Walkers, 2014) of R statistical software (R Development Core Team, 2019).

To further explore the cortical response before and after tDCS stimulation, the different conditions were then compared through a cluster-based permutation test (Maris & Oostenveld, 2007) implemented in the FieldTrip MATLAB toolbox for M/EEG analysis (freely available at http://fieldtrip.fcdonders.nl/; Oostenveld, Fries, Maris, & Schoffelen, 2011). This procedure solves the multiple comparisons problem by permuting the data and clustering them based on temporal and spatial proximity. More precisely, a big number *N* of data permutations are performed by shuffling the stimulation conditions, and then t-tests are computed at each time point for each permutation. Samples with statistics corresponding to a p-value smaller than a critical value are clustered together based on temporal and spatial proximity.

Cluster-level statistics are calculated by taking the sum of the t-values within each cluster. Finally, the cluster-corrected threshold is computed as the permutation distribution of the maximum cluster-level statistics (Maris & Oostenveld, 2007). This procedure avoids a priori definition of time windows and electrode clusters of interest.

In our analyses, for each comparison, 10000 permutations were performed with a permutation-significance level of p = 0.05 for the time-window between 0 and 300 milliseconds from the TMS onset.

To perform the analysis at sources level coherently, we started from the results of the cluster analysis at sensors. The same analysis and the whole procedure were also used to analyse data from sham sessions.

6.4.2.1 Cathodal stimulation - Sensor analysis

GMFP

In the model that was finally used to describe the GMFP values, the main effect of *Condition* did not result significant. This result means that GMFP did not change when TEPs were recorded before and after cathodal tDCS stimulation. Specifically, the model did not include the main effect of *Condition* in the 0-50 ms ($\chi^2(2) = 0.12$; p=.73), in the 50-100 ms ($\chi^2(2) = 1.04$; p=.31) and in the 100-150 ms ($\chi^2(2) = 0.04$; p=.85) time-windows. Bayesian repeated ANOVA analysis provided only a low moderate support in favour of the null hypothesis. This result was true for all the three time-windows (0-50 ms: $BF_{01}= 2.8$; 50-100 ms: $BF_{01}= 2.3$; 100-150 ms: $BF_{01}= 3.0$; JASP – version 0.11.1.0; JASP team, 2017).

LMFP

Analyses performed on LMFP values did not indicate any effect of cathodal tDCS in any of the considered clusters of electrodes. Below the results for the four clusters of electrodes are given in details.

Concerning C1, the cluster corresponding to the left PPC, namely the TMS hot spot, and covered from CP1, CP3, P1, and P3 electrodes, LRT indicated not to include *Condition* in models for any time-window (0-50 ms: $\chi^2(2) = 2*10^{-4}$; p=.98; 50-100 ms: $\chi^2(2) = .09$; p=.76; 100-150 ms: $\chi^2(2) = 0.06$; p=.81). Also in this case, Bayesian analyses showed a moderately low support to the null hypothesis, indicating no effect of tDCS on LMFP computed in this specific cluster, in any of the three time-windows (0-50 ms: $BF_{01}= 2.1$; 50-100 ms: $BF_{01}= 2.9$; 100-150 ms: $BF_{01}= 3.0$).

Considering C2, the cluster under the tDCS cathode and corresponding to the electrodes CP2, CP4, P2, and P4, the model on LMFP values did not include the main effect *Condition* in the first ($\chi^2(2)= 0.81$; p=.37) second ($\chi^2(2)= 0.09$; p=.76) and third ($\chi^2(2)= 0.63$; p=.43) time-window. In particular, Bayesian analyses gave a moderately low support to the null hypothesis, indicating no effect of tDCS on LMFP computed in this specific cluster for the first ($BF_{01}= 2.1$), the second ($BF_{01}= 3.0$) and the third ($BF_{01}= 2.4$) time-window.

Similarly, in C3, the left frontal cluster (F1, F5, FC1, and FC3), the analysis did not include the main effect of *Condition* in models for any time-window (0-50 ms: $\chi^2(2) = 0.67$; p=.41; 50-100 ms: $\chi^2(2) = 0.99$; p=.31; 100-150 ms: $\chi^2(2) = 0.24$; p=.62). Again, Bayesian analyses gave a moderately low support to the null hypothesis, indicating no effect of tDCS on LMFP computed in this specific cluster in any time-window (0-50 ms: $BF_{01}= 2.5$; 50-100 ms: $BF_{01}= 2.7$; 100-150 ms: $BF_{01}= 2.6$).

As last, on C4, the right frontal cluster (F2, F6, FC2, and FC6), the final model did not include the main effect of *Condition* neither in the 0-50ms ($\chi^2(2) = 0.12$; p=.73), nor in the 50-100ms ($\chi^2(2) = 1.64$; p=.20), nor in the 100-150ms ($\chi^2(2) = 0.06$; p=.81) time-windows. Even in this case, Bayesian analysis gave a moderately low support to the null hypothesis, indicating no effect of tDCS on LMFP computed in this specific cluster in any of the time-windows (0-50 ms: $BF_{01}= 2.5$; 50-100 ms: $BF_{01}= 2.6$; 100-150ms: $BF_{01}= 2.6$).

6.4.2.2 Cathodal Stimulation - Cluster analysis

To explore the possible presence of a modulatory effect due to cathodal tDCS stimulation, without assuming a priori certain time window and regions of interest, we performed also a cluster analysis taking into consideration the 0 - 300 ms TEP time window, from the TMS onset. The time interval was chosen observing the presence of relevant picks from in the butterfly plots, which occurred, as usual (Casarotto et al., 2010), in the first 300ms.

As described in the Chapter Three (see Paragraph 3.6.3) this is a statistical procedure that allows analysing the TEPs amplitude by correcting for multiple comparisons, and then by permuting the data and clustering them based on their spatial and temporal proximity. All samples with a statistic corresponding to a P-value smaller than .05 are thus clustered together because of spatial proximity.

The butterfly plot in Figure 6.2 shows average TEPs recorded on left PPC before and after tDCS stimulations. A cluster-based analysis testing the effect of tDCS stimulation (Pre vs Post) revealed a significant positive cluster ($p < 0.02$; Pre > Post) in frontoparietal electrodes in a time-range from 180 to 230 ms from the TMS onset. TEPs’ scalp topographies of statistically significant differences (Figure 6.6) showed that the positive cluster was associated with frontocentral electrodes and covered a bilateral portion of brain regions.

In order to compare more directly and coherently the results of the two TMS-EEG studies described in this work, the Cluster analysis was run also on the TMS-EEG data collected with cathodal tDCS stimulation at rest. The cluster-based analysis tested the tDCS effects comparing both During and After tDCS condition to the Pre (Pre vs During and Pre vs Post). No significant positive nor negative clusters were found for both the comparisons.

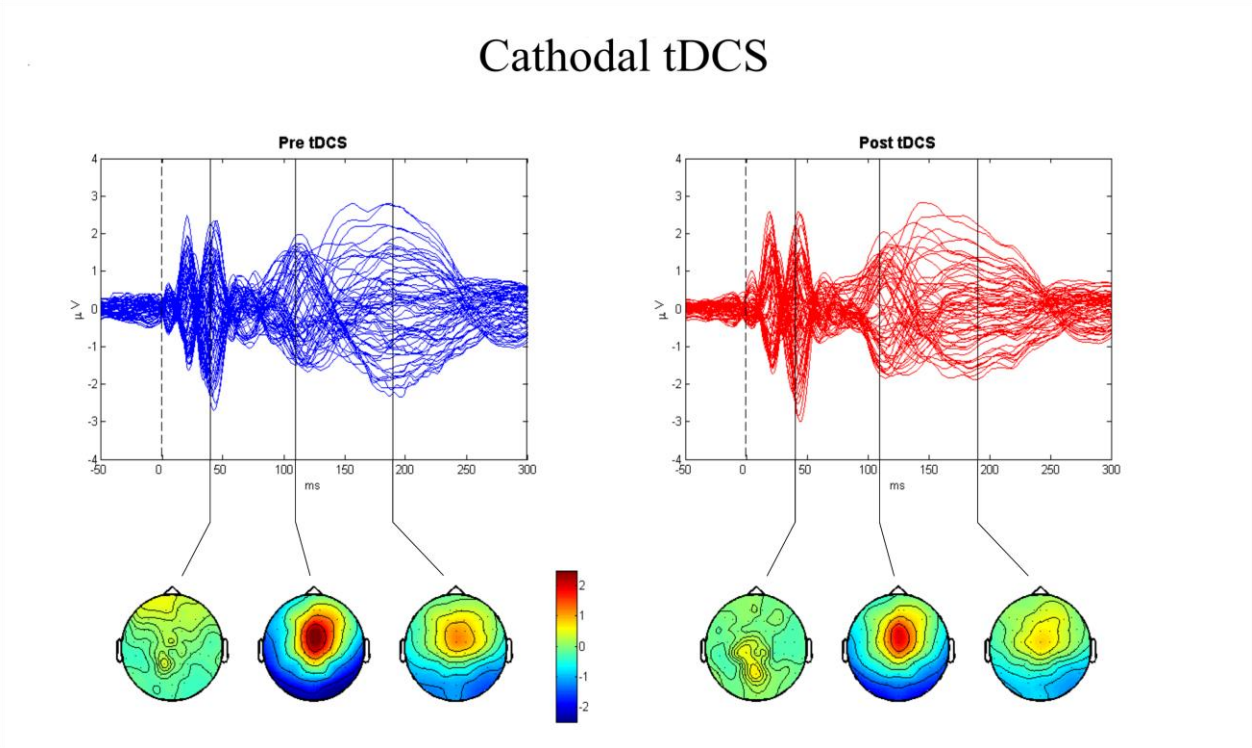

Figure 6.2: *Results of the GMFP. In the upper bound are depicted the butterfly plot of the 60 channels' TEPs for the two conditions: pre-tDCS in blue, and post-tDCS in red. The lower row represents the mean topographies computed in correspondence of the local maxima for the following time windows: 0-50 ms; 100-150 ms; and 150-200 ms.*

6.4.3 Cathodal Stimulation - Source modelling analyses

As mentioned above, for the Sources analysis, we started from the results of the Cluster analysis at the sensors level. We follow the identical procedure to sources reconstruction as described in Chapter Four (see Paragraph 4.4.7However, despite the previous TMS-EEG study at rest, but here we did not compute the Global SCD and Local SCD over the three time windows (0–50 ms; 50–100 ms and 100-150 ms). We cumulated these indexes of cortical activation in the time-window from 180 to 240 ms that was the one in which the significant cluster has been found. On this data, a linear mixed model with the factor *Condition* (Pre vs Post) was run, both for Global SCD and for the four ROIs (left and right BA7 and BA6).

Source modelling analyses confirmed results from the cluster analysis at sensors level. The best-fitted model on Global SCD included the main effect *Condition* ($\chi^2(2) = 6.4$; p=.01) with a decrease of TEPs amplitude after tDCS stimulation (see Figure 6.3).

Similarly, for both left and right BA7 and for left BA6 the factor *Condition* was included in the final model as main effect: left BA7($\chi^2(2) = 5.87$; p=.02), right BA7 ($\chi^2(2) = 6.0$; p=.01); and left BA6 ($\chi^2(2) = 7.9$; p=.005). Only for the right BA6, no effect of real cathodal tDCS stimulation was highlighted on local SCD ($\chi^2(2) = 1.5$; p=.22).

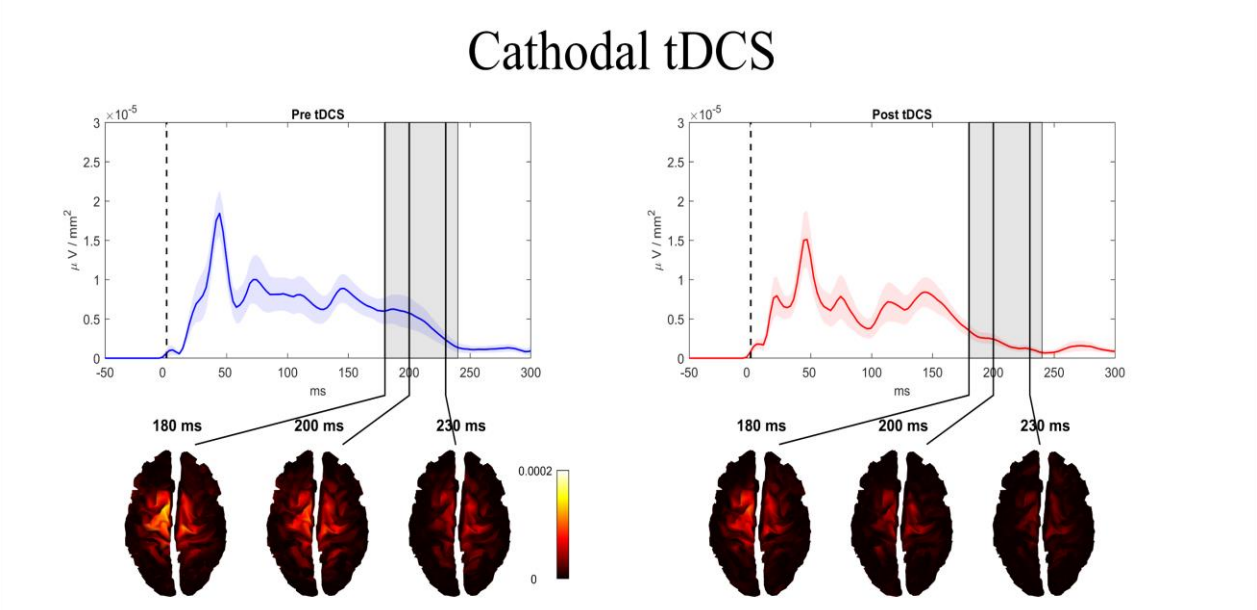

Figure 6.3: *Active vertexes and current spread at the local maxima in the GMFP time-windows revealed by the cluster analysis. For each recording session, the GMFP is shown on first top row. The gray bars define the time window where cluster-based analyses evidenced significant results. The second row shows the estimated cortical sources in time coincidence with the maximum GMFP value, in the 180-230 ms time window.*

6.4.3.1 Sham stimulation - Sensor analysis

GMFP

As expected, sham stimulation did not modulate global indices of cortical excitability. In particular, the final model run on GMFP did not include the main effect of *Condition* in any time-window (0-50 ms: $\chi^2(2) = 0.17$; p=.68; 50-100 ms: $\chi^2(2) = 0.14$; p=.71; 100-150 ms: $\chi^2(2) = 0.57$; p=.45). Bayesian analyses showed a moderately low support to the null hypothesis for the inclusion of the factor *Condition* in the final model (0-50 ms: BF_{01}= 3.0; 50-100 ms: BF_{01}= 2.9; 100-150 ms: BF_{01}= 2.9)

LMFP

Analyses run on LMFP confirmed the lack of any possible effect of sham tDCS in modulating local cortical excitability, in any of the considered clusters of electrodes. In cluster C1, LRT values were non-significant for the first ($\chi^2(2) = 0.15$; p=.69), the second ($\chi^2(2) = 0.56$; p=.46) and the third ($\chi^2(2) = 1.14$; p=.29) time-window.

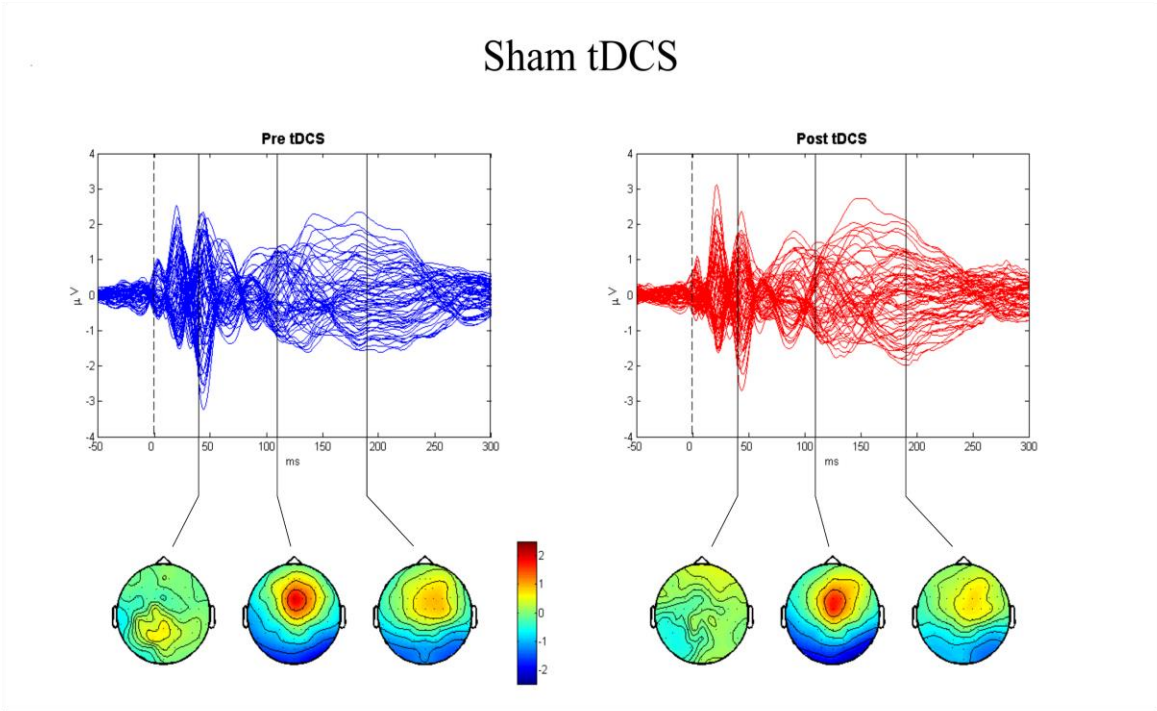

Figure 6.4: *Results of the GMFP. In the upper bound are depicted the butterfly plot of the 60 channels' TEPs for the two conditions: pre-tDCS in blue, and post-tDCS in red. The lower row represents the mean topographies computed in correspondence of the local maxima for the following time windows: 0-50 ms; 100-150 ms; and 150-200 ms.*

The same holds for cluster C2. LRT values were not significant for the factor *Condition* in any time-window (0-50ms: $\chi^2(2) = 0.002$; p=.96; 50-100ms; $\chi^2(2) = 0.02$; p=.89; 100-150ms: $\chi^2(2) = 1.14$; p=.29). Similarly, in cluster C3, LRT indicated not to include factor *Condition* for any time-

window (0-50ms: $\chi 2(2) = 0.12$; p=.73; 50-100ms: $\chi 2(2) = 0.96$; p=.33; 100-150ms: $\chi 2(2) = 1.59$; p=.21) in the final model. Finally, also for the cluster C4, LRT values were non-significant for the first ($\chi^2(2) = 0.02$; p=.89), the second ($\chi^2(2) = 1.13$; p=.29) and the third ($\chi^2(2) = 0.07$; p=.79) time-window.

All the Bayesian analysis revealed a moderately low support to the null hypothesis as shown below: for the first cluster C1 0-50 ms: BF_{01}= 2.7; 50-100 ms: BF_{01}= 2.5; 100-150 ms: BF_{01}= 2.0; for the C2 0-50 ms: BF_{01}= 3.0; 50-100 ms: BF_{01}= 1.3; 100-150 ms: BF_{01}= 2.3; for the third cluster C3 0-50 ms: BF_{01}= 2.9; 50-100 ms: BF_{01}= 2.4; 100-150 ms: BF_{01}= 2.3; and for the last cluster C 0-50 ms: BF_{01}= 2.5; 50-100 ms: BF_{01}= 2.7; 100-150 ms: BF_{01}= 2.6.

6.4.3.2 Sham stimulation - Cluster analysis

For the sham stimulation condition, also the cluster-based analysis was performed in order to test the effect of tDCS stimulation (Pre vs Post). Results revealed neither positive nor negative significant clusters (Figure 6.6).

6.4.3.3 Sham Stimulation - Source modelling analyses

In order to carry out an exploration at a different signal level, we decided to perform the Source modelling analysis, although no significant results were found at sensors level with cluster permutation. The Source modelling analyses on sham data confirmed the results from the sensor analyses, but only at a global level.

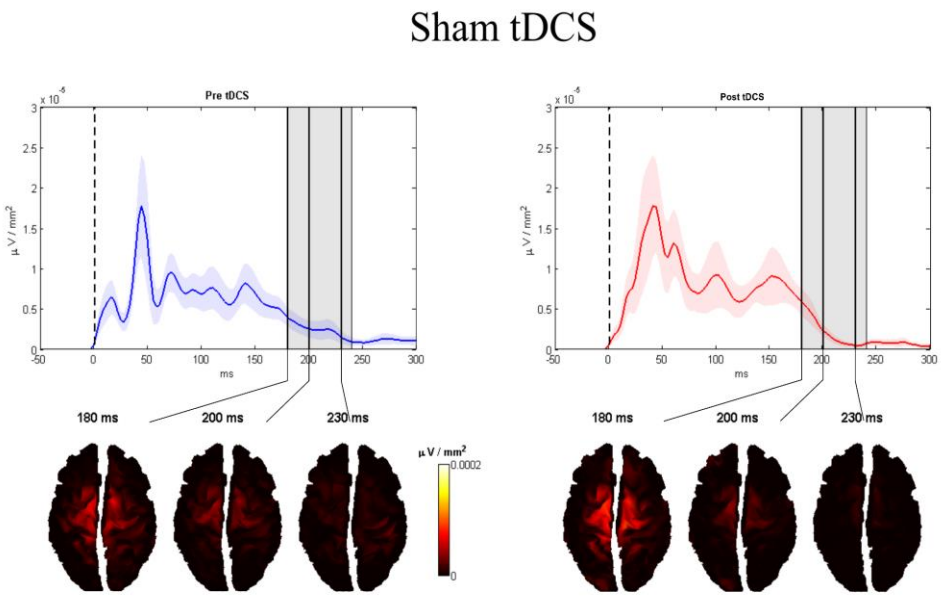

Figure 6.5: *Active vertexes and current spread at the local maxima in the GMFP time-windows revealed by the cluster analysis. For each recording session, the GMFP is shown on first top row. The gray bars define the time window where cluster-based analyses evidenced significant results. The second row shows the estimated cortical sources in time coincidence with the maximum GMFP value, in the 180-230 ms time window.*

Global SCD final model did not include *Condition* ($\chi^2(2) = 0.13$; p=.72), indicating no effect of sham stimulation on cortical excitability (see Figure 6.5).

The same holds for both left ($\chi^2(2) = 0.03$; p=.85) and right ($\chi^2(2) = 0.15$; p=.69) BA7, as well as for left BA6 ($\chi^2(2) = 0.56$; p=.45), where LRT indicated no inclusion of the factor Condition in the final model. Differently for what emerged for sensors data, at sources level, for the right BA 6, the main effect of *Condition* resulted significant ($\chi^2(2) = 5.19$; p=.02). In particular, results in this ROI showed wider TEPs after tDCS stimulation, compared to the ones before.

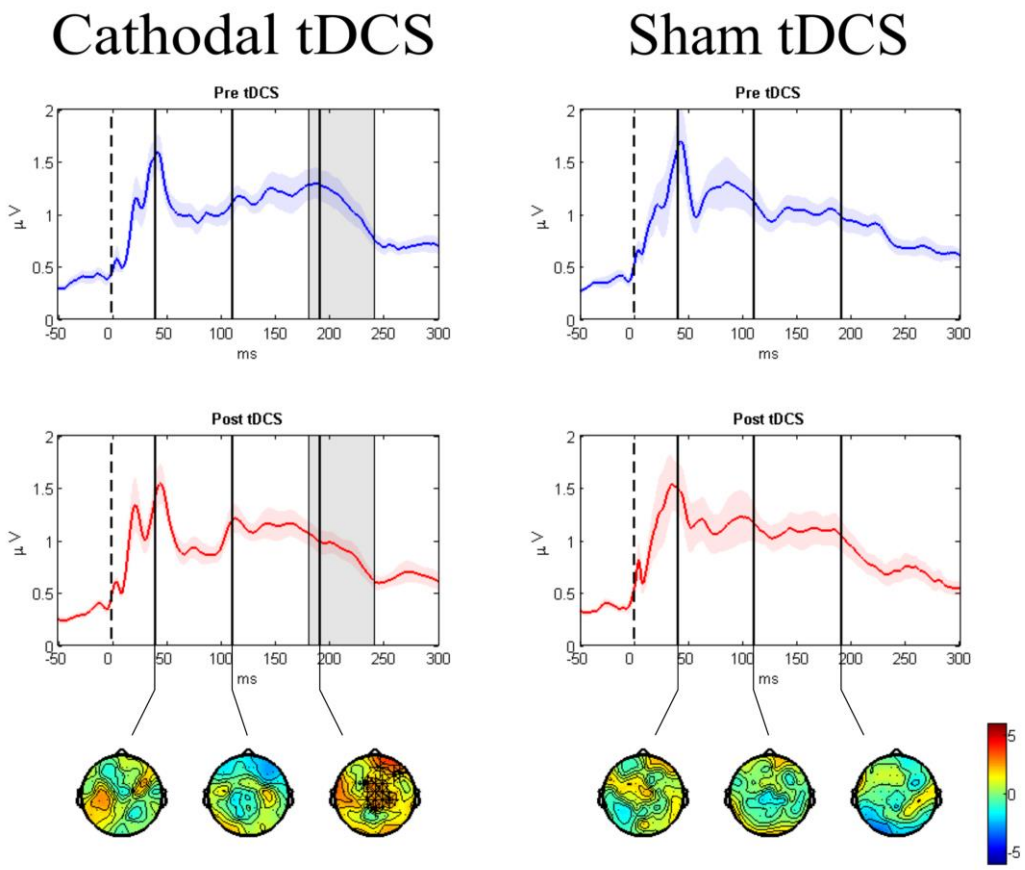

Figure 6.6: *Results of Cluster analysis. GMFP plot and topoplot of the pre tDCS (blue trace) and post tDCS (red trace) sessions for the two tDCS stimulation condition (cathodal and sham). The gray bars define the time window where cluster-based analyses evidenced significant results. In the last row topoplots show the significant clusters evidenced by the cluster analysis.*

6.5 Discussion

In this study, we sought to investigate the effects on cortical excitability induced by 15 minutes of cathodal stimulation over the right PPC during task performance. To this purpose, we measured TEPs using TMS-EEG technique before and after tDCS stimulation, during which the participants were involved in a VWMT and in a modified version of the PCT. As in the previous TMS-EEG study, described in the Chapter Four, we performed two TMS-EEG recording sessions: one before tDCS and the other 10 minutes after the end of the tDCS stimulation session, with TMS on left PPC. As a control condition, all the sixteen participants underwent an additional session in which sham tDCS was delivered. Indices of local and global activity were computed at the sensors level. Differently from previous studies, in order to avoid the use of a priori temporal windows (e.g. 0-50, 50-100ms, 100-150ms) we performed also a cluster-based analysis and the cortical source analysis focused in the time window where the cluster analysis evidenced significant results.

Starting from behavioural data, we partially replicated the results of the second behavioural study. The most relevant result concerns the main effect of the stimulation condition on reaction times, in the PCT. In particular, also in this study, we observed an increase of RTs in the cathodal condition, compared to sham one. This is a relevant aspect that seems to confirm the potential of cathodal tDCS over right PPC to disrupt the ability to spatially reorienting visual attention, a cognitive ability required in PCT, by modulating the activity of the brain areas underlying that function. For the aim of the project, the effectiveness of cathodal tDCS to modulate the behaviour is a crucial point that allows to study efficiently, using TMS-EEG, the underlying neurophysiological mechanisms of action taking place during task execution. By reproducing the behavioural data, indeed, we could state that the possible modulation effects on cortical excitability, observed through the recording of TEPs by the use of TMS-EEG, are potentially linked to the behaviour effects. However, we did not perfectly replicate the results obtained in the pilot study. In particular, here, we observed the opposite side effect. The new data showed an increase in RTs when the target appeared on the left side of the screen, while, in the second behavioural study, the same result was observed for ipsilateral stimuli.

Our results seem to be in line with previous data present in literature, which demonstrated that PPC controls stimuli presented in the contralateral hemifield. Therefore, tDCS stimulation applied on the right PPC seems to modulate the performance in a polarity-dependent way only for contralateral stimuli, with a reduction of RTs in case of anodal stimulation (Bolognini et al., 2010b), and a reduction in detecting stimuli on the left hemifield during the cathodal one (Sparing et al., 2009). The neglect clinical data seem to go in the same direction. This neuropsychological disorder is typically due to a damage in the right hemisphere and causes an inability to directly orient the attention towards the left hemifield, i.e. the one contralateral to the lesion (Molenberghs et al., 2012; Vallar, 1998).

Nevertheless, the discrepancy in our behavioural data seems to underline, once again, that high order cognitive functions are usually linked to the activity of a more complex network of areas (Lo et al., 2017). For instance, in a ERPs study, researchers investigated the brain mechanisms underlying the orienting attention processes by localizing the different stages of processing after the appearance of an exogenous cue (Tian, Klein, Satel, Xu & Yao, 2011). The authors observed that the neural activations were approximately divided into three stages and involved a widespread network of cortical regions. In an early stage, comprised from 110 to 240 ms, activations in the prefrontal cortex, in the contralateral occipitotemporal cortex and in the bilateral intraparietal cortex were observed. In the middle stage (240–350 ms), activations were mainly found in the frontal cortex and the parietal cortex. In the late phase (350–650 ms), the greater activations were in the occipitoparietal cortex. Still, unlike in the earliest stage, the activation shifted to the hemisphere ipsilateral to the cued location. These findings suggest that the orienting attention processes seem to be related to both attentional and motor response processes, involving brain regions of both neural networks (Tian et al., 2011).

Thus, as mentioned before, other studies converge in demonstrating that the right PPC underlies more general visuospatial orienting attention processes (Szczepanski, Konen, & Kastner, 2010). This brain area was more involved in the presence of bilateral stimuli since it was implicated in orienting attention toward both sides of the space (Spering at al., 2009). Moreover, in a more recent study, in which tDCS was employed to generate a hemispheric asymmetry, accordingly to current functional–anatomical models of attentional control, the authors observed a decrease in the effectiveness of peripheral cues in both hemifields. They assumed that exogenous orienting always relies on ventral and dorsal regions in the right hemisphere, irrespective of hemifield (Duecker, Schuhmann, Bien, Jacobs, & Sack, 2017).

Taken together, these considerations highlight how a deeper understanding of the involvement of the right PPC in orienting attention needs to be further investigated. This is particularly true in light of the relevant clinical implications and considering the possibility of using tDCS effectively for rehabilitation purposes. In this respect, it could be crucial to investigate the modulatory effects induced by anodal tDCS stimulation on the same cognitive functions. This would give us a more complete panorama about the role of right PPC in the visuospatial orienting attention processes. However, this issue is outside the primary purpose of this project and therefore, has not been further investigated.

Concerning neurophysiological data, at sensors level, we mirrored the analysis performed in the first TMS-EEG study, and no significant modulation of cortical excitability was observed. In comparison to the pre-tDCS session, after cathodal stimulation, no significant changes were observed

in TEPs amplitude, neither at a global (GMFP) nor at a local level (LMFP for 4 clusters of electrodes). To directly compare the results of the two TMS-EEG studies, we analysed the data considering the same TEPs' temporal windows, namely an early (0-50 ms), a middle (50-100 ms) and a late (100-150 ms) window, chosen to assess different TEP's components. No significant results were found for any index at any temporal window, thus obtaining after cathodal stimulation results similar to those after sham. A Bayesian analysis was then performed to test the validity of the results and to verify the actual absence of a tDCS effect on cortical excitability. The results showed a moderately low support of the null hypothesis. These results led us to go deeper in exploring the possible presence of a cortical excitability modulation through a cluster-based analysis.

Cluster analysis has the main advantage of not requiring an a priori definition of electrode clusters and time-windows of interest. Through a series of *N* permutations, indeed, all the values that reach a critical threshold are clustered, based on temporal and spatial contiguity. The cluster analysis revealed a frontoparietal lateralised positivity between 180 and 230 ms from the TMS onset. This means that, after cathodal tDCS stimulation, delivered during a task performance, the cortical excitability decreases in a relatively later time-window, in comparison to what was observed for anodal tDCS, and involving a lateralised network of brain regions.

Source modelling confirmed this result from cluster analysis. In fact, SCD changed after stimulation respect to pre-tDCS condition, when it was computed at a global level and in three out of the four BAs matching the clusters of the LMFP analysis. In particular, computing the data in the time-window derived from the cluster analysis (180-230 ms), the significant change was found bilaterally for BA 7 and for left BA 6, but not for right BA 6.

Two main conclusions can be drawn from this result. First, the present results seem to define how, at a functional level, the cathodal tDCS affects cortical circuits when the stimulation is applied during task performance, suggesting that, at least in the domain of right PPC stimulation, what changes the cathodal stimulation from inert to effective is the concurrent execution of a task. Second, the observed effects suggest that cathodal tDCS stimulation affects those cortical areas directly involved in a task.

Starting from the first point, our results seem to demonstrate that cathodal stimulation produces effects in systems with high levels of basal activity, in line with the idea that the effects of tDCS may depend, in an opposite way, on the background level of activity in the system (Matsunaga et al., 2004). Moreover, as already observed for anodal tDCS (Pisoni et al., 2017), also cathodal tDCS functional effects are restricted to those areas that are much more activated from task execution. A possible explanation could be the crucial role played to the location and the frequency of active synapses (Lafon et al., 2016). This means that the tDCS neurophysiological modulation is strictly

connected to the spontaneous firing and synaptic efficacy; the concurrent area activation through a task execution determine long-lasting plastic changes (Fritsch et al. 2010). In the animal model study, performed by Fritsch and co-workers (2010), indeed, M1 mouse slices needed simultaneous DC and synaptic activation in order to induce Long Term Potentiation-like changes.

According to this data, our results showed that, in those areas involved in visuospatial attentional processes (the left and right ROI BA 6 and 7), an offline reduction of cortical excitability is probably linked to a synaptic activity during task execution.

All these findings seem to converge in partially supporting the activity-selectivity hypothesis, according to which functional tDCS specificity may derive from either active neuronal networks that are preferentially modulated by tDCS, or from input-selectivity, where bias is applied to different synaptic inputs (Bikson & Rahman 2013). The cortical state of the neural population at the time of stimulation may be a crucial factor to take into account the effectiveness of tDCS stimulation. In the Bortoletto et al. (2015) work, the authors find that anodal tDCS on M1 during fast motor practice task hindered learning, as shown by the worsening of motor performance. Conversely, anodal tDCS combined with slow motor practice task, that does not induce changes in cortical excitability and motor learning per se, induced a performance enhancement. The interaction between the task- and the stimulation-induced increase in excitability may explain these findings. The authors describe their results in accordance with the "neural noise theory". According to this theory, the effects of tDCS depend on the strength of the signal and on the signal-to-noise ratio (e.g. Miniussi et al., 2013). Specifically, the signal is the neural activity operationally linked to the task, and the noise is related to the random neural activity. Since tDCS involves the relatively indiscriminate modulation of a large number of neurons, its impact could be read as a change in the relationship between noise and signal in the neural activity. As tDCS adds neuronal activity to the ongoing neural activity, its effects are state-dependent (Bortoletto et al., 2015). Neurons that are already activated at a high level by the task may receive less benefit from an excitatory stimulation because they are already close to the saturation level. Conversely, an inhibitory stimulation could induce more consistent modulatory effects on the same neurons with a high level of basal activity.

Taken together, the present results contribute to clarify the more controversial mechanisms underlying cathodal tDCS stimulation. This knowledge could be a starting point in optimizing tDCS protocols as well as new strategies to enhance learning. However, for a deeper understanding of the interaction between tDCS and the concurrent task-associated neural activity, also the effects of anodal stimulation related to this specific cognitive function need to be better explored. Regarding the second conclusion on the spatial specificity of tDCS neurophysiological effects, in our study changes in cortical excitability were found in frontoparietal areas involved in the orientation of visuospatial

attention. Different studies have shown that a dorsal frontoparietal network is globally associated with attention orientation, even if the regions in the system are engaged differently over time and across the hemispheres concerning the type of attention (endogenous vs exogenous - Mayer et al., 2017). Within this framework, attentional performance critically depends on the interaction between the hemispheres.

No significant change on cortical excitability was found when sham stimulation was delivered. The only exception is at sources level where, only in correspondence of the right ROI BA 6, we found an increase in SCD in the Post compared to Pre tDCS condition.

What occurs in the sham control condition can be considered as sort of baseline, reflecting modulations likely due to the task execution. Therefore, the significant increase of SCD in the right BA6 after sham may be attributed to the involvement of this area in the visuospatial orienting attention.

The involvement of premotor areas in attentional processes was well established in previous studies that investigate the role of these areas in both covert and overt mechanisms of orienting attention (e.g. Brovelli, Lachaux, Kahane & Boussaoud, 2005; Nobre, Giltelman, Dias & Mesulam, 2000). During attentional tasks, high activations in the primary nodes of the frontoparietal system were indeed observed. In particular, frontal areas resulted more active in lateral motor and premotor cortex of both hemispheres, and in the region of the frontal eye fields. Whereas, posterior parietal areas were more active around the posterior intraparietal sulcus, extending into inferior parietal lobule (Nobre et al., 2000). Specifically, the activation of the areas in the frontoparietal system was enhanced in the covert attention task. Frontal and parietal cortices, indeed, may jointly play an essential role in the causal top-down control of spatial attention. In particular, it seems that the activation of a frontoparietal attentional network is linked with the amount of top-down information provided by predictive cues, that influences the ability to re-orient, and not to directly orient, the visuospatial attention (Thiel et al., 2004; Vossel et al., 2006).

The lack of this effect on right BA6 after cathodal stimulation can be interpreted then as an effect of the stimulation: cathodal tDCS might have reduced cortical excitability in this area, cancelling the effect of activation due to the task execution and observed in the sham condition. It could be possible that the right BA6, plays a peculiar role in the excitability-inhibitory processes in the network. During task execution, this area could compensate for the destructive effects of cathodal tDCS on the other regions in the system. Further studies need to be performed in order to disentangle this issue.

To conclude, the information provided by our results mainly concern the dependence of tDCS effects on the state of activity of the stimulated region. For both polarities, anodal (Pisoni et al., 2017)

and cathodal, delivering stimulation during a task would confine the neurophysiological effect on the task relevant areas, thus accounting for the specificity of the behavioural effect usually observed. In the case of cathodal stimulation, at least for parietal cortex stimulation, the concurrent task activity seems to be essential to observe cortical excitability modulations. The information provided can be a starting point to improve the tDCS protocol design in the direction of achieving greater effectiveness for the treatments of neurological and psychiatric diseases. Moreover, understanding the basis of the interaction between tDCS and the concurrent task-associated neural activity could result indeed in optimized tDCS protocols and in new strategies to enhance learning.

Chapter Seven: “Conclusion”

In this thesis, we have set ourselves the aim to investigate the neurophysiological counterpart of cathodal tDCS effect, through the integrated TMS-EEG system. The interest and the scientific value of this work derive from the consideration that tDCS is one of the non-invasive neuromodulatory techniques of increasing diffusion, both in the research and in the clinical field. The reason why tDCS is becoming so widely used, also in comparison to TMS, is because it is a relatively easy-to-use, portable and undoubtedly less expensive than the other techniques. However, not much is yet known about the mechanisms underpinnings its action, especially as regards the modulatory effects induced in those brain areas that underlie higher cognitive functions.

The overview of the literature on the tDCS mechanisms of action highlighted several relevant points which oriented the experimental design of the studies we run.

First, the well-known and maybe simplistic view about the tDCS polarity-dependent effects is not well established. This is particularly true for all the brain areas outside the sensorimotor networks, where, in particular, the effects of cathodal tDCS stimulation appear to be somewhat controversial or even absent at all (Jacobson et al., 2012). Accordingly, recent evidence-based guidelines for clinical use of tDCS (Lefaucheur et al., 2017) do not include this polarity of stimulation for the treatment of any disease. Thus, considering the behavioural outcomes of cathodal tDCS are less predictable of those induced by anodal stimulation, a systematic and comprehensive study of its cortical effects acquires a critical relevance. This point prompts us to focus on the cathodal polarity of stimulation and to adopt the same procedure of previous studies on anodal tDCS. In this way, we could compare the two polarities effects on cortical excitability and connectivity, targeting the right PPC, a brain area outside the sensorimotor cortex.

Moreover, different fMRI studies showed that beyond modulating the excitability of the stimulated area, tDCS could also alter cortical connectivity from the targeted area, thus affecting broader brain networks (e.g. Amadi et al., 2014; Stagg et al., 2013). This is somehow in contrast with the specificity of the behavioural effects observed in various domains, at least following anodal tDCS. From our point of view, TMS-EEG could represent an optimal technique to localize the effects of tDCS during task performance.

The idea that comparing resting versus active state dependant effects could be a crucial step on advancing the knowledge on tDCS mechanism of action came from previous in vitro/in vivo studies on animal (Fritsch et al., 2010; Ranieri et al., 2012) and computational model (Lafon et al., 2016), which seem to converge in demonstrating that the level of basal activity in the neural system could be playing a fundamental role for the neuromodulation processes. On the animal model, the

authors showed that, without a simultaneous synaptic activation, DC stimulation elicits only a short-lasting synaptic enhancement. Long-lasting LTPs are induced in compresence of simultaneous synaptic activation (Fritsch et al., 2010; Ranieri et al., 2012). In the computational model, described by Lafon et al. (2016), was also remarked a non-linearity in the two polarity-driven mechanisms of action. Specifically, cathodal DC stimulation, if compared to the anodal one, creates an opposite shift in the threshold of Input/Output function, but with an overall weaker impact because of these two counterbalancing opposite effects on the two neuron's compartments (Lafon et al., 2016).

Following these hints, both the comparison between resting state and active state and between anodal versus cathodal tDCS seemed to be relevant issues which deserved to be further explored. For this reason, we planned a series of studies, mirroring our first study on anodal tDCS (Romero Lauro et al., 2014) in which we focused on the effect of cathodal tDCS, explored at resting state and during task execution. We decided to use the integrated TMS-EEG system. From one side, the EEG allows measuring in real-time the changes in cortical excitability also in those areas functionally and structurally connected to the targeted one. On the other hand, the TEPs represent an index of cortical excitability even for those areas otherwise not directly functional measurable. For the sake of comparability, all the relevant tDCS and TMS parameters (site, intensity, duration, etc.) were kept constant.

Our results seem to confirm the non-linearity between the effects produced by the two different stimulation polarities at rest, that do not match the well-known anodic-excitatory and cathodic-inhibitory coupling, which emerged when sensorimotor areas are targeted (Kirimoto et al., 2011; Nitsche & Paulus, 2000, 2001). In particular, these data highlighted how cathodal tDCS, compared to anodal polarity, seems to be less effective in modulating cortical excitability at rest. It could be due to a more considerable inter-individual variability observed in response to cathodal tDCS, as well as to the different mechanisms that underling the two stimulation polarities. Future studies are needed to disentangle between these alternative explanations.

Differently, our subsequent TMS-EEG study showed that cathodal tDCS induces changes in cortical excitability if administered during task performance. Thus, these results corroborate the hypothesis suggested by computational studies and animal models, that to observe long-lasting effects with cathodal tDCS, the target area must be already activated by a task. Moreover, as for the anodal stimulation (Pisoni et al., 2017), the observed changes in cortical excitability are limited to those areas strictly involved in the task. Once again, these results seem to partially support the activity-selectivity hypothesis according to which functional tDCS specificity may derive from either active neuronal networks that are preferentially modulated by tDCS, or from input-selectivity, where bias is applied to different synaptic inputs (Bikson & Rahman 2013).

As mentioned above, to mirror previous studies, we were forced to keep tDCS and TMS-EEG parameters fixed, even though when investigating higher-order cognitive functions, the duration of tDCS stimulation is usually longer (e.g. Brunoni et al., 2012, 2014; Bolognini et al., 2010a). It could be therefore interesting to replicate the behavioural and the second TMS-EEG study by increasing the tDCS stimulation duration, such to investigate whether this parameter affects the observed effects. For the same reason, the studies have been focused on the cortical reactivity only; even if the investigation of the cortical oscillatory activity would be of great interest, too. To do that, it would be needed to replicate the studies by applying anodal tDCS during a task involving the right PPC and studying in particular the oscillatory activity. This could become a starting point to a more complete and exhaustive comprehension of the tDCS polarity-dependent effects, since it would provide a more direct comparison between the two polarities.

To conclude, taken together our findings converge in noticing the existence of a non-linear polarity dependency in the mechanisms of action of the two polarities, and in underling the relevance to take into account the level of basal activity in those areas directly stimulated. Moreover, our data acquired particular significance concerning the possibility of using even cathodal tDCS in the clinical setting, suggesting to possibly coupling it with a concurrent activity to maximize its effectiveness. Our results hold relevant implications for a better refinement of tDCS protocol in research and rehabilitative settings and open new avenues of future research in the direction of increasing the knowledge on tDCS mechanisms of action as the best way guide the choice of the parameters to be used.

Acknowledgments

I would like to thank my supervisor, Dr Leonor Josefina Romero Lauro, for the opportunity to work on this exiting project and for allowing me to grow up in the scientific and research word.

I owe a huge gratitude to Dr Alberto Pisoni and Dr Giulia Mattavelli. Thank you both for made me feel part of the group in any moment, and for your constant and helpful advices and feedback during all these years. I'm quite sure that it's only thanks to your guidance, and moreover to yours patience, that I learned the technical and programming skills necessary to complete this work; furthermore your knowledge surrounding TMS-EEG in general have been invaluable.

I would also like to thank all the other members of the group, like Dr Alessandra Vergallito; and the students and interns that helped and supported me along all the way. Above everyone, I want to thank Lilia for the crucial support in the lab during the data collection; for the many stimulating discussions and debates focusing on the sense of the research in general; and, most important, thanks for your moral support. I thank the interns Gaia and Gabriel that contributed with their positive vibes and enthusiastic energy to make the last period in lab simpler and more colourful.

Besides, I would like to thank all the participants who gave up some hours of their free time to take part in my experiments; without you, nothing would have been possible.

Appendix 1

frontiers in Neuroscience

ORIGINAL RESEARCH
published: 15 May 2018
doi: 10.3389/fnins.2018.00319

Tracking the Effect of Cathodal Transcranial Direct Current Stimulation on Cortical Excitability and Connectivity by Means of TMS-EEG

Erica Varoli[1,2], *Alberto Pisoni*[2,3], *Giulia C. Mattavelli*[2,3], *Alessandra Vergallito*[2,3], *Alessia Gallucci*[3], *Lilia D. Mauro*[3], *Mario Rosanova*[4,5], *Nadia Bolognini*[2,3,6], *Giuseppe Vallar*[2,3,6] *and Leonor J. Romero Lauro*[2,3]*

[1] Ph.D. Program in Neuroscience, Department of Medicine and Surgery, University Milano-Bicocca, Monza, Italy, [2] NeuroMi - Milan Center of Neuroscience, Milan, Italy, [3] Department of Psychology, University of Milano-Bicocca, Milan, Italy, [4] Department of Biomedical and Clinical Sciences "L. Sacco", University of Milan, Milan, Italy, [5] Fondazione Europea per la Ricerca Biomedica Onlus, Milan, Italy, [6] Laboratory of Neuropsychology, IRCCS Istituto Auxologico, Milan, Italy

OPEN ACCESS

Edited by:
Domenica Veniero, University of Glasgow, United Kingdom

Reviewed by:
Vera Moliadze, Universitätsklinikum Schleswig-Holstein, Germany
Debora Desideri, Universität Tübingen, Germany

***Correspondence:**
Leonor J. Romero Lauro
leonor.romero1@unimib.it

Specialty section:
This article was submitted to Perception Science, a section of the journal Frontiers in Neuroscience

Received: *13 February 2018*
Accepted: *24 April 2018*
Published: *15 May 2018*

Citation:
Varoli E, Pisoni A, Mattavelli GC, Vergallito A, Gallucci A, Mauro LD, Rosanova M, Bolognini N, Vallar G and Romero Lauro LJ (2018) Tracking the Effect of Cathodal Transcranial Direct Current Stimulation on Cortical Excitability and Connectivity by Means of TMS-EEG. Front. Neurosci. 12:319. doi: 10.3389/fnins.2018.00319

Transcranial direct current stimulation (tDCS) is increasingly used in both research and therapeutic settings, but its precise mechanisms remain largely unknown. At a neuronal level, tDCS modulates cortical excitability by shifting the resting membrane potential in a polarity-dependent way: anodal stimulation increases the spontaneous firing rate, while cathodal decreases it. However, the neurophysiological underpinnings of anodal/cathodal tDCS seem to be different, as well as their behavioral effect, in particular when high order areas are involved, compared to when motor or sensory brain areas are targeted. Previously, we investigated the effect of anodal tDCS on cortical excitability, by means of a combination of Transcranial Magnetic Stimulation (TMS) and Electroencephalography (EEG). Results showed a diffuse rise of cortical excitability in a bilateral fronto-parietal network. In the present study, we tested, with the same paradigm, the effect of cathodal tDCS. Single pulse TMS was delivered over the left posterior parietal cortex (PPC), before, during, and after 10 min of cathodal or sham tDCS over the right PPC, while recording HD-EEG. Indexes of global and local cortical excitability were obtained both at sensors and cortical sources level. At sensors, global and local mean field power (GMFP and LMFP) were computed for three temporal windows (0–50, 50–100, and 100–150 ms), on all channels (GMFP), and in four different clusters of electrodes (LMFP, left and right, in frontal and parietal regions). After source reconstruction, Significant Current Density was computed at the global level, and for four Broadmann's areas (left/right BA 6 and 7). Both sensors and cortical sources results converge in showing no differences during and after cathodal tDCS compared to pre-stimulation sessions, both at global and local level. The same holds for sham tDCS. These data highlight an asymmetric impact of anodal and cathodal stimulation on cortical excitability, with a diffuse effect of anodal and no effect of cathodal tDCS over the parietal

cortex. These results are consistent with the current literature: while anodal-excitatory and cathodal-inhibitory effects are well-established in the sensory and motor domains, both at physiological and behavioral levels, results for cathodal stimulation are more controversial for modulation of exitability of higher order areas.

Keywords: cathodal tDCS, TMS-EEG, cortical excitability, posterior parietal cortex, neuromodulation

INTRODUCTION

Although tDCS is one of the most used non-invasive brain stimulation techniques, there are relatively few studies addressing the mechanisms underlying its action (for a review see Stagg and Nitsche, 2011; Medeiros et al., 2012). A deeper understanding of the neurophysiological underpinnings of tDCS effects would be crucial to achieving a better refinement of stimulation protocols for clinical and research purposes.

Many hints on the neuronal mechanism of online and offline tDCS effects come from the translational approach of animal models. The first pioneering *in vitro* studies (Bindman et al., 1962, 1964; Creutzfeldt et al., 1962; Purpura and McMurtry, 1965) provided evidence for a polarity-dependent modulatory action, according to which anodal tDCS increase neurons' spontaneous firing rate and evoked potentials, whereas cathodal tDCS leads to the opposite effect. Recent *in vitro* animal models unveiled the complexity of tDCS effects, showing that the modulation of neuronal excitability results from the interaction of several factors, including the specific cell morphology and type, the interaction between neuronal compartments, the effects on afferent fibers and glial cells (Bikson et al., 2004; Radman et al., 2009; Gellner et al., 2016). When the duration of the stimulation exceeds 5 min, tDCS can induce long-lasting after-effects, presumably deriving from changes in synaptic strength. These after-effects are dependent upon continuous protein synthesis during stimulation (Gartside, 1968), likely mediated by mechanisms such as Long-Term Potentiation and Depression (LTP and LTD; Hattori et al., 1990; Moriwaki, 1991; Liebetanz et al., 2002; Fritsch et al., 2010; Ranieri et al., 2012; Rohan et al., 2015). The synaptic activity induced by tDCS increases Ca^{2+} intracellular amount, affecting calcium and sodium membrane channels (Islam et al., 1995), and it is dependent on enhanced brain-derived neurotrophic factor (BDNF) secretion and TrkB-activation (Fritsch et al., 2010).

The main limitation of studies with animal models is related to the issue of translating these findings to human beings, considering the relevant differences in the parameter, settings.

For instance, current intensity safety boundaries are set within 0.4–0.8 A/m^2 (Nitsche et al., 2008) for humans, while animal studies intensity ranges between 5 to over 50 A/m^2, often leading to inflammation, microglia activation and neurodegeneration on both anesthetized and alert animals (Rohan et al., 2015; Gellner et al., 2016; Koo et al., 2016; Monai et al., 2016; Podda et al., 2016).

In humans, the mechanisms underlying tDCS effects have been mainly investigated by means of pharmacological interventions (for a review: Medeiros et al., 2012), computational models of current flow (e.g., Miranda et al., 2013; Lafon et al., 2016), and recording stimulation-effects on cortical excitability and connectivity by means of other techniques. Among these, Functional Magnetic Resonance Imaging (fMRI; e.g.,Stagg and Nitsche, 2011; Zheng et al., 2011), Positron Emission Tomography (PET; e.g., Lang et al., 2005), EEG (e.g., Accornero et al., 2007) and coupling TMS with Electromyography (e.g., Nitsche and Paulus, 2000), or EEG (e.g., Pellicciari et al., 2013; Romero Lauro et al., 2014; Bolognini and Miniussi, 2016) are the most common.

Robust evidence of tDCS-induced polarity-dependent shifts of cortical excitability have been shown by applying tDCS over the primary motor (M1; Priori et al., 1998; Nitsche and Paulus, 2000, 2001; Nitsche et al., 2003; Kirimoto et al., 2011), somatosensory (Kirimoto et al., 2011), and visual (Antal et al., 2004; Accornero et al., 2007) cortices, and measuring the amplitude of evoked activity.

In the domain of motor cortex, concerning Motor Evoked Potentials (MEPs) modulation, a certain amount of evidence suggests that the after-effects of both anodal and cathodal tDCS share a mechanism involving glutamatergic synapses (Stagg and Nitsche, 2011), but solely anodal tDCS plastic effects depend upon the modulation of GABAergic interneurons (Nitsche et al., 2004; Stagg et al., 2009; Stagg and Nitsche, 2011). Anodal tDCS indeed elicites a reduction of short-intracortical inhibition (SICI) and an increase in I-wave mediated intracortical facilitation (ICF), both measures of GABAergic interneuronal activity (Nitsche et al., 2005). Accordingly, by using Magnetic Resonance Spectroscopy (MRS) Stagg et al. (2009) demonstrated a reduction of GABA concentration within M1 10 min after anodal tDCS.

Beyond modulating the excitability of the stimulated area, tDCS can also alter cortical connectivity from the targeted area, thus affecting broader brain networks. Stagg et al. (2013) showed that anodal tDCS increased perfusion in a wide set of brain areas including the left primary sensory cortex (S1), the midcingulate cortex, the paracingulate cortex and the left parietal cortex. It was also found an increased connectivity between the stimulated area and the contralateral homologous one (i.e., right DLPFC) and the left sensorimotor cortex, but a decreased connectivity with the bilateral thalamus. Cathodal tDCS, instead, decreased perfusion in the bilateral thalami and right middle and inferior temporal gyri and led to a decrease of connectivity between the left DLPFC and an extensive region in the left temporal, parietal, and occipital lobes. In contrast, an increased functional connectivity was observed after cathodal but not anodal tDCS over M1 within the motor and non-motor network, such as the default mode brain network (Amadi et al., 2014).

Recently, the effects on cortical excitability and connectivity of anodal tDCS applied on non-motor areas were tracked using TMS-EEG. Thorugh the activation of a cortical area with TMS, it is possible to record in real time the cortical response over the cortex by means of HD-EEG recordings. TMS-evoked potentials (TEPs) recorded with this technique reflect cortical excitability and connectivity of the targeted area, representing a direct measure of the neural state. TMS-EEG studies on tDCS effects on cortical excitability showed an increase of TEPs during and 10 min after the end of anodal tDCS, which were not restricted to the stimulated area, but rather affected different cortical networks according to the brain activation state. Effects spread following structural connections at resting state (Romero Lauro et al., 2014, 2015), whereas they were confined to functionally relevant areas when tDCS was applied during task execution (Pisoni et al., 2017).

In the present study, we aimed at further complementing previous knowledge on the neurophysiological basis of tDCS by applying the same TMS-EEG co-registration approach to explore the effects induced by cathodal tDCS. Addressing the cortical effects of cathodal tDCS acquires **a critical** relevance considering that the behavioral outcomes of this stimulation are more uncertain in comparison to those induced by anodal tDCS (e.g., Jacobson et al., 2012 for a review). Indeed, whereas polarity-dependent opposite effects – anodal excitatory and cathodal inhibitory–, are usually reported when stimulating the primary sensory, motor or visual cortices (but see, e.g., Batsikadze et al., 2013; Sczesny-Kaiser et al., 2016 for different results), the evidence becomes more controversial when higher cognitive functions and the underlying brain areas are targeted (Jacobson et al., 2012). Typically, anodal tDCS has been found to enhance the targeted cognitive function, whereas cathodal stimulation is reported as less effective or is not explored at all. For instance, recent evidence-based guidelines for clinical use of tDCS (Lefaucheur et al., 2017) do not include cathodal stimulation for any disease.

To mirror previous data (Romero Lauro et al., 2014, 2015), in the present study we replicate the methodology but reversing the stimulation polarity applying cathodal tDCS over the right PPC, and tracking its effects on cortical excitability and connectivity performing TMS-EEG co-registrations before, during and 10 min after the end of the stimulation. Since our participants did not take part in the previous study, we decided to not directly compare the three groups (anodal, cathodal, and sham), rather we compared stimulation effects within the same stimulation condition; i.e., pre-post cathodal tDCS and pre-post sham stimulation. We hypothesized a reduction of cortical excitability and connectivity, during and following the stimulation.

MATERIALS AND METHODS

Participants

Fifteen healthy, right-handed volunteers (five males, mean age 25.4 years, *SD* 3.5, range 21–32) participated in the study. To define the sample size, we run a-priori computations in GPower to determine the number of participants needed to highlight a potential effect of stimulation with a power of 0.90 and an alpha level of $p = 0.05$. In detail, we ran two a-priori sample size computations, one with the smallest significant effect found in Romero Lauro et al. (2014), and the other with the mean value of the reported significant effect sizes (eta squared of 0.34 and 0.42, respectively). Each participant completed an Adult Safety Screening Questionnaire (Keel et al., 2001), and gave informed written consent before the experiment. Participants did not report contraindications to non-invasive brain stimulation (Rossi et al., 2009), namely no history of medical disorders, no substance abuse, no use of central nervous system-effective medication, no psychiatric and neurological disorders, including brain surgery, tumor, or intracranial metal implantation. The study took place in the TMS-EEG laboratory of the University of Milano-Bicocca, was approved by the local Ethics Committee, and it was carried out in accordance with the ethical standards of the revised Helsinki Declaration.

Procedure

For each participant, the experimental session consisted of three blocks of TMS-EEG recordings performed before (pre-tDCS), during (during-tDCS) and 10 min after cathodal tDCS (post-tDCS) applied over the right PPC. Each recording lasted about 7 min during which participants were in a resting condition, fixating a white cross in a black screen (17″). The second group of 15 participants took part in a control Sham session. Six participants of this sample were taken from a previous study (Romero Lauro et al., 2014), while the remaining nine were recruited from the present sample. Sham sessions were identical to the cathodal ones, but tDCS was turned off 30 s after the start. The order of the two sessions (cathodal and sham tDCS) was counterbalanced across subjects.

TMS Stimulation

TMS was delivered with an Eximia™ TMS stimulator (Nexstim™, Helsinki, Finland) using a focal figure-of-eight bi-pulse 70 mm-coil. As in Romero Lauro et al. (2014), stimulation target was the left PPC, between P1 and CP1 EEG electrodes. High-resolution (1 × 1 × 1 mm) structural magnetic resonance images (MRI) were acquired for each participant using a 3 T Intera Philips body scanner (Philips Medical Systems, Best, NL). TMS target was identified on individual MRIs using a Navigated Brain Stimulation (NBS) system (Nexstim™, Helsinki, Finland), which employs infrared-based frameless stereotaxy to map the position of the coil and participant's head, within the reference space of the individual's MRI space. Mean MNI coordinates for the target site were X = −31 (*SD* = 5.2) Y = −70 (*SD* = 6.6) Z = 54 (*SD* = 3.7). The NBS system allowed to continuously monitoring the position and orientation of the coil, thus assuring precision and reproducibility of the stimulation across sessions. Moreover, the NBS system estimated on-line the distribution and intensity (V/m) of the intracranial electric field induced by TMS. It uses a locally best-fitting spherical model, accounting for the head and brain shape of each participant, and taking into consideration the distance from scalp, coil position, and orientation. Mean stimulation intensity, expressed as a percentage of the maximal output of the stimulator, was 58% (range = 50–63%), corresponding to an electric field of 100

± 14 V/m. The coil was placed tangentially to the scalp, and adjusted for each participant in order to direct the electric field perpendicularly to the shape of the cortical gyrus, following the same procedure of previous studies (Casarotto et al., 2010; Mattavelli et al., 2013; Romero Lauro et al., 2014). Since TMS over parietal sites can activate temporal and frontal muscles, hence eliciting artifacts in the EEG recordings, the site of the stimulation was individually adjusted, in order to avoid or reduce as much as possible muscle twitches. TMS pulses were delivered at an inter-stimulus interval (ISI) randomly jittered between 2,000 and 2,300 ms (0.4–0.5 Hz). One hundred and eighty TMS pulses were delivered for each block.

tDCS Parameters

tDCS was delivered by a battery-driven constant current stimulator (Eldith™, Neuroconn, Ilmenau, Germany) using a pair of rubber electrodes and a conductive paste (Ten20 conductive EEG paste, Kappamedical™, USA) to attach them to participants' head and reduce impedance. An intracephalic montage was used. The cathode (size = 9 cm^2; current density = 0.08 mA/cm^2) was placed over the right PPC under the EEG cap, in a site corresponding to P2 electrode, which was previously removed from the cap together with the CP2 electrode, as in Romero Lauro et al. (2014). The anode (size = 25 cm^2, current density = 0.03 mA/cm^2) was positioned over the left supraorbital area. A constant current of 0.75 mA was applied for 15 min, with 8 s of fade-in/fade-out period. Different sized electrodes were used to increase the focality of stimulation (Nitsche et al., 2008). For sham tDCS, the same electrodes arrangement and stimulation parameters were used, but the stimulator was turned off after 30 s (Gandiga et al., 2006). The feasibility of concomitant EEG recording and tDCS application has been recently probed (Wirth et al., 2011; Faria et al., 2012; Schestatsky et al., 2013). In order to avoid tDCS induced artifacts in the EEG trace, the tDCS electrodes and the conductive gel never came in contact with the surrounding EEG recording leads and they were far away from the ground electrodes (see **Figure 1**). Transient EEG artifacts were observed only during the fade-in and fade-out phases of tDCS stimulation, while TMS-EEG trials were never affected by those transient artifacts. The study was performed in single blind, and no adverse effects were reported.

EEG Recording Data During TMS

TEPs were continuously recorded using a TMS compatible 60-channels amplifier (Nexstim Ltd., Helsinki, Finland), which gates the TMS artifact and prevents saturation by means of a proprietary sample-and-hold circuit (Virtanen et al., 1999). EEG signals were referenced to two electrodes placed over the forehead and used as ground. Eye movements were recorded with two additional electrodes placed near the eyes, in order to monitor ocular artifacts both in the vertical and horizontal axes. As in previous studies (Massimini et al., 2005; Casarotto et al., 2010), in order to prevent auditory potentials due to TMS pulses, a masking noise, which reproduced scrambled TMS "click" time varying frequency components, was continuously played into earplugs worn by participants during the experimental sessions. Electrodes impedance was kept below 5 kΩ, and EEG signals were recorded with a sampling rate of 1,450 Hz.

EEG Data Analysis

EEG data were pre-processed using Matlab R2016b® (Mathworks, Natick, MA, USA). First, recordings were down-sampled to 725 Hz. Continuous signal was then split in single trials, from 800 ms before to 800 ms after the TMS pulse. Trials with artifacts due to eye blinks/movements, or spontaneous muscle activity were removed following a semi-automatic procedure (Casali et al., 2010), and the visual inspection of the signal by trained experimenters (AP, EV). The average number of trials considered in the analysis was 123 (SD ± 3) for the pre-tDCS, 123 (SD ± 5) for the during tDCS block, and 122 (SD ± 3) for the post-tDCS condition. TEPs were computed by averaging selected artifact-free single trials and by filtering them between 2 and 40 Hz. Bad or missing channels, as P2 and CP2 for each session, were interpolated using the spherical interpolation function of EEGLAB (Delorme and Makeig, 2004). TEPs were then average referenced and baseline corrected between −300 and −50 ms before the TMS pulse. For each condition, as an index of global excitability, Global Mean Field Power (GMFP, Casarotto et al., 2010; Romero Lauro et al., 2014, 2015; Pisoni et al., 2017) was computed on averaged TEPs of 60 channels for three temporal windows defined in an interval between 0 and 150 ms from TMS pulse onset. The three time windows were: 0–50, 50–100, and 100–150 ms. To further identify the specific contributions of different cortical regions to the modulation of global cortical excitability, indexes of local excitability (Local Mean Field Power, LMFP) were measured following the same procedure used for GMFP. Four clusters of electrodes, with 4 electrodes each, were selected based on anatomical locations. Two parietal clusters: the left one corresponding to TMS hotspot (CP1, CP3, P1, and P3), and the right one corresponding to the area covered by the tDCS cathode (CP2, CP4, P2, and P4). Two frontal clusters corresponded to the areas structurally and functionally connected to the parietal ones: the left frontal cluster (F1, F5, FC1, and FC3) and the right frontal cluster (F2, F6, FC2, and FC6). In order to obtain a synthetic index of global and local cortical excitability, GMFP and LMFP values were cumulated within the three time windows (0–50, 50–100, and 100–150 ms after the TMS pulse) and for each experimental condition (pre-, during-, and post-tDCS).

Source Modeling

Source modeling was performed in order to assess the impact of tDCS on cortical excitability, avoiding the potential confound of volume conduction and allowing a better definition of the spatial distribution of the tDCS effects (as in Romero Lauro et al., 2015). The analysis was run on 14 out of the 15 participants enrolled in the experiment, since in one of the subjects MRI data were not suitable for source reconstruction (see for details on the procedure see Casali et al., 2013). First, meshes of cortex, skull, and scalp compartments (containing 3,004, 2,000, and 2,000 vertices, respectively) were obtained following the 3-spheres BERG method (Berg and Scherg, 1994), as implemented in the Brainstorm software package

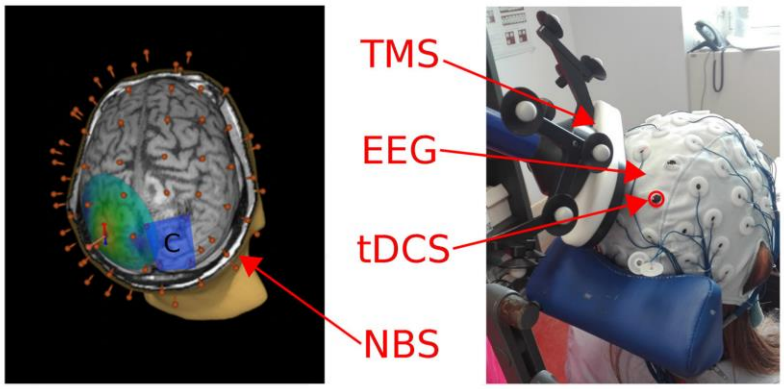

FIGURE 1 | Left: A 3D reconstruction of the individual MRI is depicted, showing the electrical field induced by TMS on the left parietal cortex. The blue rectangle represents the cathode patch position over the right parietal cortex, the 60 red points correspond to the position of the EEG cap electrodes. **Right**: A picture of the experimental setting used to deliver tDCS and TMS concurrently while recording EEG (during-tDCS condition).

(http://neuroimage.usc.edu/brainstorm). This method includes 3 concentric spheres with different homogeneous conductivities, representing the best-fitting sphere of inner and outer skull and scalp. The model was constrained to the meshes of these tissues obtained from the individual MRIs of the experimental subjects in the Statistical Parametric Mapping software package (SPM5, http://www.fil.ion.ucl.ac.uk/spm/software/spm5/): for each participant, binary masks of skull and scalp obtained from individual MRIs were warped to the canonical meshes of the Montreal Neurological Institute (MNI) atlas. Then, the inverse transformation was applied to the MNI mesh of the cortex for approximating to real anatomy. The cortex, in particular, was reconstructed as a 3D grid of 3004 fixed dipoles, normally oriented with respect to the cortical surface. For each participant, EEG sensor position was aligned to the canonical anatomical markers (pre-auricular points and nasion), and the forward model was computed. The inverse solution was computed on the average of all artifact-free TMS-EEG trials using the weighted minimum norm estimate with smoothness prior, following the same procedures as in Casali et al. (2010). This method is advantageous because it provides stable solution also in the presence of noise (Silva et al., 2004), and it does not require any a priori assumption about the nature of the source distribution (Hämäläinen and Ilmoniemi, 1994). After source reconstruction, a statistical threshold was computed in order to assess when and where the post-TMS cortical response differed from pre-TMS activity (i.e., to identify TMS-evoked response). To do so, a non-parametric permutation-based procedure was applied (Pantazis et al., 2003). A binary spatial-temporal distribution of statistically significant sources was obtained and thus only information from significant cortical sources was used for further analyses. As a measure of global cortical activation, we cumulated the absolute Significant Current Density (global SCD, measured in mA/mm^2, Casali et al., 2010) overall 3,004 cortical vertexes and over the three time windows (0–50, 50–100, and 100–150 ms) for each recording session (pre-tDCS, during-tDCS and post-tDCS). Finally, in order to mirror the LMFP EEG data analysis of the study, for each time window and each experimental condition, a local SCD was computed in the vertexes within four different Brodmann's areas (BAs), identified by means of an automatic tool of anatomical classification (WFUPickAtlas tool; http://www.ansir.wfubmc.edu). These BAs approximately corresponded to the original four clusters of LMFP (left/right BA 6 and 7).

Statistical Analyses

To estimate whether tDCS affected global or local cortical excitability, GMFP and LMFP values were submitted to a series of linear mixed effects models (Baayen et al., 2008) in R statistical computing software environment (R Core Team, 2014) with the "lme4" package (version 0.6-82, Bates et al., 2014). In particular, GMFP was considered as a continuous dependent variable, while *Condition* (factorial, 3 levels: pre-, during- and post-tDCS) and *Time Window* (factorial, 3 levels: 0–50; 50–100; and 100–150 ms) were tested as fixed factors. The by-subject intercept was included as random factor. The inclusion of a main effect or interaction in the final model was assessed by means of Likelihood Ratio Test (LRT, see Baayen et al., 2008), including a parameter if it significantly increased the model's goodness of fit. The same procedure was adopted for LMFP values, which were analyzed separately for each electrodes cluster. A further test with a Bayesian ANOVA on the same values was performed to test for the null hypothesis (Rouder et al., 2009; Etz et al., 2018) by means of the Bayesian ANOVA analysis using "JASP" software environment (version 0.8.2.0, JASP Team, 2017).

The same analysis was performed for source modeling data on global and local SCD values.

The whole procedure was also adopted to analyze sham session data.

RESULTS

Cathodal Stimulation—Sensor Analysis

GMFP

The final model on GMFP values did not include the main effect of *Condition* in the 0–50 ms [$\chi^2_{(2)} = 1.15$; $p = 0.56$], in the 50–100 ms [$\chi^2_{(2)} = 0.26$; $p = 0.87$] and in the 100–150 ms [$\chi^2_{(2)} = 1.62$; $p = 0.44$] time windows. GMFP thus did not change when recorded before, during or after cathodal tDCS (see **Figure 2A**). Bayesian analysis, indeed, provided moderate support in favor of the null hypothesis for the first ($BF_{01} = 5.1$), the second ($BF_{01} = 4.6$), and the third ($BF_{01} = 5.3$) time window.

LMFP

Analyses run on LMFP values did not support any effect of cathodal tDCS in any of the considered clusters of electrodes (see **Figure 3A**).

In particular, concerning C1, the cluster under the tDCS cathode, LRT indicated not to include *Condition* in the model run on LMFP values in the first [$\chi^2_{(2)} = 1.53$; $p = 0.46$],

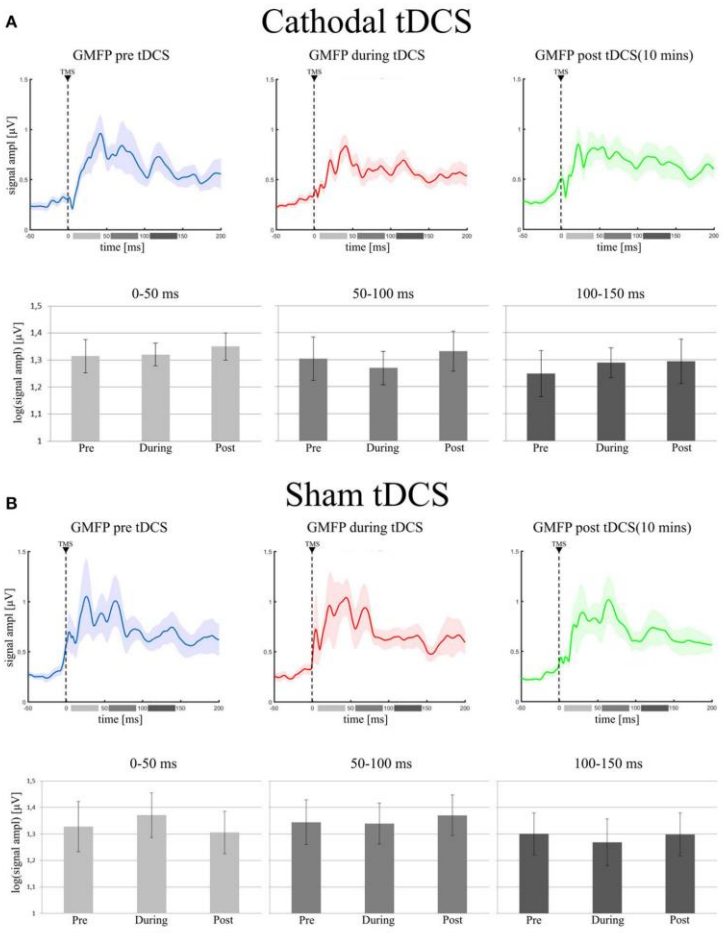

FIGURE 2 | (A) (Cathodal tDCS): in the upper row it is shown the Grand Average of GMFP in the three experimental conditions (pre tDCS = blue trace; during tDCS = red trace; post tDCS = green trace). Shadowed areas represent ± SE. In the lower row, the bar histograms represent the mean values of the log-GMFP in the three time-windows of our interest (0–50 ms = light gray, 50–100 ms = gray, 100–150 ms = dark gray) for each recording session. The error bars represent ± SE. **(B)** (Sham tDCS) shows the same data, but for the sham group: the Grand Average of GMFP and the mean values of log-GMFP, in the upper and lower row, respectively.

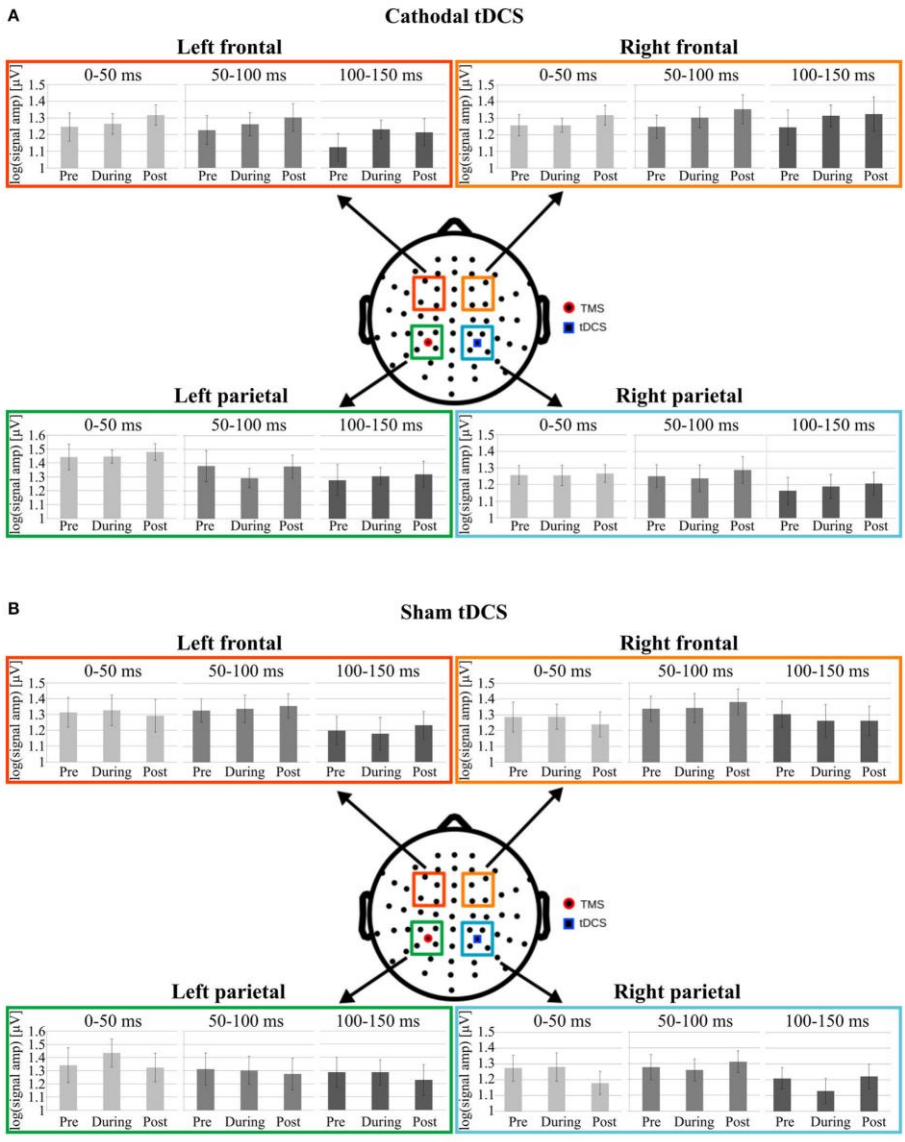

FIGURE 3 | Data from Cathodal and Sham groups are respectively shown in **(A,B)**. Mean log-LMFP for the four clusters of interest. Colored squares on the head model represent the electrodes clusters in the parietal and frontal regions. The blue square in the right parietal region represents the location of the tDCS cathode, whereas the red dot in the left parietal cluster represents the TMS position. For each cluster, the bar graphs represent mean log-LMFP in the baseline, during and post tDCS conditions, for the three temporal windows: 0–50 ms (light gray), 50–100 ms (gray), and 100–150 ms (dark gray). Error bars represent ± SE.

second [$\chi^2_{(2)} = 0.63$; $p = 0.73$], and third [$\chi^2_{(2)} = 1.36$; $p = 0.51$] time window. Critically, Bayesian analyses moderately supported the null hypothesis, indicating no effect of tDCS on LMFP computed in this cluster for the first ($BF_{01} = 5.5$), the second ($BF_{01} = 3.9$) and the third ($BF_{01} = 5.7$) time window.

Analyzing C2, the cluster under the TMS coil, LRT indicated to not include *Condition* in models for any time window [0–50 ms: $\chi^2_{(2)} = 1.12$; $p = 0.57$; 50–100 ms: $\chi^2_{(2)} = 0.99$; $p = 0.61$; 100–150 ms: $\chi^2_{(2)} = 1.22$; $p = 0.54$]. Crucially, Bayesian analyses moderately supported the null hypothesis, indicating no effect of tDCS on LMFP computed in this cluster in any time window (0–50 ms: $BF_{01} = 6$; 50–100 ms: $BF_{01} = 5.3$; 100–150 ms: $BF_{01} = 5.5$).

Similarly, in C3 LRT indicated to not include *Condition* in models for any time window [0–50 ms: $\chi^2_{(2)} = 1.03$; $p = 0.6$; 50–100 ms: $\chi^2_{(2)} = 2.78$; $p = 0.25$; 100–150 ms: $\chi^2_{(2)} = 1.08$; $p = 0.58$]. Yet, Bayesian analyses moderately supported the null hypothesis, indicating no effect of tDCS on LMFP computed in this cluster in any time window (0–50 ms: $BF_{01} = 3.8$; 50–100 ms: $BF_{01} = 3$; 100–150 ms: $BF_{01} = 4.9$).

The final model on C4 values did not include the main effect of *Condition* in the 0–50 ms [$\chi^2_{(2)} = 1.4$; $p = 0.49$] in the 50–100 ms [$\chi^2_{(2)} = 2.38$; $p = 0.30$] or in the 100–150 ms [$\chi^2_{(2)} = 3$; $p = 0.22$] time windows. Even in this case, Bayesian analysis supported moderately the null hypothesis, indicating no effect of tDCS on LMFP computed in this cluster in any time window (0–50 ms: $BF_{01} = 4.5$; 50–100 ms: $BF_{01} = 4.4$; 100–150 ms: $BF_{01} = 3.5$).

Cathodal Stimulation—Source Modeling Analyses

Source modeling analyses confirmed results from the sensor analyses. A full report of statistical results of analyses run on Global and Local SCD is reported in **Table 1**.

The final model on Global SCD did not include *Condition* in any time window, indicating no effect of cathodal tDCS on cortical activation induced by TMS (see **Figure 4A**).

Similarly, for both left and right BA7 LRT indicated no inclusion of the factor *Condition* in the final model, suggesting no influence of cathodal tDCS on local cortical activity in the left and right parietal cortices.

The same result holds for the left and right BA6, where no effect of tDCS was highlighted on local SCD.

TABLE 1 | List of *p* values resulting from the source modeling analysis performed for each time window (0–50, 50–100, and 100–150 ms) within the four Brodmann's areas (BAs), that corresponded approximately to the four clusters.

	BA 7 L	BA 7 R	BA 6 L	BA 6 R
CATHODAL				
0–50 (ms)	$p = 0.736$	$p = 0.729$	$p = 0.513$	$p = 0.605$
50–100 (ms)	$p = 0.232$	$p = 0.204$	$p = 0.683$	$p = 0.787$
100–150 (ms)	$p = 0.484$	$p = 0.582$	$p = 0.835$	$p = 0.656$

In particular, BA 7 L is the Left parietal cluster (TMS site; CP1, CP3, P1, and P3); BA 7 R is the Right parietal cluster (tDCS cathode; CP2, CP4, P2, and P4); BA 6 L is the Left frontal cluster (F1, F5, FC1, and FC3); BA 6 R is the Right frontal cluster (F2, F6, FC2, and FC6).

Sham Stimulation—Sensor Analysis

GMFP

As expected, sham stimulation did not modulate global indices of cortical excitability. In particular, the final model run on GMFP did not include the main effect of *Condition* in any time window [0–50 ms: $\chi^2_{(2)} = 1.2$; $p = 0.55$; 50–100 ms: $\chi^2_{(2)} = 0.43$; $p = 0.81$; 100–150 ms: $\chi^2_{(2)} = 0.18$; $p = 0.91$ see **Figure 2B**]. Bayesian analyses, moderately supported the null hypothesis for the inclusion of the factor *Condition* in the final model (0–50 ms: $BF_{01} = 3.9$; 50–100 ms: $BF_{01} = 5.1$; 100–150 ms: $BF_{01} = 5.4$).

LMFP

Analyses run on LMFP confirm the lack of any effect of sham tDCS in any of the considered clusters of electrodes in modulating local cortical excitability (see **Figure 3B**).

In C1, LRT values were non-significant for the first [$\chi^2_{(2)} = 2.4$; $p = 0.3$], the second [$\chi^2_{(2)} = 0.98$; $p = 0.61$] and the third [$\chi^2_{(2)} = 2.29$; $p = 0.32$] time window. Bayesian analyses moderately supported the null hypothesis, indicating no effect of sham tDCS on LMFP computed in this cluster (0–50 ms: $BF_{01} = 2.3$; 50–100 ms: $BF_{01} = 4.73$; 100–150 ms: $BF_{01} = 3.3$).

The same holds for C2. LRT values were not significant for the factor *Condition* in any time window [0–50 ms: $\chi^2_{(2)} = 1.28$; $p = 0.53$; 50–100 ms: $\chi^2_{(2)} = 0.86$; $p = 0.65$; 100–150 ms: $\chi^2_{(2)} = 0.2$; $p = 0.9$]. Similarly, Bayesian analyses moderately supported the data under the null hypothesis for the first ($BF_{01} = 3.4$), the second ($BF_{01} = 5.4$), and the third ($BF_{01} = 5$) time window.

Similarly, in C3 LRT indicated not to include factor *Condition* for any time window [0–50 ms: $\chi^2_{(2)} = 1.94$; $p = 0.38$; 50–100 ms: $\chi^2_{(2)} = 0.74$; $p = 0.69$; 100–150 ms: $\chi^2_{(2)} = 0.09$; $p = 0.95$] in the final model. Yet, Bayesian analyses moderately supported the data under the null hypothesis for the first ($BF_{01} = 4.7$), the second ($BF_{01} = 5$), and the third ($BF_{01} = 5.4$) time window.

Finally, also for C4 LRT values were non-significant for the first [$\chi^2_{(2)} = 0.08$; $p = 0.95$], the second [$\chi^2_{(2)} = 0.3$; $p = 0.86$] and the third [$\chi^2_{(2)} = 0.22$; $p = 0.89$] time window. Even in this case, Bayesian analyses moderately supported the null hypothesis, indicating no effect of sham tDCS on LMFP computed in this cluster (0–50 ms: $BF_{01} = 5.4$; 50–100 ms: $BF_{01} = 5.4$; 100–150 ms: $BF_{01} = 5.1$).

Sham Stimulation—Source Modeling Analyses

Source modeling analyses on sham recordings mirrored results from the sensor analyses. A full report of statistical results of analyses run on Global and Local SCD is reported in **Table 2.**

Global SCD final model did not include *Condition* in any time window, indicating no effect of sham stimulation on cortical excitability (see **Figure 4B**).

The same holds for both left and right BA7 and BA6, where LRT indicated no inclusion of the factor *Condition* in the final model.

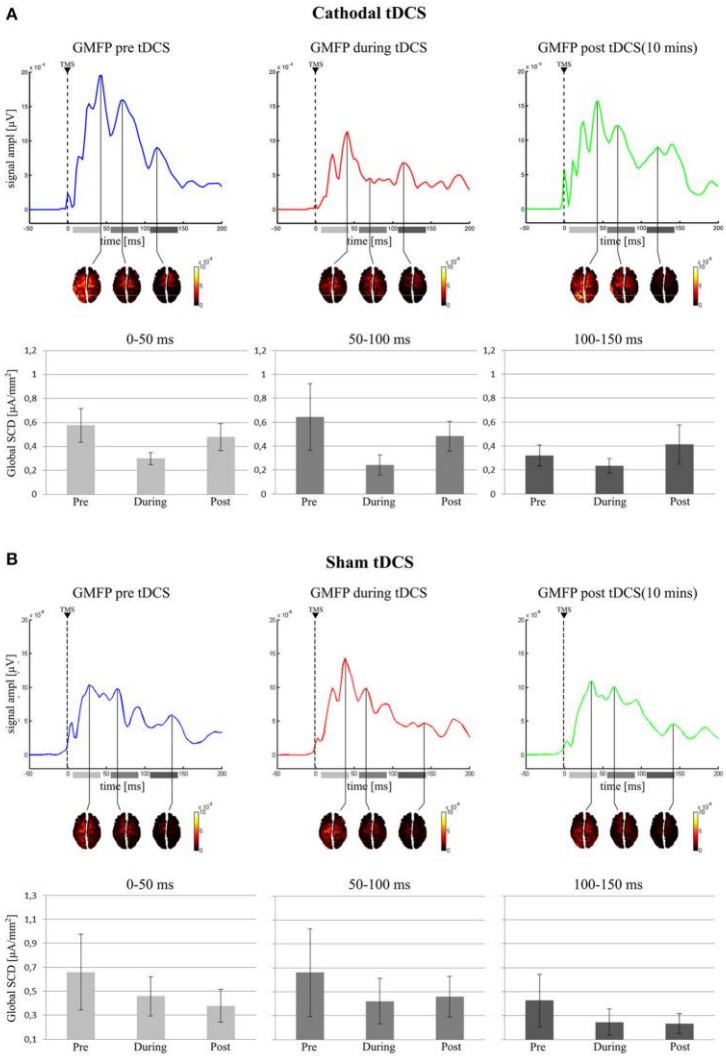

FIGURE 4 | Active vertexes and current spread at the local maxima in the GMFP for the three time-windows. In the **(A)** (Cathodal tDCS), for each recording session, the GMFP is shown on first top row, with the area beneath the curve divided in the three tested time windows (0–50 ms: light gray; 50–100 ms: gray; 100–150 ms: dark gray). The second row shows the estimated cortical sources in time coincidence with the maximum GMFP value, for each time window. In the last row are reported the mean values of the Global SCD for each condition and in each time window. **(B)** (Sham tDCS) shows the same results but for the sham group.

DISCUSSION

In this study, we ought to investigate the effects on cortical excitability induced by 10 min of cathodal stimulation over the right PPC. To this purpose, we measured TEPs by means of TMS-EEG recordings before, during and 10 min after the end of the stimulation. TMS was applied over the left PPC. As a control condition, 15 participants underwent an additional session in which sham tDCS was delivered. Since not all the participants took part in both this and Romero Lauro et al.'s experiment, we separately compared stimulation effects in the three groups, i.e., anodal, cathodal, and sham. Indices of local and global

TABLE 2 | *p*-values deriving from the sham data extracted from the same analyses described in **Table 1**.

	BA 7 L	BA 7 R	BA 6 L	BA 6 R
SHAM				
0–50 (ms)	$p = 0.174$	$p = 0.081$	$p = 0.117$	$p = 0.237$
50–100 (ms)	$p = 0.109$	$p = 0.319$	$p = 0.149$	$p = 0.088$
100–150 (ms)	$p = 0.966$	$p = 0.992$	$p = 0.998$	$p = 0.995$

activity were computed both at the sensors and cortical sources level.

At the sensors level, no significant modulation of cortical excitability was observed during and after cathodal stimulation in comparison to the pre-tDCS session, neither at a global (GMFP) nor at a local level (LMFP for 4 clusters of electrodes). Furthermore, no significant results were found for any of the considered TEPs' temporal windows, namely an early (0–50 ms), a middle (50–100 ms), and a late (100–150 ms) one, chosen to assess different TEP's components. Source modeling confirmed the results observed at the sensor level, since SCD did not change during or after stimulation with respect to the pre-tDCS condition, both when computed at a global level or in BAs, matching the clusters of the LMFP analysis. A similar pattern of results without any significant changes in cortical excitability among the three pre-, during- and post-tDCS conditions was found when sham tDCS was delivered. This result confirms the reliability of the TMS-EEG approach and no effect of test-retest of TEP-derived indices of brain activation (Lioumis et al., 2009; Casarotto et al., 2010; Kerwin et al., 2017).

The absence of significant changes among pre-, during- and after-tDCS conditions by itself does not provide evidence that the three conditions are the same. To further check this chance, a Bayesian analysis was performed to directly test the null hypothesis of no change among the three conditions. Despite subtle differences, all the results of the Bayesian analysis converge in suggesting a moderate indication toward the null hypothesis.

Although results suggest a null effect of cathodal tDCS on cortical excitability, further corroborating evidence from different approaches is needed to support such a negative conclusion. Importantly, evidence of the modulatory effects of cathodal tDCS has been provided so far by different approaches. First of all, a reduction of neurons' firing rate was observed after cathodal tDCS in animal studies (Creutzfeldt et al., 1962; Bindman et al., 1964; Purpura and McMurtry, 1965). Furthermore, when applied over M1, cathodal tDCS resulted in a decrease of corticospinal excitability assessed by MEPs (Nitsche and Paulus, 2000; Lang et al., 2004), led to a widespread decrease of regional blood flow as measured by PET (Lang et al., 2005, but see also Baudewig et al., 2001), and increased the inter-hemispheric coherence of the resting fMRI signal between the left and right homologs regions of the motor system (i.e., M1 and SMA) as well as the functional connectivity in the motor and default mode networks (Amadi et al., 2014).

The conclusion that instead can be firmly drawn from the present set of results is that cathodal effects on cortical excitability differ from the ones induced by anodal tDCS. The present study indeed mirrored a previous one from our group (Romero Lauro et al., 2014, 2015), where the same procedure and data analysis were performed to track the effects of anodal tDCS. These previous results unveiled a significant rise of cortical excitability during and after anodal tDCS at a global level, both when measured by GMPF and by SCD. Analyses at the local level showed that the rise of cortical excitability spread along a bilateral fronto-parietal network, presumably following structural/functional connections along the default mode brain network. The significant findings in these previous studies confirm the feasibility of TMS-EEG approach to tap tDCS effects on cortical excitability. Moreover, TEPs have been shown to be a reliable measure of cortical excitability when the same parameters are maintained (Casarotto et al., 2010). The lack of significant effects in the present study cannot be attributed thus to the experimental paradigm, rather indicates a crucial imbalance between the anodal and the cathodal impact on cortical excitability.

In literature, several studies show an asymmetry between anodal and cathodal tDCS effects, for example in a qualitative review and meta-analysis, Jacobson et al. (2012) revealed how the coupling of anodal-excitatory and cathodal-inhibitory effect is robust in the motor and perceptual domains, but controversial when cognitive functions are addressed. In most of the cases, indeed, when memory, language or, generally, when higher-order cortical regions are tested, as in our study, an excitatory/enhancing effect of anodal tDCS is observed, whereas cathodal tDCS effects are less effective or ineffective. For instance, in a double-blind sham-controlled, within-subjects study, 20 min of anodal but not cathodal tDCS over the left peri-sylvian area improved the performance of healthy subjects in an associative verbal learning task (Flöel et al., 2008). Similarly, the anodal, but not the cathodal, tDCS over the left dorsolateral prefrontal cortex (DLPFC) enhanced the performance at a complex task, such as the remote associates task, involving both language processing and executive abilities (Cerruti and Schlaug, 2009). In the domain of working memory, anodal tDCS over left DLPFC increased accuracy in a sequential letter task whereas cathodal effect did not differ from that of sham stimulation (Fregni et al., 2005). The frequent lack of significant behavioral effects induced by cathodal tDCS is possibly the reasons why many studies, performed both in healthy and clinical population, focused only on testing the anodal vs. sham modality of stimulation (Jacobson et al., 2012). It has to be noted that previous studies investigating tDCS-induced cognitive modulations did not target M1. It follows that cathodal effects highlighted by targeting M1 could be due to a greater sensitivity of this area to cathodal tDCS, having a different cortical organization compared to the rest of the homotypic isocortex.

Nevertheless, there are examples of tDCS effects limited to anodal polarity also in the heterotypic isocortex, such as in the motor (Baudewig et al., 2001; Priori, 2003), visual (Antal et al., 2004; Sczesny-Kaiser et al., 2016), and somatosensory systems (Matsunaga et al., 2004). Within the motor domain, for instance, there is evidence of greater effectiveness of anodal than cathodal stimulation. Indeed, anodal tDCS applied to M1 during task

execution enhanced motor speed and dexterity (Nitsche et al., 2003), and also motor learning and adaptation (Nitsche et al., 2003; Boggio et al., 2006; Galea and Celnik, 2009; Hunter et al., 2009; Reis et al., 2009). In contrast, cathodal tDCS showed no effect on learning (Nitsche et al., 2003; Galea and Celnik, 2009; Reis et al., 2009), or on reaction times (Nitsche et al., 2003).

Critically, with a methodology more similar to that applied in the present research, a previous TMS-EEG study (Pellicciari et al., 2013) found the coupling of anodal-excitatory and cathodal-inhibitory modulation on TEPs by stimulating M1; however, also in this case, the effect of the two polarities was different, since increased excitability after anodal stimulation was found over both hemispheres whereas the cathodal stimulation induced opposite effects over the two hemispheres, namely reduced excitability over the stimulated hemisphere and facilitation in the contralateral one.

The mechanisms underlying this asymmetry in the effectiveness of tDCS polarity-dependent effects are still unclear. Jacobson et al. (2012) suggested that the lack of cathodal-inhibitory effects when tapping cognitive functions, as compared to the case of the motor system, could be due to several factors, including the recruitment of broader cortical networks, the greater susceptibility to external noise of the behavioral measured adopted, the influence of the initial activation state and the greater occurrence of bilateral interactions supporting contralateral compensation. Among these explanations, the most compelling seems to be the initial activation state of the target area. More specifically, whereas addressing motor functions could be done using simple tasks (i.e., reaction times) or passively (i.e., recording MEPs), exploring tDCS effects on cognitive functions entails the use of complex tasks, prompting high activations of the target regions. Hence, the anodal-excitatory effect is additive, enhancing the actual activation state level. In contrast, the cathodal inhibitory effect might be counterbalanced by the task-induced activation, leading to null effects. However, the hypothesis of a link among anodal tDCS—increased neuronal excitability/enhanced behavioral performance, at odd with cathodal tDCS—decreased neuronal excitability/reduced behavioral performance, run the risk to oversimplify the pattern of possible behavioral and neurophysiological outcomes, especially outside the sensorimotor domain. This simplistic proposal does not take into account the complex combination of excitatory and inhibitory connections within broader cortical networks, the dependence upon the network state activation, the level of performance or task engagement, the well-known inter-individual variability and other factors affecting the current diffusion in the brain, such as different neural population and orientation (see Fertonani and Miniussi, 2017).

An alternative explanation is that the effects of tDCS may depend in an opposite way on the background level of activity in the system (Matsunaga et al., 2004). For instance, if cathodal stimulation reduces the level of neural discharge, then it may produce effects in systems with high levels of basal activity. However, if the resting state is characterized by low levels of spontaneous discharge, then cathodal tDCS may have little or no effect.

For these reasons, a possible explanation about the absence of effects induced by cathodal tDCS in our study could be found in the computational model describe in Lafon et al. (2016).

In this study, a combination of computational modeling and *in vitro* experiments were used to explore how Direct Current Stimulation (DCS) affected the neuron's input/output function, namely the synaptic efficacy (input, I) and the likelihood of eliciting an action potential (output, O), by modeling a 2-compartment neuron, including the soma and the dendrites, and by recording *in vitro* from hippocampal pyramidal cells.

Results showed that opposing polarization of soma and dendrite may account for the asymmetry in the strength of the effects of stimulation for opposite polarities. In particular, anodal tDCS modulates I/O functions by increasing the likelihood that neurons elicit an action potential in response to a fixed input and, in addition, increasing the synaptic current entering the cell. The opposite occurs for cathodal stimulation, i.e., a decrease in output likelihood by soma hyperpolarization. However, in cathodal tDCS this effect is canceled by the depolarization of the dendrites, hence increasing the probability of spike initiation at this location. Therefore, cathodal, compared to anodal, tDCS creates an opposite shift in the threshold of I/O function, but with a weaker impact because of these two counterbalancing opposite effects on the two neuron's compartments.

By applying this model to the conventional M1-SO electrodes' montage, Lafon et al. (2016) analyzed which portion of cortical tissue in human cortex is exposed to tangential or radial current flows. In particular, they simulated and averaged the population effects on the I/O function for the anodal or cathodal tDCS. Data suggest that while anodal stimulation induces an increase in the population-level I/O function, cathodal tDCS do not modulate neuronal efficiency at the population level.

A polarity asymmetry has also been shown in the induction of LTP effects. For instance, in M1 mice slices, only anodal, but not cathodal, DCS coupled with simultaneous synaptic activation was able to induce LTP (Fritsch et al., 2010). In a similar vein, in a recent study (Kronberg et al., 2017) DCS applied during plasticity induction on rat hippocampal slices resulted in asymmetric effect on synaptic plasticity since both anodal and cathodal enhanced LTP and reduced LTD. Crucially and in line with Lafon's et al. results, this study unveiled how the effect of DCS are dependent upon the location and frequency of active synapses, more than from the polarity of stimulation.

Another important point is that in our study TMS-EEG recordings were collected while our participants were in a resting state. We have recently shown how cortical excitability, as measured by means of TEPs, is modulated by the activation state of the target area (Pisoni et al., 2017). In particular, during task execution the induced rise of cortical excitability spread following functional rather than structural connections, encompassing only task-relevant brain regions. Whether cathodal effects on cortical excitability would be different by administering a task involving the target region is a crucial question, calling for further research.

Possible limitations could derive from the dimensions of the electrodes and the montage used here. In a recent study, indeed, Roy et al. (2014) used a combination of EEG and high-definition tDCS, with a 4 × 1 ring electrodes configuration. For future

studies, this could be an ideal montage to better observe the real-time effects of tDCS on cortical excitability. In line with this observation, another indication for future studies could be to use a high-resolution tDCS to probe with TMS the same tDCS target area. Finally, as highlighted by Saturnino et al. (2015), the main tDCS effects might be between the two electrodes, thus directly stimulating with TMS the region targeted with the cathode could lad to different results. Future research is then needed to explore this issue, noting that in the case of anodal stimulation even when targeting the contralateral homologous brain region TMS-EEG highlighted a vast change in cortical excitability.

In conclusion, the results of the present study show no significant modulation of cortical excitability as measured by TEPs, when the cathodal tDCS is applied over the right parietal cortex. In contrast, previous studies showed a significant rise of cortical excitability both stimulating the same area at resting state (Romero Lauro et al., 2014, 2015), or a different one during task execution (Pisoni et al., 2017). Taken together these results show an asymmetric impact of anodal and cathodal stimulation on cortical excitability, in line with previous behavioral, neurophysiological and computational modeling studies. This asymmetry warrants further research to better understand the underlying mechanism and should be taken into account in study design for both research and clinical purposes.

AUTHOR CONTRIBUTIONS

EV, AP, GM, AV, and LR: designed the study; EV, AP, GM, AV, AG, and LM: performed the experiments; EV, AP, and LR: analyzed the data; EV, AP, and LR: mainly contributed to the manuscript; GM, AV, MR, NB, and GV: contributed to the manuscript.

REFERENCES

Accornero, N., Voti, P. L., La Riccia, M., and Gregori, B. (2007). Visual evoked potentials modulation during direct current cortical polarization. *Exp. Brain Res.* 178, 261–266. doi: 10.1007/s00221-006-0733-y

Amadi, U., Ilie, A., Miranda, H., and Stagg, C. J. (2014). Polarity-specific effects of motor transcranial direct current stimulation on fMRI resting state networks. *Neuroimage* 88, 155–161. doi: 10.1016/j.neuroimage.2013.11.037

Antal, A., Kincses, T. Z., Nitsche, M. A., Bartfai, O., and Paulus, W. (2004). Excitability changes induced in the human primary visual cortex by transcranial direct current stimulation: direct electrophysiological evidence. *Invest. Ophthalmol. Vis. Sci.* 45, 702–707. doi: 10.1167/iovs.03-0688

Baayen, R. H., Davidson, D. J., and Bates, D. M. (2008). Mixed-effects modeling with crossed random effects for subjects and items. *J. Mem. Lang.* 59, 390–412. doi: 10.1016/j.jml.2007.12.005

Bates, D., Maechler, M., Bolker, B., and Walker, S. (2014). *lme4: Linear Mixed-Effects Models Using Eigen and S4. R Package Version*. Available online at: http://CRAN.R-project.org/package=lme4

Batsikadze, G., Moliadze, V., Paulus, W., Kuo, M. F., and Nitsche, M. A. (2013). Partially non-linear stimulation intensity-dependent effects of direct current stimulation on motor cortex excitability in humans. *J. Physiol.* 591, 1987–2000. doi: 10.1113/jphysiol.2012.249730

Baudewig, J., Nitsche, M. A., Paulus, W., and Frahm, J. (2001). Regional modulation of BOLD MRI responses to human sensorimotor activation by transcranial direct current stimulation. *Magnet. Reson. Med.* 45. 196–201. doi: 10.1002/1522-2594(200102)45:2<196::AID-MRM1026>3.0.CO;2-1

Berg, P., and Scherg, M. (1994). A fast method for forward computation of multiple-shell spherical head models. *Electroencephalogr. Clin. Neurophysiol.* 90, 58–64. doi: 10.1016/0013-4694(94)90113-9

Bikson, M., Inoue, M., Akiyama, H., Deans, J. K., Fox, J. E., Miyakawa, H., et al. (2004). Effects of uniform extracellular DC electric fields on excitability in rat hippocampal slices *in vitro*. *J. Physiol.* 557, 175–190. doi: 10.1113/jphysiol.2003.055772

Bindman, L. J., Lippold, O. C., and Redfearn, J. W. (1962). Long-lasting changes in the level of the electrical activity of the cerebral cortex produced by polarizing currents. *Nature* 196, 584–585. doi: 10.1038/196584a0

Bindman, L. J., Lippold, O. C., and Redfearn, J. W. (1964).The action of brief polarizing currents on the cerebral cortex of the rat (1)during current flow and (2) in the production of long-lasting after-effects. *J. Physiol.* 172, 369–382. doi: 10.1113/jphysiol.1964.sp007425

Boggio, P. S., Castro, L. O., Savagim, E. A., Braite, R., Cruz, V. C., Rocha, R. R., et al. (2006). Enhancement of non-dominant hand motor function by anodal transcranial direct current stimulation. *Neurosci. Lett.*, 404, 232–236. doi: 10.1016/j.neulet.2006.05.051

Bolognini, N., and Miniussi, C. (2016). "Multimodal association of tDCS with electroencephalography," in *Transcranial Direct Current Stimulation in Neuropsychiatric Disorders: Clinical Principles and Management*, eds A. Brunoni, M. Nitsche, and C. Loo (Cham: Springer International Publishing), 153–168.

Casali, A. G., Casarotto, S., Rosanova, M., Mariotti, M., and Massimini, M. (2010). General indices to characterize the electrical response of the cerebral cortex to TMS. *Neuroimage* 49, 1459–1468. doi: 10.1016/j.neuroimage.2009.09.026

Casali, A. G., Gosseries, O., Rosanova, M., Boly, M., Sarasso, S., Casali, K. R., et al. (2013). A theoretically based index of consciousness independent of sensory processing and behavior. *Sci. Trans. Med.* 5:198ra105. doi: 10.1126/scitranslmed.3006294

Casarotto, S., Romero Lauro, L. J., Bellina, V., Casali, A. G., Rosanova, M., Pigorini, A., et al. (2010). EEG responses to TMS are sensitive to changes in the perturbation parameters and repeatable over time. *PLoS ONE* 5:e10281. doi: 10.1371/journal.pone.0010281

Cerruti, C., and Schlaug, G. (2009). Anodal transcranial direct current stimulation of the prefrontal cortex enhances complex verbal associative thought. *J. Cogn. Neurosci.* 21, 1980–1987. doi: 10.1162/jocn.2008.21143

Creutzfeldt, O. D., Fromm, G. H., and Kapp, H. (1962). Influence of transcortical d-c currents on cortical neuronal activity. *Exp. Neurol.* 5, 436–452. doi: 10.1016/0014-4886(62)90056-0

Delorme, A., and Makeig, S. (2004). EEGLAB: an open source toolbox for analysis of single-trial EEG dynamics including independent component analysis. *J. Neurosci. Methods* 134, 9–21. doi: 10.1016/j.jneumeth.2003.10.009

Etz, A., Gronau, Q. F., Dablander, F., Edelsbrunner, P. A., and Baribault, B. (2018). How to become a Bayesian in eight easy steps: an annotated reading list. *Psychonomic Bull. Rev.* 25, 219–234. doi: 10.3758/s13423-017-1317-5

Faria, P., Fregni, F., Sebastião, F., Dias, A. I., and Leal, A. (2012). Feasibility of focal transcranial DC polarization with simultaneous EEGrecording: preliminary assessment in healthy subjects and human epilepsy. *Epilepsy Behav.* 25, 417–425. doi: 10.1016/j.yebeh.2012.06.027

Fertonani, A., and Miniussi, C. (2017). Transcranial electrical stimulation: what we know and do not know about mechanisms. *Neuroscientist* 23, 109–123. doi: 10.1177/1073858416631966

Flöel, A., Rösser, N., Michka, O., Knecht, S., and Breitenstein, C. (2008). Noninvasive brain stimulation improves language learning. *J. Cogn. Neurosci.* 20, 1415–1422. doi: 10.1162/jocn.2008.20098

Fregni, F., Boggio, P. S., Nitsche, M., Bermpohl, F., Antal, A., Feredoes, E., et al. (2005). Anodal transcranial direct current stimulation of prefrontal cortex enhances working memory. *Exp. Brain Res.* 166, 23–30. doi: 10.1007/s00221-005-2334-6

Fritsch, B., Reis, J., Martinowich, K., Schambra, H. M., Ji, Y., Cohen, L. G., et al. (2010). Direct current stimulation promotes BDNF-dependent synaptic plasticity: potential implications for motor learning. *Neuron* 66, 198–204. doi: 10.1016/j.neuron.2010.03.035

Galea, J. M., and Celnik, P. (2009). Brain polarization enhances the formation and retention of motor memories. *J. Neurophysiol.* 102, 294–301. doi: 10.1152/jn.00184.2009

Gandiga, P. C., Hummel, F. C., and Cohen, L. G. (2006). Transcranial DC stimulation (tDCS): a tool for double-blind sham-controlled clinical studies in brain stimulation. *Clin. Neurophysiol.* 117, 845–850. doi: 10.1016/j.clinph.2005.12.003

Gartside, I. B. (1968). Mechanism of sustained increases of firing rate in neurones of the rat cerebral cortex after polarization: role of protein synthesis. *Nature* 220, 383–384. doi: 10.1038/220383a0

Gellner, A. K., Reis, J., and Fritsch, B. (2016). Glia: a neglected player in non-invasive direct current brain stimulation. *Front. Cell. Neurosci.* 10:188. doi: 10.3389/fncel.2016.00188

Hämäläinen, M. S., and Ilmoniemi, R. J. (1994). Interpreting magnetic fields of the brain: minimum norm estimates. *Med. Biol. Eng. Comput.* 32, 35–42. doi: 10.1007/BF02512476

Hattori, Y., Moriwaki, A., and Hori, Y. (1990). Biphasic effects of polarizing current on adenosine sensitive generation of cyclic AMP in rat cerebral cortex. *Neurosci. Lett.* 116, 320–324. doi: 10.1016/0304-3940(90)90094-P

Hunter, T., Sacco, P., Nitsche, M. A., and Turner, D. L. (2009). Modulation of internal model formation during force field-induced motor learning by anodal transcranial direct current stimulation of primary motor cortex. *J. Physiol.* 587, 2949–2961. doi: 10.1113/jphysiol.2009.169284

Islam, N., Aftabuddin, M., Moriwaki, A., Hattori, Y., and Hori, Y. (1995). Increase in the calcium level following anodal polarization in the rat brain. *Brain Res.* 684, 206–208. doi: 10.1016/0006-8993(95)00434-R

Jacobson, L., Koslowsky, M., and Lavidor, M. (2012). tDCS polarity effects in motor and cognitive domains: a meta-analytical review. *Exp. Brain Res.* 216, 1–10. doi: 10.1007/s00221-011-2891-9

JASP Team (2017). *JASP (Version 0.8. 2). [Computer Software]*. Amsterdam: JASP.

Keel, J. C., Smith, M. J., and Wassermann, E. M. (2001). A safety screening questionnaire for transcranial magnetic stimulation. *Clin. Neurophysiol.* 112:720. doi: 10.1016/S1388-2457(00)00518-6

Kerwin, L. J., Keller, C. J., Wu, W., Narayan, M., and Etkin, A. (2017). Test-retest reliability of transcranial magnetic stimulation EEG evoked potentials. *Brain Stimul.* 11, 536–544. doi: 10.1016/j.brs.2017.12.010

Kirimoto, H., Ogata, K., Onishi, H., Oyama, M., Goto, Y., and Tobimatsu, S. (2011). Transcranial direct current stimulation over the motor association cortex induces plastic changes in ipsilateral primary motor and somatosensory cortices. *Clin. Neurophysiol.* 122, 777–783. doi: 10.1016/j.clinph.2010.09.025

Koo, H., Kim, M. S., Han, S. W., Paulus, W., Nitche, M. A., Kim, Y. H., et al. (2016). After-effects of anodal transcranial direct current stimulation on the excitability of the motor cortex in rats. *Restor. Neurol. Neurosci.* 34, 859–868. doi: 10.3233/RNN-160664

Kronberg, G., Bridi, M., Abel, T., Bikson, M., and Parra, L. C. (2017). Direct current stimulation modulates LTP and LTD: activity dependence and dendritic effects. *Brain Stimul.* 10, 51–58. doi: 10.1016/j.brs.2016.10.001

Lafon, B., Rahman, A., Bikson, M., and Parra, L. C. (2016). Direct current stimulation alters neuronal input/output function. *Brain Stimul.* 10, 36–45. doi: 10.1016/j.brs.2016.08.014

Lang, N., Nitsche, M. A., Paulus, W., Rothwell, J. C., and Lemon, R. N. (2004). Effects of transcranial direct current stimulation over the human motor cortex on corticospinal and transcallosal excitability. *Exp. Brain Res.* 156, 439–443. doi: 10.1007/s00221-003-1800-2

Lang, N., Siebner, H. R., Ward, N. S., Lee, L., Nitsche, M. A., Paulus, W., et al. (2005). How does transcranial DC stimulation of the primary motor cortex alter regional neuronal activity in the human brain? *Eur. J. Neurosci.* 22, 495–504. doi: 10.1111/j.1460-9568.2005.04233.x

Lefaucheur, J. P., Antal, A., Ayache, S. S., Benninger, D. H., Brunelin, J., Cogiamanian, F., et al. (2017). Evidence-based guidelines on the therapeutic use of transcranial direct current stimulation (tDCS). *Clin. Neurophysiol.* 128, 56–92. doi: 10.1016/j.clinph.2016.10.087

Liebetanz, D., Nitsche, M. A., Tergau, F., and Paulus, W. (2002). Pharmacological approach to the mechanisms of transcranial DC-stimulation-induced after effects of human motor cortex excitability. *Brain* 125, 2238–2247. doi: 10.1093/brain/awf238

Lioumis, P., Kičić, D., Savolainen, P., Mäkelä, J. P., and Kähkönen, S. (2009). Reproducibility of TMS-evoked EEG responses. *Hum. Brain Mapp.* 30, 1387–1396. doi: 10.1002/hbm.20608

Massimini, M., Ferrarelli, F., Huber, R., Esser, S. K., Singh, H., and Tononi, G. (2005). Breakdown of cortical effective connectivity during sleep. *Science* 309, 2228–2232. doi: 10.1126/science.1117256

Matsunaga, K., Nitsche, M. A., Tsuji, S., and Rothwell, J. C. (2004). Effect of transcranial DC sensorimotor cortex stimulation on somatosensory evoked potentials in humans. *Clin. Neurophysiol.* 115, 456–460. doi: 10.1016/S1388-2457(03)00362-6

Mattavelli, G., Rosanova, M., Casali, A. G., Papagno, C., and Romero Lauro, L. J. (2013). Top-down interference and cortical responsiveness in face processing: a TMS-EEG study. *Neuroimage* 76, 24–32. doi: 10.1016/j.neuroimage.2013.03.020

Medeiros, L. F., de Souza, I. C. C., Vidor, L. P., de Souza, A., Deitos, A., Volz, M. S., et al. (2012). Neurobiological effects of transcranial direct current stimulation: a review. *Front. Psychiatry* 3:110. doi: 10.3389/fpsyt.2012.00110

Miranda, P. C., Mekonnen, A., Salvador, R., and Ruffini, G. (2013). The electric field in the cortex during transcranial current stimulation. *Neuroimage* 70, 48–58. doi: 10.1016/j.neuroimage.2012.12.034

Monai, H., Ohkura, M., Tanaka, M., Oe, Y., Konno, A., Hirai, H., et al. (2016). Calcium imaging reveals glial involvement in transcranial direct current stimulation-induced plasticity in mouse brain. *Nat. Commun.* 7:11100. doi: 10.1038/ncomms11100

Moriwaki, A. (1991). Polarizing currents increase noradrenaline-elicited accumulation of cyclic AMP in rat cerebral cortex. *Brain Res.* 544, 248–252. doi: 10.1016/0006-8993(91)90061-Y

Nitsche, M. A., Cohen, L. G., Wassermann, E. M., Priori, A., Lang, N., Antal, A., et al. (2008). Transcranial direct current stimulation: state of the art 2008. *Brain Stimul.* 1, 206–223. doi: 10.1016/j.brs.2008.06.004

Nitsche, M. A., Grundey, J., Liebetanz, D., Lang, N., Tergau, F., and Paulus, W. (2004). Catecholaminergic consolidation of motor cortical neuroplasticity in humans. *Cereb. Cortex* 14, 1240–1245. doi: 10.1093/cercor/bhh085

Nitsche, M. A., Liebetanz, D., Antal, A., Lang, N., Tergau, F., and Paulus, W. (2003). Modulation of cortical excitability by weak direct current stimulation-technical, safety and functional aspects. *Suppl. Clin. Neurophysiol.* 56, 255–276. doi: 10.1016/S1567-424X(09)70230-2

Nitsche, M. A., and Paulus, W. (2000). Excitability changes induced in the human motor cortex by weak transcranial direct current stimulation. *J. Physiol.* 527, 633–639. doi: 10.1111/j.1469-7793.2000.t01-1-00633.x

Nitsche, M. A., and Paulus, W. (2001). Sustained excitability elevations induced by transcranial DC motor cortex stimulation in humans. *Neurology* 57, 1899–1901. doi: 10.1212/WNL.57.10.1899

Nitsche, M. A., Seeber, A., Frommann, K., Klein, C. C., Rochford, C., Nitsche, M. S., et al. (2005). Modulating parameters of excitability during and after transcranial direct current stimulation of the human motor cortex. *J. Physiol.* 568(Pt 1), 291–303. doi: 10.1113/jphysiol.2005.092429

Pantazis, D., Nichols, T. E., Baillet, S., and Leahy, R. M. (2003). "Spatiotemporal localization of significant activation in MEG using permutation tests," in *Information Processing in Medical Imaging* (Berlin; Heidelberg: Springer), 512–523.

Pellicciari, M. C., Brignani, D., and Miniussi, C. (2013). Excitability modulation of the motor system induced by transcranial direct current stimulation: a multimodal approach. *Neuroimage* 83, 569–580. doi: 10.1016/j.neuroimage.2013.06.076

Pisoni, A., Mattavelli, G., Papagno, C., Rosanova, M., Casali, A., and Romero Lauro, L. (2017). Cognitive enhancement induced by anodal tDCS drives circuit-specific cortical plasticity. *Cereb. Cortex* 28, 1132–1140. doi: 10.1093/cercor/bhx021.

Podda, M. V., Cocco, S., Mastrodonato, A., Fusco, S., Leone, L., Barbati, S. A., et al. (2016). Anodal transcranial direct current stimulation boosts synaptic plasticity and memory in mice via epigenetic regulation of Bdnf expression. *Sci. Reports* 6:22180. doi: 10.1038/srep22180

Priori, A. (2003). Brain polarization in humans: a reappraisal of an old tool for prolonged non-invasive modulation of brain excitability. *Clin. Neurophysiol.* 114, 589–595. doi: 10.1016/S1388-2457(02)00437-6

Priori, A., Berardelli, A., Rona, S., Accornero, N., and Manfredi, M. (1998). Polarization of the human motor cortex through the scalp. *Neuroreport* 9, 2257–2260. doi: 10.1097/00001756-199807130-00020

Purpura, D. P., and McMurtry, J. G. (1965). Intracellular activities and evoked potential changes during polarization of motor cortex. *J. Neurophysiol.* 28, 166–185. doi: 10.1152/jn.1965.28.1.166

R Core Team (2014). *R: A Language and Environment for Statistical Computing*. Vienna: R Foundation for Statistical Computing. 512–523. Available online at: http://www.R-project.org/

Radman, T., Ramos, R. L., Brumberg, J. C., and Bikson, M. (2009). Role of cortical cell type and morphology in subthreshold and suprathreshold uniform electric field stimulation *in vitro*. *Brain Stimul.* 2, 215–228. doi: 10.1016/j.brs.2009.03.007

Ranieri, F., Podda, M. V., Riccardi, E., Frisullo, G., Dileone, M., Profice, P., et al. (2012). Modulation of LTP at rat hippocampal CA3-CA1 synapses by direct current stimulation. *J. Neurophysiol.* 107, 1868–1880. doi: 10.1152/jn.00319.2011

Reis, J., Schambra, H. M., Cohen, L. G., Buch, E. R., Fritsch, B., Zarahn, E., et al. (2009). Noninvasive cortical stimulation enhances motor skill acquisition over multiple days through an effect on consolidation. *Proc. Natl. Acad. Sci. U.S.A* 106, 1590–1595. doi: 10.1073/pnas.0805413106

Rohan, , J. G., Carhuatanta, K. A., McInturf, S. M., Miklasevich, M. K., and Jankord, R. (2015). Modulating hippocampal plasticity with *in vivo* brain stimulation. *J. Neurosci.* 35, 12824–12832. doi: 10.1523/JNEUROSCI.2376-15.2015

Romero Lauro, L. J., Pisoni, A., Rosanova, M., Casarotto, S., Mattavelli, G., Bolognini, N., et al. (2015). Localizing the effects of anodal tDCS at the level of cortical source: a reply to Bailey et al., 2015. *Cortex* 74, 323–328. doi: 10.1016/j.cortex.2015.04.023

Romero Lauro, L. J., Rosanova, M., Mattavelli, G., Convento, S., Pisoni, A., Opitz, A., et al. (2014). TDCS increases cortical excitability: direct evidence from TMS-EEG. *Cortex* 58, 99–111. doi: 10.1016/j.cortex.2014.05.003

Rossi, S., Hallett, M., Rossini, P. M., Pascual-Leone, A., and Safety of TMS Consensus Group (2009). Safety, ethical considerations, and application guidelines for the use of transcranial magnetic stimulation in clinical practice and research. *Clin Neurophysiol.* 120, 2008–2039. doi: 10.1016/j.clinph.2009.08.016

Rouder, J. N., Speckman, P. L., Sun, D., Morey, R. D., and Iverson, G. (2009). Bayesian t tests for accepting and rejecting the null hypothesis. *Psychon. Bull. Rev.* 16, 225–237. doi: 10.3758/PBR.16.2.225

Roy, A., Baxter, B., and He, B. (2014). High-definition transcranial direct current stimulation induces both acute and persistent changes in broadband cortical synchronization: a simultaneous tDCS–EEG study. *IEEE Trans. Biomed. Eng.* 61, 1967–1978. doi: 10.1109/TBME.2014.2311071

Saturnino, G. B., Antunes, A., and Thielscher, A. (2015). On the importance of electrode parameters for shaping electric field patterns generated by tDCS. *Neuroimage* 120, 25–35.

Schestatsky, P., Morales-Quezada, L., and Fregni, F. (2013). Simultaneous EEG monitoring during transcranial direct current stimulation. *J. Visual. Exp.* 76:50426. doi: 10.3791/50426

Sczesny-Kaiser, M., Beckhaus, K., Dinse, H. R., Schwenkreis, P., Tegenthoff, M., and Höffken, O. (2016). Repetitive transcranial direct current stimulation induced excitability changes of primary visual cortex and visual learning effects—a pilot study. *Front. Behav. Neurosci.* 10:116. doi: 10.3389/fnbeh.2016.00116

Silva, C., Maltez, J. C., Trindade, E., Arriaga, A., and Ducla-Soares, E. (2004). Evaluation of L 1 and L 2 minimum norm performances on EEG localizations. *Clin. Neurophysiol.* 115, 1657–1668. doi: 10.1016/j.clinph.2004.02.009

Stagg, C. J., Best, J. G., Stephenson, M. C., O'Shea, J., Wylezinska, M., Kincses, Z. T., et al. and Johansen-Berg, H. (2009). Polarity-sensitive modulation of cortical neurotransmitters by transcranial stimulation. *J. Neurosci.* 29, 5202–5206. doi: 10.1523/JNEUROSCI.4432-08.2009

Stagg, C. J., Lin, R. L., Mezue, M., Segerdahl, A., Kong, Y., Xie, J., et al. (2013). Widespread modulation of cerebral perfusion induced during and after transcranial direct current stimulation applied to the left dorsolateral prefrontal cortex. *J. Neurosci.* 33, 11425–11431. doi: 10.1523/JNEUROSCI.3887-12.2013

Stagg, C. J., and Nitsche, M. A.,(2011). Physiological basis of transcranial direct current stimulation. *Neuroscientist* 17, 37–53. doi: 10.1177/1073858410386614

Virtanen, J., Ruohonen, J., Näätänen, R., and Ilmoniemi, R. J. (1999). Instrumentation for the measurement of electric brain responses to transcranial magnetic stimulation. *Med. Biol. Eng. Comput.* 37, 322–326. doi: 10.1007/BF02513307

Wirth, M., Rahman, R. A., Kuenecke, J., Koenig, T., Horn, H., Sommer, W., et al. (2011). Effects of transcranial direct current stimulation (tDCS) on behaviour and electrophysiology of language production. *Neuropsychologia* 49, 3989–3998. doi: 10.1016/j.neuropsychologia.2011.10.015

Zheng, X., Alsop, D. C., and Schlaug, G. (2011). Effects of transcranial direct current stimulation (tDCS) on human regional cerebral blood flow. *Neuroimage* 58, 26–33. doi: 10.1016/j.neuroimage.2011.06.018

Conflict of Interest Statement: The authors declare that the research was conducted in the absence of any commercial or financial relationships that could be construed as a potential conflict of interest.

Appendix 2

Supplementary materials

Supplementary Table S1. In the following table are reported the results of the mixed-effect analysis on accuracy in the Posner Task, only for the sham stimulation condition.

Parameter	χ^2	*P*	*Removal order*	*Estimate*	*z value*	*p*
Intercept	-	-	*Not removed*	5.8768	13.306	<.001
Cue validity	-	-	*Not removed*	-1.5976	-4.071	<.001
Cue validity:Target side	*0.1351*	*.7132*	1	-	-	-
Target side	*0.8182*	*.3657*	2	-	-	-

Supplementary Table S2. In the following table are reported the results of the mixed-effect analysis on log-transformed RTs in the Posner Task, only for the sham stimulation condition.

Parameter	χ^2	*P*	*Removal order*	*Estimate*	*t value*	*p*
Intercept	-	-	*Not removed*	5.797	415.588	<.001
Cue validity	-	-	*Not removed*	$6.454*10^{-3}$	0.982	.326
Target side	-	-	*Not removed*	$-9.068*10^{-3}$	-1.381	.167
Cue validity:Target side	-	-	*Not removed*	$2.401*10^{-2}$	2.589	.009

Supplementary Table S3. In the following table are reported the results of the mixed-effect analysis on accuracy in the Posner Task performed using the whole sample.

Parameter	χ^2	*P*	*Removal order*	*Estimate*	*z value*	*p*
Intercept	-	-	*Not removed*	5.2487	21.50	<.001
Cue validity	-	-	*Not removed*	-1.3211	-5.42	<.001
Cue validity:Target side:Stimulation condition	*0.001*	*.9752*	1	-	-	-

Target side:Stimulation condition	*2.7965*	*.09447*	2	-	-	-
Stimulation condition:Cue validity	*0.8482*	*.3571*	3	-	-	-
Stimulation condition	*0.377*	*.5392*	4	-	-	-
Cue validity:Target side	*0.2153*	*.6426*	5	-	-	-
Target side	*0.1675*	*.6824*	6	-	-	-

Supplementary Table S4. In the following table are reported the results of the mixed-effect analysis on log-transformed RTs in the Posner Task performed using the whole sample.

Parameter	χ^2	*P*	*Removal order*	*Estimate*	*t value*	*p*
Intercept	-	-	*Not removed*	5.813	480.735	<.001
Stimulation condition	-	-	*Not removed*	$-1.663*10^{-2}$	-2.830	.0047
Target side	-	-	*Not removed*	$-2.437*10^{-2}$	-4.158	<.001
Cue validity	-	-	*Not removed*	$-1.090*10^{-2}$	-1.862	.0626
Stimulation condition:Target side	-	-	*Not removed*	$1.517*10^{-2}$	2.237	.0253
Target side:Cue validity	-	-	*Not removed*	$2.106*10^{-2}$	3.105	.0019
Stimulation condition:Cue validity	-	-	*Not removed*	$1.937*10^{-2}$	2.856	.0043
Cue validity:Target side:Stimulation condition	*0.4175*	*.5182*	1	-	-	-

Supplementary Table S5. In the following table are reported the results of the mixed-effect analysis on accuracy in the Posner Task, only for the group Sub1, which performed the Posner task as second task.

Parameter	χ^2	*P*	*Removal order*	*Estimate*	*z value*	*p*
Intercept	-	-	*Not removed*	5.9224	2345.1	<.001

Cue validity	-	-	*Not removed*	-1.8776	-743.6	<.001
Cue validity:Target side:Stimulation condition	*0.0838*	*.7722*	1	-	-	-
Stimulation condition:Target side	*0.0768*	*.7817*	2	-	-	-
Stimulation condition:Cue validity	*0.063*	*.8018*	3	-	-	-
Stimulation condition	*3.395*	*.0654*	4	-	-	-
Cue validity:Target side	*0.0258*	*.8725*	5	-	-	-
Target side	*0.69*	*.4062*	6	-	-	-

Supplementary Table S6. In the following table are reported the results of the mixed-effect analysis on log-transformed RTs in the Posner Tas, only for the group Sub1, which performed the Posner task as second task.

Parameter	χ^2	*P*	*Removal order*	*Estimate*	*t value*	*p*
Intercept	-	-	*Not removed*	5.795	317.834	<.001
Stimulation condition	-	-	*Not removed*	$-2.356*10^{-2}$	-3.533	<.001
Target side	-	-	*Not removed*	$-1.819*10^{-2}$	-2.737	.006
Cue validity	-	-	*Not removed*	1.450*10-2	3.083	.002
Stimulation condition:Target side	-	-	*Not removed*	1.951*10-2	2.074	.038
Stimulation condition:Target side:Cue validity	*0.4325*	*.5107*	1	-	-	-
Stimulation condition:Cue validity	*2.8556*	*.0911*	2	-	-	-
Target side:Cue validity	*3.1351*	*.0766*	3	-	-	-

Supplementary Table S7. In the following table are reported the results of the mixed-effect analysis on accuracy in the Posner Task, only for the group Sub2, which performed the Posner task as first task.

Parameter	χ^2	*P*	*Removal order*	*Estimate*	*z value*	*p*
Intercept	-	-	*Not removed*	4.8616	17.001	<.001
Cue validity	-	-	*Not removed*	-1.055	-3.647	<.001
Stimulation condition:Cue validity:Target side	*0.101*	*.7506*	1	-	-	-
Stimulation condition:Target side	*3.366*	*.066*	2	-	-	-
Stimulation condition:Cue validity	*2.472*	*.116*	3	-	-	-
Stimulation condition	*0.421*	*.516*	4	-	-	-
Target side:Cue validity	*0.259*	*.610*	5	-	-	-
Target side	*0.017*	*.987*	6	-	-	-

Supplementary Table S8. In the following table are reported the results of the mixed-effect analysis on log-transformed RTs in the Posner Task, only for the group Sub2, which performed the Posner task as first task.

Parameter	χ^2	*P*	*Removal order*	*Estimate*	*t value*	*p*
Intercept	-	-	*Not removed*	5.815	376.666	<.001
Stimulation condition	-	-	*Not removed*	$-3.286*10^{-3}$	-0.391	.696
Target side	-	-	*Not removed*	$-9.976*10^{-3}$	-1.459	.145
Cue validity	-	-	*Not removed*	$-6.648*10^{-3}$	-0.972	.331
Target side:Cue validity	-	-	*Not removed*	$1.157*10^{-2}$	1.190	.234
Stimulation condition:Cue validity	-	-	*Not removed*	$2.259*10^{-2}$	2.325	.02
Stimulation condition:Target side:Cue validity	*0.081*	*.776*	1	-	-	-

Stimulation condition:Target side	*1.423*	*.233*	2	-	-	-

*Note: each table summarizes the model-simplification procedure, including the goodness-of-fit tests and their results. Parameters were not removed (i.e. Cue validity and Target side in Table S2) when they were part of higher order interactions (i.e. Cue validity * Target side). The rightmost part of each table reports the effects of the included variables, after having removed outliers.*

Appendix 3

Supplementary materials

Supplementary Table S1. Results of the mixed-effect analysis on accuracy in the Posner Cueing Task

Parameter	$\chi 2$	*p*	*Removal order*	*Estimate*	*z-value*	*p*
Intercept	-	-	*Not removed*	4.3879	29.05	<.001
Cue validity	-	-	*Not removed*	-1.0370	-3.488	<.001
Target side	-	-	*Not removed*	-0.5302	-1.940	.0524
Cue validity:Target side:Stimulation condition	*0.642*	*.423*	*1*			
Target side:Stimulation condition	*0.0234*	*.8785*	*2*	-	-	-
Stimulation condition : Cue validity	*0.0008*	*.9779*	*3*	-	-	-
Stimulation condition	0.2977	.5853	*4*	-	-	-
Cue validity:Target side	2.8407	.0919	*5*	-	-	-

Supplementary Table S2. Results of the mixed-effect analysis on log-transformed RTs in the Posner Task

Parameter	$\chi 2$	*p*	*Removal order*	*Estimate*	*t-value*	*p*
Intercept	-	-	*Not removed*	5.782	234.325	<.001
Stimulation condition	-	-	*Not removed*	-0.003	-0.428	.6684
Target side	-	-	*Not removed*	0.004		.6643
Cue validity	-	-	*Not removed*	-0.009	-5.42	.2039
Stimulation condition : Target side	-	-	*Not removed*	-0.022		.0279
Cue validity:Target side	-	-	*Not removed*	0.019		.0484
Cue validity: Target side : Stimulation condition	*.0029*	*.9569*	*1*	-	-	-
Stimulation condition:Cue validity	*.9378*	*.3328*	*2*	-	-	-

Note: each table summarizes the model-simplification procedure, including the goodness-of-fit tests and their results. Parameters were not removed (i.e. Stimulation condition and Target side in Table S2) when they were part of higher order interactions (i.e. Stimulation condition Target side). The rightmost part of each table reports the effects of the included variables, after having removed outliers.*

References

Accornero, N., Voti, P. L., La Riccia, M., & Gregori, B. (2007). Visual evoked potentials modulation during direct current cortical polarization. Experimental Brain Research, 178(2), 261-266.

Amadi, U., Ilie, A., Miranda, H., & Stagg, C. J. (2014). Polarity-specific effects of motor transcranial direct current stimulation on fMRI resting state networks. Neuroimage, 88, 155-161.

Amassian, V. E., Cracco, R. Q., Maccabee, P. J., & Cracco, J. B. (1992). Cerebello-frontal cortical projections in humans studied with the magnetic coil. Electroencephalography and Clinical Neurophysiology/Evoked Potentials Section, 85(4), 265-272.

Ambrus, G. G., Al-Moyed, H., Chaieb, L., Sarp, L., Antal, A., & Paulus, W. (2012). The fade-in–short stimulation–fade out approach to sham tDCS–reliable at 1 mA for naive and experienced subjects, but not investigators. Brain stimulation, 5(4), 499-504.

Andersen, R. A., & Cui, H. (2009). Intention, action planning, and decision making in parietal-frontal circuits. Neuron, 63(5), 568-583.

Anderson, D. E., Vogel, E. K., & Awh, E. (2011). Precision in visual working memory reaches a stable plateau when individual item limits are exceeded.

Antal, A., & Herrmann, C. S. (2016). Transcranial alternating current and random noise stimulation: possible mechanisms. Neural plasticity, 2016.

Antal, A., Boros, K., Poreisz, C., Chaieb, L., Terney, D., & Paulus, W. (2008). Comparatively weak after-effects of transcranial alternating current stimulation (tACS) on cortical excitability in humans. Brain stimulation, 1(2), 97-105.

Antal, A., Kincses, T. Z., Nitsche, M. A., & Paulus, W. (2003). Modulation of moving phosphene thresholds by transcranial direct current stimulation of V1 in human. Neuropsychologia, 41(13), 1802-1807.

Antal, A., Kincses, T. Z., Nitsche, M. A., Bartfai, O., & Paulus, W. (2004). Excitability changes induced in the human primary visual cortex by transcranial direct current stimulation: direct electrophysiological evidence. Investigative Ophthalmology & Visual Science, 45(2), 702e707.

Antal, A., Kriener, N., Lang, N., Boros, K., & Paulus, W. (2011). Cathodal transcranial direct current stimulation of the visual cortex in the prophylactic treatment of migraine. Cephalalgia, 31(7), 820-828.

Antal, A., Nitsche, M. A., & Paulus, W. (2001). External modulation of visual perception in humans. Neuroreport, 12(16), 3553-3555.

Antal, A., Terney, D., Poreisz, C., & Paulus, W. (2007). Towards unravelling task-related modulations of neuroplastic changes induced in the human motor cortex. European Journal of Neuroscience, 26(9), 2687-2691.

Ashburner, J., Barnes, G., Chen, C. C., Daunizeau, J., Flandin, G., & Friston, K. (2011). SPM8. Functional Imaging Laboratory, Institute of Neurology, 12.

Aston-Jones, G., & Cohen, J. D. (2005). Adaptive gain and the role of the locus coeruleus–norepinephrine system in optimal performance. Journal of Comparative Neurology, 493(1), 99-110.

Awh, E., Barton, B., & Vogel, E. K. (2007). Visual working memory represents a fixed number of items regardless of complexity. Psychological science, 18(7), 622-628.

Baayen, R. H., Davidson, D. J., & Bates, D. M. (2008). Mixed-effects modeling with crossed random effects for subjects and items. Journal of Memory and Language, 59(4), 390e412.

Bachtiar, V., Near, J., Johansen-Berg, H., & Stagg, C. J. (2015). Modulation of GABA and resting state functional connectivity by transcranial direct current stimulation. Elife, 4, e08789.

Baddeley, A. (2000). The episodic buffer: a new component of working memory?. Trends in cognitive sciences, 4(11), 417-423.

Bibliography

Baddeley, A. (2003). Working memory: looking back and looking forward. Nature reviews neuroscience, 4(10), 829.

Baddeley, A. (2010). Working memory. Current biology, 20(4), R136-R140.

Baddeley, A. D., & Hitch, G. (1974). Working memory. In Psychology of learning and motivation (Vol. 8, pp. 47-89). Academic press.

Baddeley, A. D., & Logie, R. H. (1999). Working memory: The multiple-component model.

Baddeley, A., Logie, R., Bressi, S., Sala, S. D., & Spinnler, H. (1986). Dementia and working memory. The Quarterly Journal of Experimental Psychology Section A, 38(4), 603-618.

Barbey, A. K., Koenigs, M., & Grafman, J. (2013). Dorsolateral prefrontal contributions to human working memory. cortex, 49(5), 1195-1205.

Barch, D. M., Sheline, Y. I., Csernansky, J. G., & Snyder, A. Z. (2003). Working memory and prefrontal cortex dysfunction: specificity to schizophrenia compared with major depression. Biological psychiatry, 53(5), 376-384.

Barker, A. T., Jalinous, R., & Freeston, I. L. (1985). Non-invasive magnetic stimulation of human motor cortex. The Lancet, 325(8437), 1106-1107.

Bashinski, H. S., & Bacharach, V. R. (1980). Enhancement of perceptual sensitivity as the result of selectively attending to spatial locations. Perception & Psychophysics, 28(3), 241-248.

Bastani, A., & Jaberzadeh, S. (2013). Differential modulation of corticospinal excitability by different current densities of anodal transcranial direct current stimulation. PloS one, 8(8), e72254.

Bates, D., Maechler, M., Bolker, B., & Walker, S. (2014). lme4: Linear mixed-effects models using Eigen and S4. R package version, 1(7), 1-23.

Bates, D., Maechler, M., Bolker, B., & Walker, S. (2015). lme4: Linear mixed-effects models using Eigen and S4. R package version 1.1–7. 2014.

Batsikadze, G., Moliadze, V., Paulus, W., Kuo, M. F., & Nitsche, M. A. (2013). Partially non-linear stimulation intensity-dependent effects of direct current stimulation on motor cortex excitability in humans. The Journal of physiology, 591(7), 1987-2000.

Baudewig, J., Nitsche, M. A., Paulus, W., & Frahm, J. (2001). Regional modulation of BOLD MRI responses to human sensorimotor activation by transcranial direct current stimulation. Magnetic Resonance in Medicine, 45(2), 196-201.

Beaudreau, S. A., & Finger, S. (2006). Medical electricity and madness in the 18th century: the legacies of Benjamin Franklin and Jan Ingenhousz. Perspectives in biology and medicine, 49(3), 330-345.

Berg, P., & Scherg, M. (1994). A fast method for forward computation of multiple-shell spherical head models. Electroencephalography and clinical Neurophysiology, 90(1), 58-64.

Berryhill, M. E., Peterson, D. J., Jones, K. T., & Stephens, J. A. (2014). Hits and misses: leveraging tDCS to advance cognitive research. Frontiers in psychology, 5, 800.

Berryhill, M. E., Wencil, E. B., Coslett, H. B., & Olson, I. R. (2010). A selective working memory impairment after transcranial direct current stimulation to the right parietal lobe. Neuroscience letters, 479(3), 312-316.

Bikson, M., & Rahman, A. (2013). Origins of specificity during tDCS: anatomical, activity-selective, and input-bias mechanisms. Frontiers in human neuroscience, 7, 688.

Bikson, M., Datta, A., Rahman, A., & Scaturro, J. (2010). Electrode montages for tDCS and weak transcranial electrical stimulation: role of “return” electrode’s position and size. Clinical neurophysiology: official journal of the International Federation of Clinical Neurophysiology, 121(12), 1976.

Bikson, M., Grossman, P., Thomas, C., Zannou, A. L., Jiang, J., Adnan, T., ... & Brunoni, A. R. (2016). Safety of transcranial direct current stimulation: evidence based update 2016. Brain stimulation, 9(5), 641-661.

Bikson, M., Inoue, M., Akiyama, H., Deans, J. K., Fox, J. E., Miyakawa, H., & Jefferys, J. G. R. (2004). Effects of uniform extracellular DC electric fields on excitability in rat hippocampal slices in vitro. Journal of Physiology, 557(1), 175-190.

Bikson, M., Rahman, A., & Datta, A. (2012). Computational models of transcranial direct current stimulation. Clinical EEG and neuroscience, 43(3), 176-183.

Bindman, L. J., Lippold, O. C., & Redfearn, J. W. (1962). Long-lasting changes in the level of the electrical activity of the cerebral cortex produced by polarizing currents. Nature, 196, 584-585.

Bindman, L. J., Lippold, O. C., & Redfearn, J. W. (1964). The action of brief polarizing currents on the cerebral cortex of the rat (1)during current flow and (2) in the production of long-lasting after-effects. Journal of Physiology, 172, 369–382.

Boggio, P. S., Castro, L. O., Savagim, E. A., Braite, R., Cruz, V. C., Rocha, R. R., ... & Fregni, F. (2006). Enhancement of non-dominant hand motor function by anodal transcranial direct current stimulation. Neuroscience letters, 404(1), 232-236.

Bolognini, N., Fregni, F., Casati, C., Olgiati, E., & Vallar, G. (2010b). Brain polarization of parietal cortex augments training-induced improvement of visual exploratory and attentional skills. Brain research, 1349, 76-89.

Bolognini, N., Olgiati, E., Rossetti, A., & Maravita, A. (2010a). Enhancing multisensory spatial orienting by brain polarization of the parietal cortex. European Journal of Neuroscience, 31(10), 1800-1806.

Bolognini, N., Spandri, V., Olgiati, E., Fregni, F., Ferraro, F., & Maravita, A. (2013). Long-term analgesic effects of transcranial direct current stimulation of the motor cortex on phantom limb and stump pain: a case report. Journal of pain and symptom management, 46(4), e1-e4.

Bolognini, N., Vallar, G., Casati, C., Latif, L. A., El-Nazer, R., Williams, J., ... & Fregni, F. (2011). Neurophysiological and behavioral effects of tDCS combined with constraint-induced movement therapy in poststroke patients. Neurorehabilitation and neural repair, 25(9), 819-829.

Bortoletto, M., Pellicciari, M. C., Rodella, C., & Miniussi, C. (2015). The interaction with task-induced activity is more important than polarization: a tDCS study. Brain stimulation, 8(2), 269-276.

Bortoletto, M., Veniero, D., Thut, G., & Miniussi, C. (2015). The contribution of TMS–EEG coregistration in the exploration of the human cortical connectome. Neuroscience & Biobehavioral Reviews, 49, 114-124.

Brady, T. F., Konkle, T., & Alvarez, G. A. (2011). A review of visual memory capacity: Beyond individual items and toward structured representations. Journal of vision, 11(5), 4-4.

Brovelli, A., Lachaux, J. P., Kahane, P., & Boussaoud, D. (2005). High gamma frequency oscillatory activity dissociates attention from intention in the human premotor cortex. Neuroimage, 28(1), 154-164.

Brunelin, J., Mondino, M., Haesebaert, F., Saoud, M., Suaud-Chagny, M. F., & Poulet, E. (2012). Efficacy and safety of bifocal tDCS as an interventional treatment for refractory schizophrenia.

Brunoni, A. R., Boggio, P. S., De Raedt, R., Benseñor, I. M., Lotufo, P. A., Namur, V., ... & Vanderhasselt, M. A. (2014a). Cognitive control therapy and transcranial direct current stimulation for depression: a randomized, double-blinded, controlled trial. Journal of affective disorders, 162, 43-49.

Brunoni, A. R., & Vanderhasselt, M. A. (2014b). Working memory improvement with non-invasive brain stimulation of the dorsolateral prefrontal cortex: a systematic review and meta-analysis. Brain and cognition, 86, 1-9.

Brunoni, A. R., Ferrucci, R., Fregni, F., Boggio, P. S., & Priori, A. (2012). Transcranial direct current stimulation for the treatment of major depressive disorder: a summary of preclinical, clinical and translational findings. Progress in Neuro-Psychopharmacology and Biological Psychiatry, 39(1), 9-16.

Brunoni, A., Nitsche, M., & Loo, C. (2016). Transcranial direct current stimulation in neuropsychiatric disorders. Switzerland: Springer International Publishing.

Casali, A. G., Casarotto, S., Rosanova, M., Mariotti, M., & Massimini, M. (2010). General indices to characterize the electrical response of the cerebral cortex to TMS. Neuroimage, 49(2), 1459-1468.

Bibliography

Casali, A. G., Gosseries, O., Rosanova, M., Boly, M., Sarasso, S., Casali, K. R., ... & Massimini, M. (2013). A theoretically based index of consciousness independent of sensory processing and behavior. Science translational medicine, 5(198), 198ra105-198ra105.

Casarotto, S., Canali, P., Rosanova, M., Pigorini, A., Fecchio, M., Mariotti, M., ... & Massimini, M. (2013). Assessing the effects of electroconvulsive therapy on cortical excitability by means of transcranial magnetic stimulation and electroencephalography. Brain topography, 26(2), 326-337.

Casarotto, S., Comanducci, A., Rosanova, M., Sarasso, S., Fecchio, M., Napolitani, M., ... & Gosseries, O. (2016). Stratification of unresponsive patients by an independently validated index of brain complexity. Annals of neurology, 80(5), 718-729.

Casarotto, S., Romero Lauro, L. J., Bellina, V., Casali, A. G., Rosanova, M., Pigorini, A., ... & Massimini, M. (2010). EEG responses to TMS are sensitive to changes in the perturbation parameters and repeatable over time. PLoS One, 5(4), e10281.

Casula, E. P., Tarantino, V., Basso, D., Arcara, G., Marino, G., Toffolo, G. M., ... & Bisiacchi, P. S. (2014). Low-frequency rTMS inhibitory effects in the primary motor cortex: Insights from TMS-evoked potentials. Neuroimage, 98, 225-232.

Chambers, C. D., Payne, J. M., & Mattingley, J. B. (2007). Parietal disruption impairs reflexive spatial attention within and between sensory modalities. Neuropsychologia, 45(8), 1715-1724.

Cieslik, E. C., Mueller, V. I., Eickhoff, C. R., Langner, R., & Eickhoff, S. B. (2015). Three key regions for supervisory attentional control: evidence from neuroimaging meta-analyses. Neuroscience & biobehavioral reviews, 48, 22-34.

Cipollari, S., Veniero, D., Razzano, C., Caltagirone, C., Koch, G., & Marangolo, P. (2015). Combining TMS-EEG with transcranial direct current stimulation language treatment in aphasia. Expert Review of Neurotherapeutics, 15(7), 833-845.

Clemens, B., Jung, S., Mingoia, G., Weyer, D., Domahs, F., & Willmes, K. (2014). Influence of anodal transcranial direct current stimulation (tDCS) over the right angular gyrus on brain activity during rest. PloS one, 9(4), e95984.

Coffman, B. A., Clark, V. P., & Parasuraman, R. (2014). Battery powered thought: enhancement of attention, learning, and memory in healthy adults using transcranial direct current stimulation. Neuroimage, 85, 895-908.

Cohen, J. D., Perlstein, W. M., Braver, T. S., Nystrom, L. E., Noll, D. C., Jonides, J., & Smith, E. E. (1997). Temporal dynamics of brain activation during a working memory task. Nature, 386(6625), 604.

Cohen, M. X. (2017). Rigor and replication in time-frequency analyses of cognitive electrophysiology data. International Journal of Psychophysiology, 111, 80-87.

Conde, V., Tomasevic, L., Akopian, I., Stanek, K., Saturnino, G. B., Thielscher, A., ... & Siebner, H. R. (2019). The non-transcranial TMS-evoked potential is an inherent source of ambiguity in TMS-EEG studies. Neuroimage, 185, 300-312.

Convento, S., Vallar, G., Galantini, C., & Bolognini, N. (2013). Neuromodulation of early multisensory interactions in the visual cortex. Journal of Cognitive Neuroscience, 25(5), 685-696.

Corbetta, M., & Shulman, G. L. (2002). Control of goal-directed and stimulus-driven attention in the brain. Nature reviews neuroscience, 3(3), 201.

Corbetta, M., Patel, G., & Shulman, G. L. (2008). The reorienting system of the human brain: from environment to theory of mind. Neuron, 58(3), 306-324.

Counter, S. A., & Borg, E. (1992). Analysis of the coil generated impulse noise in extracranial magnetic stimulation. Electroencephalography and Clinical Neurophysiology/Evoked Potentials Section, 85(4), 280-288.

Cowan, N. (2001). The magical number 4 in short-term memory: A reconsideration of mental storage capacity. Behavioral and brain sciences, 24(1), 87-114.

Cowan, N. (2010). The magical mystery four: How is working memory capacity limited, and why?. Current directions in psychological science, 19(1), 51-57.

Cowan, N., & Morey, C. C. (2006). Visual working memory depends on attentional filtering. Trends in cognitive sciences, 10(4), 139-141.

Cowan, N., Elliott, E. M., Saults, J. S., Morey, C. C., Mattox, S., Hismjatullina, A., & Conway, A. R. (2005). On the capacity of attention: Its estimation and its role in working memory and cognitive aptitudes. Cognitive psychology, 51(1), 42-100.

Cowan, N., Naveh-Benjamin, M., Kilb, A., & Saults, J. S. (2006). Life-span development of visual working memory: When is feature binding difficult?. Developmental psychology, 42(6), 1089.

Cracco, R. Q., Amassian, V. E., Maccabee, P. J., & Cracco, J. B. (1989). Comparison of human transcallosal responses evoked by magnetic coil and electrical stimulation. Electroencephalography and Clinical Neurophysiology/Evoked Potentials Section, 74(6), 417-424.

Creutzfeldt, O. D., Fromm, G. H., & Kapp, H. (1962). Influence of transcortical dc currents on cortical neuronal activity. Experimental neurology, 5(6), 436-452.

Curtis, C. E., & D'Esposito, M. (2003). Persistent activity in the prefrontal cortex during working memory. Trends in cognitive sciences, 7(9), 415-423.

Darki, F., & Klingberg, T. (2014). The role of fronto-parietal and fronto-striatal networks in the development of working memory: a longitudinal study. Cerebral cortex, 25(6), 1587-1595.

Datta, A., Bansal, V., Diaz, J., Patel, J., Reato, D., & Bikson, M. (2009). Gyri-precise head model of transcranial direct current stimulation: improved spatial focality using a ring electrode versus conventional rectangular pad. Brain stimulation, 2(4), 201-207.

Datta, A., Elwassif, M., Battaglia, F., & Bikson, M. (2008). Transcranial current stimulation focality using disc and ring electrode configurations: FEM analysis. Journal of neural engineering, 5(2), 163.

Delorme, A., & Makeig, S. (2004). EEGLAB: an open source toolbox for analysis of single-trial EEG dynamics including independent component analysis. Journal of Neuroscience Methods, 134, 9e21.

D'Esposito, M., Aguirre, G. K., Zarahn, E., Ballard, D., Shin, R. K., & Lease, J. (1998). Functional MRI studies of spatial and nonspatial working memory. Cognitive Brain Research, 7(1), 1-13.

Dmochowski, J. P., Bikson, M., & Parra, L. C. (2012). The point spread function of the human head and its implications for transcranial current stimulation. Physics in Medicine & Biology, 57(20), 6459.

Dmochowski, J. P., Datta, A., Bikson, M., Su, Y., & Parra, L. C. (2011). Optimized multi-electrode stimulation increases focality and intensity at target. Journal of neural engineering, 8(4), 046011.

Dosenbach, N. U., Fair, D. A., Cohen, A. L., Schlaggar, B. L., & Petersen, S. E. (2008). A dual-networks architecture of top-down control. Trends in cognitive sciences, 12(3), 99-105.

Dubljević, V., Saigle, V., & Racine, E. (2014). The rising tide of tDCS in the media and academic literature. Neuron, 82(4), 731-736.

Duecker, F., Schuhmann, T., Bien, N., Jacobs, C., & Sack, A. T. (2017). Moving beyond attentional biases: Shifting the interhemispheric balance between left and right posterior parietal cortex modulates attentional control processes. Journal of cognitive neuroscience, 29(7), 1267-1278.

Duncan, J., & Owen, A. M. (2000). Common regions of the human frontal lobe recruited by diverse cognitive demands. Trends in neurosciences, 23(10), 475-483.

Elliott, P. (2014). Electricity and the brain: an historical evaluation. In The Stimulated Brain (pp. 3-33). Academic Press.

Eriksson, J., Vogel, E. K., Lansner, A., Bergström, F., & Nyberg, L. (2015). Neurocognitive architecture of working memory. Neuron, 88(1), 33-46.

Bibliography

Esmaeilpour, Z., Shereen, A. D., Ghobadi-Azari, P., Datta, A., Woods, A. J., Ironside, M., ... & Ekhtiari, H. (2019). Methodology for tDCS integration with fMRI. medRxiv, 19006288.

Etz, A., Gronau, Q. F., Dablander, F., Edelsbrunner, P. A., & Baribault, B. (in press). How to become a Bayesian in eight easy steps: An annotated reading list. Psychonomic Bulletin & Review.

Fan, J., McCandliss, B. D., Sommer, T., Raz, A., & Posner, M. I. (2002). Testing the efficiency and independence of attentional networks. Journal of cognitive neuroscience, 14(3), 340-347.

Faria, P., Fregni, F., Sebastião, F., Dias, A. I., & Leal, A. (2012). Feasibility of focal transcranial DC polarization with simultaneous EEGrecording: Preliminary assessment in healthy subjects and human epilepsy. Epilepsy & Behavior, 25(3), 417e425.

Ferdjallah, M., Bostick, F. X., & Barr, R. E. (1996). Potential and current density distributions of cranial electrotherapy stimulation (CES) in a four-concentric-spheres model. IEEE Transactions on Biomedical Engineering, 43(9), 939-943.

Ferrarelli, F., Massimini, M., Peterson, M. J., Riedner, B. A., Lazar, M., Murphy, M. J., ... & Tononi, G. (2008). Reduced evoked gamma oscillations in the frontal cortex in schizophrenia patients: a TMS/EEG study. American Journal of Psychiatry, 165(8), 996-1005.

Fertonani, A., & Miniussi, C. (2017). Transcranial electrical stimulation: what we know and do not know about mechanisms. The Neuroscientist, 23(2), 109-123.

Fertonani, A., Pirulli, C., & Miniussi, C. (2011). Random noise stimulation improves neuroplasticity in perceptual learning. Journal of Neuroscience, 31(43), 15416-15423.

Filmer, H. L., Dux, P. E., & Mattingley, J. B. (2015). Dissociable effects of anodal and cathodal tDCS reveal distinct functional roles for right parietal cortex in the detection of single and competing stimuli. Neuropsychologia, 74, 120-126.

Finger, S. (2006). Benjamin Franklin, electricity, and the palsies: on the 300th anniversary of his birth. Neurology, 66(10), 1559-1563.

Fitzgerald, P. B. (2010). TMS-EEG: a technique that has come of age?. Clinical Neurophysiology, 121(3), 265-267.

Fogassi, L., & Luppino, G. (2005). Motor functions of the parietal lobe. Current opinion in neurobiology, 15(6), 626-631.

Friedman, H. R., & Goldman-Rakic, P. S. (1994). Coactivation of prefrontal cortex and inferior parietal cortex in working memory tasks revealed by 2DG functional mapping in the rhesus monkey. Journal of Neuroscience, 14(5), 2775-2788.

Fritsch, B., Gellner, A. K., & Reis, J. (2017). Transcranial electrical brain stimulation in alert rodents. JoVE (Journal of Visualized Experiments), (129), e56242.

Fritsch, B., Reis, J., Martinowich, K., Schambra, H. M., Ji, Y., Cohen, L. G., & Lu, B. (2010). Direct current stimulation promotes BDNF-dependent synaptic plasticity: potential implications for motor learning. Neuron, 66(2), 198-204.

Fuggetta, G., Fiaschi, A., & Manganotti, P. (2005). Modulation of cortical oscillatory activities induced by varying single-pulse transcranial magnetic stimulation intensity over the left primary motor area: a combined EEG and TMS study. Neuroimage, 27(4), 896-908.

Gandiga, P. C., Hummel, F. C., & Cohen, L. G. (2006). Transcranial DC stimulation (tDCS): a tool for double-blind sham-controlled clinical studies in brain stimulation. Clinical neurophysiology, 117(4), 845-850.

Gartside, I. B. (1968). Mechanism of sustained increases of firing rate in neurones of the rat cerebral cortex after polarization: role of protein synthesis. Nature, 220, 383-384.

Gellner, A. K., Reis, J., & Fritsch, B. (2016). Glia: a neglected player in non-invasive direct current brain stimulation. Frontiers in cellular neuroscience, 10.

Gelman, A., & Hill, J. (2006). Data analysis using regression and multilevel/hierarchical models. Cambridge university press.

Giordano, J., Bikson, M., Kappenman, E. S., Clark, V. P., Coslett, H. B., Hamblin, M. R., ... & Nitsche, M. A. (2017). Mechanisms and effects of transcranial direct current stimulation. Dose-Response, 15(1), 1559325816685467.

Giustolisi, B., Vergallito, A., Cecchetto, C., Varoli, E., & Lauro, L. J. R. (2018). Anodal transcranial direct current stimulation over left inferior frontal gyrus enhances sentence comprehension. Brain and language, 176, 36-41.

Gross, J. (2014). Analytical methods and experimental approaches for electrophysiological studies of brain oscillations. Journal of neuroscience methods, 228, 57-66.

Hämäläinen, M. S., & Ilmoniemi, R. J. (1994). Interpreting magnetic fields of the brain: minimum norm estimates. Medical & Biological Engineering & Computing, 32(1), 35-42.

Hampstead, B. M., Brown, G. S., & Hartley, J. F. (2014). Transcranial direct current stimulation modulates activation and effective connectivity during spatial navigation. Brain stimulation, 7(2), 314-324.

Harris, A. R., Schwerdtfeger, K., & Strauss, D. J. (2011). Adapted filter banks for feature extraction in transcranial magnetic stimulation evoked responses. Medical & biological engineering & computing, 49(2), 221-231.

Hattori, Y., Moriwaki, A., & Hori, Y. (1990). Biphasic effects of polarizing current on adenosine sensitive generation of cyclic AMP in rat cerebral cortex. Neuroscience Letters, 116, 320–324.

Haxby, J. V., Petit, L., Ungerleider, L. G., & Courtney, S. M. (2000). Distinguishing the functional roles of multiple regions in distributed neural systems for visual working memory. Neuroimage, 11(5), 380-391.

Heilman, K. M., & Van Den Abell, T. (1980). Right hemisphere dominance for attention: the mechanism underlying hemispheric asymmetries of inattention (neglect). Neurology, 30(3), 327-327.

Heilman, K. M., Bowers, D., Coslett, H. B., Whelan, H., & Watson, R. T. (1985). Directional hypokinesia: prolonged reaction times for leftward movements in patients with right hemisphere lesions and neglect. Neurology, 35(6), 855-855.

Heimrath, K., Sandmann, P., Becke, A., Müller, N. G., & Zaehle, T. (2012). Behavioral and electrophysiological effects of transcranial direct current stimulation of the parietal cortex in a visuo-spatial working memory task. Frontiers in psychiatry, 3, 56.

Heinen, K., Sagliano, L., Candini, M., Husain, M., Cappelletti, M., & Zokaei, N. (2016). Cathodal transcranial direct current stimulation over posterior parietal cortex enhances distinct aspects of visual working memory. Neuropsychologia, 87, 35-42.

Herrmann, C. S., Rach, S., Vosskuhl, J., & Strüber, D. (2014). Time–frequency analysis of event-related potentials: a brief tutorial. Brain topography, 27(4), 438-450.

Hill, A. T., Fitzgerald, P. B., & Hoy, K. E. (2016). Effects of anodal transcranial direct current stimulation on working memory: a systematic review and meta-analysis of findings from healthy and neuropsychiatric populations. Brain stimulation, 9(2), 197-208.

Hill, A. T., Rogasch, N. C., Fitzgerald, P. B., & Hoy, K. E. (2019). Impact of concurrent task performance on transcranial direct current stimulation (tDCS)-Induced changes in cortical physiology and working memory. Cortex, 113, 37-57.

Hill, A. T., Rogasch, N. C., Fitzgerald, P. B., & Hoy, K. E. (2016). TMS-EEG: A window into the neurophysiological effects of transcranial electrical stimulation in non-motor brain regions. Neuroscience & Biobehavioral Reviews, 64, 175-184.

Hill, A. T., Rogasch, N. C., Fitzgerald, P. B., & Hoy, K. E. (2017). Effects of prefrontal bipolar and high-definition transcranial direct current stimulation on cortical reactivity and working memory in healthy adults. Neuroimage, 152, 142-157.

Huang, N. E. (2014). Hilbert-Huang transform and its applications (Vol. 16). World Scientific.

Bibliography

Huntley, J. D., & Howard, R. J. (2010). Working memory in early Alzheimer's disease: a neuropsychological review. International Journal of Geriatric Psychiatry: A journal of the psychiatry of late life and allied sciences, 25(2), 121-132.

Ikkai, A., & Curtis, C. E. (2011). Common neural mechanisms supporting spatial working memory, attention and motor intention. Neuropsychologia, 49(6), 1428-1434.

Ilmoniemi, R. J., & Kičić, D. (2010). Methodology for combined TMS and EEG. Brain topography, 22(4), 233.

Ilmoniemi, R. J., Virtanen, J., Ruohonen, J., Karhu, J., Aronen, H. J., Näätänen, R., & Katila, T. (1997). Neuronal responses to magnetic stimulation reveal cortical reactivity and connectivity. Neuroreport, 8(16), 3537-3540.

Im, C. H., Park, J. H., Shim, M., Chang, W. H., & Kim, Y. H. (2012). Evaluation of local electric fields generated by transcranial direct current stimulation with an extracephalic reference electrode based on realistic 3D body modeling. Physics in Medicine & Biology, 57(8), 2137.

Iramina, K., Maeno, T., Nonaka, Y., & Ueno, S. (2003). Measurement of evoked electroencephalography induced by transcranial magnetic stimulation. Journal of applied physics, 93(10), 6718-6720.

Islam, N., Aftabuddin, M., Moriwaki, A., Hattori, Y., & Hori, Y. (1995). Increase in the calcium level following anodal polarization in the rat brain. Brain Research, 684, 206–208.

Ives, J. R., Rotenberg, A., Poma, R., Thut, G., & Pascual-Leone, A. (2006). Electroencephalographic recording during transcranial magnetic stimulation in humans and animals. Clinical neurophysiology, 117(8), 1870-1875.

Jackson, M. P., Rahman, A., Lafon, B., Kronberg, G., Ling, D., Parra, L. C., & Bikson, M. (2016). Animal models of transcranial direct current stimulation: methods and mechanisms. Clinical Neurophysiology, 127(11), 3425-3454.

Jackson, M. P., Truong, D., Brownlow, M. L., Wagner, J. A., McKinley, R. A., Bikson, M., & Jankord, R. (2017). Safety parameter considerations of anodal transcranial direct current stimulation in rats. Brain, behavior, and immunity, 64, 152-161.

Jacobson, L., Koslowsky, M., & Lavidor, M. (2012). tDCS polarity effects in motor and cognitive domains: a meta-analytical review. Experimental brain research, 216(1), 1-10.

Jahankhani, P., Kodogiannis, V., & Revett, K. (2006, October). EEG signal classification using wavelet feature extraction and neural networks. In IEEE John Vincent Atanasoff 2006 International Symposium on Modern Computing (JVA'06) (pp. 120-124). IEEE.

Jamil, A., Batsikadze, G., Kuo, H. I., Labruna, L., Hasan, A., Paulus, W., & Nitsche, M. A. (2017). Systematic evaluation of the impact of stimulation intensity on neuroplastic after-effects induced by transcranial direct current stimulation. The Journal of physiology, 595(4), 1273-1288.

Jarbo, K., & Verstynen, T. D. (2015). Converging structural and functional connectivity of orbitofrontal, dorsolateral prefrontal, and posterior parietal cortex in the human striatum. Journal of Neuroscience, 35(9), 3865-3878.

JASP Team. (2017). JASP (Version 0.8. 2).

Johnson, M. K., McMahon, R. P., Robinson, B. M., Harvey, A. N., Hahn, B., Leonard, C. J., ... & Gold, J. M. (2013). The relationship between working memory capacity and broad measures of cognitive ability in healthy adults and people with schizophrenia. Neuropsychology, 27(2), 220.

Jones, K. T., & Berryhill, M. (2012). Parietal contributions to visual working memory depend on task difficulty. Frontiers in psychiatry, 3, 81.

Juan, C. H., Tseng, P., & Hsu, T. Y. (2017). Elucidating and modulating the neural correlates of visuospatial working memory via noninvasive brain stimulation. Current Directions in Psychological Science, 26(2), 165-173.

Kammer, T., & Baumann, L. W. (2010). Phosphene thresholds evoked with single and double TMS pulses. Clinical Neurophysiology, 121(3), 376-379.

Kang, E. K., Kim, Y. K., Sohn, H. M., Cohen, L. G., & Paik, N. J. (2011). Improved picture naming in aphasia patients treated with cathodal tDCS to inhibit the right Broca's homologue area. Restorative neurology and neuroscience, 29(3), 141-152.

Karnath, H. O., Himmelbach, M., & Küker, W. (2003). The cortical substrate of visual extinction. Neuroreport, 14(3), 437-442.

Keel, J. C., Smith, M. J., & Wassermann, E. M. (2001). A safety screening questionnaire for transcranial magnetic stimulation. Clinical neurophysiology: official journal of the International Federation of Clinical Neurophysiology, 112(4), 720-720.

Keeser, D., Meindl, T., Bor, J., Palm, U., Pogarell, O., Mulert, C., ... & Padberg, F. (2011). Prefrontal transcranial direct current stimulation changes connectivity of resting-state networks during fMRI. Journal of Neuroscience, 31(43), 15284-15293.

Kekic, M., Boysen, E., Campbell, I. C., & Schmidt, U. (2016). A systematic review of the clinical efficacy of transcranial direct current stimulation (tDCS) in psychiatric disorders. Journal of psychiatric research, 74, 70-86.

Kerwin, L. J., Keller, C. J., Wu, W., Narayan, M., & Etkin, A. (2017). Test-retest reliability of transcranial magnetic stimulation EEG evoked potentials. Brain stimulation.

Kirimoto, H., Ogata, K., Onishi, H., Oyama, M., Goto, Y., & Tobimatsu, S. (2011). Transcranial direct current stimulation over the motor association cortex induces plastic changes in ipsilateral primary motor and somatosensory cortices. Clinical Neurophysiology, 122(4), 777e783.

Kleinman, J. T., Newhart, M., Davis, C., Heidler-Gary, J., Gottesman, R. F., & Hillis, A. E. (2007). Right hemispatial neglect: frequency and characterization following acute left hemisphere stroke. Brain and cognition, 64(1), 50-59.

Klingberg, T., Forssberg, H., & Westerberg, H. (2002). Increased brain activity in frontal and parietal cortex underlies the development of visuospatial working memory capacity during childhood. Journal of cognitive neuroscience, 14(1), 1-10.

Kravitz, D. J., Saleem, K. S., Baker, C. I., & Mishkin, M. (2011). A new neural framework for visuospatial processing. Nature Reviews Neuroscience, 12(4), 217.

Krishnamurthy, V., Gopinath, K., Brown, G. S., & Hampstead, B. M. (2015). Resting-state fMRI reveals enhanced functional connectivity in spatial navigation networks after transcranial direct current stimulation. Neuroscience letters, 604, 80-85.

Kronberg, G., Bridi, M., Abel, T., Bikson, M., & Parra, L. C. (2017). Direct current stimulation modulates LTP and LTD: activity dependence and dendritic effects. Brain Stimulation: Basic, Translational, and Clinical Research in Neuromodulation, 10(1), 51-58.

Kuo, H. I., Bikson, M., Datta, A., Minhas, P., Paulus, W., Kuo, M. F., & Nitsche, M. A. (2013). Comparing cortical plasticity induced by conventional and high-definition 4× 1 ring tDCS: a neurophysiological study. Brain stimulation, 6(4), 644-648.

Kuo, M. F., Grosch, J., Fregni, F., Paulus, W., & Nitsche, M. A. (2007a). Focusing effect of acetylcholine on neuroplasticity in the human motor cortex. Journal of Neuroscience, 27(52), 14442-14447.

Kuo, M. F., Paulus, W., & Nitsche, M. A. (2007b). Boosting focally-induced brain plasticity by dopamine. Cerebral cortex, 18(3), 648-651.

Kuznetsova, A., Brockhoff, P. B., & Christensen, R. H. B. (2015). Package 'lmertest'. R package version, 2(0).

Làdavas, E., Del Pesce, M., & Provinciali, L. (1989). Unilateral attention deficits and hemispheric asymmetries in the control of visual attention. Neuropsychologia, 27(3), 353-366.

Lafon, B., Rahman, A., Bikson, M., & Parra, L. C. (2016). Direct current stimulation alters neuronal input/output function. Brain Stimulation, 10, 36-45.

Bibliography

Lang, N., Nitsche, M. A., Paulus, W., Rothwell, J. C., & Lemon, R. N. (2004). Effects of transcranial direct current stimulation over the human motor cortex on corticospinal and transcallosal excitability. Experimental Brain Research, 156(4), 439-443.

Lang, N., Siebner, H. R., Ward, N. S., Lee, L., Nitsche, M. A., Paulus, W., …, & Frackowiak, R. S. (2005). How does transcranial DC stimulation of the primary motor cortex alter regional neuronal activity in the human brain?. European Journal of Neuroscience, 22(2), 495-504.

Lee, J. Y., Nagano, Y., Taylor, J. P., Lim, K. L., & Yao, T. P. (2010). Disease-causing mutations in parkin impair mitochondrial ubiquitination, aggregation, and HDAC6-dependent mitophagy. The Journal of cell biology, 189(4), 671-679.

Lee, L., Siebner, H. R., Rowe, J. B., Rizzo, V., Rothwell, J. C., Frackowiak, R. S., & Friston, K. J. (2003). Acute remapping within the motor system induced by low-frequency repetitive transcranial magnetic stimulation. Journal of Neuroscience, 23(12), 5308-5318.

Lees, A. J., & Smith, E. (1983). Cognitive deficits in the early stages of Parkinson's disease. Brain, 106(2), 257-270.

Lefaucheur, J. P., Antal, A., Ayache, S. S., Benninger, D. H., Brunelin, J., Cogiamanian, F., ... & Marangolo, P. (2017). Evidence-based guidelines on the therapeutic use of transcranial direct current stimulation (tDCS). Clinical Neurophysiology, 128(1), 56-92.

Lehmann, D., & Skrandies, W. (1980). Reference-free identification of components of checkerboard-evoked multichannel potential fields. Electroencephalography and clinical neurophysiology, 48(6), 609-621.

Lewis, P. M., & Rosenfeld, J. V. (2016). Electrical stimulation of the brain and the development of cortical visual prostheses: an historical perspective. Brain research, 1630, 208-224.

Li, L. M., Leech, R., Scott, G., Malhotra, P., Seemungal, B., & Sharp, D. J. (2015). The effect of oppositional parietal transcranial direct current stimulation on lateralized brain functions. European Journal of Neuroscience, 42(11), 2904-2914.

Li, L. M., Uehara, K., & Hanakawa, T. (2015). The contribution of interindividual factors to variability of response in transcranial direct current stimulation studies. Frontiers in cellular neuroscience, 9, 181.

Li, S., Cai, Y., Liu, J., Li, D., Feng, Z., Chen, C., & Xue, G. (2017). Dissociated roles of the parietal and frontal cortices in the scope and control of attention during visual working memory. Neuroimage, 149, 210-219.

Liebetanz, D., Koch, R., Mayenfels, S., König, F., Paulus, W., & Nitsche, M. A. (2009). Safety limits of cathodal transcranial direct current stimulation in rats. Clinical Neurophysiology, 120(6), 1161-1167.

Liebetanz, D., Nitsche, M. A., Tergau, F., & Paulus, W. (2002). Pharmacological approach to the mechanisms of transcranial DC-stimulation-induced after effects of human motor cortex excitability. Brain, 125, 2238–2247.

Lioumis, P., Kičić, D., Savolainen, P., Mäkelä, J. P., & Kähkönen, S. (2009). Reproducibility of TMS-Evoked EEG responses. Human brain mapping, 30(4), 1387-1396.

Litvak, V., Komssi, S., Scherg, M., Hoechstetter, K., Classen, J., Zaaroor, M., ... & Kahkonen, S. (2007). Artifact correction and source analysis of early electroencephalographic responses evoked by transcranial magnetic stimulation over primary motor cortex. Neuroimage, 37(1), 56-70.

Lo, O. Y., van Donkelaar, P., & Chou, L. S. (2019). Effects of transcranial direct current stimulation over right posterior parietal cortex on attention function in healthy young adults. European Journal of Neuroscience.

Luck, S. J., & Vogel, E. K. (1997). The capacity of visual working memory for features and conjunctions. Nature, 390(6657), 279.

Luck, S. J., & Vogel, E. K. (2013). Visual working memory capacity: from psychophysics and neurobiology to individual differences. Trends in cognitive sciences, 17(8), 391-400.

Maris, E., & Oostenveld, R. (2007). Nonparametric statistical testing of EEG-and MEG-data. Journal of neuroscience methods, 164(1), 177-190.

Martin, D. M., Liu, R., Alonzo, A., Green, M., & Loo, C. K. (2014). Use of transcranial direct current stimulation (tDCS) to enhance cognitive training: effect of timing of stimulation. Experimental brain research, 232(10), 3345-3351.

Massimini, M., Ferrarelli, F., Huber, R., Esser, S. K., Singh, H., & Tononi, G. (2005). Breakdown of cortical effective connectivity during sleep. Science, 309(5744), 2228-2232.

Massimini, M., Ferrarelli, F., Murphy, M. J., Huber, R., Riedner, B. A., Casarotto, S., & Tononi, G. (2010). Cortical reactivity and effective connectivity during REM sleep in humans. Cognitive neuroscience, 1(3), 176-183.

Matsunaga, K., Nitsche, M. A., Tsuji, S., & Rothwell, J. C. (2004). Effect of transcranial DC sensorimotor cortex stimulation on somatosensory evoked potentials in humans. Clinical Neurophysiology, 115(2), 456e460.

Mattavelli, G., Rosanova, M., Casali, A. G., Papagno, C., & Romero Lauro, L. J. (2013). Top-down interference and cortical responsiveness in face processing: a TMS-EEG study. Neuroimage, 76, 24-32.

McLaren, M. E., Nissim, N. R., & Woods, A. J. (2018). The effects of medication use in transcranial direct current stimulation: a brief review. Brain stimulation, 11(1), 52-58.

McNab, F., & Klingberg, T. (2008). Prefrontal cortex and basal ganglia control access to working memory. Nature neuroscience, 11(1), 103.

Medeiros, L. F., de Souza, I. C. C., Vidor, L. P., de Souza, A., Deitos, A., Volz, M. S., …, & Torres, I. L. (2012). Neurobiological effects of transcranial direct current stimulation: a review. Frontiers in psychiatry, 3.

Merrill, D. R., Bikson, M., & Jefferys, J. G. (2005). Electrical stimulation of excitable tissue: design of efficacious and safe protocols. Journal of neuroscience methods, 141(2), 171-198.

Meyer, B. U., Diehl, R., Steinmetz, H., Britton, T. C., & Benecke, R. (1991). Magnetic stimuli applied over motor and visual cortex: influence of coil position and field polarity on motor responses, phosphenes, and eye movements. Electroencephalography and clinical neurophysiology. Supplement, 43, 121-134.

Meyer, K. N., Du, F., Parks, E., & Hopfinger, J. B. (2018). Exogenous vs. endogenous attention: Shifting the balance of fronto-parietal activity. Neuropsychologia, 111, 307-316.

Miller, E. K., & Cohen, J. D. (2001). An integrative theory of prefrontal cortex function. Annual review of neuroscience, 24(1), 167-202.

Milner, A. D., & Goodale, M. A. (1995). Oxford psychology series, No. 27.

Miniussi, C., & Thut, G. (2010). Combining TMS and EEG offers new prospects in cognitive neuroscience. Brain topography, 22(4), 249.

Miniussi, C., Brignani, D., & Pellicciari, M. C. (2012). Combining transcranial electrical stimulation with electroencephalography: a multimodal approach. Clinical EEG and Neuroscience, 43(3), 184-191.

Miniussi, C., Harris, J. A., & Ruzzoli, M. (2013). Modelling non-invasive brain stimulation in cognitive neuroscience. Neuroscience & Biobehavioral Reviews, 37(8), 1702-1712.

Miocinovic, S., Somayajula, S., Chitnis, S., & Vitek, J. L. (2013). History, applications, and mechanisms of deep brain stimulation. JAMA neurology, 70(2), 163-171.

Miranda, P. C., Lomarev, M., & Hallett, M. (2006). Modeling the current distribution during transcranial direct current stimulation. Clinical neurophysiology, 117(7), 1623-1629.

Miranda, P. C., Mekonnen, A., Salvador, R., & Ruffini, G. (2013). The electric field in the cortex during transcranial current stimulation. NeuroImage, 70, 48-58.

Molenberghs, P., Mesulam, M. M., Peeters, R., & Vandenberghe, R. R. (2007). Remapping attentional priorities: differential contribution of superior parietal lobule and intraparietal sulcus. Cerebral Cortex, 17(11), 2703-2712.

Molenberghs, P., Sale, M. V., & Mattingley, J. B. (2012). Is there a critical lesion site for unilateral spatial neglect? A meta-analysis using activation likelihood estimation. Frontiers in Human Neuroscience, 6, 78.

Bibliography

Moliadze, V., Antal, A., & Paulus, W. (2010). Electrode-distance dependent after-effects of transcranial direct and random noise stimulation with extracephalic reference electrodes. Clinical Neurophysiology, 121(12), 2165-2171.

Monte-Silva, K., Kuo, M. F., Hessenthaler, S., Fresnoza, S., Liebetanz, D., Paulus, W., & Nitsche, M. A. (2013). Induction of late LTP-like plasticity in the human motor cortex by repeated non-invasive brain stimulation. Brain stimulation, 6(3), 424-432.

Monte-Silva, K., Kuo, M. F., Thirugnanasambandam, N., Liebetanz, D., Paulus, W., & Nitsche, M. A. (2009). Dose-dependent inverted U-shaped effect of dopamine (D2-like) receptor activation on focal and nonfocal plasticity in humans. Journal of Neuroscience, 29(19), 6124-6131.

Moriwaki, A. (1991). Polarizing currents increase noradrenaline-elicited accumulation of cyclic AMP in rat cerebral cortex. Brain Research. 544, 248–252.

Moruzzi, G., & Magoun, H. W. (1995). Brain stem reticular formation and activation of the EEG. 1949. The Journal of neuropsychiatry and clinical neurosciences, 7(2), 251.

Mutanen, T., Mäki, H., & Ilmoniemi, R. J. (2013). The effect of stimulus parameters on TMS–EEG muscle artifacts. Brain stimulation, 6(3), 371-376.

Nagel, B. J., Herting, M. M., Maxwell, E. C., Bruno, R., & Fair, D. (2013). Hemispheric lateralization of verbal and spatial working memory during adolescence. Brain and cognition, 82(1), 58-68.

Nasseri, P., Nitsche, M. A., & Ekhtiari, H. (2015). A framework for categorizing electrode montages in transcranial direct current stimulation. Frontiers in human neuroscience, 9, 54.

Nee, D. E., & D'Esposito, M. (2016). The hierarchical organization of the lateral prefrontal cortex. Elife, 5, e12112.

Nikouline, V., Ruohonen, J., & Ilmoniemi, R. J. (1999). The role of the coil click in TMS assessed with simultaneous EEG. Clinical Neurophysiology, 110(8), 1325-1328.

Nikulin, V. V., Kičić, D., Kähkönen, S., & Ilmoniemi, R. J. (2003). Modulation of electroencephalographic responses to transcranial magnetic stimulation: evidence for changes in cortical excitability related to movement. European Journal of Neuroscience, 18(5), 1206-1212.

Nitsche, M. A., & Paulus, W. (2000). Excitability changes induced in the human motor cortex by weak transcranial direct current stimulation. The Journal of physiology, 527(3), 633-639.

Nitsche, M. A., & Paulus, W. (2001). Sustained excitability elevations induced by transcranial DC motor cortex stimulation in humans. Neurology, 57(10), 1899e1901.

Nitsche, M. A., Cohen, L. G., Wassermann, E. M., Priori, A., Lang, N., Antal, A., …& Pascuale-Leone, A. (2008). Transcranial direct current stimulation: state of the art 2008. Brain Stimulation, 1(3), 206-223.

Nitsche, M. A., Doemkes, S., Karakose, T., Antal, A., Liebetanz, D., Lang, N., ... & Paulus, W. (2007). Shaping the effects of transcranial direct current stimulation of the human motor cortex. Journal of neurophysiology, 97(4), 3109-3117.

Nitsche, M. A., Fricke, K., Henschke, U., Schlitterlau, A., Liebetanz, D., Lang, N., ... & Paulus, W. (2003a). Pharmacological modulation of cortical excitability shifts induced by transcranial direct current stimulation in humans. The Journal of physiology, 553(1), 293-301.

Nitsche, M. A., Grundey, J., Liebetanz, D., Lang, N., Tergau, F., & Paulus, W. (2004). Catecholaminergic consolidation of motor cortical neuroplasticity in humans. Cerebral Cortex, 14(11), 1240e1245.

Nitsche, M. A., Kuo, M. F., Karrasch, R., Wächter, B., Liebetanz, D., & Paulus, W. (2009). Serotonin affects transcranial direct current–induced neuroplasticity in humans. Biological psychiatry, 66(5), 503-508.

Nitsche, M. A., Liebetanz, D., Antal, A., Lang, N., Tergau, F., & Paulus, W. (2003). Modulation of cortical excitability by weak direct current stimulation-technical, safety and functional aspects. Supplements to Clinical Neurophysiology, 56, 255e276.

Nitsche, M. A., Liebetanz, D., Schlitterlau, A., Henschke, U., Fricke, K., Frommann, K., ... & Tergau, F. (2004a). GABAergic modulation of DC stimulation-induced motor cortex excitability shifts in humans. European Journal of Neuroscience, 19(10), 2720-2726.

Nitsche, M. A., Nitsche, M. S., Klein, C. C., Tergau, F., Rothwell, J. C., & Paulus, W. (2003). Level of action of cathodal DC polarisation induced inhibition of the human motor cortex. Clinical Neurophysiology, 114(4), 600-604.

Nitsche, M. A., Seeber, A., Frommann, K., Klein, C. C., Rochford, C., Nitsche, M. S., …, & Paulus, W. (2005). Modulating parameters of excitability during and after transcranial direct current stimulation of the human motor cortex. The Journal of Physiology, 568(Pt 1), 291e303.

Nobre, A. C., Gitelman, D. R., Dias, E. C., & Mesulam, M. M. (2000). Covert visual spatial orienting and saccades: overlapping neural systems. Neuroimage, 11(3), 210-216.

Noetscher, G. M., Yanamadala, J., Makarov, S. N., & Pascual-Leone, A. (2014). Comparison of cephalic and extracephalic montages for transcranial direct current stimulation—a numerical study. IEEE Transactions on Biomedical Engineering, 61(9), 2488-2498.

Nystrom, L. E., Braver, T. S., Sabb, F. W., Delgado, M. R., Noll, D. C., & Cohen, J. D. (2000). Working memory for letters, shapes, and locations: fMRI evidence against stimulus-based regional organization in human prefrontal cortex. Neuroimage, 11(5), 424-446.

Oldfield, R. C. (1971). The assessment and analysis of handedness: the Edinburgh inventory. Neuropsychologia, 9(1), 97-113.

Olesen, P. J., Westerberg, H., & Klingberg, T. (2004). Increased prefrontal and parietal activity after training of working memory. Nature neuroscience, 7(1), 75.

Oostenveld, R., Fries, P., Maris, E., & Schoffelen, J. M. (2011). FieldTrip: open source software for advanced analysis of MEG, EEG, and invasive electrophysiological data. Computational intelligence and neuroscience, 2011, 1.

Opitz, A., Paulus, W., Will, S., Antunes, A., & Thielscher, A. (2015). Determinants of the electric field during transcranial direct current stimulation. Neuroimage, 109, 140-150.

Owen, A. M., McMillan, K. M., Laird, A. R., & Bullmore, E. (2005). N-back working memory paradigm: A meta-analysis of normative functional neuroimaging studies. Human brain mapping, 25(1), 46-59.

Pantazis, D., Nichols, T., Baillet, S., & Leahy, R. (2003). Spatiotemporal localization of significant activation in MEG using permutation tests. In Information Processing in Medical Imaging (pp. 512-523). Springer Berlin/Heidelberg.

Parent, A. (2004). Giovanni Aldini: from animal electricity to human brain stimulation. Canadian Journal of Neurological Sciences, 31(4), 576-584.

Pascual-Leone, A., Tormos, J. M., Keenan, J., Tarazona, F., Cañete, C., & Catalá, M. D. (1998). Study and modulation of human cortical excitability with transcranial magnetic stimulation. Journal of Clinical Neurophysiology, 15(4), 333-343.

Pascual-Leone, A., Walsh, V., & Rothwell, J. (2000). Transcranial magnetic stimulation in cognitive neuroscience–virtual lesion, chronometry, and functional connectivity. Current opinion in neurobiology, 10(2), 232-237.

Paulus, W., Nitsche, M. A., & Antal, A. (2016). Application of transcranial electric stimulation (tDCS, tACS, tRNS): From motor-evoked potentials towards modulation of behaviour. European Psychologist, 21(1), 4.

Paus, T., Sipila, P. K., & Strafella, A. P. (2001). Synchronization of neuronal activity in the human primary motor cortex by transcranial magnetic stimulation: an EEG study. Journal of Neurophysiology, 86(4), 1983-1990.

Pellicciari, M. C., Brignani, D., & Miniussi, C. (2013). Excitability modulation of the motor system induced by transcranial direct current stimulation: a multimodal approach. Neuroimage, 83, 569-580.

Pellicciari, M. C., Veniero, D., & Miniussi, C. (2017). Characterizing the cortical oscillatory response to TMS pulse. Frontiers in cellular neuroscience, 11, 38.

Perlstein, W. M., Carter, C. S., Noll, D. C., & Cohen, J. D. (2001). Relation of prefrontal cortex dysfunction to working memory and symptoms in schizophrenia. American Journal of Psychiatry, 158(7), 1105-1113.

Bibliography

Pesaran, B., Pezaris, J. S., Sahani, M., Mitra, P. P., & Andersen, R. A. (2002). Temporal structure in neuronal activity during working memory in macaque parietal cortex. Nature neuroscience, 5(8), 805.

Petersen, S. E., & Posner, M. I. (2012). The attention system of the human brain: 20 years after. Annual review of neuroscience, 35, 73-89.

Petrides, M., & Pandya, D. N. (1999). Dorsolateral prefrontal cortex: comparative cytoarchitectonic analysis in the human and the macaque brain and corticocortical connection patterns. European Journal of Neuroscience, 11(3), 1011-1036.

Piccolino, M. (2000). The bicentennial of the Voltaic battery (1800–2000): the artificial electric organ. Trends in neurosciences, 23(4), 147-151.

Pigorini, A., Casali, A. G., Casarotto, S., Ferrarelli, F., Baselli, G., Mariotti, M., ... & Rosanova, M. (2011). Time–frequency spectral analysis of TMS-evoked EEG oscillations by means of Hilbert–Huang transform. Journal of neuroscience methods, 198(2), 236-245.

Pinheiro, J., Bates, D., DebRoy, S., & Sarkar, D. (2008). the R Development Core team. 2012. Nlme: Linear and nonlinear mixed effects models. R package version, 3, 1-137.

Pirulli, C., Fertonani, A., & Miniussi, C. (2013). The role of timing in the induction of neuromodulation in perceptual learning by transcranial electric stimulation. Brain stimulation, 6(4), 683-689.

Pisoni, A., Mattavelli, G., Papagno, C., Rosanova, M., Casali, A., & Romero Lauro, L. (2017). Cognitive Enhancement Induced by Anodal tDCS Drives Circuit-Specific Cortical Plasticity. Cerebral Cortex, 1-9.

Posner, M. I. (1980). Orienting of attention. Quarterly journal of experimental psychology, 32(1), 3-25.

Posner, M. I., & Petersen, S. E. (1990). The attention system of the human brain. Annual review of neuroscience, 13(1), 25-42.

Posner, M. I., Nissen, M. J., & Ogden, W. C. (2014). Attended and Unattended Processing Modes: The Role of Set for Spatial Location Editors' Introduction. In Modes of Perceiving and Processing Information (pp. 145-166). Psychology Press.

Postle, B. R. (2006). Working memory as an emergent property of the mind and brain. Neuroscience, 139(1), 23-38.

Priori, A. (2003). Brain polarization in humans: a reappraisal of an old tool for prolonged non-invasive modulation of brain excitability. Clinical Neurophysiology, 114(4), 589-595.

Priori, A., Berardelli, A., Rona, S., Accornero, N., & Manfredi, M. (1998). Polarization of the human motor cortex through the scalp. Neuroreport, 9(10), 2257e2260.

Purpura, D. P., & McMurtry, J. G. (1965). Intracellular activities and evoked potential changes during polarization of motor cortex. Journal of Neurophysiology, 28, 166e185.

Radman, T., Ramos, R. L., Brumberg, J. C., & Bikson, M. (2009). Role of cortical cell type and morphology in subthreshold and suprathreshold uniform electric field stimulation in vitro. Brain Stimulation, 2, 215–228.

Ragazzoni, A., Pirulli, C., Veniero, D., Feurra, M., Cincotta, M., Giovannelli, F., ... & Miniussi, C. (2013). Vegetative versus minimally conscious states: a study using TMS-EEG, sensory and event-related potentials. PloS one, 8(2), e57069.

Ranieri, F., Podda, M. V., Riccardi, E., Frisullo, G., Dileone, M., Profice, P., …, & Grassi, C. (2012). Modulation of LTP at rat hippocampal CA3-CA1 synapses by direct current stimulation. Journal of Neurophysiology, 107, 1868–1880.

Raz, A., & Buhle, J. (2006). Typologies of attentional networks. Nature Reviews Neuroscience, 7(5), 367.

Robison, M. K., McGuirk, W. P., & Unsworth, N. (2017). No evidence for enhancements to visual working memory with transcranial direct current stimulation to prefrontal or posterior parietal cortices. Behavioral neuroscience, 131(4), 277.

Rogasch, N. C., & Fitzgerald, P. B. (2013). Assessing cortical network properties using TMS–EEG. Human brain mapping, 34(7), 1652-1669.

Rohan , J. G., Carhuatanta, K. A., Mcinturf, S. M., Miklasevich, M. K., & Jankord, R. (2015). Modulating hippocampal plasticity with in vivo brain stimulation. Journal of Neuroscience, 35, 12824–12832.

Romero Lauro, L. J., Pisoni, A., Rosanova, M., Casarotto, S., Mattavelli, G., Bolognini, N., & Vallar, G. (2015). Localizing the effects of anodal tDCS at the level of cortical source: A Reply to Bailey et al., 2015. Cortex, 74(2016), 323-328.

Romero Lauro, L. J., Rosanova, M., Mattavelli, G., Convento, S., Pisoni, A., Opitz, A., …, & Vallar, G. (2014). TDCS increases cortical excitability: Direct evidence from TMS-EEG. Cortex, 58(2014), 99-111.

Rosanova, M., Casali, A., Bellina, V., Resta, F., Mariotti, M., & Massimini, M. (2009). Natural frequencies of human corticothalamic circuits. Journal of Neuroscience, 29(24), 7679-7685.

Rosanova, M., Gosseries, O., Casarotto, S., Boly, M., Casali, A. G., Bruno, M. A., ... & Massimini, M. (2012). Recovery of cortical effective connectivity and recovery of consciousness in vegetative patients. Brain, 135(4), 1308-1320.

Rose, E. J., & Ebmeier, K. P. (2006). Pattern of impaired working memory during major depression. Journal of affective disorders, 90(2-3), 149-161.

Rossi, S., Hallett, M., Rossini, P. M., Pascual-Leone, A., & Safety of TMS Consensus Group. (2009). Safety, ethical considerations, and application guidelines for the use of transcranial magnetic stimulation in clinical practice and research. Clinical neurophysiology, 120(12), 2008-2039.

Rottschy, C., Langner, R., Dogan, I., Reetz, K., Laird, A. R., Schulz, J. B., ... & Eickhoff, S. B. (2012). Modelling neural correlates of working memory: a coordinate-based meta-analysis. Neuroimage, 60(1), 830-846.

Rouder, J. N., Speckman, P. L., Sun, D., Morey, R. D., & Iverson, G. (2009). Bayesian t tests for accepting and rejecting the null hypothesis. Psychonomic bulletin & review, 16(2), 225-237.

Rounis, E., Stephan, K. E., Lee, L., Siebner, H. R., Pesenti, A., Friston, K. J., ... & Frackowiak, R. S. (2006). Acute changes in frontoparietal activity after repetitive transcranial magnetic stimulation over the dorsolateral prefrontal cortex in a cued reaction time task. Journal of Neuroscience, 26(38), 9629-9638.

Roy, L. B., Sparing, R., Fink, G. R., & Hesse, M. D. (2015). Modulation of attention functions by anodal tDCS on right PPC. Neuropsychologia, 74, 96-107.

Ruffini, G., Fox, M. D., Ripolles, O., Miranda, P. C., & Pascual-Leone, A. (2014). Optimization of multifocal transcranial current stimulation for weighted cortical pattern targeting from realistic modeling of electric fields. Neuroimage, 89, 216-225.

Sadleir, R. J., Vannorsdall, T. D., Schretlen, D. J., & Gordon, B. (2010). Transcranial direct current stimulation (tDCS) in a realistic head model. Neuroimage, 51(4), 1310-1318.

Saiote, C., Turi, Z., Paulus, W., & Antal, A. (2013). Combining functional magnetic resonance imaging with transcranial electrical stimulation. Frontiers in human neuroscience, 7, 435.

Salvador, R., Wenger, C., & Miranda, P. C. (2015). Investigating the cortical regions involved in MEP modulation in tDCS. Frontiers in cellular neuroscience, 9, 405.

Santarnecchi, E., Brem, A. K., Levenbaum, E., Thompson, T., Kadosh, R. C., & Pascual-Leone, A. (2015). Enhancing cognition using transcranial electrical stimulation. Current Opinion in Behavioral Sciences, 4, 171-178.

Sarmiento, C. I., San-Juan, D., & Prasath, V. B. S. (2016). Letter to the Editor: Brief history of transcranial direct current stimulation (tDCS): from electric fishes to microcontrollers. Psychological medicine, 46(15), 3259-3261.

Sarnthein, J., Petsche, H., Rappelsberger, P., Shaw, G. L., & Von Stein, A. (1998). Synchronization between prefrontal and posterior association cortex during human working memory. Proceedings of the National Academy of Sciences, 95(12), 7092-7096.

Bibliography

Sauseng, P., Freunberger, R., Feldheim, J. F., & Hummel, F. C. (2011). Right prefrontal TMS disrupts interregional anticipatory EEG alpha activity during shifting of visuospatial attention. Frontiers in psychology, 2, 241.

Sauseng, P., Klimesch, W., Schabus, M., & Doppelmayr, M. (2005). Fronto-parietal EEG coherence in theta and upper alpha reflect central executive functions of working memory. International Journal of Psychophysiology, 57(2), 97-103.

Schestatsky, P., Morales-Quezada, L., & Fregni, F. (2013). Simultaneous EEG monitoring during transcranial direct current stimulation. Journal of Visualized Experiments, (76).

Schlaug, G., & Renga, V. (2008). Transcranial direct current stimulation: a noninvasive tool to facilitate stroke recovery. Expert review of medical devices, 5(6), 759-768.

Schlösser, R. G., Wagner, G., & Sauer, H. (2006). Assessing the working memory network: studies with functional magnetic resonance imaging and structural equation modeling. Neuroscience, 139(1), 91-103.

Schneider, W., Eschman, A., & Zuccolotto, A. (2002). E-prime (version 2.0). Computer software and manual]. Pittsburgh, PA: Psychology Software Tools Inc.

Sczesny-Kaiser, M., Beckhaus, K., Dinse, H. R., Schwenkreis, P., Tegenthoff, M., & Höffken, O. (2016). Repetitive Transcranial Direct Current Stimulation Induced Excitability Changes of Primary Visual Cortex and Visual Learning Effects—A Pilot Study. Frontiers in behavioral neuroscience, 10.

Shen, W. W. (1999). A history of antipsychotic drug development. Comprehensive psychiatry, 40(6), 407-414.

Shomstein, S. (2012). Cognitive functions of the posterior parietal cortex: top-down and bottom-up attentional control. Frontiers in integrative neuroscience, 6, 38.

Siebner, H. R., Bergmann, T. O., Bestmann, S., Massimini, M., Johansen-Berg, H., Mochizuki, H., ... & Pascual-Leone, A. (2009). Consensus paper: combining transcranial stimulation with neuroimaging. Brain stimulation, 2(2), 58-80.

Silva, C., Maltez, J. C., Trindade, E., Arriaga, A., & Ducla-Soares, E. (2004). Evaluation of L 1 and L 2 minimum norm performances on EEG localizations. Clinical neurophysiology, 115(7), 1657-1668.

Silvanto, J., Muggleton, N., & Walsh, V. (2008). State-dependency in brain stimulation studies of perception and cognition. Trends in cognitive sciences, 12(12), 447-454.

Smith, E. E., Jonides, J., Koeppe, R. A., Awh, E., Schumacher, E. H., & Minoshima, S. (1995). Spatial versus object working memory: PET investigations. Journal of cognitive neuroscience, 7(3), 337-356.

Sparing, R., Thimm, M., Hesse, M. D., Küst, J., Karbe, H., & Fink, G. R. (2009). Bidirectional alterations of interhemispheric parietal balance by non-invasive cortical stimulation. Brain, 132(11), 3011-3020.

Stagg, C. J., & Nitsche, M. A. (2011). Physiological basis of transcranial direct current stimulation. Neuroscientist, 17, 37–53.

Stagg, C. J., Lin, R. L., Mezue, M., Segerdahl, A., Kong, Y., Xie, J., & Tracey, I. (2013). Widespread modulation of cerebral perfusion induced during and after transcranial direct current stimulation applied to the left dorsolateral prefrontal cortex. The Journal of Neuroscience, 33(28), 11425e11431.

Starck, J., Rimpiläinen, I., Pyykkö, I., & Esko, T. (1996). The noise level in magnetic stimulation. Scandinavian audiology, 25(4), 223-226.

Steinberg, H. (2013). Letter to the editor: transcranial direct current stimulation (tDCS) has a history reaching back to the 19th century. Psychological medicine, 43(3), 669-671.

Stone, D. B., & Tesche, C. D. (2009). Transcranial direct current stimulation modulates shifts in global/local attention. Neuroreport, 20(12), 1115-1119.

Suchan, J., Rorden, C., & Karnath, H. O. (2012). Neglect severity after left and right brain damage. Neuropsychologia, 50(6), 1136-1141.

Suh, H. S., Lee, W. H., & Kim, T. S. (2012). Influence of anisotropic conductivity in the skull and white matter on transcranial direct current stimulation via an anatomically realistic finite element head model. Physics in Medicine & Biology, 57(21), 6961.

Swaab-Barneveld, H., De Sonneville, L., Cohen-Kettenis, P., Gielen, A., Buitelaar, J. A. N., & Van Engeland, H. (2000). Visual sustained attention in a child psychiatric population. Journal of the American Academy of Child & Adolescent Psychiatry, 39(5), 651-659.

Szczepanski, S. M., Konen, C. S., & Kastner, S. (2010). Mechanisms of spatial attention control in frontal and parietal cortex. Journal of Neuroscience, 30(1), 148-160.

Taylor, S. (2007). Electroconvulsive therapy: a review of history, patient selection, technique, and medication management. Southern Medical Journal, 100(5), 494-499.

Team, R. (2013). R development core team. RA Lang Environ Stat Comput, 55, 275-286.

Terney, D., Chaieb, L., Moliadze, V., Antal, A., & Paulus, W. (2008). Increasing human brain excitability by transcranial high-frequency random noise stimulation. Journal of Neuroscience, 28(52), 14147-14155.

Thiel, C. M., Zilles, K., & Fink, G. R. (2004). Cerebral correlates of alerting, orienting and reorienting of visuospatial attention: an event-related fMRI study. Neuroimage, 21(1), 318-328.

Thut, G., Ives, J. R., Kampmann, F., Pastor, M. A., & Pascual-Leone, A. (2005). A new device and protocol for combining TMS and online recordings of EEG and evoked potentials. Journal of neuroscience methods, 141(2), 207-217.

Tian, Y., Klein, R. M., Satel, J., Xu, P., & Yao, D. (2011). Electrophysiological explorations of the cause and effect of inhibition of return in a cue–target paradigm. Brain topography, 24(2), 164-182.

Tiitinen, H., Virtanen, J., Ilmoniemi, R. J., Kamppuri, J., Ollikainen, M., Ruohonen, J., & Näätänen, R. (1999). Separation of contamination caused by coil clicks from responses elicited by transcranial magnetic stimulation. Clinical neurophysiology, 110(5), 982-985.

Todd, J. J., & Marois, R. (2005). Posterior parietal cortex activity predicts individual differences in visual short-term memory capacity. Cognitive, Affective, & Behavioral Neuroscience, 5(2), 144-155.

Tseng, P., Hsu, T. Y., Chang, C. F., Tzeng, O. J., Hung, D. L., Muggleton, N. G., ... & Juan, C. H. (2012). Unleashing potential: transcranial direct current stimulation over the right posterior parietal cortex improves change detection in low-performing individuals. Journal of Neuroscience, 32(31), 10554-10561.

Vallar, G. (1998). Spatial hemineglect in humans. Trends in cognitive sciences, 2(3), 87-97.

Vandenberghe, R., & Gillebert, C. R. (2009). Parcellation of parietal cortex: convergence between lesion-symptom mapping and mapping of the intact functioning brain. Behavioural brain research, 199(2), 171-182.

Veniero, D., Bortoletto, M., & Miniussi, C. (2009). TMS-EEG co-registration: on TMS-induced artifact. Clinical Neurophysiology, 120(7), 1392-1399.

Vernet, M., Bashir, S., Yoo, W. K., Perez, J. M., Najib, U., & Pascual-Leone, A. (2013). Insights on the neural basis of motor plasticity induced by theta burst stimulation from TMS–EEG. European Journal of Neuroscience, 37(4), 598-606.

Villamar, M. F., Volz, M. S., Bikson, M., Datta, A., DaSilva, A. F., & Fregni, F. (2013a). Technique and considerations in the use of 4x1 ring high-definition transcranial direct current stimulation (HD-tDCS). JoVE (Journal of Visualized Experiments), (77), e50309.

Villamar, M. F., Wivatvongvana, P., Patumanond, J., Bikson, M., Truong, D. Q., Datta, A., & Fregni, F. (2013b). Focal modulation of the primary motor cortex in fibromyalgia using 4× 1-ring high-definition transcranial direct current stimulation (HD-tDCS): immediate and delayed analgesic effects of cathodal and anodal stimulation. The Journal of Pain, 14(4), 371-383.

Virtanen, J., Ruohonen, J., Naatanen, R., & Ilmoniemi, R. J. (1999). Instrumentation for the measurement of electric brain responses to transcranial magnetic stimulation. Medical and Biological Engineering and Computing, 37(3), 322-326.

Bibliography

Vogel, E. K., & Machizawa, M. G. (2004). Neural activity predicts individual differences in visual working memory capacity. Nature, 428(6984), 748.

Vogel, E. K., McCollough, A. W., & Machizawa, M. G. (2005). Neural measures reveal individual differences in controlling access to working memory. Nature, 438(7067), 500.

Vossel, S., Thiel, C. M., & Fink, G. R. (2006). Cue validity modulates the neural correlates of covert endogenous orienting of attention in parietal and frontal cortex. Neuroimage, 32(3), 1257-1264.

Wagner, T., Fregni, F., Fecteau, S., Grodzinsky, A., Zahn, M., & Pascual-Leone, A. (2007). Transcranial direct current stimulation: a computer-based human model study. Neuroimage, 35(3), 1113-1124.

Wagner, T., Valero-Cabre, A., & Pascual-Leone, A. (2007). Noninvasive human brain stimulation. Annu. Rev. Biomed. Eng., 9, 527-565.

Wallace, D., Cooper, N. R., Paulmann, S., Fitzgerald, P. B., & Russo, R. (2016). Perceived comfort and blinding efficacy in randomised sham-controlled transcranial direct current stimulation (tDCS) trials at 2 mA in young and older healthy adults. PloS one, 11(2), e0149703.

Walsh, V., & Cowey, A. (2000). Transcranial magnetic stimulation and cognitive neuroscience. Nature Reviews Neuroscience, 1(1), 73.

Walsh, V., & Pascual-Leone, A. (2003). Transcranial magnetic stimulation: a neurochronometrics of mind. MIT press.

Wexler, A. (2017). Recurrent themes in the history of the home use of electrical stimulation: transcranial direct current stimulation (tDCS) and the medical battery (1870–1920). Brain stimulation, 10(2), 187-195.

Wirth, M., Rahman, R. A., Kuenecke, J., Koenig, T., Horn, H., Sommer, W., & Dierks, T. (2011). Effects of transcranial direct current stimulation (tDCS) on behaviour and electrophysiology of language production. Neuropsychologia, 49(14), 3989-3998.

Woods, A. J., Antal, A., Bikson, M., Boggio, P. S., Brunoni, A. R., Celnik, P., ... & Knotkova, H. (2016). A technical guide to tDCS, and related non-invasive brain stimulation tools. Clinical neurophysiology, 127(2), 1031-1048.

Wörsching, J., Padberg, F., Ertl-Wagner, B., Kumpf, U., Kirsch, B., & Keeser, D. (2016). Imaging transcranial direct current stimulation (tDCS) of the prefrontal cortex—correlation or causality in stimulation-mediated effects?. Neuroscience & Biobehavioral Reviews, 69, 333-356.

Wörsching, J., Padberg, F., Helbich, K., Hasan, A., Koch, L., Goerigk, S., ... & Keeser, D. (2017). Test-retest reliability of prefrontal transcranial Direct Current Stimulation (tDCS) effects on functional MRI connectivity in healthy subjects. Neuroimage, 155, 187-201.

Xu, Y., & Chun, M. M. (2006). Dissociable neural mechanisms supporting visual short-term memory for objects. Nature, 440(7080), 91.

Yavari, F., Jamil, A., Samani, M. M., Vidor, L. P., & Nitsche, M. A. (2018). Basic and functional effects of transcranial Electrical Stimulation (tES)—An introduction. Neuroscience & Biobehavioral Reviews, 85, 81-92.

You, D. S., Kim, D. Y., Chun, M. H., Jung, S. E., & Park, S. J. (2011). Cathodal transcranial direct current stimulation of the right Wernicke's area improves comprehension in subacute stroke patients. Brain and language, 119(1), 1-5.

Zaehle, T., Rach, S., & Herrmann, C. S. (2010). Transcranial alternating current stimulation enhances individual alpha activity in human EEG. PloS one, 5(11), e13766.

Zaghi, S., Acar, M., Hultgren, B., Boggio, P. S., & Fregni, F. (2010). Noninvasive brain stimulation with low-intensity electrical currents: putative mechanisms of action for direct and alternating current stimulation. The Neuroscientist, 16(3), 285-307.

Zago, S., Priori, A., Ferrucci, R., & Lorusso, L. (2016). Historical Aspects of Transcranial Electric Stimulation. In Transcranial Direct Current Stimulation in Neuropsychiatric Disorders (pp. 3-19). Springer, Cham.

Zheng, X., Alsop, D. C., & Schlaug, G. (2011). Effects of transcranial direct current stimulation (tDCS) on human regional cerebral blood flow. Neuroimage, 58(1), 26-33.